



University
of Glasgow

Bryson, Michelle S (2011) *The role of chemokines and their receptors in non-Hodgkin's lymphoma*.
PhD thesis.

<http://theses.gla.ac.uk/2675/>

Copyright and moral rights for this thesis are retained by the author

A copy can be downloaded for personal non-commercial research or study, without prior permission or charge

This thesis cannot be reproduced or quoted extensively from without first obtaining permission in writing from the Author

The content must not be changed in any way or sold commercially in any format or medium without the formal permission of the Author

When referring to this work, full bibliographic details including the author, title, awarding institution and date of the thesis must be given

THE ROLE OF CHEMOKINES AND THEIR RECEPTORS IN NON-HODGKIN'S LYMPHOMA

Michelle Bryson

September 2010

This thesis is submitted to the University of Glasgow in
accordance with the requirements for the degree of
Doctor of Philosophy in the Faculty of Medicine

Division of Immunology, Infection and Inflammation
University of Glasgow
University Avenue
Glasgow
G12 8QQ

© Michelle Bryson

Abstract

Chemokines are a family of low-molecular weight proteins that mediate their effects through binding with chemokine receptors (a group of seven trans-membrane spanning G-protein coupled receptors). Chemokines are well known for their role in leukocyte trafficking, although they also mediate a range of other physiological functions including cell proliferation, growth and differentiation. Chemokines are integral to the development and functioning of the immune system and are implicated in the pathogenesis of a wide range of diseases including autoimmune disorders, HIV infection and malignancies.

Non-Hodgkin's lymphoma (NHL) is a malignancy of the lymphoid system, which can affect any tissues in the body but has a predilection for the secondary lymphoid organs and the bone marrow. NHL represents a heterogeneous group of disorders with variations in presentation and prognosis. Whilst there have been improvements in overall survival in the last few decades following developments in treatment there is still a significant mortality associated with NHL as well as significant morbidity associated with the treatments required to control the disease or affect a cure.

There is increasing evidence that chemokines and their receptors play a role in the pathogenesis of NHL with increased chemokine receptor expression seen in certain subtypes. Chemokines have also been shown to influence prognosis in particular NHL subtypes. This thesis describes studies to examine the relationship between constitutive chemokine receptor expression and NHL subtype with subsequent correlation between chemokine receptor expression and outcome. Results from studies on clinical samples obtained from patients with a range of B-cell NHL subtypes revealed significant differences in chemokine receptor expression between subtypes. Predominantly these differences were noted with the receptors CCR4 and CCR7. CCR4 has previously been examined in relation to T-cell lymphomas and high CCR4 expression has been associated with an adverse prognosis in adult T-cell leukaemia/lymphoma. However, systematic examination of CCR4 in B-cell NHL has not been done before. In this study CCR4 expression was seen in samples of diffuse large B-cell lymphoma (DLBCL), mantle cell lymphoma (MCL), MALT lymphoma and Burkitt's lymphoma. Furthermore high CCR4 expression was associated with a significantly improved survival in patients with DLBCL. CCR7 expression was significantly higher in cases of MCL and chronic lymphocytic lymphoma/small lymphocytic lymphoma (CLL/SLL), this however did not equate to

differences in outcome. The high expression of CCR7 in MCL and CLL/SLL does however make this receptor an ideal target for the development of targeted therapies.

Further studies in this thesis describe strategies used to target the chemokine system with cytotoxic agents. CCR7 was chosen for targeting experiments due to its restricted expression (naïve T-cells, memory T-cells, dendritic cells and subsets of B-cells) in normal tissues, the fact that it controls homing of leukocytes to lymph nodes, and that is the second most commonly reported chemokine receptor detected in cancers. The first approach for targeting the chemokine system used radio-labelled chemokines to induce cytotoxicity in cells expressing the cognate receptor. Unfortunately, the results from this were not conclusive and further studies are required to explore this approach.

The second approach described in this thesis entailed the potential use of oncolytic adenoviral gene therapy. This approach requires the redirection of adenoviral tropism from the coxsackie and adenovirus receptor (CAR) and through CCR7. This was successfully achieved in cell lines engineered to express and those endogenously expressing CCR7 by ‘shrouding’ the virus in CCL19. However, background infection was high and this led to the engineering of an adenoviral vector incorporating a peptide within the viral knob protein to allow for more efficient ‘shrouding’ of the virus and thus more efficient redirection of the virus. However, final experiments with this vector were not performed due to time constraints.

The final part of this thesis relates to the characterisation of EL4 cells (a murine T-cell lymphoma cell line) for use as a potential *in-vivo* mouse model for targeting experiments. Following injection into the flank of C57/BL6 with these cells, measurable tumours develop. It was demonstrated that this cell line expressed CCR7, and finally after a number of modifications, it was shown that adenoviral tropism could be redirected through chemokine receptors on the surface of these cells.

In summary the results in this thesis shows for the first time that CCR4 is expressed across a number of B-cell NHL subtypes and that this is associated with outcome in DLBCL. Results also demonstrate that therapeutic targeting of CCR7 is a reasonable therapeutic approach in NHL. In addition, redirection of oncolytic adenoviral vectors through chemokine receptors provides a potential strategy for obtaining this targeted therapy. Finally, EL4 cells have the potential to be used as an *in-vivo* mouse model for CCR7 targeted therapies.

Table of Contents

Abstract	ii
List of Tables	ix
List of Figures	x
Acknowledgements	xiv
Author's declaration	xvi
Abbreviations	xvii
CHAPTER ONE	1
INTRODUCTION	1
1.1 Overview of the Immune System	1
1.1.1 Haematopoiesis	1
1.1.2 Innate Immunity.....	2
1.1.2.1 External Barriers to Infection	2
1.1.2.2 Cellular Components of the Innate Immune System	3
1.1.3 Chemical Components of the Immune System.....	3
1.1.4 Adaptive Immunity	5
1.1.4.1 Organisation of the Immune System	5
1.1.4.2 Generation of Antigen Specific Receptors in Lymphocytes	7
1.1.5 B Lymphocytes.....	7
1.1.5.1 B Lymphocyte Receptor (Immunoglobulin) Rearrangement.....	8
1.1.5.2 B-cell Activation.....	9
1.1.5.3 T-cell Dependent Activation, Isotype Switching and Somatic Hypermutation	9
1.1.5.4 T-cell Independent Responses	10
1.1.6 T-lymphocytes.....	11
1.1.6.1 Maturation in the Thymus.....	11
1.1.6.2 Innocence to experience: Meeting of the Naïve T-cell and Antigen	12
1.1.6.3 Antigen Processing and the MHC Molecules	13
1.1.6.4 Antigen Recognition by T-cells.....	13
1.1.6.5 T-cell Receptor Signalling.....	13
1.1.6.6 T cell Sub-sets	14
1.1.7 Regulation of Autoimmune Responses	15
1.1.8 Interactions Within and Outside of the Immune System	16
1.2 Chemokines and their Receptors	17
1.2.1 Historical Perspective.....	17
1.2.2 Nomenclature and Structural Classification of Chemokines	17
1.2.3 Functional Classification of Chemokines.....	21
1.2.4 N-terminal Domain of Chemokines.....	22
1.2.5 Chemokine Regulation.....	22
1.2.5.1 Regulation by Glycosaminoglycans	22
1.2.5.2 Post-translational Control.....	23
1.2.6 Chemokine Receptors	23
1.2.6.1 Receptor Activation and Guanine Nucleotide Binding Proteins.....	24
1.2.6.2 Signalling Pathways and Intracellular Control of Migration.....	25
1.2.6.3 Desensitisation, Internalisation and Recycling of Receptors.....	26
1.2.6.4 Decoy Receptors	27
1.2.7 Chemokines and Organisation of the Immune System.....	28
1.2.7.1 Chemokine Control of Lymphocyte Trafficking	28
1.2.8 T Lymphocyte Development in the Thymus	29
1.2.9 Chemokines during B cell Development.....	31
1.2.10 Homing of Naïve Lymphocytes to Lymph Nodes	31
1.2.11 Migration within and out of Secondary Lymphoid Organs.....	32
1.2.12 Tissue Specific Homing of Leukocytes	32
1.2.13 Chemokines and T cell Subsets	34
1.2.13.1 Memory T cells	34
1.2.13.2 Helper T-cells	35

1.2.13.3 Regulatory T cells	36
1.2.14 Germinal Centre Organisation and B cell Immune Responses	36
1.2.15 Initiation of Immune Responses by Constitutive Chemokines	36
1.3 Non-Hodgkin's Lymphoma	38
1.3.1 Historical Perspective	38
1.3.2 Epidemiology of Lymphoma	40
1.3.3 Aetiology of NHL	42
1.3.4 Clinical Features	43
1.3.5 Diagnosis of NHL	44
1.3.6 Classification of NHL	48
1.3.7 General Principles of Treatment	48
1.3.8 Pathophysiology of NHL	50
1.3.8.1 Genetic and Molecular Aspects of B-cell Neoplasms	50
1.3.8.2 Antigenic Stimulation	51
1.3.8.3 Role of the microenvironment	51
1.3.9 B-cell Neoplasms Studied in this Thesis	53
1.3.9.1 Diffuse large B-cell lymphoma	53
1.3.9.2 Follicular Lymphoma	55
1.3.9.3 Mantle Cell Lymphoma	57
1.3.9.4 Chronic Lymphocytic Leukaemia/ Small Lymphocytic Lymphoma	59
1.3.9.5 Burkitt's Lymphoma	62
1.3.9.6 Marginal Zone Lymphoma	63
1.3.10 Summary	65
1.4 Chemokines and Lymphoma	66
1.4.1 Chemokines and Malignancy	66
1.4.2 Chemokines and Lymphoma Development	68
1.4.3 Lymphoma Subtype and Chemokine Expression	70
1.4.4 Expression and Clinical Stage	72
1.4.5 Expression and Prognosis	72
1.4.6 Using the Chemokine System as Targeted Therapy	73
1.4.6.1 General Principles	73
1.4.6.2 Small Molecule Antagonists of Chemokine Receptors	73
1.4.6.3 Antibody Therapy Targeting the Chemokine System	74
1.4.6.4 Chemotoxins and Gene Therapy	75
1.5 Adenoviral Vectors	76
1.5.1 Overview	76
1.5.2 Structure of the Adenovirus	76
1.5.3 Components of Adenoviral DNA and Viral Replication	77
1.5.4 The Coxsackie and Adenovirus Receptor	78
1.5.5 Entry of Adenovirus into Cells	79
1.5.6 Adenovirus and Gene Therapy	81
1.5.7 Targeting Specific Cells with Adenoviral Vectors	83
1.5.7.1 Conditionally-Replicating Adenovirus and Tissue-Specific Promoters	83
1.5.7.2 Redirection of adenoviral tropism	84
1.6 Aims of Study	86
CHAPTER TWO	87
MATERIALS AND METHODS	87
2.1 Materials	87
2.1.1 Antibodies	87
2.1.2 Bacteriology	88
2.1.3 Cell Culture	89
2.1.4 Cell Lines	90
2.1.5 Chemicals	90
2.1.6 Miscellaneous	91
2.1.7 Molecular Biology	92
2.1.7.1 Plasmids	92
2.1.7.2 Oligonucleotides	93
2.1.7.3 Restriction Enzymes	94
2.2 Methods	95
2.2.1 Obtaining Ethical Committee Approval for use of Patient Samples	95

2.2.2 Tissue Culture.....	95
2.2.2.1 Freezing Cells.....	95
2.2.2.2 Defrosting cells.....	96
2.2.2.3 Counting Cells.....	96
2.2.2.4 Transfection of Cells.....	96
2.2.2.4.1 Stable Transfection of HEK.293 and CHO Cells Using Effectene®.....	96
2.2.2.4.2 Transient Transfection of CHO Cells using Polyfect®.....	97
2.2.2.4.3 Transfection of EL4 Cells by Nucleoporation.....	97
2.2.3 Analysis of Cell Fluorescence by FACS.....	98
2.2.4 Molecular Biology.....	101
2.2.4.1 Oligonucleotide Synthesis.....	101
2.2.4.2 Nucleic Acid Preparation.....	101
2.2.4.2.1 Genomic DNA Extraction.....	101
2.2.4.2.2 RNA Extraction using Trizol®.....	101
2.2.4.2.3 DNAase Treatment of RNA.....	102
2.2.4.2.4 cDNA Synthesis from RNA.....	102
2.2.4.3 Polymerase Chain Reaction (PCR).....	102
2.2.4.3.1 Reverse Transcriptase PCR (RT-PCR).....	102
2.2.4.3.2 Overlap-extension PCR.....	103
2.2.4.4 Agarose Gel Electrophoresis.....	104
2.2.4.5 Restriction Enzyme Digests.....	104
2.2.4.6 Partial Digests.....	105
2.2.4.7 Gel Purification of DNA Fragments and PCR Products.....	105
2.2.4.8 Cloning of PCR Products into TOPO® Vectors.....	105
2.2.4.9 Annealing of Oligonucleotides.....	105
2.2.4.10 DNA Ligation using the Roche Rapid Ligation Kit.....	106
2.2.4.11 Site Directed Mutagenesis.....	106
2.2.4.12 Preparation of Chemically Competent Cells.....	107
2.2.4.13 Transformation using Chemically Competent Cells.....	107
2.2.4.14 Transformation Using Electrically Competent Cells.....	108
2.2.4.15 Plasmid DNA Preparation (Mini/Maxipreps).....	108
2.2.4.16 DNA Sequencing.....	108
2.2.5 In-vitro assays.....	109
2.2.5.1 Antibody Staining for Surface Receptor Expression.....	109
2.2.5.2 CCL19-Biotin Uptake.....	109
2.2.5.3 Radiolabelled Ligand Uptake.....	110
2.2.5.4 MTT Proliferation Assay.....	110
2.2.5.5 Chemotaxis Assays.....	111
2.2.5.5.1 Chemotaxis using 24 well HTS Transwell® Plates.....	111
2.2.5.5.2 QCM™ Chemotaxis 3µm 96-Well Cell Migration Assay.....	111
2.2.6 Adenovirus Preparation, Modification and Infections.....	112
2.2.6.1 Expanding Adenoviral Stocks.....	112
2.2.6.2 Adenoviral Titre Assay using the BD Adeno-X™ Rapid Titre Kit.....	113
2.2.6.3 Shrouding of Adenovirus with Chemokine.....	114
2.2.6.4 Infection of Mammalian Cells.....	115
2.2.6.5 Assessment of Mammalian Cell Infection by Staining for Beta-galactosidase.....	115
2.2.6.6 Assessment of Mammalian Cell Infection using the Promega Luciferase assay.....	116
2.2.6.7 Assessment of Mammalian Cell Infection by FACS.....	116
2.2.6.8 Preparation of Adenovirus for Visualisation by Electron Microscope.....	116
2.2.7 In-vivo Assays.....	117
2.2.7.1 Maintenance of Mice.....	117
2.2.7.2 Infection of Mice with Adenovirus.....	117
2.2.7.3 Assessment of Virus Infection in Mouse Tissues.....	117
2.2.7.3.1 Cryopreservation of Mouse Tissues and Preparation of Slides.....	117
2.2.7.3.2 β-galactosidase Staining of Mouse Tissues.....	118
2.2.8 Statistical Analysis.....	118

CHAPTER THREE..... 119

ANALYSIS OF CHEMOKINE RECEPTOR EXPRESSION IN NON-HODGKIN'S LYMPHOMA. 119

3.1 Introduction.....	119
3.2 Use of Cell Lines to Verify Oligonucleotides for the Detection of Chemokine Receptors.....	120
3.2.1 Identifying Cell Lines to be used.....	120

3.2.2 RT-PCR Results on Cell Lines.....	120
3.2.3 Topocloning and Sequencing to Verify the Chemokine Receptor Primers.....	123
3.3 Testing of Chemokine Receptor Antibodies Using Cell Lines.....	123
3.4 Testing of Patient Samples	125
3.4.1 Comparison of Chemokine Receptor Expression within Each NHL Subtype.	126
3.4.2 Comparison of Constitutive Chemokine Receptor Expression Between Lymphoma Subtypes	134
3.4.2.1 CCR4 Expression	134
3.4.2.2 CCR6 Expression	136
3.4.2.3 CCR7 Expression	138
3.4.2.4 CCR9 Expression	140
3.4.2.5 CCR10 Expression.....	142
3.4.2.6 CXCR4 Expression.....	143
3.4.2.7 CXCR5 Expression.....	144
3.5 Correlation of Constitutive Chemokine Receptor Expression with Clinical Outcome.....	145
3.5.1 Correlation Between CCR4 Expression and Clinical Course	146
3.5.1.1 Overall Survival and CCR4 Expression	146
3.5.1.2 Stage of Lymphoma at Presentation and CCR4 Expression.....	147
3.6 Summary	149
CHAPTER FOUR.....	150
IN-VITRO STUDIES OF CCR7.....	150
4.1 Introduction.....	150
4.2 Constructs and Cell Lines.....	151
4.2.1 Assessment of hCCR7 Expression by Flow Cytometry	152
4.2.2 Functional assessment of hCCR7 Expression by biotin-CCL19 Uptake	153
4.3 Functional Analysis of CCR7 in Raji Cells.....	157
4.3.1 Biotin-CCL19 Uptake in Raji Cells.....	157
4.3.2. Chemotaxis Assays on Raji cells	159
4.4 Cell killing by exposure to a radio-labelled chemokine	162
CHAPTER FIVE.....	170
REDIRECTION OF ADENOVIRAL TROPISM THROUGH CHEMOKINE RECEPTORS	170
5.1 Introduction.....	170
5.2 Infection of HEK293 and HEK.hCCR7 Cells Following Chemical shrouding of Adenovirus with Chemokine	171
5.3 Infection of CHO and CHO.hCCR5 Cells with Adenovirus shrouded with CCL3.....	175
5.4 Optimisation of Infection Rates.....	177
5.4.1 Effect of Incubation Time with NeutrAvidin™ on the Rate of Infection.....	177
5.4.2 Effect of Incubation Time with Chemokine on the Rate of Infection.....	178
5.4.3 Effect of NeutrAvidin™ concentration on infection rates.....	178
5.5 Infection of Raji Cells with Adenovirus shrouded in CCL19	180
5.6 Increasing the Specificity of Cell Targeting using Different Promoters.....	183
5.6.1 Comparison of infection rates in HEK293 and A2780 cells following infection with Ad5.hTERT.Luc.....	183
5.6.2 Comparison of Infection in HEK293 and HEK.hCCR7 Cells with Ad5.hTR.Luc shrouded with CCL19	184
5.7 Assessment of NeutrAvidin™ binding to adenovirus using electron microscopy.....	185
5.8 Modification of the adenoviral knob protein.....	188
5.8.1 Construction of a Vector for Homologous Recombination with the pAdEasy Vector.....	189
5.8.2 Homologous Recombination with pAdEasy and pCR2.1.Ad5.AP.Tet.....	197
5.8.3 Development of pCR2.1.Ad5.AP.Kan	197
5.8.4 Homologous Recombination with pAdEasy and pCR2.1.Ad5.AP.Kan.....	199
5.8.5 Sub-cloning to obtain pAdEasy.AP	199
5.9 Incorporation of a reporter gene into pAdEasy.AP	202
5.10 Summary.....	204
CHAPTER SIX.....	205
EL4 CELLS AS AN <i>IN-VIVO</i> NON-HODGKIN'S LYMPHOMA MOUSE MODEL.....	205
6.1 Introduction.....	205
6.2 Assessment of mCCR7 Expression in EL4 Cells.....	206

6.2.1 Assessment of Murine CCR7 Expression by RT-PCR.....	206
6.3 Assessment of functional mCCR7 expression EL4 cells.....	207
6.3.1 Biotin-CCL19 Uptake by EL4 Cells.....	207
6.3.2 Chemotaxis Assay with EL4 Cells using CCL19.....	209
6.4 Adenoviral Infection of EL4 Cells	210
6.4.1 Initial Infection Experiments with Chemically shrouded Adenovirus.	211
6.4.2.1 Determination of the Optimum Anti-hexon Antibody Concentration.....	211
6.5 Effect of Increasing mCCR7 Expression on the rate of Infection	213
6.5.1 Development of pEF6.mCCR7and Transfection into EL4 Cells.....	213
6.5.2 Functional Analysis of EL4 Cells with Increased mCCR7 Expression	215
6.5.2.1 Biotinylated-CCL19 Uptake in EL4.mCCR7 Cells.....	215
6.5.2.2 Migration of EL4 and EL4.mCCR7 cells towards CCL19.....	217
6.5.3 Adenoviral Infection in EL4 and EL4.mCCR7 Cells	218
6.6 Investigating Other Causes of Sub-optimal Infection of EL4 Cells	219
6.6.1 Expression of CCX-CKR in EL4 Cells	220
6.6.2 Development of CCX-CKR Expressing Cell Lines.....	221
6.6.3 Infection with Adenovirus shrouded with CCL19 in Cells Expressing CCX-CKR or CCR7 ...	222
6.7 Optimising the Infection of EL4 Cells Further.....	226
6.7.1 Infection of EL4 cells with a higher MOI.....	226
6.7.2 Development of an Adenoviral Vector using EF1- α as a Promoter	228
6.8 Expression of CAR, α_v -integrin and CCX-CKR in Murine Tissues and Cells.....	229
6.10 Summary.....	236
CHAPTER SEVEN.....	237
DISCUSSION.....	237
7.1 Non-Hodgkin's Lymphoma and Chemokine Receptor Expression.....	237
7.2 Chemokine Receptor Expression and Function: Differences Between Normal B-cells and Malignant B-cells.....	239
7.3 CCR4 and Non-Hodgkin's Lymphoma	240
7.3.1 CCR4 Expression	240
7.3.2 CCR4 Targeted Therapy.....	243
7.4 CCR7 and NHL.....	245
7.4.1 CCR7 Expression	245
7.4.2 CCR7 Targeted Therapy	247
7.5 Using the Chemokine System to Target Specific Cell Populations with Cytotoxins	249
7.5.1 Chemotoxins and Chemokine-toxin Conjugates.....	249
7.5.2 Adenoviral Vectors Gene Therapy – Oncolytic Vectors.....	250
7.6 Development of a Murine Lymphoma Model.....	251
7.7 Summary and Future Directions.....	253
APPENDICES	255
8.1 WHO Classification of Tumours of the Lymphoid Tissues	255
8.2 Eastern Cooperative Oncology Group Performance Status [404].....	259
References.....	260

List of Tables

Table 1.1: Expression pattern and stage of immunoglobulin rearrangement according to maturational stage of B cell development.	8
Table 1.2: Overview of the CC chemokines and their cognate receptors.	19
Table 1.3: Overview of the CXC, XC and CX3C chemokines and their cognate receptors.	20
Table 1.4: Immunophenotypic profile of B-cell non-Hodgkin's lymphomas.	45
Table 1.5: Cotswolds revision of the Ann Arbour Staging Classification [217].	48
Table 1.6: Revised-International Prognostic Index	54
Table 1.7: Overall survival and progression free survival (PFS) in patients with follicular lymphoma based upon FLIPI score	56
Table 1.8: Outline of the two clinical staging systems for CLL/SLL.....	61
Table 1.9: Adhesion molecule and chemokine receptor expression on lymphoma subtypes	71
Table 3.1: Expression of constitutive chemokine receptor RNA in Raji, Daudi and MOLT-4 cells.	122
Table 3.2: Summary of mean chemokine receptor expression across different NHL subtypes.	133
Table 6.1: Expression of CAR, α_v-integrins and CCX-CKR in mouse tissues and leukocytes.....	233

List of Figures

Figure 1.1: Overview of haematopoiesis demonstrating the different cytokine profiles required for cellular differentiation.	2
Figure 1.2: Location of primary and secondary lymphoid organs in man.	6
Figure 1.3: Anatomical organisation of lymph nodes showing the route taken by naïve B-cells through the structure.....	6
Figure 1.4: Localisation and antigen expression during B-lymphocyte maturation.....	9
Figure 1.5: Steps of T-cell maturation within the thymus.	12
Figure 1.6: Positioning of the cysteine residues in the different structural classes of chemokines.	21
Figure 1.7: Outline of the 7 transmembrane structure of the chemokine receptor	25
Figure 1.8: Outline of major signalling pathways activated following receptor activation and their outcome on cellular function.....	26
Figure 1.9: Multistep paradigm of leukocyte adhesion and activation.....	29
Figure 1.10: Positioning of thymocytes within the thymus and chemokine receptor expression at different developmental stages.	30
Figure 1.11: Known and proposed functions for constitutive chemokines and their receptors..	34
Figure 1.12: Illustrations and images of Hodgkin’s Disease	39
Figure 1.13: Graphical representation of the incidence of NHL and the mortality rates associated with NHL in the UK	41
Figure 1.14: Radiological images from patients with lymphoma	47
Figure 1.15: Demonstration of chemokine receptor expression at different stages of B-cell differentiation and the corresponding lymphoma sub-types.	69
Figure 1.16: Diagrammatic representation of the adenoviral particle.....	77
Figure 1.17: An overview adenoviral internalization following attachment to CAR	80
Figure 1.18: Diagram demonstrating the various components of adenoviral genome in the different vector generations.....	83
Figure 2.1: Gating for single-colour flow cytometry.....	98
Figure 2.2: Determination of cell viability using ViaProbe	99
Figure 2.3: Setting up the flow cytometer for 2 colour analysis of lymphocytes.....	100
Figure 3.1: Expression of constitutive chemokine receptor expression in human lymphoma cell lines.....	121
Figure 3.2: Confirmation of hCCR10 RNA expression in L1.2.hCCR10 cells.....	122
Figure 3.3: Results of single colour flow cytometry on Raji, Daudi or L1.2hCCR10 cells with chemokine receptor antibodies	124
Figure 3.4: Distribution of chemokine receptor expression in 16 follicular lymphoma cases..	127

Figure 3.5: Distribution of chemokine receptor expression in 17 diffuse large B-cell lymphoma cases.....	128
Figure 3.6: Distribution of chemokine receptor expression in 17 mantle cell lymphoma cases	129
Figure 3.7: Distribution of chemokine receptor expression in 9 Burkitt's lymphoma cases.....	130
Figure 3.8: Distribution of chemokine receptor expression in MALT lymphoma cases	131
Figure 3.9: Distribution of chemokine receptor expression in 24 CLL/SLL	132
Figure 3.10: Comparison of CCR4 expression between the lymphoma subtypes	135
Figure 3.11: Comparison of CCR6 expression between the lymphoma subtypes.....	137
Figure 3.12: Comparison of CCR7 expression between the lymphoma subtypes	139
Figure 3.13: Comparison of CCR9 expression between the lymphoma subtypes.....	141
Figure 3.14: Comparison of CCR10 expression between the lymphoma subtypes	142
Figure 3.15: Comparison of CXCR4 expression between the lymphoma subtypes.....	143
Figure 3.16: Comparison of CXCR5 expression between the lymphoma subtypes.....	144
Figure 3.17: Kaplan-Meier charts comparing survival between NHL patients with high or low levels of CCR4 expression on B-cells.....	147
Figure 3.18: Correlation between clinical stage and CCR4 expression in patients with DLBCL, MCL or follicular lymphoma.. ..	148
Figure 4.1: pcDNA3.1.hCCR7 used to engineer hCCR7 expressing cell lines	152
Figure 4.2: hCCR7 surface expression in HEK293.hCCR7 cells	153
Figure 4.3: Biotin-CCL19 uptake by pools of HEK.hCCR7 cells.....	155
Figure 4.4: Biotin-CCL19 uptake by HEK.hCCR7 cells	156
Figure 4.5: Biotin-CCL19 uptake in Raji cells.....	158
Figure 4.6: Chemotaxis of Raji cells using Transwell® chemotaxis plates.....	160
Figure 4.7: Calibration curve for QCMTM Chemotaxis Assay using Raji cells.....	161
Figure 4.8: QCM™ Chemotaxis assay using Raji cells.....	162
Figure 4.9: Calibration curve for the MTT Cell assay.	164
Figure 4.10: Comparison of cell numbers at day 2 and 4 between wells exposed or not exposed to radiolabelled chemokine.	166
Figure 4.11: Cell numbers following 2, 4, 8 or 12 days incubation with radiolabelled chemokine.. ..	167
Figure 5.1: Outline of strategy to redirect adenoviral tropism	172
Figure 5.2: Infection of HEK293 and HEK.hCCR7 cells with Ad5.CMV.LacZ shrouded with biotin-CCL19.	174
Figure 5.3: Analysis of Ad5.CMV.LacZ infection in HEK293 and HEK.hCCR7 cells	174

Figure 5.4: CAR expression in CHO and HEK293 cells.	176
Figure 5.5: Infection of CHO and CHO.hCCR5 cells with Ad5.CMV.LacZ shrouded with biotin-CCL3.....	176
Figure 5.6: Infection rates with different durations of Ad5.CMV.LacZ incubation with NeutrAvidin™.....	177
Figure 5.7: Infection rates with different incubation times with CCL3.....	178
Figure 5.8: Effect of NeutrAvidin™ concentration on Ad5.CMV.LacZ infection rates.	179
Figure 5.9: HEK.hCCR7 cells infected with Ad5.CMV.LacZ incubated with NeutrAvidin™ at different concentrations.....	180
Figure 5.10: CAR expression in Raji Cells.....	181
Figure 5.11: Raji cells infected with Ad5.CMV.LacZ shrouded with CCL19.....	182
Figure 5.12: Infection of Raji cells with CCL19 shrouded Ad5.CMV.LacZ.	182
Figure 5.13: Infection of HEK293 and A2780 cells with Ad5.hTR.Luc, Ad5.hTERT.Luc and Ad5.SV40.Luc.....	184
Figure 5.14: Infection of HEK.hCCR7 cells with CCL19 shrouded Ad5.hTR.Luc.....	185
Figure 5.15: Electron micrograph of non-labelled adenovirus.....	187
Figure 5.16: Ad5.CMV.LacZ-NeutrAvidin™ conjugates incubated with biotin gold.....	187
Figure 5.17: Strategy to improve efficiency of adenovirus shrouding with chemokines.	188
Figure 5.18: Homologous recombination using the Stratagene AdEasy™ Adenoviral System.	190
Figure 5.19: Map of adenoviral vector containing the acceptor peptide.....	192
Figure 5.20: Overlap extension PCR.....	193
Figure 5.21: <i>Xba</i> I digest of overlap extension PCR product.....	194
Figure 5.22: Vectors created for homologous recombination with pAdEasy.....	195
Figure 5.23: <i>Xba</i> I digest on RT-PCR product from pCR2.1.Ad5.AP.Tet construct.....	196
Figure 5.24: Vector map of pCR2.1.Ad5.AP.Kan.....	198
Figure 5.25: Vector maps of pCR2.1.Ad5.AP.Kan and pBL.Ad5.AP.Kan.....	200
Figure 5.26: DNA preparation of ligation with pAdEasy and pBluescript.Spe1.Pac1.Frag.AP fragments.....	201
Figure 5.27: <i>Xba</i> I digest on RT-PCR product from pAdEasy.AP construct.	202
Figure 5.28: Vector maps of pAdEasy.AP.GFP and pAdEasy.AP.LacZ.....	203
Figure 6.1: mCCR7 expression in EL4 cells.....	206
Figure 6.2: Surface mCCR7 expression in EL4 cells.....	207
Figure 6.3: Biotin-CCL19 uptake by EL4 cells.....	208
Figure 6.4: Migration of EL4 cells in response to CCL19 and CXCL12.....	209

Figure 6.5: CAR and α_v -integrin expression in EL4 cells	210
Figure 6.6: Determination of anti-hexon antibody concentrations for use in adenoviral experiments.	212
Figure 6.7: Vector map of pEF6.mCCR7.....	213
Figure 6.8: mCCR7 expression in pools of EL4.mCCR7 cells.....	214
Figure 6.9: Expression of mCCR7 in pools of EL4.mCCR7 cells.....	215
Figure 6.10: Biotin-CCL19 uptake in EL4.mCCR7 pools.....	216
Figure 6.11: Uptake of biotin-CCL19 by EL4.mCCR7 cells.	216
Figure 6.12: QCM™ Calibration curve using EL4 cells.	217
Figure 6.13: Migration of EL4 and EL4.mCCR7 cells towards CCL19.....	218
Figure 6.14: Detection of Ad5.CMV.LacZ infection in EL4 cells using anti-hexon antibody	219
Figure 6.15: Expression of mCCR7 and mCCX-CKR in EL4 cells by RT-PCR.	220
Figure 6.16: Analysis of hCCX-CKR and hCCR7 expression in transfected CHO cells.....	221
Figure 6.17: Infection of CHO and HEK293 cells expressing hCCR7 or hCCX-CKR.....	223
Figure 6.18: Adenoviral infection of HEK.hCCR7 and HEK.hCCX-CKR cells.	224
Figure 6.19: Adenoviral infection of CHO.hCCR7 and CHO.hCCX-CKR cells.	225
Figure 6.20: Infection of EL4 cells with CCL19 shrouded Ad5.CMV.LacZ at MOI of 200.	227
Figure 6.21: Vector maps of pShuttle.CMV.IRES.GFP and pShuttle.EF6.IRES.GFP.	229
Figure 6.22: Expression of CAR and α_v -integrin in murine tissues and leukocytes.....	231
Figure 6.23: Expression of CCX-CKR in mouse tissues and leukocytes.	232
Figure 6.24: Infection of C57/Bl6 Mice with CCL19 shrouded Ad5.CMV.LacZ.	235

Acknowledgements

First of all I would like to thank Gerry Graham for giving me, a mere medic, the opportunity to work on this project. A big thanks also goes to Leukaemia Lymphoma Research who funded this study along with, all of the patients who were gracious enough to donate clinical samples for research. As much as I dislike the cliché it has to be said that it has been a long and interesting journey and I have learned a lot. Not least of which is how to pack up laboratory equipment to safely move it from one site to another, from the Beatson Institute to the Robertson Building and finally to the Glasgow Biomedical Research Centre. Skills, which came in handy when moving from the rainy Rainbow-laden skies of Glasgow to the sunny, blue skies of the Gold Coast in Australia (see the journey cliché works). Along the way I have had help from a number of people from all over the University, all of whom have impressed me with their willingness and patience, they include in no particular order: Rob, Derek, the three Clares (McCulloch, Burt and Shepherd), Clive, Emma, Paz, Pauline, Kenny, boy Chris, girl Chris, Mark M, Mark S, Ross, Antonio, Vicky, Catherine, Alasdair, Tim, Tam, Iain, Valerie, Judith, Laura, Maureen, Lesley, Aileen, Alan, Nicol Keith, Lawrence Tetley and Ruth Jarrett. I also had plenty of support outside of the laboratory with a particular mention to Pat Tansey and Sandy Sharp, my Haematology mentors and role models. My friends Lindsay, Julie and Fiona kept me sane/drank throughout this time, whilst Dave and my sister Karen provided much needed support during the difficult times. I also have to mention my life long friend Jon, it took me a long time to finish this, but your PhD still took longer! I could go on, but I would finally like to thank my colleagues here at the Gold Coast Hospital; Jeremy, Tara, Jasotha, Andrew and Marco, whilst I'm sure that you have appreciated learning all about chemokines, I am sure that you'll appreciate it even more that you will no longer have to hear me say,

“After I have submitted my PhD thesis I will.....”

Dedicated to the Memory of:
My father John Norman Bryson (1951-2005)
and
My grandfather Fredrick Leslie Palmer (1912-1992)

Author's declaration

“ I declare that, except where explicit reference is made to the contribution of others, that this dissertation is the result of my own work and has not been submitted for any other degree at the University of Glasgow or any other institution

Signature _____

Printed Name _____”

Abbreviations

°C	degrees celcius
µg	microgram
µl	microlitre
-/-	knock-out
+/-	heterozygote
+/+	wild type
-RT	without reverse transcriptase
Ab	antibody
ABC	activated B Celll
Ad5	adenovirus serotype 5
ADAM	a disintegrin and metalloproteinase
ADCC	antibody dependent cell-mediation cytotoxicity
Adv	adenoviral vector
Ag	antigen
AID	activation-induced cytidine deaminase
AIDS	acquired immunodeficiency syndrome
AIHA	autoimmune haemolytic anaemia
AP2	adaptor protein 2
APC	antigen presenting cell
ASCT	autologous stem cell transplant
ATLL	acute T lymphoblastic leukaemia/lymphoma
BEAM	BCNU, etoposide, ara-c, melphalan
BCL-2	B cell lymphoma 2
BCR	B cell receptor
BM	bone marrow
bp	base pair
Ca ²⁺	calcium ion
CAM	cell adhesion molecule
CAR	coxsackie and adenovirus receptor
CCL	CC chemokine ligand
CCR	CC chemokine receptor
CD	cluster of differentiation
CDC	Complement dependent cytotoxicity

CHO	Chinese hamster ovary
CHOP	cyclophosphamide, hydroxydoxorubicin, oncovin, prednisolone
CLA	cutaneous lymphocyte antigen
CLL	chronic lymphocytic leukaemia
CMJ	cortico-medullary junction
CMV	cytomegalovirus
CNS	central nervous system
CO ₂	carbon dioxide
COREC	Central Office for Research Ethics Committees
CRG	Chemokine Research Group
CRUK	Cancer Research UK
CSF	cerebro-spinal fluid
CT scan	computerised tomography scanning
CTL	cytotoxic T lymphocytes
CXCL	CXC chemokine ligand
CXCR	CXC chemokine receptor
CVP	cyclophosphamide, vincristine, prednisolone
DARC	Duffy antigen/ receptor for chemokines
DC	dendritic cell
ddH ₂ O	distilled water
DEPC	diethylpyrocarbonate
DLBCL	diffuse large B cell lymphoma
DMEM	Dulbecco's modified Eagle's medium
DMSO	dimethyl sulphoxide
DN	double negative
DNA	deoxyribonucleic acid
DP	double positive
dsRNA	double stranded RNA
EBV	Epstein Barr Virus
ECL	extracellular loop
ECM	extracellular matrix
ECOG	Eastern cooperative Oncology Group
<i>E.coli</i>	<i>Escherichia coli</i>
EDTA	ethylenediaminetetraacetic acid
EFS	event free survival
EPO	erythropoietin
EPOCH	etoposide, prednisolone, oncovin, cyclophosphamide, doxorubicin

FACS	fluorescence activated cell sort
FISH	fluorescent <i>in-situ</i> hybridisation
FITC	fluorescein isothiocyanate
FDG-PET	<u>fluorodeoxyglucose</u> -positron emission tomography
FCS	fetal calf serum
FDC	follicular dendritic cell
FOXP-3	forkhead box P3
g	gram
G418	geneticin
GAG	glycosaminoglycans
GAP	GTPase activating protein
GBRC	Glasgow Biomedical Research Centre
GC	germinal centre
G-CSF	granulocyte colony stimulating factor
GDP	guanine biphosphate
GEF	GDP exchange factors
GELA	Goupe d'Etude des Lymphomes de l'Adulte
GEP	gene expression profiling
GFP	green fluorescent protein
GM-CSF	granulocyte/Macrophage colony stimulating factor
GPCR	G-protein coupled receptors
GTP	guanine triphosphate
Hb	haemoglobin
HCV	hepatitis C virus
HEK	human embryonic kidney
HEV	high endothelial venule
HHV	human herpes virus
HIV	human immunodeficiency virus
<i>H.pylori</i>	<i>Helicobacter pylori</i>
HRP	horseradish peroxidase
HSC	haematopoietic stem cell
HTLV	human T-lymphotropic virus
ICAM-1	intracellular adhesion molecule-1
IFN- γ	interferon-gamma
Ig	immunoglobulin
HEK	human embryonic kidney
HEV	high endothelial venule
HHV	human herpes virus

kb	kilobase pairs
kDA	kiloDalton
kg	kilogram
l	litre
LDH	lactate dehydrogenase
LN	lymph node
LPD	lymphoproliferative disorder
LPS	lipopolysaccharide
M	molar
MadCAM-1	mucosal addressin cellular adhesion molecule-1
MALT	mucosa-associated lymphoid tissue
MAPK	mitogen activated protein kinase
MCL	mantle cell lymphoma
MFI	mean fluorescence intensity
mg	milligram
MHC	major histocompatibility complex
min	minute
ml	milliliter
mM	millimolar
MMP	matrix metalloproteinase
MRI	magnetic resonance imaging
mRNA	messenger RNA
MZ	marginal zone
MZL	marginal zone lymphoma
NCBI	National Centre for Biotechnology Information
NHL	non-Hodgkin's lymphoma
nm	nanometre
nM	nanomolar
NK	natural killer
NZY	NZ amine, yeast
OD	optical density
ORF	open reading frame
OS	overall survival
OTC	ornithine transcarbamylase
PEG	polyethylene glycol
PFS	progression free survival

PI3K	phosphatidylinositol 3-kinase
PIP ₂	phosphatidylinositol 4,5-biphosphate
PIP ₃	phosphatidylinositol 3,4,5-biphosphate
Plt	paucity of lymph node T cells
PTLD	post-transplant lymphoproliferative disorder
RAG	recombination activation genes
R-DHAP	rituximab, dexamethasone, ara-c, platinum
RGS	regulator of G-protein signaling
R-ICE	rituximab, ifosphamide, cytarabine, etoposide
RNA	ribonucleic acid
rpm	revolutions per minute
RPMI	Roswell Park Memorial Institute medium
RT	room temperature
RT-PCR	reverse-transcription PCR
S1P	sphingosine 1-phosphate
S1PR1	sphingosine 1-phosphate receptor 1
SCF	stem cell factor
SCZ	sub-cortical zone
sIg	surface immunoglobulin
SLL	small lymphocytic lymphoma
SOC	super optimal broth (catabolic repression)
TAC1	transmembrane activator and calcium-modulator and cyclophilin ligand interactor
TCR	T-cell receptor
T _{FH}	T follicular helper cell
Th1	T helper cell type 1
Th2	T helper cell type 2
Th17	T helper cell IL17
TI	thymus independent
TNF α	tissue necrosis factor- α
TPO	thrombopoietin
Treg	T regulatory cell
TSP	thymus settling progenitor
VCAM-1	vascular cellular adhesion molecule-1
VEGF	vascular endothelial growth factor
VLA-4	very late antigen-4
WHO	World Health Organisation

w/v

weight per unit of volume

CHAPTER ONE

INTRODUCTION

1.1 Overview of the Immune System

During our life we encounter a diverse range of infectious organisms. These vary in size and composition from the barely detectable prion to large intestinal parasites. The effects of these pathogens are also highly variable; from those that can kill within hours such as the Ebola virus, to those with which we can coexist in an uneasy symbiosis for numerous years. In response to this constant bombardment we have developed a highly complex and sophisticated defence system, the immune system. The immune system can be broadly divided into the innate and adaptive systems. The innate system is generally non-specific and is not affected by prior contact with infectious agents. In contrast acquired immunity occurs in response to specific microorganisms. However, the immune system is complex and the division between the innate and adaptive systems are not always clear.

1.1.1 Haematopoiesis

This process results in the production of the cells, which form a large component of the immune system. Definitive haematopoiesis originates from aortic endothelial cells arising from the aorta-gonado-mesonephros region of the embryo; this is followed by migration of cells to initiate haematopoiesis within the foetal liver [1]. Shortly after birth, haematopoietic stem cells (HSCs) from the liver migrate to the bone marrow that becomes the primary site of haematopoiesis throughout life, except under pathological states when the spleen and even the liver can become sites for haematopoiesis [2]. As haematopoietic cells are relatively short lived and have no capacity for self-renewal, it falls upon the HSCs which do have self-renewing capacity to continuously provide the pool needed for a functioning immune system. HSC are able to differentiate into all lineages of the haematopoietic system of which 'white cells' provide a functioning immune system [3]. In response to a variety of cytokines produced by stromal cells within the microenvironment (see figure 1.1), HSCs undergo a system of continuous differentiation [4]. Once the cell is partially differentiated its ability to proliferate becomes restricted and it is destined to follow a distinct differentiation pathway.

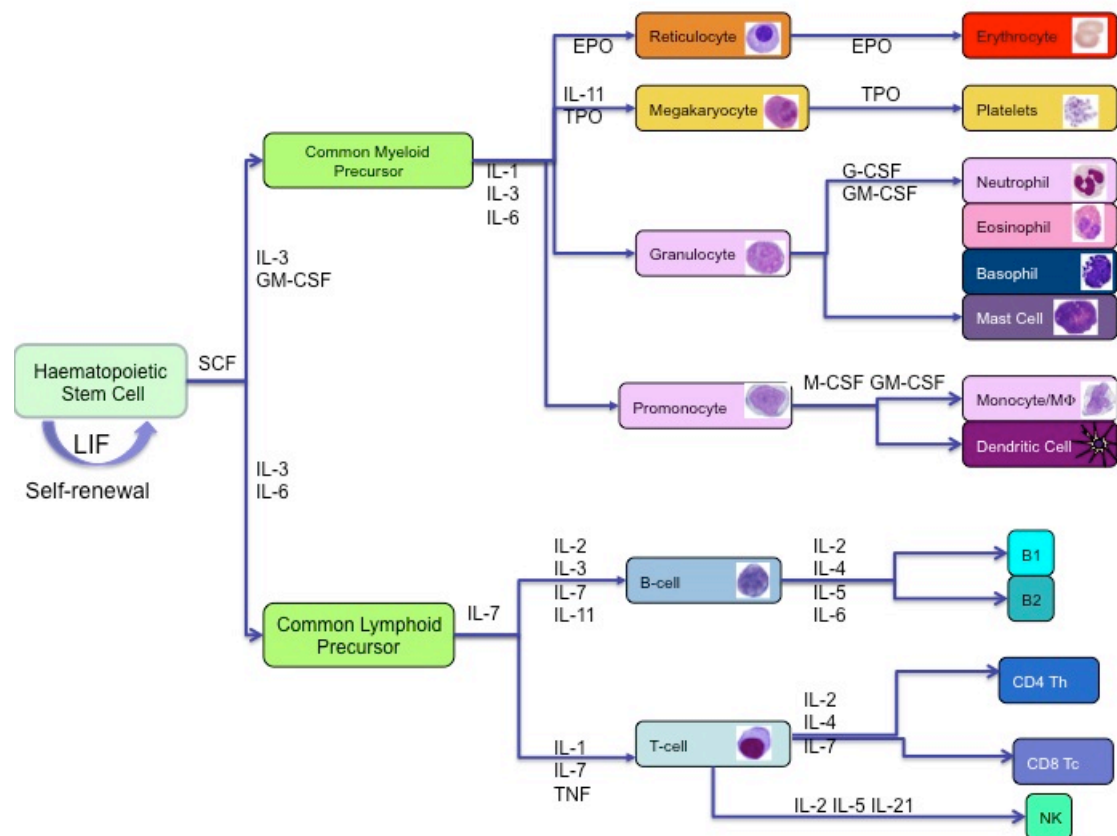


Figure 1.1: Overview of haematopoiesis demonstrating the different cytokine profiles required for cellular differentiation. Adapted from Delves et. al, 2006 [4]

1.1.2 Innate Immunity

The innate immune system is able to act without any prior exposure to the pathogen attempting to evade it. What follows is a limited overview of this system, with a later emphasis on the adaptive immune system.

1.1.2.1 External Barriers to Infection

The skin is the first major line of defence preventing, microorganisms from gaining initial access. Intact skin is impermeable to most major infectious agents, and also provides a hostile environment for bacteria via excretion of low pH lactic and fatty acids in the sweat and sebum. Secretions from mucous membranes also prevent invasion, including gastric acid, lysozymes, nasal secretions and saliva, blocking adherence of inhaled or ingested organisms. Physical mechanisms have developed including, cilia within the respiratory tract that push foreign material back out into the environment. Furthermore, commensal bacteria colonise our mucous membranes and assist in our defence by suppressing the

growth of potentially pathogenic bacteria by competing for essential nutrients or by producing inhibitory substances [4].

1.1.2.2 Cellular Components of the Innate Immune System

If a microorganism does bypass the external barriers then it has to face the humoral and cellular defence mechanisms in place. Perhaps the most important amongst the cellular components are the phagocytes, literally meaning, “eating cells”, these engulf microorganisms via a process termed phagocytosis.

Neutrophils are a key initial line of defence against microorganisms, which they destroy by phagocytosis and digestion. These are short-lived polymorphonuclear cells, normally found in the circulation [5]. Neutrophil recruitment to inflamed tissues is a key feature of the innate immune system, allowing localised eradication of invading pathogens. In contrast the longer-lived tissue macrophages form the mononuclear phagocyte system. They are found in connective tissues and basement membranes of small blood vessels. Macrophages are especially numerous within the liver (Kupffer cells), lung (alveolar macrophages), kidney, splenic sinusoids and medullary sinuses of lymph nodes. In these locations they are ideally placed to filter foreign antigens. These cells are also major players in humoral mechanisms of immunity [6]. Macrophages have the additional advantage of being able to combat intracellular as well as extracellular pathogens.

Other cells of the immune system include mast cells, basophils, eosinophils and natural killer cells. The first three cell types have roles in allergies, hypersensitivity reactions and parasite eradication. Eosinophils are of particular interest with the release of eosinophilic granules in the absence of parasitic infection being the hallmark of allergic reactions [7]. Natural killer (NK) cells are large granular lymphocytes, which, account for 10-15% of circulating lymphocytes [8]. These cells are predominantly involved in the eradication of infected or abnormal host cells by either inducing humoral responses or via antibody dependant cell mediated cytotoxicity (ADCC). [9, 10].

1.1.3 Chemical Components of the Immune System

Cells do not function in isolation and cellular recruitment to sites of inflammation is essential for the efficient destruction of pathogens. This is achieved through cellular responses to, or interaction with, peptides including cytokines, adhesion molecules, interferons and chemokines.

Cell adhesion molecules (CAMs) are transmembrane receptors, which mediate cellular adhesion and signalling. They are predominantly expressed on haematopoietic and endothelial cells; integrins interact with the extracellular matrix (ECM), and selectins, cadherins and the immunoglobulin super family CAMs mediate adhesion to adjacent cells [11]. These molecules can be expressed constitutively, or become up or down regulated in response to a number of stimuli including a variety of pro-inflammatory cytokines. CAMs can regulate numerous cellular functions including development, apoptosis, haemostasis, homing and activation [12]. Addressins are tissue specific adhesion molecules that act along with chemokines in the targeting of lymphocytes to lymphoid tissue at particular anatomical sites including the gut, lung, skin and peripheral lymph nodes.

Cytokines form a complex system of over 250 proteins and glycoproteins [13] secreted by both haematopoietic and non-haematopoietic cells, which have a diverse range of effects on a variety of cell types. These effects result from intracellular signalling following interaction with specific cell surface receptors. Cytokines can be categorised by function such as those stimulating haematopoietic cell growth and differentiation including granulocyte-macrophage colony stimulating factor (GM-CSF), granulocyte colony stimulating factor (G-CSF) and erythropoietin. Cytokines produced by, and exerting, their effect on leucocytes are termed interleukins [14]. Tissue necrosis factors (TNF), produced primarily by monocytes and macrophages [15], were initially named for their ability to kill tumour cells in-vitro [16]; more importantly they mediate inflammatory and metabolic responses during disease states [13]. Chemokines are discussed in more detail later. Cytokines have a central role in cell-to-cell communication and have a major role in the control and development of the innate and adaptive immune systems.

Interferons form a major class of cytokines first described in 1957 due their inhibitory effect on viral replication [17]. Whilst initially described in relation to their role in antiviral defence mechanisms they do have other biological effects including cell growth, differentiation and apoptosis [18]. Interferons (IFNs) are divided into, type 1 (viral IFNs) including the IFNs α , β and ω and their subclasses, and type 2 (immune IFN) encompasses only IFN γ [19]. Type I IFNs are induced in response to viral infections, whilst mitogenic or antigenic stimuli induce IFN γ [18]. Additionally, type 1 IFNs have, two other protective effects. Firstly, they induce up regulation of MHC class I molecules, thereby enhancing pathogen antigen presentation and increasing susceptibility to attack by cytotoxic T cells. Secondly, they promote up regulation of inhibitors of viral RNA and DNA production. NK

cells and CD4⁺ Th1 cells only produce IFN γ whilst CD8⁺ cytotoxic cells produce the remaining interferons [18]. IFN γ helps immune responses by increasing MHC class II expression, regulating cytokine expression and promoting activation of immune effector cells. IFNs are in widespread clinical use for conditions as varied as hepatitis C infection, myeloproliferative disorders, multiple sclerosis and carcinoid tumours.

1.1.4 Adaptive Immunity

The innate immune system is non-specific and certain microorganisms have developed strategies to evade it. Additionally it can cause substantial collateral damage to the host. The hallmark of the adaptive immune system is its ability to target specific microorganisms and reduce host tissue damage. Central to adaptive immunity are B and T-lymphocytes and the application of their receptors with specificity towards particular microbes. Following microbe recognition a series of events occur leading to targeted effector responses. What follows is a general overview of this system.

1.1.4.1 Organisation of the Immune System

Lymphocytes emerging from the thymus or bone marrow (primary lymphoid organs) are antigen naïve, relocating to secondary lymphoid tissues from the peripheral circulation, which include lymph nodes; spleen, tonsils and mucosa associated lymphoid tissue (see figure 1.2). Only a few naïve T and B-cells are able to react with specific foreign particles and systems are in place enabling them to encounter their specific antigens. Lymphoid tissues provide the microenvironment for this process, containing antigen presenting cells and a variety of stromal cells able to produce the cytokines necessary to maintain T and B-lymphocytes. Adhesion molecules are expressed by lymphoid tissues, in an ordered array, allowing cells to move through tissue, thereby increasing the chance of contact with antigen.

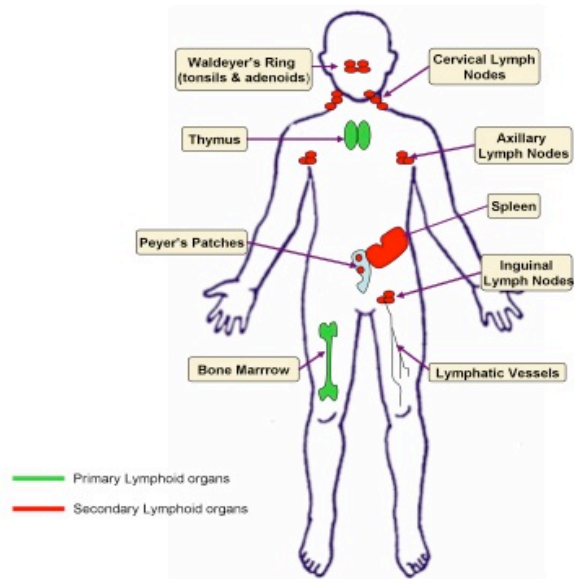


Figure 1.2: Location of primary and secondary lymphoid organs in man.

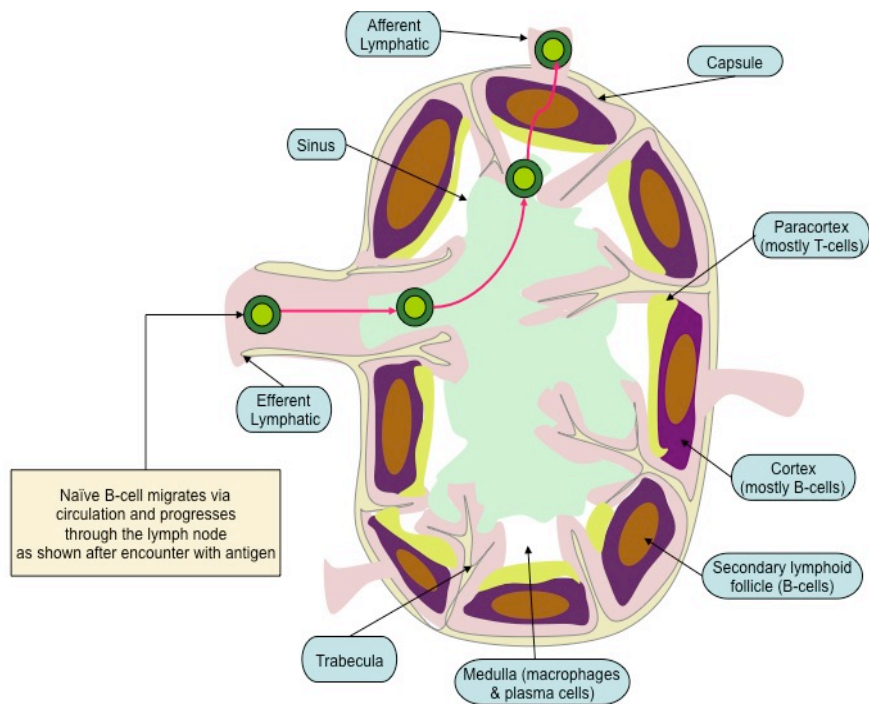


Figure 1.3: Anatomical organisation of lymph nodes showing the route taken by naïve B-cells through the structure.

1.1.4.2 Generation of Antigen Specific Receptors in Lymphocytes

T and B-cell clones are continually created throughout life, although production falls after the second decade in adults [14]. Lymphocyte antigen receptors are the means by which foreign antigens can be recognised, and they are key in the initiation of effector responses. Antigen receptors on B-cells are immunoglobulins (Ig), and those on T-cells are T-cell receptors (TCR). Each receptor has unique antigen specificity. Each individual has billions of lymphocytes, each with a particular receptor providing an incredibly diverse range of antigen recognition, achieved through somatic DNA recombination [20].

1.1.5 B Lymphocytes

B-cells are characterised by expression of cell surface immunoglobulins [21] and antibody production following activation. This is the humoral immune response. Early B-cell development occurs in the bone marrow and involves IgH and IgL rearrangement, these Ig proteins also play a role in the regulation of B-cell development [22]. The development of the B-cells can be followed by cell surface expression of certain molecules and the stage of IgH and IgL rearrangement [23] and as shown in table 1.1 and figure 1.4. Early in B-cell development the membrane-bound molecule Ig acts as the B-cell receptor (BCR) [24]. During this time the BCR internalises antigen and processes it to act as antigen presenting cells for T-cell responses. B-cells are then negatively selected within the bone marrow. Exposure of surface immunoglobulin positive (sIg⁺) B-cells to autoantigen leads to maturation arrest and apoptosis of those with high affinity [25], whilst those with no avidity are released into the circulation where they migrate to the spleen or lymph nodes and complete maturation. The final result is a B- cell producing one Ig and subsequently one specific antibody (Ab).

Different antibody classes have differing anatomical localisations. IgM is found predominantly in the intravascular space and IgG is the predominant class found in blood and tissues [14]. IgA is secreted by B-cells in mucosa associated lymphoid tissues (MALT); found in the gut, bronchus, urogenital and oro-pharangeal areas [26]. Antibodies function in one of three ways. Firstly, they can neutralise antigen by directly binding to it. Secondly, coating antigen facilitates recognition by other cells through, the Ab Fc portion and thus induces phagocytosis. Finally, it can activate complement, enhancing opsonisation or directly kill the pathogen [27]. Therefore antibody production

not only forms part of the adaptive immune system but forms a role within the innate system too.

1.1.5.1 B Lymphocyte Receptor (Immunoglobulin) Rearrangement

Immunoglobulin rearrangement occurs in B-cells within the bone marrow environment, prior to antigen exposure [28]. Each immunoglobulin (Ig) molecule consists of heavy and light chains within which are found variable (V) and constant (C) domains. Both heavy and light chain gene sequences contain more than one gene segment each of which has numerous potential genes [29] that can be utilised giving rise to a huge number of combinations. Rearrangement of the V domains in heavy and light chain genes is followed by RNA splicing into the C region genes [30]. These rearrangements are guided by a number of non-coding flanking DNA sequences [30], DNA modifying enzymes and recombination activation genes (RAG-1 and RAG-2) [31]. Additional variability is introduced by the fact that splicing is an inaccurate process and frame shift errors occur, deoxyribonucleotidyltransferase is able to insert nucleotides into the gene sequence and finally following antigen exposure; somatic hypermutation of the Ig heavy chain occurs [32]. As B-cells develop, the Ig receptor is present as an IgM molecule that can also internalise antigen and present it to T-cells acting as APCs. Subsequently the B-cells co-express IgD. The final stage of B-cell maturation, follows activation.

<i>Stage</i>	<i>Heavy Chain</i>	<i>Light Chain</i>	<i>Ig</i>	<i>CD19</i>	<i>CD20</i>
<i>Progenitor B cell</i>	germline	germline	-	-	-
<i>Early Pro-B cell</i>	D-J rearrangement	germline	-	-	-
<i>Late Pro-B cell</i>	V-DJ rearrangement	germline	-	-	-
<i>Large Pre-B cell</i>	VDJ rearranged	germline	m	?	-
<i>Small Pre-B cell</i>	VDJ rearranged	VJ rearranged	m	?	-
<i>Immature B cell</i>	VDJ rearranged	VJ rearranged	IgM	+	-
<i>Mature B cell</i>	VDJ rearranged	VJ rearranged	IgM, IgD	+	+

Table 1.1: Expression pattern and stage of immunoglobulin rearrangement according to maturational stage of B cell development along with expression of cell surface markers CD19 and CD20.

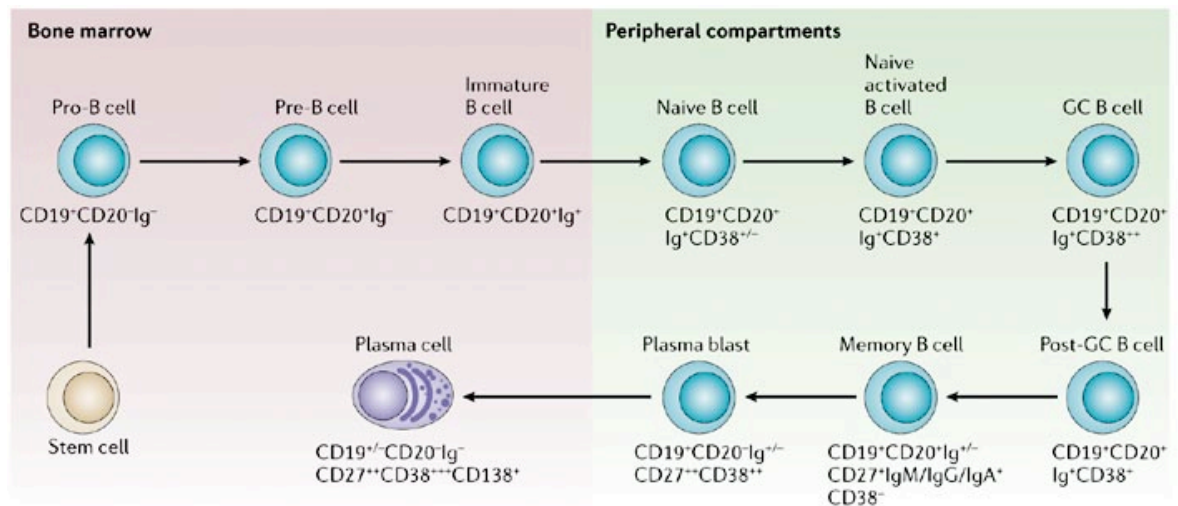


Figure 1.4: Localisation and antigen expression during B-lymphocyte maturation. (Taken from Edwards and Cambridge, 2006 [33]).

1.1.5.2 B-cell Activation

B-cell activation occurs following interaction of antigen with the BCR. This can occur in one of two ways. Firstly, binding of the BCR to antigen directly initiates a number of intracellular signals. Secondly, the BCR can deliver the antigen to intracellular sites where it is processed and then presented along with MHC class II molecules on the cell surface. The cells then recognise the antigens and further B cell proliferation and differentiation to antibody secreting cells ensues. The resulting plasma cells can produce and secrete one of the Ig subclasses (IgA, IgG, IgM, IgE and IgD). Antibodies are able to recognise the conformational structure of antigens in turn leading to further B-cell activation [34]. The result is an enormous number of B-lymphocytes each producing only one type of heavy chain and one type of light chain, with potential to recognise the variety of microbes encountered throughout life. Two broad mechanisms of B-cell activation have been described; T cell dependent and independent activation.

1.1.5.3 T-cell Dependent Activation, Isotype Switching and Somatic Hypermutation

Primary B-cell activation occurs within the T-cell rich areas of secondary lymphoid organs. Class II molecules presented with antigenic peptides are recognised by antigen primed Th cells, which then release a number of activating signals to the B-cell, stimulating proliferation and maturation. To achieve this Th cells forms contact with B-cells by a number of mechanisms, central to which is the CD40L on the Th cell and CD40 on the B- cell surface [35]. Other molecules include CD30L and CD30, IL-4, and BLys

and TACI [27]. However, this initial response is short lived and can only form IgM molecules which, have limited effector functions, therefore a further process is required.

Primary follicles are then formed at the B cell-T cell border (marginal zone), during which clonal expansion of both the B and T-cells occur over several days, with migration of germinal centre cells to this area. A proportion of the activated B-cells undergo intense B-cell proliferation here to form the germinal centre [36]. A rim of resting B-cells and a meshwork of follicular dendritic cells (FDCs) surround the germinal centre, forming the mantle zone. Initially, B-cells have reduced sIg expression, the centroblasts, forming the densely packed dark zone, where somatic hypermutation occurs. Somatic hypermutation consists of a series of predominantly single point mutations within the IgV gene leading to subtle alterations in the specificity and affinity of the resulting protein [37]. A small number of B-cells result which have higher affinity and specificity for the foreign antigen, these cells are then provided with further survival signals such as increased BCL-X_L expression, mediated by CD40/CD40L and BLys/TACI, whilst B-cells (the majority) with poor antigen affinity apoptose [38, 39].

Subsequently, sIg is up regulated, and the cells become less densely packed and interconnect with FDCs, becoming centrocytes, at which point isotype switching occurs. Isotype switching entails the replacement of the IgM C_H region with that of IgG, IgA or IgE through the up regulation of mRNA production and splicing. The type of immunoglobulin molecule produced is influenced by the cytokine release from the Th cells, with IL-4 driving IgG1 and IgE, TGF β driving IgG2b and IgA, IL-5 driving IgA and IFN γ driving IgG2a and IgG3 production? [27]. B cells are then induced to become either, memory B-cells or plasma cells yet; the exact mechanism by which differentiation to either of these cells types occurs is unclear.

1.1.5.4 T-cell Independent Responses

Thymus independent (TI) antigens include bacterial polysaccharides, lipopolysaccharides (LPS) and proteins. These TI antigens fall into two categories. TI-1 antigens include LPS, which can directly induce proliferation and differentiation of most B-cells regardless of their antigen specificity. This is termed polyclonal activation [40]. This response is more rapid than the Th dependant responses, and does not induce isotype switching, maturation or the formation of memory B-cells, and is therefore short lived. TI-2 antigens can induce the production of IgG and IgM antibodies, but only in mature B-cells [41]. The B-cells react to the bacterial capsular antigen and thus this response of importance for our defence

against encapsulated bacteria such as *Haemophilus influenzae*, as these bacteria are able to avoid T cell priming.

1.1.6 T-lymphocytes

1.1.6.1 Maturation in the Thymus

T-cell maturation and TCR (T-cell receptor) rearrangement occurs in the thymus, with T-cell precursors (also known as thymus-settling progenitors (TSPs)). TSPs populate the thymus via entry through the cortical-medullary junction (CMJ) after which they migrate to the sub-cortical-zone [42]. Maturation then ensues with both negative and positive selection steps [43] along with TCR rearrangement. Furthermore expression of particular CD antigens characterise particular stages of T-cell maturation (see figure 1.5)

T cell receptor (TCR) rearrangement occurs in a fashion analogous to that of immunoglobulin rearrangement [44]. The same enzyme systems are used to produce two types of T-cell receptor. TCRs have two forms; TCR $\alpha\beta$ and TCR $\gamma\delta$ [45]. TCR $\alpha\beta$ is predominantly expressed on CD4⁺CD8⁻ or CD4⁻CD8⁺ lymphocytes, whilst TCR $\gamma\delta$ is expressed on CD4⁻CD8⁻ T cells? [46]. As with B-cells, the TCRs incorporate different V, D and J genes to develop a diverse receptor repertoire [45]. TCR $\alpha\beta$ s form approximately 90% of the TCR repertoire with TCR $\gamma\delta$ making up the final 10%. TCRs are associated with particular anatomical localisations with TCR $\alpha\beta$ located predominantly in the secondary lymphoid organs, and TCR $\gamma\delta$ s in epithelial tissues, enabling earlier and more general responses to foreign antigens [47]. In contrast to B-cells, these receptors recognise short antigen peptide sequences expressed by antigen presenting cells in combination with class I or II MHC molecules [34].

Positive selection occurs within the cortex, where cells bearing TCRs able to bind MHC class I or II molecules have a survival advantage over the others which die 'by neglect' [48]. MHC class I binding cells develop into CD8⁺ T cells whilst MHC class II binding cells become CD4⁺ T-cells. Negative selection steps follow in the medulla where T-cells having high affinity for self-antigens are induced to undergo apoptosis, reducing the risk of autoimmunity. The antigen naïve T cells then egress into the peripheral circulation (see figure 1.5).

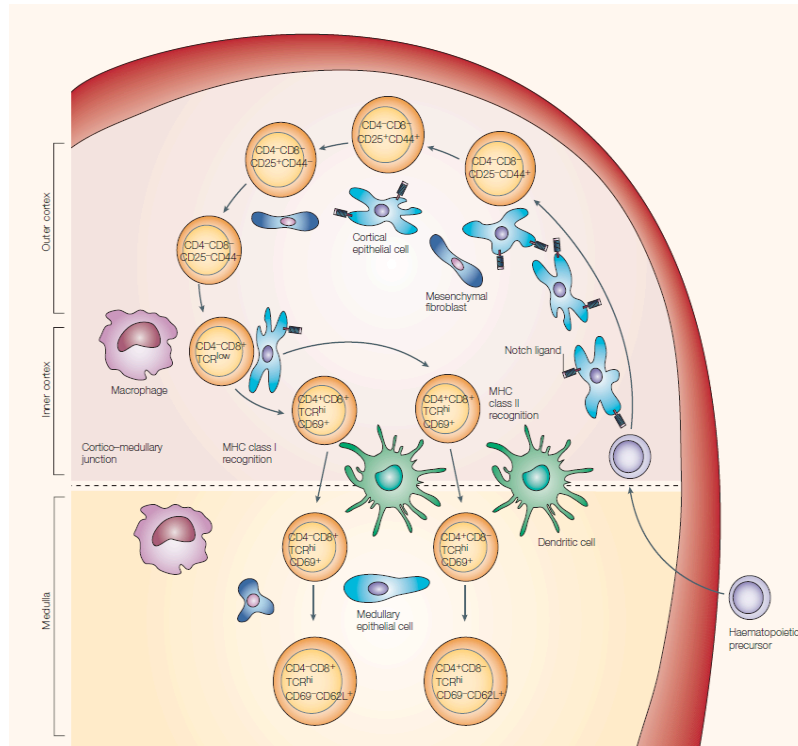


Figure 1.5: Steps of T-cell maturation within the thymus. (Taken from Zúñiga-Pflücker, 2004 [49])

1.1.6.2 Innocence to experience: Meeting of the Naïve T-cell and Antigen

T-cell activation and subsequent initiation of immune response requires interaction between the T-cell and its antigen via presentation on antigen presenting cells (APCs) such as dendritic cells or macrophages. The probability of these low frequency cell types meeting is increased by firstly, continuous migration of naïve T-cells between and within lymph nodes ‘searching’ for foreign antigens [50]. Lymphocytes traffic between the lymph nodes via blood and lymphatic vessels finally entering the lymph nodes via the high endothelial venules (HEV) mediated by L-selectin [51] in combination with chemokines and their receptors. During intra-lymph node migration T- cells transiently bind to numerous APCs postulated to be guided by chemokine gradients. Secondly, dendritic cells that have taken up antigen from infected tissue are stimulated to migrate to draining lymph nodes [52] via up regulation of lymphoid homing chemokine receptors such as CCR7 [53]. Once a T-cell has had contact with an APC bearing its antigen, activation takes place over 48-72 hours.

1.1.6.3 Antigen Processing and the MHC Molecules

Antigenic peptides are processed and presented with major histocompatibility complex (MHC) molecules and is a prerequisite for T-cell activation. MHC molecules fall into 2 classes. Intracellular antigens cut into short peptides within the cytosol of APCs are subsequently bound and presented with MHC class I molecules [54], which can then be recognised for targeting by cytotoxic T-cells. Extracellular antigens taken in via endocytic pathways are processed by APCs including dendritic cells, B-cells and macrophages, and subsequently this antigen is processed and re-expressed with MHC class II molecules [55]. Under normal circumstances MHC class II expression is restricted to APCs.

1.1.6.4 Antigen Recognition by T-cells

CD4⁺ and CD8⁺ have differing functions, and so the MHC molecule used to present an antigen determines the effector response generated [56]. MHC class I molecules are expressed on all nucleated cells highlighting the fact that many cells can be infected with viruses or express abnormal tumour peptides [34]. MHC class I-antigen complexes are open to highly targeted attack by CD8⁺ cytotoxic T-cells [57]. In contrast CD4 activation is regulated by limited expression of MHC class II molecules expressed by APCs [34] helping to limit CD4 effector responses which entails the release of cytokines leading to subsequent activation of surrounding cells. Inappropriate antigen presentation or effector cell attack is limited as TCR binding to the antigen-MHC complex alone is insufficient to induce cellular activation; stimulation with co-receptors is also required.

1.1.6.5 T-cell Receptor Signalling

TCRs are complexed with CD3 molecules [58]. Following antigen binding, receptor aggregation occurs, resulting in signal transduction and ultimately gene activation and T-cell proliferation [14]. Additional co-receptors participate in signal activation following TCR engagement. CD28 is a major stimulatory molecule [59] which, binds to CD80. Other major co-stimulatory molecules include CD86 which binds CTLA-4 [60] and CD40 which binds CD40L [48]. These molecules are found in large numbers on dendritic cells, with expression up regulation after stimulation [60], so dendritic cells are the most potent stimulators of naïve T-cells. Following activation; division and clonal expansion occurs [14]; the majority of these are effector cells, although memory T-cells are also produced. Up regulation of organ specific homing receptors in diseased tissues aids homing of activated T-cells, via responses to molecules released from these sites. Long-lived memory cells can then reside in these tissues, thereby eliciting a rapid immune response if the same

foreign antigen/MHC combination is encountered again. These cells can reside in tissues for as long as ten years.

1.1.6.6 T cell Sub-sets

T helper (Th) cells characteristically express CD4 and include Th1, Th2, Th-17 and T follicular helper cells (T_{FH}). Th1 cells mediate cell dependent immune responses through the release of cytokines such as IL-2 and IFN γ ? [61], leading to T-cell proliferation, cytotoxic T-cell activation, and stimulation of macrophages and NK-cells. Therefore Th1 cells are critical for responses against intracellular pathogens. These cytokines also provide a positive feedback loop by stimulating differentiation of Th0 cells to Th1, whilst simultaneously blocking Th2 differentiation [62]. In contrast Th2 cells mediate antibody responses and are a central defence against extracellular pathogens, particularly parasites [62]. Th2 cells release a variety of cytokines including IL4, IL5, IL6 and IL10 which, favour antibody production. IL-4 directly induces IgE production [63], whilst IL-5 promotes eosinophil development. As with Th1 cells a positive feedback loop occurs with IL-4 stimulating differentiation to Th2 cells whilst simultaneously suppressing Th1 development.

Th-17 cells are characterised by secretion of IL-17, and their development is suppressed by cytokines produced by Th1 and Th2 cells, demonstrating that they are a separate Th subset. They appear to have a role in both inflammatory and antibody mediated responses [64].

T_{FH} cells provide assistance for immunoglobulin production by B-cells within the germinal centre. These cells are characterised by CXCR5 expression, and facilitate migration to CXCL13 rich germinal centres, and thus interaction with germinal centre B-cells [65, 66]. Additionally, high expression of co-stimulatory molecules such as CD40L on T_{FH} cells highlights their role in providing cognate assistance to B-cells within the germinal centres [67].

Cytotoxic, CD8+, T cells (T_c) are directly cytotoxic to specific antigen bearing cells. As they recognise MHC class I associated peptides, they have a major role in the control of intracellular pathogens [57]. Following antigen binding these cells kill in one of three ways. Firstly, by releasing cytokines such as IFN γ and TNF α ?? IFN γ causes up regulation of antigen and Fas expression on cell surfaces thereby enhancing targeted cell lysis. TNF α engages with target cell receptors and induces apoptosis directly? [68]. The other

mechanisms involve direct cell-cell contact, including mediation by FasL on the Tc cell surface binding to Fas receptor (CD95) on the target cells triggering apoptosis [69]. The second cell-cell mediated mechanism involves the release of highly toxic, pre-synthesised, secretory lysosomes containing perforin and granzymes which, interact with the target cell and cause cell death [70, 71]. As with Th cells, Tc are subdivided according to the cytokine profile they release with Tc1 cells releasing IFN γ , TNF α and IL-2 and Tc2 cells releasing IL-4, IL-5 and IL-10 [72]. However, the exact role for these two subsets is not as clear as with Th cells. CD8+ cytotoxic cells are predominantly involved in antiviral and probably anti-tumour activity.

T regulatory (Treg) cells play a role in the control of the immune system by silencing self-reactive T-cells [73], thereby reducing autoimmunity. Differing subsets of Tregs have been described based upon their cell surface expression, cytokine production profiles and postulated mechanisms of action, these include CD4+CD25+FOXP3+ and CD4+CD25-FOXP3+ cells producing either IL-10 or TGF β (tissue growth factor β) and mediating cytokine or cell-cell contact mediated effects [73]. The mechanisms of suppression by these cells have not been fully elucidated. However binding of Treg and T effector cells with CTLA-4 has been shown to mediate ligation of CD80/CD86 inducing suppressive signals [74], and reduce both proliferation and IFN γ production [75]. Another possible mechanism is that of simple competition between Treg and T effector cells for APCs and survival signals [76]. The role of these cells in immunosurveillance and the pathogenesis of autoimmune disease and malignancies are becoming clearer.

1.1.7 Regulation of Autoimmune Responses

As has been described, lymphocytes with affinity for self-antigens do arise through the mechanisms required for formation B and T-cell receptors formation. Yet, a number of mechanisms are in place to reduce the proliferation of these lymphocytes and the subsequent autoimmunity that would result. These include positive and negative selection in the thymus, the positive selection of B-cells in the bone marrow environment, and the anergy and apoptosis of lymphocytes in the periphery due to the lack of co-stimulatory molecule activation. Yet, of course some of these cells do escape these quality control processes leading to the development of autoimmune diseases.

1.1.8 Interactions Within and Outside of the Immune System

Understandably, research into immune based therapies for a wide range of disorders has been a major focus of research groups and pharmaceutical companies. This has led to the development of many products in clinical use today. Examples include the use of cytokines and their antagonists, monoclonal antibodies, cellular therapies and therapeutic vaccinations. It should be noted though that immune reactions are complex and changes in one part of the system can lead to unforeseen changes in others. This has been highlighted with the use of CD28 agonists in early clinical trials and the unforeseen consequence of multi-organ failure occurring in study participants [77]. Despite this, it is clear that there is a huge therapeutic potential to be gained from further understanding of the immune system.

1.2 Chemokines and their Receptors

In the previous section gave a basic overview of the immune system. Chemokines form an integral part of the immune system, and are studied in this thesis. In this section an overview of the chemokine system will be discussed, along with a more detailed discussion of the role of chemokines in the adaptive immune system.

1.2.1 Historical Perspective

Chemokines are a group of small (~8-14kDa) structurally related peptides [78]. These peptides primarily perform as chemoattractants, thereby explaining the derivation of their name; CHEMOattractant cytoKINES. To date over 40 chemokines have been discovered since the first one; CXCL4/PF4 was described in 1977 [79]. Initially, the chemokines were shown to be clearly associated with inflammatory conditions, leading to the conclusion that, they played an integral role in the recruitment of leucocytes to sites of inflammation. Subsequently, it was shown that chemokines also displayed a distinct and conserved structural homology as well as having potent chemotactic effects on leucocytes. However, chemokines are also able to influence various other aspects of cell function, such as adhesion, proliferation, maturation, differentiation, apoptosis, replication, and malignant transformation. Therefore since 1977 research into chemokines and their receptors have implicated them in the pathophysiology of many disease processes including infection, autoimmune disease and cancer. Of most interest, perhaps, is the discovery that 2 chemokine receptors, CXCR4 [80] and CCR5 [81] act as co-receptors for HIV entry into cells. Soon after a population of individuals that carry a mutation in CCR5 (CCR5 Δ 32) were indentified, which in the homozygous state renders the individual resistant to HIV infection and in the heterozygous state less likely to develop AIDS [82, 83]. Consequently, an antagonist to CCR5, Maraviroc has been developed and shows efficacy in reducing HIV viral loads in infected individuals [84]. Other agents targeting the chemokine system are now in clinical use or in clinical trials and will be discussed in more detail later.

1.2.2 Nomenclature and Structural Classification of Chemokines

Initially the names of chemokines highlighted the function for which they were first discovered, e.g. MIP1 α or monocyte inflammatory protein 1 α . However it has become clear that individual chemokines have a number of functions and so, to avoid confusion an international system of nomenclature has been introduced based upon their structural classification. Chemokines can be divided into four families according to the arrangement

of the first two cysteine residues at the N-terminus of the molecule. The two major families are CXC (or alpha) and CC (or beta) depending upon the presence or absence of an intervening amino acid between these first two cysteine residues (Figure 1.4). Two other groups include the C (lymphotactin and SCM-1) and CX₃C (fractalkine) chemokines, the first lacks two of the first three cysteine residues and the second has three amino acids between the first two cysteine residues.

Chemokines are named according to the order in which their gene was characterised and by their cysteine motif. So, MIP-1 α becomes CCL3 and IL-8 becomes CXCL8 and so on. At present this nomenclature accounts for 43 human chemokines [78]. In this thesis the international nomenclature will be used. Chemokine cell signalling is mediated through seven-transmembrane G protein-coupled receptors (GPCRs). These receptors are expressed on a number of different cell types, but are predominantly expressed on cells of the haematopoietic system. The international system of nomenclature is also used for the chemokine receptors where L is replaced by R, e.g. CXCR4, CCR5 etc. Table 1.2 and 1.3 demonstrates the chemokines and their receptors known at the present time (it excludes the atypical chemokine receptors which will be briefly discussed later).

However, the chemokine system is not straightforward with different chemokines being able to bind to more than one receptor and with most receptors having more than one ligand. This apparent 'redundancy' in the system reflects subtlety and intricacy, which we are only just beginning to understand.

Characteristic chemokine conformation results from interactions between the cysteine residues, via disulphide bonds [85]. The bonds form between the 1st and 3rd and the 2nd and 4th residues, numbered according to their position in the peptide sequence. The first 2 cysteine residues are located together (with or without intervening amino acids) at the N-terminus, the 3rd is found central to the molecule and the fourth close to the C-terminus. An understanding of the structure of chemokines is essential in the understanding of their function and ultimately in the development of agents to act either as agonists or antagonists.

<i>SYSTEMATIC NAME</i>	<i>COMMON NAME</i>	<i>RECEPTORS</i>
<i>CCL1</i>	I-309	CCR8
<i>CCL2</i>	MCP-1	CCR1, 2
<i>CCL3</i>	MIP-1 α	CCR1, 5
<i>CCL4</i>	MIP-1 β	CCR1, 5, 8
<i>CCL5</i>	RANTES	CCR1, 3, 5
<i>CCL7</i>	MCP-3	CCR1, 2, 3, 5
<i>CCL8</i>	MCP-2	CCR1, 2, 3, 5
<i>CCL11</i>	Eotaxin	CCR2, 3, 5
<i>CCL13</i>	MCP-4	CCR1, 2, 3, 5
<i>CCL14</i>	HCC-1	CCR1, 5
<i>CCL15</i>	MIP-1 δ	CCR1, 3
<i>CCL16</i>	HCC-4	CCR1, 2, 5
<i>CCL17</i>	TARC	CCR4, 8
<i>CCL18</i>	PARC	CCR3
<i>CCL19</i>	MIP-3 β /ELC	CCR7
<i>CCL20</i>	MIP-3 α	CCR6
<i>CCL21</i>	6Ckine/SLC	CCR7
<i>CCL22</i>	MDC	CCR4
<i>CCL23</i>	MPIF-1	CCR1
<i>CCL24</i>	Eotaxin-2	CCR3
<i>CCL25</i>	TECK	CCR9
<i>CCL26</i>	Eotaxin-3	CCR2, 3
<i>CCL27</i>	CTACK	CCR10
<i>CCL28</i>		CCR3, 10

Table 1.2: Overview of the CC chemokines and their cognate receptors.

<i>SYSTEMATIC NAME</i>	<i>COMMON NAME</i>	<i>RECEPTORS</i>
<i>CXCL1</i>	GRO α	CXCR2
<i>CXCL2</i>	GRO β	CXCR2
<i>CXCL3</i>	GRO γ	CXCR2
<i>CXCL4</i>	PF4	CXCR3
<i>CXCL5</i>	ENA-78	CXCR1, 2
<i>CXCL6</i>	GCP-2	CXCR1, 2
<i>CXCL7</i>	NAP-2	CXCR2
<i>CXCL8</i>	IL-8	CXCR1, 2
<i>CXCL9</i>	MIG	CXCR3
<i>CXCL10</i>	1P-10	CXCR3
<i>CXCL11</i>	I-TAC	CXCR3, CXCR7
<i>CXCL12</i>	SDF-1	CXCR4, CXCR7
<i>CXCL13</i>	BCA-1	CXCR5
<i>CXCL14</i>	BRAK	
<i>CXCL16</i>		CXCR6
<i><u>XC Chemokines</u></i>		
<i>XCL1</i>	Lymphotactin	XCR1
<i>XCL2</i>	SCM-1 β	XCR1
<i>CX₃CL1</i>	Fractalkine	CX ₃ CR1

Table 1.3: Overview of the CXC, XC and CX₃C chemokines and their cognate receptors.

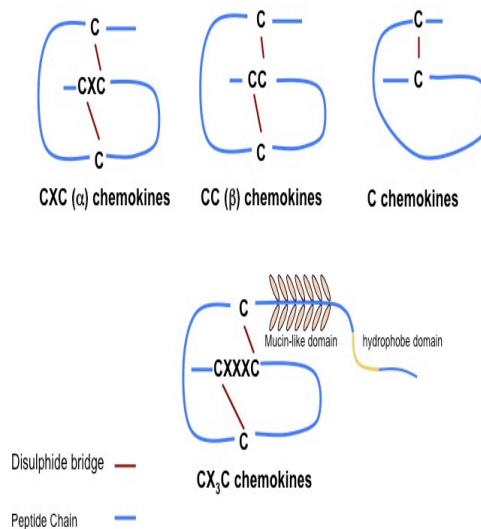


Figure 1.6: Positioning of the cysteine residues in the different structural classes of chemokines.

1.2.3 Functional Classification of Chemokines

Chemokines can be broadly classified, according to their function, into inflammatory (inducible) and constitutive (homeostatic) chemokines. This classification of chemokines highlights the integral role they play in the organisation of the immune response.

Chemokines control the directed migration of leukocytes. Under homeostatic conditions this is controlled by the constitutive chemokines through interaction with specific receptors on the cell surfaces. Furthermore, a number of constitutive chemokine receptors display compartmentalisation in their expression. For example CCR7 expression is limited to T-lymphocytes, subsets of B-cells and mature dendritic cells. In contrast CXCR4 is widely expressed and found on haematopoietic stem cells, thymocytes, B and T-cells, dendritic cells, some endothelial cells and neutrophils [86].

In contrast, inflammatory chemokine receptors such as CCR1, CCR2, CCR3, CCR5 and CXCR2 are up-regulated and responding to the corresponding up regulation of ligands expressed within damaged tissues. These receptors and their ligands are also up-regulated in chronic inflammatory diseases such as rheumatoid arthritis, inflammatory bowel disease and multiple sclerosis [87].

Under homeostatic conditions chemokines have an integral role in the organisation of the immune system. However it is worth reflecting on the differences between these two

groups of chemokines in terms of the overall impact on the immune system. Constitutive chemokines are expressed at much lower levels than the inflammatory chemokines (when induced), yet, disruption of these chemokines have more profound affects. This is demonstrated in knock-out mice, for example deletion of CCR7 leads to a severe disruption of the secondary lymphoid organs both structurally and functionally [88]. In contrast mice with deletions of the inflammatory receptors such as CCR3 have a surprisingly normal phenotype under normal circumstances, and only display a phenotype under certain inflammatory conditions [89].

Not surprisingly, chemokines have been shown to play a significant role in the pathogenesis of a number of diseases including asthma, HIV infection, autoimmune conditions and malignancy.

1.2.4 N-terminal Domain of Chemokines

The N-terminal domain of chemokines is required for receptor mediated signalling as initially established by using CCL2 analogues with differing N-terminal amino acids [90]. N-terminus truncated forms of CCL2, demonstrate binding affinity with its receptor but does not result in chemotaxis [91]. Additionally, variations in the N-terminal domain can lead to varying biological affects, for example the presence of the glutamic acid-leucine-arginine (ELR) motif on CXC chemokines (CXCL8, CXCL5 and CXCL1-3) is associated with angiogenesis, whereas those lacking the ELR motif (CXCL9-11, CXCL4 and CXCL13) are angiostatic [92]. One notable exception to this rule is CXCL12, which, while lacking the ELR, motif appears to be angiogenic [93]. Additional receptor binding sites are present on chemokines including the N-loop between the first 2 cysteines and the 3₁₀ helix [85].

1.2.5 Chemokine Regulation

Chemokine secretion and function is regulated in a number of ways including oligomerisation, heterodimerisation, interaction with glycosaminoglycans (GAGs) and post-translation control. The latter two mechanisms will be discussed briefly.

1.2.5.1 Regulation by Glycosaminoglycans

GAGs are carbohydrate structures presented on the surface of most cells [85]. Chemokine gradients facilitate directed migration of leukocytes. *In vivo* this is dependent on binding of chemokines to GAGs on endothelial cell surfaces [94]. Interaction between endothelial cells (ECs) and GAGs enables chemokines to be presented to circulating blood cells

without being removed by blood flow; thus facilitating leukocyte adhesion to vessel walls. GAGs are classified in a number of families including the heparans, based upon length and disaccharide units, and it appears that these families display differing chemokine affinities and vice versa. For example the affinity of CXCL8 for a particular sub-fraction of heparin is not demonstrated by either CXCL4 or CXCL7 [95]. Cellular bound and soluble GAG/chemokine complexes act differently, with the former enabling concentration of chemokines at a particular location thereby triggering the cognate chemokine receptor whilst, soluble GAG/chemokine complexes have an inhibitory effect [96].

1.2.5.2 Post-translational Control

Alterations in the N-terminal sequence of chemokines can affect its biological function. This occurs naturally *in vivo* via proteases such as CD26 and matrix metalloproteinases (MMPs), which truncate the N-terminal domain of post-translational secretory chemokines [85]. Truncated chemokines differ functionally from their full-length counterparts in signalling ability, receptor specificity and receptor affinity. For example CD26 cleavage of full length CCL4 leads to a truncated product which, retains the ability to down-regulate cell surface expression of CCR5 and block HIV-1 entry into cells, whilst gaining the ability to bind to CCR1 and CCR2b [97, 98]. In a situation analogous to GAG affinity, chemokine affinity as substrates for different MMPs has also been noted. Thus post-terminal truncation of the N-terminal domain adds another level to the increasingly complex *in vivo* regulation of chemokines.

1.2.6 Chemokine Receptors

To date more than 20 chemokine receptors have been described with all but 4 (DARC, D6, CXCR7 and CCX-CKR) initiating intracellular signalling events following binding with their ligands. Chemokine receptors form a group within the 7 transmembrane spanning G-protein coupled receptor family. Helical transmembrane regions are linked by 3 extracellular loops and 3 intracellular loops, with the N-terminal end positioned extracellularly and the C-terminal end intracellularly. Signalling through chemokine receptors is largely due to a DRYLAIVHA (or variation thereof) motif, located on the second intracellular loop. The role of this motif is highlighted by the fact that it is lacking in atypical, non-signalling, receptors [85]. Yet, it should be noted that, to date, the structure of chemokines is speculative, based upon presumed chemokine receptor binding sites on chemokines and on elucidated crystal structures of other GPCRs such as rhodopsin [99]. Mutagenesis studies have helped to determine receptor ligand binding sites. It has been demonstrated that binding sites in the N-terminal domain of chemokines enables correct

orientation of ligand within its receptor allowing for interaction with residues within the transmembranous helices [100]. Further binding sites are present on other extracellular loops (ECLs), offering further assistance in correct orientation of the ligand [100, 101]. Additionally, some receptors are glycosylated or tyrosine sulphated and show greater affinity for their cognate ligands [85].

1.2.6.1 Receptor Activation and Guanine Nucleotide Binding Proteins

Following ligand binding, conformational changes in the receptor occur enabling tyrosine phosphorylation within the DRYLAIVHA motif (figure 1.7). This leads to activation of the guanine nucleotide-binding (G protein) pathway via interaction of G-protein subunits with components of the DRYLAIVHA motif [102]. Usually, this involves activation of the $G\alpha_i$ protein, indicated by interruption of downstream signalling following exposure to, the $G\alpha_i$ inhibitor, *pertussis* toxin, in numerous chemokine/receptor interactions including CXCL8/CXCR1 [103]. The $G\alpha_i$ subunit contains inactive GDP and forms a heterotrimeric structure with $G\beta$ and $G\gamma$ subunits. Following activation, GDP is replaced by GTP, leading to, dissociation of the $G\alpha_i$ subunit from the $G\beta\gamma$ subunit, the latter then activates a number of downstream signalling pathways [104]. However, whilst this is the classical paradigm of G protein chemokine mediated signalling, other G proteins have also been implicated, for example $G\alpha_q$ proteins have been identified to induce signalling in granulocytes [105]. $G\alpha_i$ acts as a GTPase leading to gradual hydrolysis of GTP to GDP, which, in turn leads to re-association of the G protein subunits and quenching of signalling responses. This is facilitated by a family of GTPase activating proteins (GAP) known as regulators of G protein signalling (RGS) that inhibit G protein signalling by increasing the rate of GTP hydrolysis [106, 107], thus having a regulatory role in G protein mediated activities.

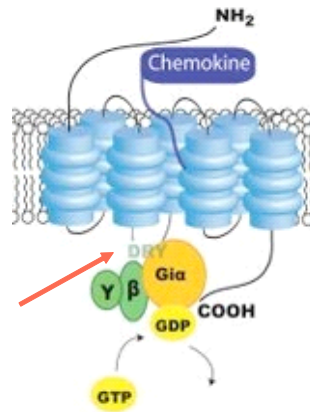


Figure 1.7: Outline of the 7 transmembrane structure of the chemokine receptor, demonstrating the N-terminus binding with the chemokine and the C-terminus activation following binding of the DRY motif (red arrow) with the G-protein complex.

1.2.6.2 Signalling Pathways and Intracellular Control of Migration

Chemokine induced signal transduction is implicated in numerous cellular functions such as growth, proliferation, adhesion and apoptosis (Figure 1.6). However, a complete exploration of these pathways is beyond the scope of this discussion, and will be limited to those involved in the control of chemotaxis.

Numerous signalling pathways have been shown to be required for chemotaxis foremost amongst these are those transduced by the phosphoinositide-3 kinases (PI3K), however, pathways will vary depending upon the cellular context and receptor ligand interaction. In brief, following ligand binding, PI3Ks are rapidly activated leading to generation of phosphatidylinositol-3,4,5-triphosphate (PIP₃), these molecules translocate to the leading edge of the cells, where Rac (part of the Rho family of GTPases), induces polymerization of actin within the leading edge. This pathway is the predominant mechanism for chemotaxis within neutrophils, but is not essential for lymphocyte migration. In lymphocytes a protein DOCK2 instead of PI3Ks is essential for lymphocyte migration. DOCK2 is a haematopoietic-specific protein which has been shown to be important for chemokine induced activation of Rac and actin polymerisation, with DOCK2^{-/-} mice displaying impaired chemokine induced B and T-lymphocyte migration and atrophied lymphoid follicles [108].

The trailing edge of the cell undergoes independent morphological changes. It is unclear how this occurs in lymphocytes, but in other leucocytes, this is mediated through Rho

activation via an alternative G protein subunit; $G\alpha_{12/13}$ [109]. Rho localises to the trailing edge, inducing retraction of this through formation of actin/myosin complexes.

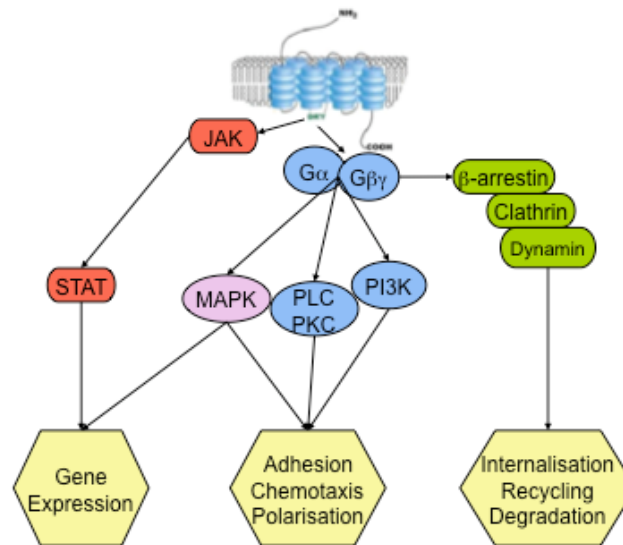


Figure 1.8: Outline of major signalling pathways activated following receptor activation and their outcome on cellular function.

1.2.6.3 Desensitisation, Internalisation and Recycling of Receptors

Following ligand binding and receptor activation, mechanisms are in place to prevent further unwarranted downstream signalling. Once activated GPCRs, undergo phosphorylation of serine and threonine residues on the C terminus [110]. This leads to steric hindrance to G protein binding and increased affinity for a group of cytosolic proteins, the β -arrestins. Binding of GPCRs to β -arrestin leads to further inhibition of steric binding. These actions effectively block further G protein mediated signalling, leading to receptor desensitisation.

Clathrin mediated endocytosis is the most frequently observed mechanism for chemokine receptor internalisation. Other mechanisms have been observed, but, in this thesis, discussion will be restricted to clathrin-mediated mechanisms as these have significance for adenoviral uptake, discussed later in section 1.5.

β -arrestins mediate receptor internalisation, by providing a link between the desensitised receptor complex and internalisation (endocytic) machinery. β -arrestin binds directly to

clathrin via a Leu-Xaa-Glu/Asp binding motif [111] whilst also, interacting with the β 2-adaptin subunit of a clathrin adaptor protein (AP2) [112]. The clathrin terminal domain orientated towards the plasma membrane, thought to act as an anchor for arrestins and AP2, facilitates recruitment of the receptor complex into clathrin-coated pits [111]. Coated pits form a bud via pinching of the plasma membrane with assistance of dynamin [113]. The buds are then released into the cytoplasm as clathrin-coated vesicles.

Once internalised, the receptor is distributed to various intracellular sites guided by one of the Rab GTPases. Rab GTPases cycle between active and inactive forms [114, 115]. Different members of the Rab family appear to have specific functions within the cell. Rab5 promotes fusion with early endosomes assisting in regulating internalisation. Rab5 dominant-negative mutants have been shown to inhibit or reduce CXCR2, CCR5 and CXCR4 internalisation [116, 117]. Rab4 and Rab11a are involved in rapid and slow receptor recycling respectively [117]. Re-sensitisation occurs during recycling, enabling re-establishment of functioning cell surface chemokine receptors.

Finally, receptor degradation occurs with some chemokine receptors following prolonged exposure to ligands, by localisation to lysosomes, mediated by Rab7 and Rab9. Degradation of both CXCR2 and CXCR4 in association with Rab7 has been observed, although not all chemokine receptors are degraded including CCR7, which undergoes recycling [118].

The fate of the chemokine itself varies and is not always clear, in most studies, degradation following uncoupling with the receptor occurs within lysosomes. Yet, this is not always the case as seen with CCL21 where binding does not appear to elicit CCR7 internalisation [119]. In other instances modified chemokines such as AOP-CCL5 have been shown to recycle back to the plasma membrane following CCR5 associated internalisation [120]. The mechanisms described above are complex, and the fate of the receptor depends not only on the ligand bound but also on the cellular context, with a number of other controlling factors yet to be determined.

1.2.6.4 Decoy Receptors

To date four decoy receptors; the Duffy antigen receptor for chemokines (DARC), D6, CXCR7 and CXC-CKR have been discovered. These receptors bind chemokines with high affinity, but differ from 'typical' chemokine receptors in a number of aspects. Firstly, neither G-protein coupled signal transduction nor Ca^{2+} fluxes have been noted following

ligand binding to these receptors [121, 122]. This relates to an absence of the DRY motif on the second intracellular loop that is required for signal transduction [123]. Decoy receptors are proposed to function by modulating immune inflammatory responses through scavenging chemokines from the microenvironment in inflamed tissues. This leads to dampening of inflammation as shown in D6 knock out mice, which demonstrate an exaggerated cutaneous inflammatory response compared to wild type mice [124]. The ability of the decoy receptor to reduce inflammatory responses may have other impacts such as reduced metastatic spread in carcinomas [125]. Additionally, membrane surface expression of these decoy receptors is not down-regulated following prolonged exposure to ligands. Instead, as has been shown with D6 (inflammatory CC chemokines) and CXCR (CCL19, 21 and 25), these receptors constitutively bind, internalise and then deliver the chemokine to lysosomes for degradation, prior to recycling to the surface [126, 127]. There is also wider expression of these receptors on non-leukocyte cells than with 'typical' chemokine receptors. These various aspects support the role of decoy receptors as control mechanisms for inflammatory responses and the potential role of these in the pathogenesis of cancer and other conditions.

1.2.7 Chemokines and Organisation of the Immune System

Chemokines have a central role in effective functioning of both the innate and adaptive immune systems. Post capillary venules express different chemokine and integrin combinations depending on their tissue location. Whilst they control the trafficking of all leukocytes, this discussion will focus predominantly on lymphocyte development and trafficking, as an understanding of this is central to later discussions regarding lymphoma biology.

1.2.7.1 Chemokine Control of Lymphocyte Trafficking

In the adult, primary lymphoid organs consist of the bone marrow and thymus. These are the sites of lymphocyte production and chemokine receptor expression of the lymphocyte precursors and particular chemokine expression profiles lead to clearly defined microenvironments within these organs.

The multi-step paradigm is thought to explain the process of adhesion and activation of leucocytes to tissues across high endothelial venules (HEV)[128]. Initially tethering and rolling of cells across endothelial surface occurs via transient interactions between selectins on cell surfaces and carbohydrate ligands or integrins. This enables the leukocyte to sample the endothelial surface for signals, such as chemokines, which trigger endothelial

adhesion and leukocyte arrest via integrin activation. Chemokines then direct the adherent cell to migrate trans-endothelially into extra-vascular tissues. The exact mechanism by which cells transmigrate through the endothelial lining is not entirely clear, but it has been shown continuous shear forces promote transmigration without the need for chemokine gradients [129]. From here the cell can migrate further through a series of chemokine gradients to target tissues. This process is diagrammatically represented in figure 1.7.

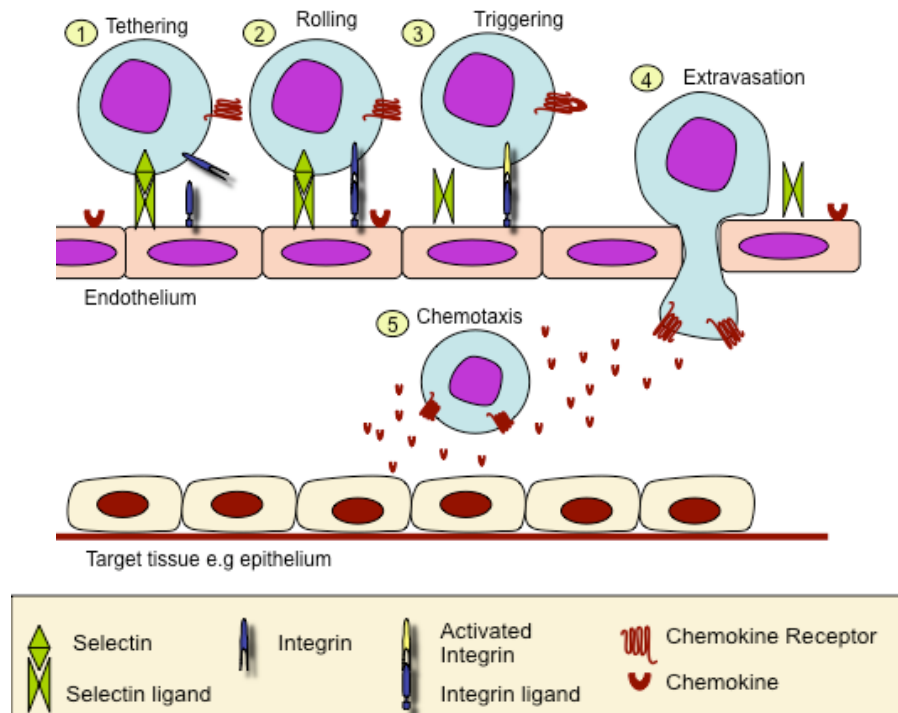


Figure 1.9: Multistep paradigm of leukocyte adhesion and activation. Cells are initially transiently tethered by selectins on endothelial surfaces. This enables leukocytes to sample the endothelial surface for signals such as chemokines, which if encountered leads to adhesion on the endothelial surface via activation of integrins. Trans-endothelial migration of the adherent cell into extra-vascular tissues is then directed by chemokines.

1.2.8 T Lymphocyte Development in the Thymus

Pre-thymocytes enter the thymus via the cortico-medullary junction (CMJ). The first step in maturation requires CCR7 induction of migration of $CD4^+CD8^-CD117^+$ or double negative 1/2 (DN1/2) thymocytes to the sub-cortical zone (SCZ). Disruption of the CCR/CCL19/CCL21 axis results in failure of this process with accumulation of DN1/2 cells at the CMJ and a reduction in more mature, $CD4^+CD8^-CD117^-$ (DN3/4) cells [130]. During positive selection CCR7 expression is up regulated, enabling the $CD4^+CD8^+$ (double positive (DP)) cells to undergo guided migration into the medulla, where final maturation to single positive (SP) cells occurs [131].

Thymocyte migration of thymocytes to the cortex depends upon CXCR4 expression. CXCR4^{-/-} precursors do not develop beyond the DN1 stage and tend to accumulate within the CMJ rather than migrating to the SCZ [132]. Failure to develop is probably due to lack of pro-survival signals in the CMJ compared to those the SCZ such as IL-7 [133]. Whilst, immature CCR9⁺ thymocytes usually accumulate within the SCZ, CCR9 directed homing might not be essential for thymocyte development. CCR9^{-/-} thymocytes appear randomly distributed throughout the thymic cortex, but despite this abnormal localisation, maturation to SP cells appears to be intact [134]. CCR4 also assists in migration of T-cells following positive selection. CCL17 and CCL22 are produced by CD30L⁺ medullary cells, and thus guide “transitional” thymocytes into the medulla as CCR4 expression is increased [135]. However, CCR4 appears to be complementary rather than essential for thymic development with grossly normal thymus development in CCR4^{-/-} mice [136].

Once development is complete, the positively/negatively selected SP cells up-regulate CCR7. CCR7 and CCL19, together with sphingosine-1-phosphate₁ (S1P₁), then enable migration of these naïve T-cells in to the circulation [137]. A summary of the position, site and receptor expression of thymocytes and different developmental stages, is shown in figure 1.8.

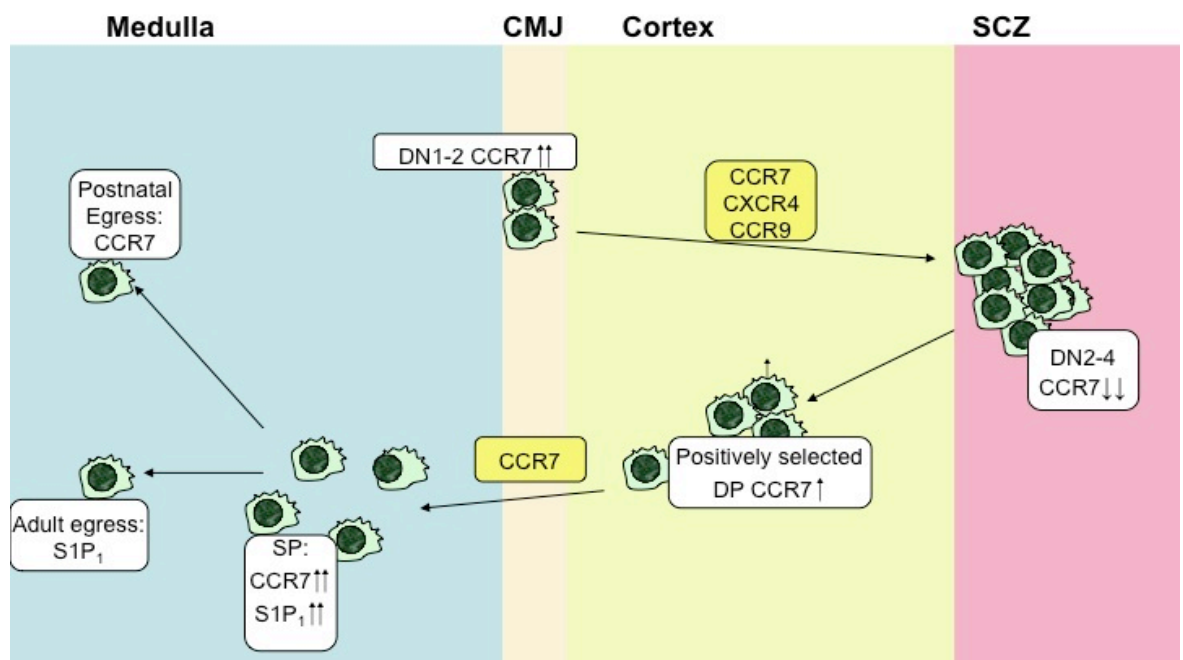


Figure 1.10: Positioning of thymocytes within the thymus and chemokine receptor expression at different developmental stages. [adapted from Stein, 2005 (138)]

1.2.9 Chemokines during B cell Development

In adults B-cells are produced by and develop within the bone marrow under normal conditions. B-cell precursors express a variety of receptors at different stages, the most important of which besides the chemokine receptors are shown in table 1.1. Chemokines and their receptors are essential for the development of the B-cell compartment. CXCR4 plays the most central role in B-cell maturation with lack of CXCR4 or CXCL12 resulting in severely impaired B-cell development and has been shown to be essential at the earliest stages of B-cell development within the foetal liver [139]. Retention of B-cell precursors within the bone marrow microenvironment relies on CXCR4 mediated signals, preventing premature release of these cells into the circulation. Interruption of the CXCR4/CXCR12 axis leads to the mobilisation of myeloid and B-cell precursors into the circulation [140]. However, immature and naïve B-cells are subsequently released appropriately into the circulation despite continuing to express high levels of CXCR12. So, how are the retention signals bypassed with maturation? This appears to be related to integrin expression. Early precursors respond to CXCR4 signals by activating adhesion molecules such as VLA-4, allowing for retention, however as B-cells undergo maturation, activation of adhesion molecules diminishes until eventually adhesion mediated retention is lost [141]. Pro-pre B-cells have also been shown to respond to CCL25, however, unlike CXCR4, CCR9 does not appear to be essential for B-cell maturation. CCR9^{-/-} mice demonstrate reduced numbers of pro-pre B-cells, yet overall B-cell development is only minimally impaired, with a seemingly normal mature B-cell population [142].

As B-cells develop their ability to respond to chemokines predominantly associated with secondary lymphoid organs (CCL19, CCL21 and CXCL13) increases, with initial responsiveness to CCL21 and CCL19. Once the B-cells have egressed into the circulation they home predominantly to the spleen at the T-B cell border. Initially, CXCR5 expression is relatively low, but later increases in response to pro-survival signals from B-cell follicles, promoting migration in to these areas [143].

1.2.10 Homing of Naïve Lymphocytes to Lymph Nodes

Naïve lymphocytes home to secondary lymphoid organs from the circulation. Migration of T-cells into secondary lymphoid organs is predominantly mediated by CCR7. Ligands for CCR7 are presented via endothelial cells on HEVs (CCL21) or on the luminal surface of HEVs following release from stromal cells in the lymph node T-cell areas (CCL19). The importance of CCR7 and its ligands are demonstrated with *plt/plt* (*plt* –paucity of lymph node T-cells) mice in which T-cell migration into and development of secondary lymphoid

organs is severely impaired. *plt/plt* mice have a deletion on chromosome 4 leading to the loss of expression of CCL19 and CCL21 [144] [145]. T_{FH} cells also express CXCR5 enabling their migration into the B- cell rich follicles, providing B-cell help. If the naïve T-lymphocyte does not encounter its cognate antigen in 12 hours, it will re-enter the circulation to restart the process in another lymphoid organ.

B-cell migration into secondary lymphoid organs shows slight differences, in part dependent upon the lymphoid tissue. In peripheral lymph nodes, both CXCR4 and CCR7 are required for integrin activation on B-lymphocytes. Whilst CXCL13 is found in peripheral lymph nodes its role is uncertain, yet homing to Peyer's patches does require CXCL13. The CXCR5/CXCL13 axis is also implicated in homing of B-cells to mesenteric lymph nodes [146]. B-cells also arrest on HEVs associated with B-cell follicles aided by CXCL13 production by follicular dendritic cells. There also appears to be a role for CXCR4 in maintaining B-cells within this area, highlighted by the observation that CXCR4^{-/-} B-cells are not maintained solely within the follicles but can also be detected within the lamina propria [147]. Specialised cells are found within the B-cell follicle. Follicular dendritic cells are able to capture and display antigen on their surface. Again in the event that the B-lymphocyte does not meet its cognate antigen, after 24 hours it is re-released into the circulation.

1.2.11 Migration within and out of Secondary Lymphoid Organs

Intra-vital microscopy has shown that T and B-cells move constantly within their microenvironment thus increasing the chances of them coming into contact with APCs or foreign antigens [148, 149]. These movements appear to be random rather than directed, however in the absence of CCL19/21 and CXCL13 chemokine gradients chemokinesis occurs, indicating that they are likely to be important in the positioning of cells [149]. In the event that the lymphocyte does not encounter its antigen it will leave the lymph node via efferent lymphatic vessels to re-enter the bloodstream. This egress appears to be regulated by shingosine-1-phosphate 1 (S1P₁) receptors rather than chemokine receptors [150].

1.2.12 Tissue Specific Homing of Leukocytes

Specific combinations of adhesion molecules and chemokines provide a system whereby leucocytes are guided to where they are required. Furthermore, the presence of chemokine gradients within tissues provides further specificity to the final stages of leukocyte

migration. These combinations can be easily detected and consequently the specificity for homing to particular tissues can be elucidated.

To clarify this concept further a well described, lymphocyte sub-set will be discussed. Gut-homing lymphocytes express integrin $\alpha_4\beta_7$, that mediates rolling and adhesion to intestinal venules through MAdCAM-1. Furthermore, it has been shown that $\alpha_4\beta_7^{\text{hi}}$ cells have memory for intestinal pathogens [136]. Chemokines play an essential role in further specifying the tissue tropism of these lymphocytes. Out with the thymus, CCL25 is almost exclusively produced by epithelial cells, which are found in crypts of the small intestine. Moreover examination of intestinal lymphocytes reveals that almost all of the T-cells and a majority of B-cells co-express CCR9 and $\alpha_4\beta_7$ [151]. Additionally, CCL25 appears to attract IgA producing plasma cells rather than those producing other immunoglobulin classes. These features therefore strongly suggest that these lymphocytes play a central role in the mucosal humoral immune response of the small intestine. Furthermore, inhibition of CCL25 inhibits migration of antigen-specific CD8⁺ T-cells to the small intestine, strengthening the case for a central role of CCR9/CCL25 interaction in lymphocyte localisation to the small intestine [152].

It should however be noted that not all chemokine receptor pairs have defined tissue-tropism. Many others are broadly expressed in normal and inflamed non-lymphoid tissues, for example CXCR3 and CCR5 are expressed by nearly all tissue infiltrating T cells. These two receptors bind to many different ligands, which are predominantly expressed during inflammation. However, there is a high degree of redundancy in the system as highlighted by the effects of CCR5 deficiency in humans (discussed previously). It should also be noted that these chemokines receptors can not compensate for the loss of any of the tissue specific chemokines receptors. Figure 1.9 provides a summary of the chemokines and their receptors involved in the homing of lymphocytes to specific areas.

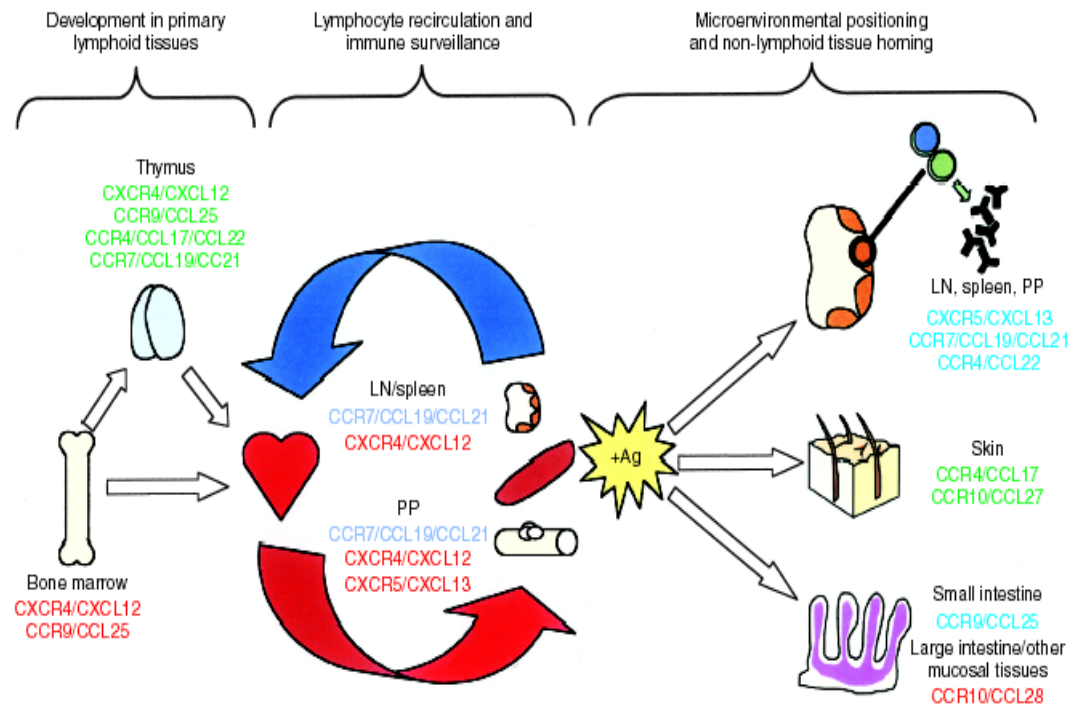


Figure 1.11: Known and proposed functions for constitutive chemokines and their receptors in lymphocyte development, trafficking and function. Taken from, Campbell et al 2003.

How do tissue specific effector and memory cells arise? Lymphocyte precursors isolated from the intestinal or cutaneous lymphatic systems later localise to these areas, suggesting that the site at which the lymphocyte is activated determines its tissue tropism. There is emerging evidence that vitamins have a role in determining tissue tropism. Vitamin D3 produced by sun-exposed DCs has been shown to induce T-cells to up-regulate CCR10 and thus induce skin-tropism, whilst simultaneously down-regulating the gut homing receptors $\alpha_4\beta_7$ and CCR9 [153]. In contrast, retinoic acid produced by mucosal cells in the gut generates gut-homing tropism in T-cells, including Th-17 cells, up-regulating $\alpha_4\beta_7$ and CCR9 [154, 155].

1.2.13 Chemokines and T cell Subsets

1.2.13.1 Memory T cells

Memory T-cells are distinguished by a $CD4^+CD45RO^+$ phenotype [156]. Currently they are classified as either central memory (T_{CM}) or effector memory (T_{EM}) lymphocytes. T_{CM} cells are characterised by high CCR7 and L-selectin expression, thus retaining their ability to home to secondary lymphoid organs. T_{CM} cells provide B-cell help and assist with immunoglobulin class switching [157]. In contrast, T_{EM} cells have low CCR7 and L-

selectin expression and after stimulation produce a range of cytokines and up-regulate the chemokine receptor expression required for migration to the inflamed tissues [157].

However, this division may be over simplistic. CCR7 expression can often be detected on effector cells within inflamed tissues, although as the T_{EM} cells migrate to more peripheral tissues, CCR7 expression tends to become down-regulated [158]. Yet, CCL19 and CCL21 are often presented on the post capillary venules under certain inflammatory conditions [159], and the presence of CCR7⁺ T_{EM} cells may reflect their homing capacity under these circumstances. Additionally, T_{CM} cells have been detected out with secondary lymphoid organs [160].

These findings demonstrate a number of points. Firstly, CCL19 and CCL21 can act as both inflammatory and homeostatic chemokines. Secondly, it reiterates the point that chemokine expression alone is not sufficient to determine the migratory paths taken by cells. Finally, the distinction between T_{EM} and T_{CM} cells is not as transparent as initially described once *in vivo* studies are carried out.

1.2.13.2 Helper T-cells

Th1 and Th2 cells express particular chemokine receptors patterns with Th1 cells expressing CXCR3 and CCR5 and Th2 cells expressing CCR4, CCR3 and CCR7, whilst both subsets express CXCR4, CCR1 and CCR2 [161, 162]. The expression of chemokine receptors and response to specific chemokines fits with their proposed roles in immunity. For example allergic reactions require the presence of Th2 cells, the ligand for CCR3 and CCR11, is up regulated in sites where such reactions take place [162]. However, as is often the case, the picture becomes less clear with *in vivo* studies. Examination of T-cell subsets in human blood revealed more heterogeneous populations, with populations of Th1 cells co-expressing chemokine receptors, thought to reflect a Th2 phenotype and vice versa, for example CXCR3⁺CCR4⁺ positive cells could be detected in both subsets [163]. This highlights that the system is far more complex and rigid categorisation of these cells and their migratory capacities is not helpful.

As described previously, these cells are characterised by low CCR7 expression and high CXCR5 expression, thereby facilitating their positioning within the CXCL13, producing germinal centres to provide germinal centre B-cell help.

Th17 cells have been implicated in the development of inflammation. Th17 cells are able to recognise signals released from inflamed tissues, and have been shown to express

CCR2, CCR5, CCR7, CXCR3 and CCR4, and CCR6 [164, 165]. There is an overlap with those chemokine receptors expressed by both Th1 and Th2 cells, likely to reflect the fact that these subsets all migrate to inflamed tissue. Th17 cells also share chemokine receptor profiles with T-regulatory cells (namely CCR4, CCR5, CCR6, CXCR3 and CXCR6) and these cells are often co-located [165]. This would be beneficial, in that the T-regulatory cells can act as a dampener to profound inflammatory responses produced by Th17 cells.

1.2.13.3 Regulatory T cells

Regulatory T-cells (Tregs) have a homeostatic function by suppressing T-cell activation and promoting self-tolerance. Tregs are currently divided into subsets dependant upon the expression of $\alpha_E\beta_7$ integrin [166]. $\alpha_E\beta_7^+$ Tregs (both CD25⁺ and CD25⁻) display a T_{EM} cell phenotype reflected in mRNA expression of CCR4, CXCR3 and CCR6 and migrate in response to the inflammatory chemokines CCL17, CXCL9 and CCL20, [167]. Thus reflecting their ability to migrate to inflamed tissues and mitigate inflammatory responses there. The $\alpha_E\beta_7^-$ Tregs are all CD25⁺, and re-circulate through lymphoid tissues, express CCR7 and respond readily to CCL19 thus homing efficiently to secondary lymphoid organs [167]. Re-circulating of these Tregs provides immunosurveillance by increasing the chance of encountering inflamed tissues.

1.2.14 Germinal Centre Organisation and B cell Immune Responses

At the time of an immune response the correct positioning of B and T-cells is vital. T-cell activation leads to up-regulation of CXCR5 and down-regulation of CCR7, whilst the converse occurs in B-cells allowing for interaction at the T-B cell border. A number of activated B-cells then form the germinal centre, becoming organised into dark and light zones. In the former centroblasts are attracted and retained via CXCL12 released by the stroma interacting with CXCR4 on the B-cell surface [168]. CXCR5 bearing cells, both B-cells and follicular T-helper cells, home to form the light zone in response to CXCL13 released by follicular dendritic cells [168, 169], where affinity maturation and class switching with assistance from T_{FH} cells occurs. The resulting B-cell populations then home according to their initial site of induction.

1.2.15 Initiation of Immune Responses by Constitutive Chemokines

The role of chemokines in the initiation of immune responses does not appear to be essential. In CCR7 deficient mice, there is a disturbed lymph node micro-architecture due to defective homing of dendritic cells and T-cells, however, immune reactions as measured by immunoglobulin production do occur, although at lower levels and with different

isotypes [88]. Additionally, *plt/plt* mice lacking expression of both CCL19 and *serCCL21* (a murine variant of CLL21), display disturbed lymphoid architecture despite this, pronounced T-cell responses could be elicited following antigen exposure, albeit delayed and with altered dendritic and T-cell localisation within lymph nodes [145]. Further work on *plt/plt* mice demonstrated a delayed/absent resolution of the inflammatory responses when compared to wild type mice [145], implicating the lack of constitutive chemokines and subsequent lymphoid organ organisation in the defective immunosurveillance and Treg function. Therefore whilst initiation is not completely impaired by the absence of certain constitutive chemokines, it is possible that resolution may well be.

1.3 Non-Hodgkin's Lymphoma

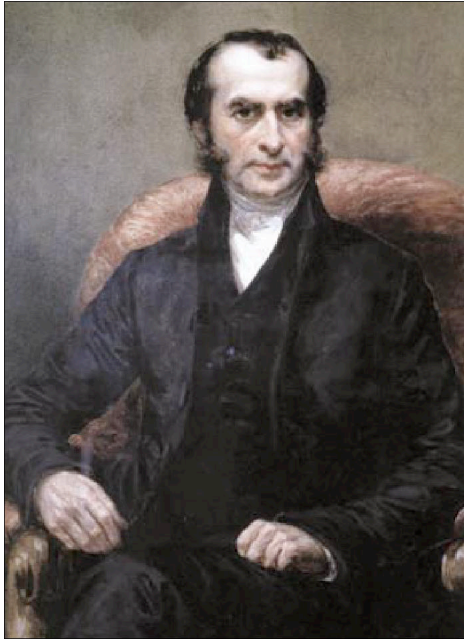
In section 1.1 the immune system and in section 1.2 the chemokine system was outlined with a particular emphasis on the adaptive immune system. Central to the adaptive immune system are lymphocytes and this section discusses the clinical and pathological aspects of one of the diseases involving the lymphoid system, and the disease under study in this project - non-Hodgkin's lymphoma.

1.3.1 Historical Perspective

Lymphoma is a malignancy of the lymphoid system. Whilst its main sites of involvement are the primary or secondary lymphoid organs, it can affect any site in the body, due to infiltration by malignant lymphocytes. The pathological appearance of the disease was first described by Thomas Hodgkin (figure 1.10a) in 1832 in his paper titled "On Some Morbid Appearances of the Absorbent Glands and Spleen" [Reviewed in 170]. It was later when Samuel Wilkes revisited the disease that it was given the eponymous name of Hodgkin's disease [171]. Some 60 years later lymphoma was further classified into Hodgkin's disease and non-Hodgkin's lymphoma (NHL). Dorothy Reed and Carl Sternberg described the presence of the cell now termed the Reed-Sternberg cell [172, 173] shown in figure 1.10d. This cell, currently thought to be a germinal B-cell, distinguishes the two broad categories of lymphoma from each other, with Hodgkin's disease having the Reed-Sternberg cell.

In the 1940's NHL was the first malignancy for which chemotherapy was used, with mustine producing a dramatic, but short-lived reduction in tumour bulk [174]. Since that time a number of advances in treatment have led to improved outcomes for those affected by NHL. First attempts at NHL classification were based on histological appearances and included three subtypes [175]; this has been replaced by numerous classification systems over the decades with increased understanding of the biology and clinical outcomes of NHL. The WHO classification, containing over 60 NHL subtypes (see appendix 8.1), is based on histological, immunophenotypical, cytogenetic and molecular characteristics and is now the current standard [176]. Lymphomas were also the first diseases in which clinical tumour staging systems were proposed. The original Rye staging was described in 1966 [177], subsequently this was revised and the Cotswold Revised Ann Arbor staging classification is now in use [178].

So, from the initial descriptions by physician and philanthropist Thomas Hodgkin in 1832 to molecularly targeted therapies in 2010, our understanding and treatment of lymphomas has come a long way.



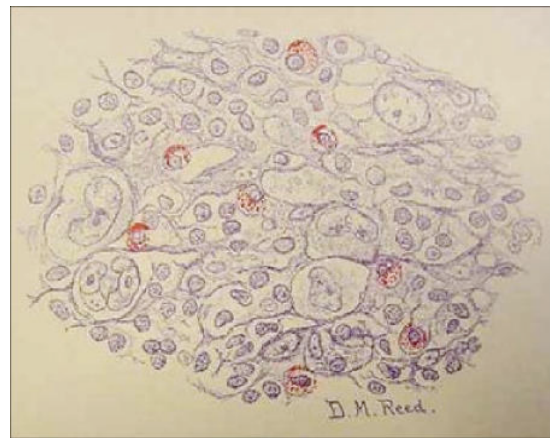
a)



b)



c)



d)

Figure 1.12: Illustrations and images of Hodgkin's Disease: a) Portrait of Thomas Hodgkin b) Hodgkin's disease watercolour drawing by Robert Carswell in 1828 of case number 7 in Hodgkin's paper, c) Photograph of abdominal lymph nodes from Thomas Hodgkin's 2nd case now kept in the Gordon Museum, GKT, King's College London, d) An image of Dorothy Reed's original illustration of Reed-Sternberg cells, demonstrating the characteristic large binucleated cells.

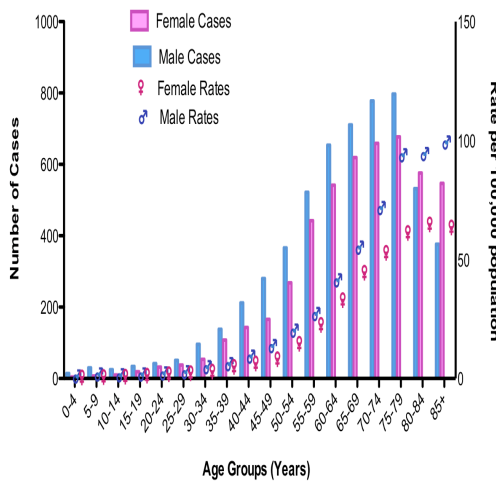
1.3.2 Epidemiology of Lymphoma

NHL is approximately six times more common than Hodgkin's lymphoma and is currently, the fifth most common malignancy in men and the seventh in women in the UK. It is more common in men, and Caucasians have a higher incidence than other races. Whilst Hodgkin's lymphoma incidence has remained stable over time, the incidence of NHL is increasing by 3-5% per year (Figure 1.11B); this appears to be a genuine worldwide trend. Whilst there is increasing incidence with advancing age (Figure 1.11A), an aging population cannot entirely account for this, as shown in figure 1.11B where the incidence is adjusted for age. There have been many theories as to why this is occurring but as yet, the actual cause is unknown. There are also differences in incidence and predominant NHL subtypes worldwide, with T-cell lymphomas being more common in the Far East and Burkitt's Lymphoma predominating in certain areas of Africa.

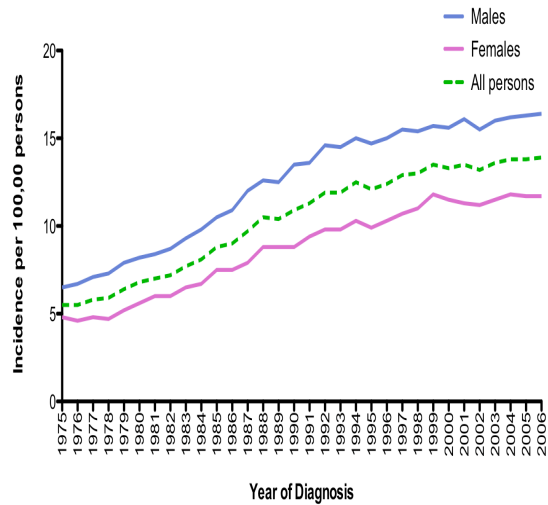
Over the last 30 years there has been an improvement in treatment outcomes with Hodgkin's lymphoma patients, with a five-year survival of 80% or more. However, improvements in overall survival for those with NHL has only gradually improved, with falling mortality rates only observed within the last 5 years or so. This latter aspect is interesting, as the mortality rates have fallen despite increasing incidence (Figure 1.11D). In the last decade an anti-CD20 monoclonal antibody, rituximab, has been used widely in the treatment of the more common B-cell lymphomas, leading to significantly improved outcomes, which may in part have contributed to the reduced mortality rates. The latest available data shows that in the UK, there were 10,569 new cases of NHL in 2006, whilst in 2008 there were 4,533 deaths relating to NHL. A major factor in overall survival is age, with older patients faring less well than younger patients with current five year survival figures for the 65-74 male group being 53% compared to 73% in the 15-44 male age group [ISD, National Services Scotland 179]. It is also interesting to note that there does not appear to be a significant impact of social deprivation or ethnicity on the incidence of NHL within the UK.

Except where specified, the statistics quoted in this section and the data used to formulate the graphs have been obtained from the Cancer Research UK, Cancer statistics pages [180].

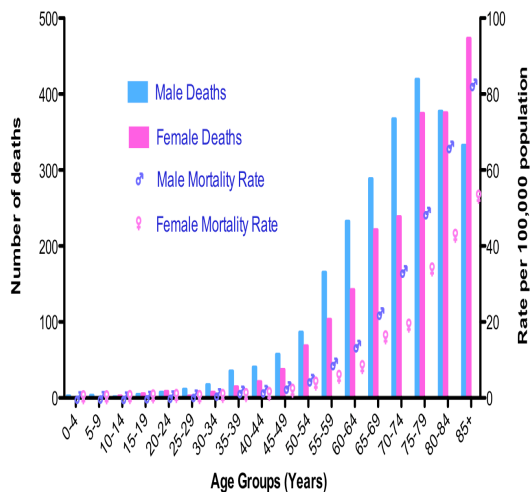
A. Numbers of new cases and incidence by age and sex of non-Hodgkin lymphoma, UK 2006



B. Age standardised incidence rates of Non-Hodgkin's lymphoma by sex in the United Kingdom, 1975-2006



C. Non-Hodgkin's Lymphoma related deaths according to age and sex, United Kingdom, 2007



D. Age standardised mortality rates due to non-Hodgkin's lymphoma, by sex in the UK from 1971-2001

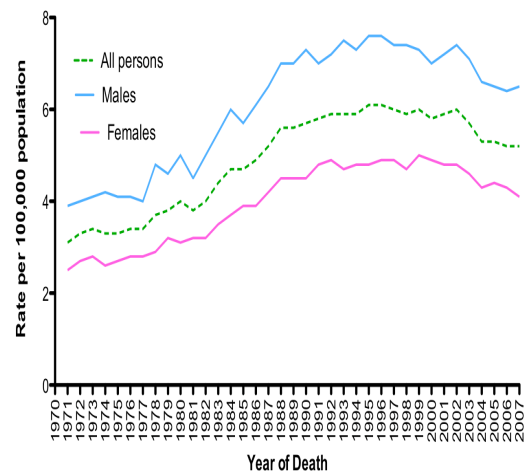


Figure 1.13: Graphical representation of the incidence of NHL and the mortality rates associated with NHL in the UK. A) Differences in NHL incidence rates according to age and sex, B) Demonstration of increasing age adjusted incidence of NHL over time, C) Differences in NHL mortality rates according to age and sex, D) Age standardised mortality rates over time Data and graphs from Cancer Research UK (2009).

1.3.3 Aetiology of NHL

In the majority of cases the aetiology of NHL is unknown. With the increasing incidence of NHL, a wide range of potential risk factors have been explored. Smoking, hair dye use and exposure to ionizing or non-ionizing radiation do not appear to increase the risk of NHL [181, 182]. Other factors show weak associations such as benzene, herbicide nitrites/nitrates exposure or working in agricultural, farming or manufacturing occupations, although of course these factors are linked [183, 184] and, there is emerging data indicating that there may be a link between silicone breast implants and primary breast ALK1-negative anaplastic large cell lymphoma [185]. Finally, other studies have shown a trend towards a lower risk of NHL with exposure to sunlight and alcohol consumption [186, 187].

In a minority of cases the causative agent can be established, including particular microorganisms, immunosuppressive agents, autoimmune disorders including rheumatoid arthritis and inherited immunodeficiency states. The most established microorganism associated with lymphoma is the Epstein-Barr virus (EBV). EBV was first discovered in samples given to Epstein by Burkitt of cases now known as Burkitt's lymphoma [188, 189]. Since that time EBV has been implicated in the pathogenesis of a number of other lymphomas including NK cell lymphomas, post-transplant lymphoproliferative disease and a proportion of Hodgkin's lymphoma cases [190].

Human immunodeficiency virus (HIV) is associated with an approximately 100 fold increased incidence of lymphoma, with a higher than normal incidence of more aggressive subtypes such as Burkitt's lymphoma and primary CNS lymphoma [176, 191]. Human T-lymphocyte virus (HTLV) is associated with adult T-cell lymphoblastic leukaemia/lymphoma, which is more common in Japan and the Caribbean reflecting increased rates of HTLV infection in these populations [192]. Hepatitis C virus (HCV) is associated with low and high grade lymphomas [193], whilst Human herpes virus 8 (HHV8) is associated with primary effusion lymphomas [194].

Chronic infection with bacteria has also been associated with the development of NHL. *Helicobacter pylori* is associated with gastric lymphomas, especially gastric MALT lymphomas [195] and eradication of this organism leads to resolution of the lymphoma in a significant proportion of those affected [196]. *Chlamydia psittaci* infection has been associated with MALTomas of the lacrimal glands [197] and *Borrelia Bergdorfi* has been

associated with NHL [198]. It is likely that further associations between viral and bacterial infections and particular NHL subtypes will become apparent over time.

Finally, there is a strong association with disorders or drugs that cause immune dysfunction. A number of immunodeficiency states, whether inherited, acquired or iatrogenic have a strong association with the development of lymphoma as well as conversely chronic inflammatory conditions such as rheumatoid arthritis [199]. EBV-driven post-transplant lymphoproliferative disorders occur on the background of immunosuppression following solid organ or bone marrow transplantation, in some instances withdrawal of immunosuppressive agents leads to regression of the lymphoma [Reviewed by 200].

1.3.4 Clinical Features

NHL presents in a variety of ways and it can, at times, be difficult to establish the diagnosis. The median age at diagnosis typically lies in the 6th or 7th decade of life. In the majority of patients painless lymphadenopathy is a presenting feature ranging from, a single node to widespread lymphadenopathy. Patients may also have splenomegaly or hepatomegaly at presentation. The presence of “B” symptoms is significant; these include unexplained fevers of greater than 38°C, drenching night sweats and unexplained weight loss of more than 10% of their body mass over 3 months, conferring an unfavourable outcome. However, lymphomas can develop in any anatomical site, and extra-nodal disease causing a range of symptoms and clinical signs depending on its location. For example, common extra-nodal sites include the skin presenting as nodules or generalised skin rashes, gut lymphomas can present with indigestion, diarrhoea or even bowel obstruction, and mediastinal involvement with features ranging from mild shortness of breath, chest pain through to potentially life threatening superior vena-cava obstruction. Less common sites include the bones presenting with fractures, spinal cord compression and/or bone pain, the central nervous system presentation including but not limited to hemiparesis, cranial nerve palsies, cognitive impairment and even cerebellar signs; more rarely, ovarian, kidney and pancreatic involvement has been described. Therefore, knowing that lymphoma can present in such a myriad of ways, it is no surprise that it can be frequently difficult to diagnose. Most of the information above can be found in standard medical or general haematology textbooks such as Postgraduate Haematology, [214].

1.3.5 Diagnosis of NHL

A number of investigations are required to confirm a diagnosis of NHL. These range from simple haematological and biochemical tests to more complex molecular testing. A full blood count is often normal, however if patients have heavy bone marrow infiltration, anaemia thrombocytopenia and/or leucopenia may result. Lymphopenia when seen often negatively impacts on the prognosis. In certain lymphoma subtypes anaemia or thrombocytopenia may occur due to autoimmune phenomena this is particularly true of chronic lymphocytic leukaemia/ small lymphocytic lymphoma (CLL/SLL). Testing for lactate dehydrogenase (LDH), albumin, and beta-2-microglobulin impact on prognostic scores. Some lymphomas may be associated with monoclonal gammopathies or hypogammaglobulinaemia, and so testing for these can be useful.

Investigating the possibility of an aetiological agent is always advisable with serology for EBV, HIV, and Hepatitis C forming part of the lymphoma work up. Hepatitis B and CMV status are also checked and have implications for treatment, the presence of the former being a relative contra-indication for rituximab and the latter guides the type of blood products used in supportive care. Other microbial testing is guided by the NHL sub-type, e.g. HTLV-1 testing in those with T-cell leukaemia/lymphoma.

A tissue biopsy is essential to establish the diagnosis and treatment should not be commenced on suspicion alone. Definitive histology is obtained by biopsy of the affected gland or tissue. Sides are examined with haematoxylin and eosin (H & E) staining initially before deciding upon immunohistochemistry panels. Various antibody panels have been developed to aid in the diagnosis of NHL subtypes and guidance on appropriate panels can be found in guidelines published by the British Committee for Standards in Haematology (www.beshguidelines.com). An outline of the immunophenotypes for the more common B-cell lymphomas is shown in table 1.4. Demonstration of clonality is an integral aspect of lymphoma diagnosis. For B-cell lymphomas this is relatively easy, B cells express either kappa or lambda light chains on the surface, with a normal $\kappa:\lambda$ ratio of 2-4:1, if there is a clonal B-cell population then this ratio is disturbed with either kappa or lambda restriction. However, T-cell clonal populations are less easy to detect and PCR is required to demonstrate a monoclonal TCR $\alpha\beta$ or $\gamma\delta$ population.

Further tests including cytogenetic analysis, fluorescent in-situ hybridisation, and molecular studies are also indicated in certain lymphomas, some of which will be explored later.

	CD20	CD79a	CD10	Bcl-6	CD5	CD23	Cyclin D1	Bcl-2	Others
<i>Follicular lymphoma</i>	+	+	+/-	+	-	-/+	-	+/-	MUM1-
<i>CLL/SLL*</i>	+	+	-	-	+	+	-	+	
<i>Lymphoplasmacytic Lymphoma</i>	+	+	-	-	-	-	-	+	CD25-/+ CD11c-
<i>B-cell PLL[#]</i>	+	+	-/+	-/+	-/+	-	-	+	
<i>Nodal marginal zone lymphoma</i>	+	+	-	-	-	-	-	+	CD11c +/-
<i>Extranodal marginal zone lymphoma</i>	+	+	-	-	-	-	-	+	CD11c +/-
<i>Splenic marginal zone lymphoma</i>	+	+	-	-	-	-	-	+	DBA44 -/+ CD25-/+
<i>Mantle cell lymphoma</i>	+	+	-	-	+	-	+	+	MUM1- CD11c-
<i>Myeloma/plasmacytoma</i>	-/+	+/-	-	-	-	-	-/+	-	MUM1+ CD138+ CD38+
<i>DLCBL[^] germinal centre type</i>	+	+	+	+	-/+	-/+	-	+/-	MUM1-
<i>DLBCL activated B-cell type</i>	+	+	-	-/+	-/+	-/+	-	+/-	MUM1+
<i>Mediastinal large B-cell lymphoma</i>	+	+	-/+	+	-	+/-	-	+	
<i>Burkitt's lymphoma</i>	+	+	+	+	-	-	-	-	MUM1

Table 1.4: Immunophenotypic profile of B-cell non-Hodgkin's lymphomas. CLL/SLL – chronic lymphocytic leukaemia/small lymphocytic lymphoma, #PLL-prolymphocytic leukaemia, ^DLBCL – diffuse large B-cell lymphoma. [Taken from 215].

Once the diagnosis of NHL has been confirmed testing is required to stage the disease. Computed Tomography (CT) scanning (figure 1.12b) is employed to determine how extensive lymphoma is enabling clinicians to determine how many lymph node groups are involved and if there is any extra-nodal organ involvement. A bone marrow biopsy is

performed on every patient requiring treatment with the presence of lymphoma in the bone marrow automatically classifying the patient with advanced disease. On occasion, the diagnosis is made on the bone marrow leading to a search for lymphoma elsewhere. Other investigations such as examination of cerebro-spinal fluid (CSF), magnetic resonance imaging (MRI) (figure 1.12d) or bone scans may also be required, depending upon the setting. Once information from CT and bone marrow studies have been collated, the patient is then staged using the Cotswold revision of the Ann Arbor staging classification [216], outlined in table 1.5.

In recent years fluorodeoxyglucose-positron emission tomography (FDG-PET) has been utilised in staging and response assessments of patients with higher grade NHLs and Hodgkin's lymphoma. Increased PET avidity reflects an increased metabolic rate and thus highly metabolic lymphomas can be distinguished from physiological activity (figure 1.12c). Its role in management of lymphomas is becoming clearer, certainly, if a patient is PET-negative at the end of treatment, they have an improved outcome and may escape consolidative treatment such as radiotherapy [178].

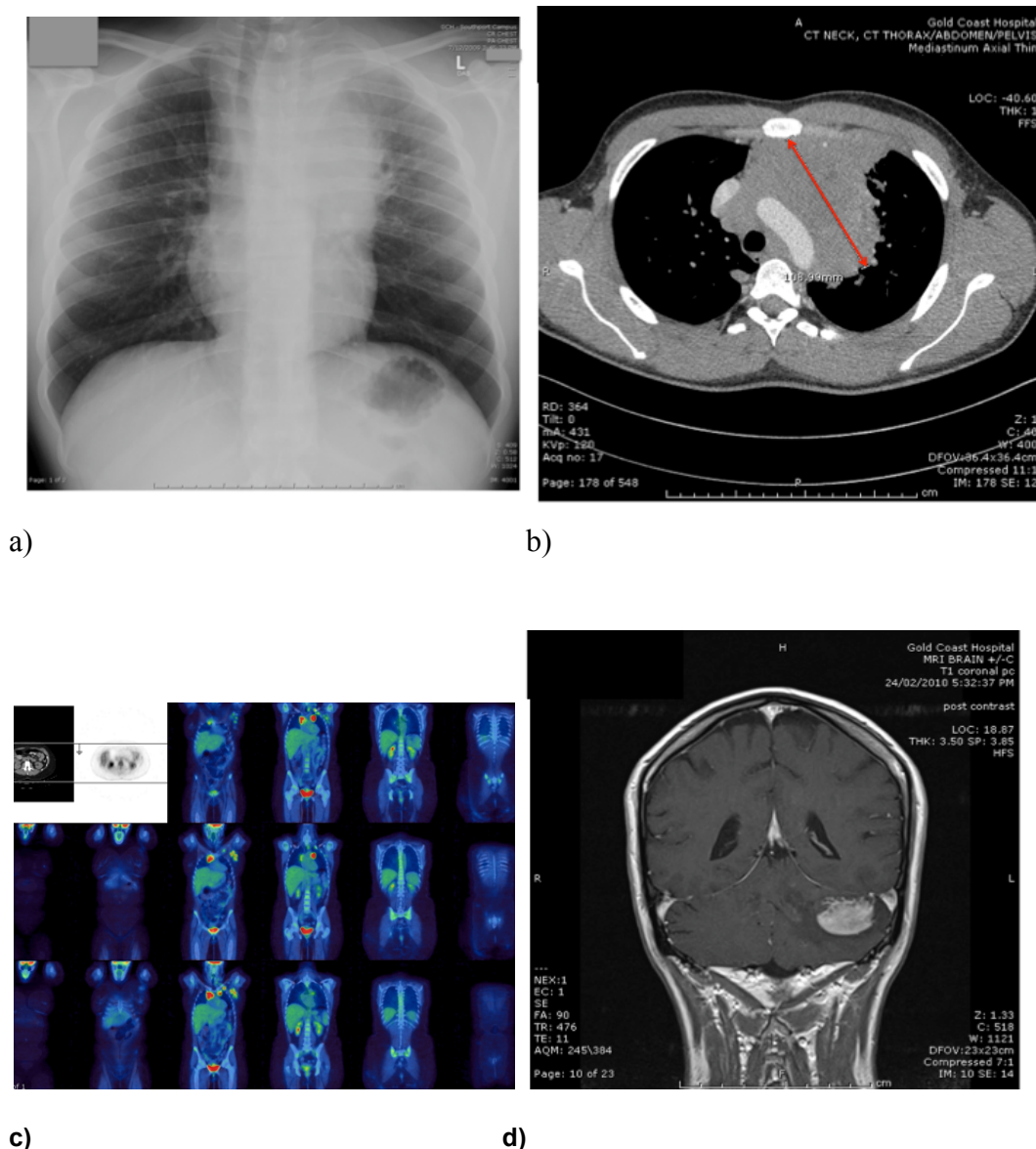


Figure 1.14: Radiological images from patients with lymphoma. a) Plain chest x-ray demonstrating a widened mediastinum due to lymphadenopathy, b) CT-scan of the same patient highlighting the mediastinal mass, c) FDG-PET scan, showing abnormal, increased avidity in the mediastinum and left axilla (red and yellow), the brain and bladder are PET avid due to the high metabolism in the brain, and excretion of the FDG through the bladder, d) MRI scan of brain, demonstrating lesion in the left cerebellum. (These images were obtained from patients seen at the Gold Coast Hospital, QLD, Australia).

<i>Stage</i>	<i>Definition</i>
<i>I</i>	Involvement of a single lymph node region or lymphoid structure (e.g. spleen, thymus, Waldeyer ring)
<i>II</i>	Involvement of two or more lymph node regions on the same side of the diaphragm (the mediastinum is a single site; hilar nodes are lateralized); the number of anatomic sites should be indicated by suffix (e.g.II ₃)
<i>III</i>	Involvement of lymph node regions or structures on both sides of the diaphragm.
<i>III₁</i>	With or without splenic, hilar, coeliac or portal nodes
<i>III₂</i>	With para-aortic, iliac or mesenteric nodes
<i>IV</i>	Involvement of extranodal site(s) beyond those designated E, including bone marrow
<i>E, involvement of a single extranodal site, or contiguous or proximal to known nodal site of disease</i> <i>Stage followed by A or B where:</i> <i>A – absence of symptoms</i> <i>B- presence of B symptoms; ≥ 10% loss of body mass in preceding 6 months, drenching night sweats, unexplained fevers of ≥ 38⁰C for 3 or more days.</i>	

Table 1.5: Cotswolds revision of the Ann Arbour Staging Classification [217].

1.3.6 Classification of NHL

Non-Hodgkin's lymphoma consists of a diverse range of tumour types, which are currently classified according to the World Health Organisation system [178]. These are based on the histology, immunocytochemistry and molecular biology (Appendix 8.4). The subtypes of lymphoma behave very differently with regards to their clinical presentation, course and distribution of disease.

1.3.7 General Principles of Treatment

Very occasionally treatment modalities such as triple therapy (proton pump inhibitor, metronidazole and amoxicillin) in the case of *H.pylori* related MALTomas, or surgery for localized gastric lymphomas may be employed. However, at present the mainstay for the treatment of NHL involves the use of immunotherapy, chemotherapy, radiotherapy or a combination of the three. The problem with the latter two treatment modalities is the degree of toxicity to non-malignant tissue. Chemotherapy is given systemically and has numerous potential short-term and long-term side effects including immunosuppression, cytopenias, emesis, alopecia, renal and hepatic toxicity, neuropathies, mucositis, cardiomyopathies, pulmonary fibrosis, haemorrhagic cystitis, infertility and unfortunately an increased risk of secondary tumours, particularly leukaemia. The development of side effects depends upon the type of chemotherapeutic agent used, its quantity and duration.

Additional modalities such as autologous or allogeneic stem cell transplantation may also be utilised in lymphoma management with similar toxicity profiles with the additional complication of graft versus host disease in the latter.

Whilst the side effects of radiotherapy are more likely to be localised, the side effects are again numerous including localised burns and mucositis, marrow suppression (pelvic irradiation), adhesions, skin malignancies, cardiac failure, pulmonary fibrosis and an increased risk of second malignancies, especially skin or breast cancer within radiotherapy fields.

Although these treatments are undoubtedly efficacious in a proportion of patients, toxicity limits the amount of treatment given and so alternate treatment modalities have been sought. Rituximab is a monoclonal human anti-CD20 antibody. CD20 is found on the surface of mature B-cells, and thus on mature B-cell tumours. Rituximab has been shown to increase response rates and 5year survival in elderly patients who receive this as an adjunct to standard chemotherapy for DLBCL [176]. It has also been shown to improve outcomes in other B-cell lymphomas and is now a standard addition to treatment for these. However there are still a significant number of patients for whom this additional treatment is ineffective, and exploration of alternative immunotherapies are ongoing, including idiotype anti-lymphoma vaccinations and the use of cytotoxic T-lymphocytes (CTLs). The use of EBV specific CTLs in EBV driven post transplant lymphoproliferative disease (PTLD), has had some success [218].

In addition to immunotherapy, molecularly targeted treatments are being trialed. The proteasome inhibitor, bortezomib, has been shown to have some activity in mantle cell lymphoma [219]. Other agents target epigenetic phenomena, and the histone deacetylase inhibitor, vorinostat, has shown efficacy in T-cell lymphomas [220]. Finally, the immunomodulatory drugs (IMiDs) thalidomide and lenalidomide have also given some promising results in those with mantle cell lymphoma [221].

It can be seen, that there is still the need to develop more specific and less toxic therapies in lymphoma and one potential avenue for such therapy development is the exploitation of the chemokine system.

1.3.8 Pathophysiology of NHL

Distinct NHL subtypes have different pathological mechanisms, but this discussion will be limited to those driving the B-cell lymphomas, reflecting the clinical sub-types examined in this thesis.

1.3.8.1 Genetic and Molecular Aspects of B-cell Neoplasms

Morphological and immunophenotypical studies of malignant B-cells have demonstrated that different subtypes appear to be “stuck” at particular stages of differentiation. Recent developments in molecular profiling have shown how malignant B-cells ‘hijack’ the regulatory mechanisms of normal B-cells to their own nefarious ends. During differentiation, modification of DNA occurs at a number of points, which can result in disruption of genes and lead to oncogenic processes.

The point at which this may occur is during V(J)D gene rearrangement. In lymphomas RAG mediated recombination may be aberrant leading to chromosomal translocations in which regulatory gene sequences drive inappropriate genes, this occurs with the t(14;18) translocation detected in follicular lymphomas and a proportion of diffuse large B-cell lymphomas (DLBCL). With t(14;18) the gene for IgH drives BCL-2, leading to over expression of the latter [201]. Aberrant over expression of BCL-2 results in inhibition of programmed cell death, providing NHL cells with a survival advantage over their normal counterparts [202]. In mantle cell lymphoma, t(11;14), is also a consequent of RAG complex dysfunction, here the IgH gene drives CCND1, encoding cyclin D1, leading to over expression and subsequent dysregulation of the cell cycle and bypassing of tumour suppressor genes such as p21 [203]. Whilst these translocations are necessary in the pathogenesis of lymphomas, they are not sufficient, and other poorly understood mechanisms are required for disease development.

Deregulation of a mutator enzyme, activation-induced cytidine deaminase (AID), may also have a role in the development of aberrant translocations mediated by the RAG complex [204]. DNA breakages also occur within the germinal centre, during somatic hypermutation and class-switch recombination. Both of these mechanisms rely on AID [205]. It perhaps no surprise then that, many lymphomas arise from the germinal centre, where AID appears to be central to these processes and thus implicated in the pathogenesis of many lymphomas. Mouse models have demonstrated that over expression of AID is associated with development of DLBCL [206]. In DLBCL, errors during somatic hypermutation dependant upon AID, lead to the accumulation of mutations in proto-

oncogenes such as PIM1 and MYC, the latter of which is involved in control of cell growth, proliferation and apoptosis [207]. Class switch recombination is also mediated by AID, with the risk of aberrant breaks in the IgH, this occurs with translocations involving the MYC locus, leading to over-expression and dysregulation of a variety of intra-cellular homeostatic mechanisms, and the eventual development of Burkitt's lymphoma [208].

Whilst these mechanisms explain the aberrant expression of proto-oncogenes and regulatory genes, how do they explain the maturation arrest observed in B-cell neoplasms? One way, in which this occurs, is demonstrated by the role of BCL-6 in DLBCL. BCL-6 is a repressor of transcription found in cells originating from the germinal centre, when this is involved in translocations, over expression leads to suppression of genes such as *Blimp-1* which is a master regulator of plasma cell differentiation [209]. Alternatively, neoplastic cells may lose their response to microenvironmental triggers of differentiation such as antigens, cytokines and other immune cells. Under normal circumstances, antigenic stimulation is required for triggering of the BCR leading to phosphorylation of I κ B α and its subsequent degradation, which usually sequesters NF- κ B within the cytoplasm. This enables NF- κ B to relocate to the nucleus where target genes involved in the prevention of apoptosis and the stimulation of autocrine signals are then activated. In malignant B-cells such as the ABC-subtype of DLBCL, constitutive activation of NF- κ B negates the need for antigenic stimulation, thus rendering the cells non-responsive to environmental components [Reviewed in 207].

1.3.8.2 Antigenic Stimulation

The role of chronic antigenic stimulation is highlighted by chronic infections with bacteria such as *Helicobacter pylori* and *Chlamydia psittaci*, and viruses such as Epstein Barr virus and Hepatitis C and their strong association with lymphoma. Eradication of these microorganisms can lead to disease regression. Gastric MALT lymphomas have a strong association with *Helicobacter pylori* infection, therapy to eradicate the bacteria leads to resolution of the lymphoma in up to 70% of cases [207], a similar picture is seen with splenic marginal zone lymphomas when hepatitis C is treated with interferon alpha therapy [210].

1.3.8.3 Role of the microenvironment

Whilst it is clear that the microenvironment has a huge role to play in the pathogenesis of Hodgkin's lymphoma, where less than 1% of the tumour bulk is comprised of the

malignant cells, our understanding of the role the microenvironment in the pathogenesis of NHL is only just beginning. Over the last decade gene expression profiling (GEP) has been utilised to better characterise both malignant and non-malignant cells within tumours, these studies have revealed that the non-malignant cells in the microenvironment also have an influence on the outcome and response to treatments.

GEP profiling applied to malignant (CD19+) and non-malignant (CD19-) cell populations from follicular lymphoma tissue reveal that two non-malignant gene-expression signatures, immune response-1 and immune response-2, are more predictive for outcome than differences in malignant cell profiles [211]. Further studies have confirmed the role of the tumour-infiltrating cells on prognosis in follicular lymphoma with poorer outcomes associated with profiles similar to those found in normal activated lymphoid tissue, with mediators of activated T-cells, macrophages and follicular dendritic cells being over-expressed, particularly CCL19, CCL20 and CCR1, along with a tendency for the T-cell population to be that of T helper 1 type. In contrast those with a more favourable outcome demonstrate non-activated T-cell signatures [212].

Examination of the cellular milieu and extra-cellular matrix in DLBCL has also demonstrated differences. Two stromal signatures are identified, the first conferring a more favourable outcome compared to the second. In stromal signature 1, there are changes consistent with a more fibrotic picture, with extra-cellular matrix deposition and infiltration by histiocytes; this is associated with a better outcome. In contrast stromal signature 2 reveals an increase in endothelial cells and pro-angiogenic cytokines such as VEGF and CXCR4, and an adverse outcome [213].

It is thought that the cellular milieu and the cytokines they release influence the behaviour of these malignancies by ensuring the most advantageous positioning within the bone marrow or lymph nodes thus enhancing their exposure to various survival signals. Additionally, understanding the nature of these microenvironments, adds to the list of potential therapeutic agents, for example a monoclonal antibody to VEGF, bevacizumab, is being investigated in phase 2 and phase 3 trials in those with DLBCL [214].

1.3.9 B-cell Neoplasms Studied in this Thesis

Below is a more detailed discussion of the six NHL sub-types studied in this project.

1.3.9.1 Diffuse large B-cell lymphoma

Diffuse large B-cell lymphoma (DLBCL) is the most common lymphoma Worldwide, accounting for 30-40% of new cases. No obvious aetiological agent has been detected for the majority of cases of DLBCL, however, a small proportion arise on a background of HIV or EBV infection. DLBCL is a high-grade lymphoma and is potentially curable. It can arise de-novo or on the background of more indolent lymphomas such as follicular lymphoma or CLL/SLL. Diagnosis depends upon finding a clonal B-cell population and the pattern of cell markers seen in DLBCL is shown in table 1.4. The most common translocation detected in DLBCL involves 3q27 and the coding region for BCL-6 [222]. The typical t(14;18) translocation of follicular lymphoma is found in 20-30% of cases of DLBCL and may reflect transformation from follicular lymphoma [223]. The translocation associated with Burkitt's lymphoma, t(8;14), and the associated oncoprotein, c-myc, is present in up to 15%. Distinguishing DLBCL from Burkitt's lymphoma may therefore be difficult [224].

DLBCL encompasses a fairly heterogeneous group of lymphomas, with gene expression profiling, revealing 4 distinct sub types; germinal centre (GC) cell type, activated B-cell (ABC) type, primary mediastinal B-cell lymphoma and type 3. Markers can be used to distinguish between these types, with MUM1 being positive in ABC type but negative in GC type [225]. However, at present this distinction does not alter therapeutic choices. The revised international prognostic index (R-IPI) for DLBCL takes in to account the impact of rituximab on outcomes in DLBCL. It is based on a number of clinical features each scoring 1 and include age greater than 60 years, Ann Arbor stage III/IV, ECOG performance status > 2 (appendix 8.5), elevated LDH, and more than 1 involved extra-nodal site. The patient are then categorised as very good, good or poor risk with an estimated 4-year overall survival of 94%, 79% and 55% respectively. (see table 1.6). The prognostic score doesn't alter initial management, but will guide patient counseling, and may assist decisions on entry into available clinical trials or consolidative treatment [226].

	<i>No. of IPI factors</i>	<i>% of patients</i>	<i>4-year EFS*, %</i>	<i>4-year OS[#], %</i>
<i>Very good</i>	0	10	94	94
<i>Good</i>	1,2	45	80	79
<i>Poor</i>	3,4,5	45	53	55

Table 1.6: Revised-International Prognostic Index and observed outcomes at 4 years [227]. * EFS – event free survival, #OS- overall survival.

CHOP (cyclophosphamide, hydroxydoxorubicin, vincristine (Oncovin) and prednisolone) has formed the backbone of DLBCL therapy since the 1970's. CHOP has traditionally been given every 21 days for 6-8 courses. For those with early, stage I-IIA disease, the addition of rituximab to CHOP (R-CHOP) has led to survival exceeding 90% in those receiving six courses of R-CHOP or undergoing dual modality (with radiotherapy) treatment [227, 228]. R-CHOP also forms the mainstay of treatment for those with advanced disease. The GELA study compared CHOP with R-CHOP in elderly patients, revealing a significantly increased survival, response rate and failure free survival in the R-CHOP arm [229]. Similar results were obtained in the MInT study with younger patients [218].

Following treatment, CT and PET scan +/- bone marrow examination depending on marrow findings at diagnosis are performed to assess response. Complete response (CR) is defined as there being no detectable disease. In a sub-group of patients, i.e. those starting with bulky disease (>10cm diameter) consolidative radiotherapy to the site of initial bulk is often employed, especially if there is still avidity by PET or a residual mass of >1.5cm in diameter.

In sub-groups of patients with DLBCL additional or alternative treatment modalities may be required. CNS prophylaxis is used in patients identified as being at high risk including those with testicular, sinus or epidural involvement, circulating lymphoma cells, more than 2 extra-nodal sites and with an elevated LDH. Those with primary CNS B-cell lymphomas have regimens incorporating high dose methotrexate; this drug is one of the few chemotherapy agents that have been shown to be effective in this subgroup [229].

Finally, patients who relapse or have suboptimal responses to treatment, require alternative, more intensive treatments. The time from CR to relapse has prognostic significance, with those relapsing within 12 months having a poorer prognosis. Repeat biopsy is essential, as other pathologies do occur including second malignancies and chronic infections such as tuberculosis. Chemotherapy is re-instituted with 'salvage' regimens such as R-DHAP (rituximab, dexamethasone, cytosine and cisplatin) or R-ICE (rituximab, ifosfamide, cytosine and etoposide). If chemosensitivity is demonstrated, eligible patients (biologically fit and younger than 70 years) proceed onto an autologous stem cell transplant (ASCT). The CORAL study has demonstrated no differences in outcome with either of the 'salvage' regimens described above with overall survival at 5 years being ~50% [230].

1.3.9.2 Follicular Lymphoma

Follicular lymphoma accounts for about 20% cases of NHL. The highest incidence is found in the USA and Western Europe, where it can account for up to 40% of cases. It is rare in those under the age of 20 years and the median age of presentation is somewhere in the sixth decade [231]. Follicular lymphoma is a low grade lymphomas and not currently curable. The current median survival is estimated at 12-14 years following diagnosis [176]. Follicular lymphoma cells are derived from follicle centre (germinal centre) B-cells. These cells demonstrate clonal restriction usually expressing surface immunoglobulin (sIg) along with the B-cell antigens (CD20, CD79a, CD22), BCL-2, BCL-6 and CD10. The translocation t(14;18) is detected in up to 90% of cases. This translocation involves the BCL-2 locus leading to interruption of the normal apoptotic pathways. Other cytogenetic abnormalities have been described and often involve BCL-6, making distinction from DLBCL difficult [232]. Primary cutaneous follicular lymphoma is usually negative for BCL-2 and t(14;18) [176].

Many patients present with advanced stage disease, with 40-70% having marrow involvement at diagnosis [176]. Despite widespread disease, the majority, are asymptomatic at diagnosis. It predominantly affects nodal sites, but extra-nodal involvement may occur, and occasionally, may only involve extra-nodal tissue. A clinical prognostic staging system has been developed, the follicular lymphoma international prognostic index or FLIPI. This is based on 5 prognostic factors; age > 60 years, haemoglobin concentration (Hb) <120g/L, elevated LDH, more than 4 nodal areas involved and Ann Arbor stage III/IV, resulting in 3 prognostic groups; low, intermediate and high risk [233]. These are outlined in table 1.7 along with the expected overall survival

figures. In 2009 a revised FLIPI score was devised based on patient data following the routine use of rituximab, this revealed differences in predictive prognostic information and the adverse risk factors were noted as age > 60 years, Hb <120g/L, bone marrow involvement, elevated serum β -2-microglobulin and the largest involved lymph node exceeding 6cm in diameter. Again the patients were assigned to a low, intermediate or high risk group [234]. However, as data in those receiving rituximab is not yet mature, only 3 year overall survival figures were given, as such it remains to be seen if this prognostic scoring system will hold true at 10 years.

In the minority of patients presenting with stage I disease, involved field radiotherapy is potentially curable. However, in the majority follicular lymphoma is not curable. The decision therefore, is not what treatment to give, but when to give it. Not all patients require immediate treatment and studies comparing a watch and wait approach with chemotherapy up front, demonstrate no improvement in overall survival between the two arms. A study by the BNLI (British National Lymphoma Investigation) group, also defined a population for whom treatment was not immediately required; absence of B symptoms, no rapid disease progression, absence of marrow compromise, no life threatening organ involvement, absence of renal infiltration or macroscopic liver involvement, no bone lesions and no masses >7cm [235]. Such guidelines are reasonable to follow in deciding when to initiate treatment, and some patients can go for a number of years without it. Currently unclear is whether or not rituximab alone is preferable than a watch and wait approach in asymptomatic patients, the results of a recently closed study addressing this question are awaited.

<i>Risk Group</i>	<i>No. Of risk factors</i>	<i>Proportion of patients (%)</i>	<i>5 year overall survival (%)</i>	<i>10 year overall survival (%)</i>
<i>Low</i>	0-1	36	91	70
<i>Intermediate</i>	2	37	78	51
<i>High</i>	≥ 3	27	53	36

Table 1.7: Overall survival and progression free survival (PFS) in patients with follicular lymphoma based upon FLIPI score [236]. See text for details about the risk factors.

Once treatment is required, a number of regimens are available. Follicular lymphoma was the first of the NHLs to demonstrate an advantage with adding rituximab up front to CHOP or CVP (cyclophosphamide, vincristine and prednisolone) [234, 237]. Following either R-

CHOP or R-CVP, maintenance with 2 years of rituximab maintenance therapy has proven successful in maintaining responses; the PRIMA study demonstrated a significant improvement in 2 year progression free survival in those receiving rituximab maintenance compared to those who did not (PFS: 82% vs. 66%) [238]. This has now become standard treatment.

Patients invariably relapse, with a pattern of progressively shorter periods of remission between treatments, frequently ending in transformation to DLBCL or the development of refractory disease. Decisions regarding treatment at first relapse depend upon age and performance status and as at presentation, a period of observation is often employed. Eligible patients are offered ASCT if they respond following immunochemotherapy, and this has been shown to improve OS and PFS [239]. In a very select young and fit group, allogeneic transplantation may be considered and long term survival has been seen in those with refractory disease [240].

For those in whom ASCT is not viable, immunochemotherapy can be used varying from intensive regimens such as R-ICE, to a single agent palliative approach with drugs such as chlorambucil or fludarabine with or without rituximab. Rituximab maintenance given every 2-3 months has been shown to be efficacious following treatment for relapsed and refractory disease, with median survival following rituximab maintenance versus observation only being 51.5 versus 14.9 months [241].

1.3.9.3 Mantle Cell Lymphoma

Mantle cell lymphoma accounts for 3-10% of cases of NHL. The median age at diagnosis is 60-65 years, with a male predominance of >2:1. Mantle cell lymphoma (MCL) is not curable in the majority and has the worst outcome of all B-cell lymphomas with a median survival of 3-5 years [242]. MCL cells are derived from the mantle zone with a variety of histological types seen. More aggressive variants consist of blastoid and pleomorphic types corresponding to the most unfavourable outcomes, contrasting with small cell and marginal-zone like variants. All MCL cells display the same immunophenotype, with sIgM/IgD, CD20, CD5, FMC-7 and CD43 positivity and negative or only weak positivity for CD23 (distinguishing them from CLL/SLL). Cyclin D1 is positive in the majority of cases [176]. The hallmark of MCL is t(11;14), resulting in deregulated over expression of cyclin D1 [176]. This abnormality has potential utility as a marker of minimal residual disease (MRD).

Presentation with early stage I/II disease is unusual and the majority present with widespread disease. MCL cells are frequently detected in the circulation, bone marrow and extranodal involvement is common, especially the gastrointestinal tract in which involvement is detected over 80% cases [243]. It is argued that endoscopic examination of the gut is required in all MCL, however, a more pragmatic approach is to reserve this investigation for those who present with early stage, and therefore potentially curable, disease prior to localised treatment, as it will not affect the management of the majority presenting with advanced disease.

A prognostic scoring system has been proposed for MCL the mantle cell lymphoma international prognostic index (MIPI), based upon age, LDH, ECOG performance status and white cell count. This prognostic index is a little more complex with a scoring system for each prognostic factor. For the low risk group median survival there is an estimated 5 year OS of 60%, the median survival for the intermediate and high risk groups are 51 months and 29 months respectively [244]. However, the MIPI was developed on the basis of 455 patients compared to the thousands in both the FLIPI and R-IPI scores, and on patients entered into clinical trials (an independent good prognostic indicator), so correlation with widespread clinical practice is yet to be verified.

For those few with genuinely limited stage disease, involved field radiotherapy following 3-4 courses of chemotherapy have been reported to induce long-term remissions of over 8 years [245]. Unfortunately, the majority present with advanced disease with most requiring treatment with immunochemotherapy with or without ASCT consolidation as first line. Rituximab has been used in MCL, initially the results were rather disappointing, but in 2008 the Nordic Lymphoma Group published their study, which for the first time did not show any relapses beyond five years post-treatment. R-CHOP alternating with R-high dose cytosine, followed by a R-BEAM (BCNU, etoposide, ara-c, melphalan) conditioned ASCT in 160 consecutive patients, recorded an overall response rate of 96%, 6 year overall survival of 70% and EFS of 56%. In contrast to the MIPI only Ki-67 was demonstrated to have prognostic significance [246]. This has now become the preferred treatment for transplant eligible patients at our centre.

For those who are not transplant eligible, treatment depends upon their performance status, those that are fitter may tolerate intense regimens, however, as these do not significantly impact on overall survival, less intense regimens may be preferable, as these will debulk the disease and lead to symptomatic improvement, but without the toxicity profile inevitably

associated with more intense regimens. Other useful regimens include those based on fludarabine and in recent years bendamustine has shown some promise [247]. In the very elderly and unfit, a palliative approach with chlorambucil with or without rituximab is often useful for symptomatic relief.

At relapse, the aim of treatment is palliative in the majority, and regimens with lower toxicity profiles are preferred, as quality of life becomes the aim. Novel agents such as bortezomib, lenalidomide and temsoralimus have shown some efficacy, and bendamustine has been particularly successful. Trials using these agents along with more conventional agents first line, either as induction (bendamustine) or as maintenance (lenalidomide) are underway [248].

1.3.9.4 Chronic Lymphocytic Leukaemia/ Small Lymphocytic Lymphoma

Chronic lymphocytic leukaemia (CLL) is the most common leukaemia occurring in adults in the West, with an annual incidence of 2-6 cases/100,000 persons. Interestingly, it is rare in the Far East, and a similarly low incidence is seen in migrants from these regions, suggesting a genetic predisposition. It has an increasing incidence with age, and the median age at diagnosis is 65, although it is being increasingly diagnosed in younger patients. There is a slight female predominance. Diagnosis is usually made on blood samples, but when diagnosed following lymph node or tissue biopsy it accounts for ~7% of NHL cases [248].

Although CLL/Small lymphocytic lymphoma (SLL) are classified as the same condition, clinically a division is made; those with circulating cells are classified as CLL, whilst those with no abnormal circulating cells have SLL. In the majority, diagnosis is made on the presence of circulating CLL cells. The diagnosis is made in those with a persistent lymphocytosis of, $\geq 5 \times 10^9/L$ with a typical immunophenotype; CD20, CD5, CD19, CD79a, CD23 (negative in MCL) positivity, weak sIgM/IgD and CD11c expression and negative for FMC7. A scoring system has been devised based on a composite of the above markers to help in distinguishing CLL/SLL from other B cell neoplasms [176]. No single B-cell lineage has been identified in CLL with two broad groups noted, IgV_H – unmutated and IgV_H-mutated. Unmutated status is associated with a poorer outcome, and can be identified by a surrogate marker, ZAP-70 [249]. Additionally, expression of CD38 is associated with a poorer outcome [250].

Genetic abnormalities are detectable in ~80% of cases. There is a strong association between the cytogenetic abnormality and the clinical picture. For example the presence deletion 13q confers a favourable prognosis with a median survival of 133 months, whereas deletion of 17p (and thus p53) has the poorest median survival of 32 months [251]. CLL/SLL is not curable with survival from diagnosis ranging from a few months to over 20 years. Two different clinical staging systems are commonly used these are the Binet [252] and Rai [253] staging systems based upon, lymphocytosis, lymphadenopathy, organomegaly, haemoglobin concentration and platelet counts. These two staging systems are summarised in table 1.8. However, if a patient is anaemic or thrombocytopenic, autoimmune haemolytic anaemia (AIHA) or immune thrombocytopenia (ITP) needs to be excluded, these phenomena occur in approximately 5% of patients. AIHA or ITP require treatment, but do not always necessitate treatment of the CLL/SLL, a full description of the management of AIHA and ITP is out with the scope of this thesis, but a number of drugs used in CLL/SLL are effective whilst others are contra-indicated.

Treatment is indicated for those with Binet stage B or Rai stage I/II disease in the presence of one or more of the following; massive splenomegaly (>6cm below costal margin), lymph node mass \geq 10cm diameter, increasing lymphocytosis of >50% in 2 months or doubling time of <6 months, AIHA or ITP failing to response to standard treatments and significant constitutional symptoms. Treatment is indicated in those with Binet stage C or Rai stage III/IV disease [254].

Once the decision to treat has been made, the staging investigations including bone marrow examination, CT scanning and cytogenetic analysis are performed. The current standard for treatment naïve patients is rituximab, fludarabine and cyclophosphamide. Treatment will be guided by the patient's age and performance status. The German CLL Study Group CLL8 trial group has recently shown an improvement in overall response of 95% with rituximab, fludarabine, cyclophosphamide (FCR) compared to 85% in the FC arm, which has equated to prolonging PFS from 33 to 52 months [255]. However, for those who are older and frailer, single agent chlorambucil or fludarabine with or without rituximab can still achieve useful responses, disease control and symptomatic relief.

CLL/SLL is not curable and the disease inevitably relapses in a pattern analogous to that seen with follicular lymphoma. A proportion of patients undergo high grade transformation to DLBCL (Richter's transformation). Treatment at relapse depends upon time since first treatment, depth of response to the initial treatment, age, performance status and the

presence of abnormalities such as deletion of 17p. The latter is recognised as having some resistance to fludarabine, and some advocate using agents such as alemtuzumab (anti-CD52 monoclonal antibody) to overcome this [256]. For those who are younger and have a donor, allogeneic transplantation is a consideration, and has been reported to induce durable remission [257]. For the others, re-induction of remission can often be achieved using the original regimen. Richter's transformation is treated as for *de-novo* DLBCL. Whilst for those who are elderly or have a poor performance status, palliative approaches with agents such as chlorambucil, corticosteroids or cyclophosphamide are reasonable.

<i>System</i>	<i>Clinical Features</i>	<i>Median Survival (years)</i>
<i>Rai Stage (simplified 3 stage)</i>		
<i>0 (Low risk)</i>	Lymphocytosis in blood and marrow only	>10
<i>I & II (Intermediate risk)</i>	Lymphadenopathy, splenomegaly +/- hepatomegaly	7
<i>III & IV (High risk)</i>	Anaemia, thrombocytopenia*	0.75-4
<i>Binet Group</i>		
<i>A</i>	Less than 3 areas of lymphadenopathy, no anaemia or thrombocytopenia	12
<i>B</i>	More than 3 involved lymph node areas, no anaemia or thrombocytopenia	7
<i>C</i>	Haemoglobin < 100g/L* Platelets < 100 x 10 ⁹ /L*	2-4

Table 1:8: Outline of the two clinical staging systems for CLL/SLL, along with median survival for each stage. * as long as autoimmune causes of cytopenias have been excluded [Taken from 257].

1.3.9.5 Burkitt's Lymphoma

Burkitt's lymphoma is a highly aggressive lymphoma, which often presents with extranodal disease or as acute leukaemia, yet has one of the highest cure rates. Clinically there are three distinct groups. Endemic Burkitt's lymphoma has an incidence of 5-10 per 100,000 in Equatorial Africa, and Papua New Guinea (PNG), with a geographical association with endemic malaria. Endemic Burkitt's lymphoma is a disease of childhood with a peak incidence occurring in the 4-7 age group and male predominance, it has a predilection for the jaw and facial bones. HIV-associated Burkitt's lymphoma has a more nodal presentation and a high risk of CNS involvement, occurring in approximately 6 of every 100 AIDS cases. Finally, the group that will be discussed here is sporadic Burkitt's lymphoma. This is rare occurring in 2-3 per million per year. It is predominantly a disease of childhood and early adulthood with a median age at diagnosis of 30 years, there is a male predominance, and abdominal disease is the most common presentation [257]. The histology in Burkitt's lymphoma is characteristic with intermediate sized cells, with round or oval nuclei. There is a high degree of proliferation leading to a number of apoptotic cells, taken up by clearer histiocytes giving the characteristic 'starry night' microscopic appearance at low power [258]. However patients can present with a predominantly leukaemic picture. Other tests are required to confirm the diagnosis, including examination for EBV, FISH for typical translocations including t(8;14), detection of c-myc or other translocations involving myc. Burkitt's lymphoma cells are typically CD20, CD19, CD10, BCL-6, CD38 positive [176].

Treatment for Burkitt's lymphoma depends upon the age at presentation, with many paediatric centres using the complex regimens for acute lymphoblastic leukaemia such as the BFM 90 protocol which achieved an event free survival (EFS) of 89% at 6 years, the median age of this cohort was 9 years [176]. In adults toxicity profiles of such regimens has led to the development of alternative regimens including the CODOX-M/IVAC protocol. The British LY06 study, achieved a 2 year overall survival of 73% and 2 year EFS of 65% using this [259]. Since that time rituximab has been incorporated into regimens, with the best results reported with dose-adjusted EPOCH and an overall survival reported of 100% and EFS of 95% at 27 months [260], however this study is still ongoing and these results whilst promising are only based on an interim analysis.

Compared to other lymphomas, Burkitt's lymphoma has a high cure rate, however a proportion of patients will relapse or develop refractory disease, for these patients,

outcomes are very poor with the disease rarely responding to chemotherapy or radiotherapy. For those with relapse, who are fit and who can demonstrate chemosensitivity, ASCT has been shown to provide a 37% 3 year overall survival compared to 7% in chemoresistant cases [261]. Therefore, in many cases it is appropriate to adopt a palliative approach.

1.3.9.6 Marginal Zone Lymphoma

Marginal zone lymphomas (MZL) account for 7-8% of all B-cell NHLs [258] but for up to 50% of primary gastric lymphomas [233]. The median age at diagnosis is 61 with a slight female preponderance. The marginal zone lymphomas fall into three broad clinical types, extranodal, splenic and nodal MZLs. MZL cells represent mature B-cells. It appears that this results from chronic antigenic stimulation as, evidenced by the observation that genes involved in autoantibody formation, V_{H4} , V_{H3} and V_{H1} , are used by these cells [262]. MZL cells are positive for mature B-cell markers (CD20 and CD79a), and marginal zone antigens CD21 and CD35, they also have sIgM or sIgD [263].

Staging procedures are similar to other lymphomas with CT scanning and bone marrow examination, the staging systems themselves are however quite complex due to the variety of potential sites. Extranodal MALT lymphomas form the bulk of MZL cases, of which about a third are primary gastric MALT lymphomas. A geographical variation has been seen with higher incidence recorded in North East Italy, where a higher rate of *H.pylori* infection was also noted [176]. Other common extranodal sites include the salivary glands (16%), ocular adenxa (10-12%), skin (8-10%), lung (6-10%), intestine (3-9%) and upper airways (5-10%), in up to 11% of cases multiple sites are involved with or without bone marrow or nodal involvement. MALT lymphomas are indolent with 5 year overall survival rates ranging from 46% in those with upper airway involvement to 100% in those with intestinal, skin, lung, breast or thyroid involvement [262]. A number of cytogenetic abnormalities have been associated with MALT lymphomas including t(11;18), t(1;14), t(14;18) and t(3;14). The first of these is unique to MALT lymphomas, the presence of this translocation is of value in that it usually occurs in *H.pylori* negative cases, or if co-existing predicts for a lack of response to eradication therapy [263].

In gastric MALT lymphomas eradication of *H.pylori*, when present, leads to regression of the lymphoma in a significant proportion of cases [263]. The same principle applies to MALT lymphomas associated with other organisms such as *Campylobacter*, *Chlamydia* or *Borrelia*. If no infective aetiology is noted, treatment depends upon symptoms and the

extent of disease. Localised disease is potentially curable with localised radiotherapy. In those with more advanced disease, cure is not achievable and treatment depends upon the extent of the disease and symptoms. In the majority a watch and wait approach is appropriate with many not requiring treatment. Reasonable responses can be gained from single agents such as chlorambucil or fludarabine, with or without rituximab. In rare cases with extensive disease, combination chemotherapy regimens such as those used for follicular lymphoma or CLL/SLL are favoured [210].

Splenic marginal zone lymphoma accounts for approximately 1% of lymphoma cases. The usual presentation is that of isolated splenomegaly. Splenic hilar nodes are often involved but disseminated lymph node involvement is unusual. Bone marrow involvement occurs in 95% of cases, and circulating villous lymphocytes can be detected in up to 15% of cases [264]. There is an association with autoimmune haemolytic anaemia. Additionally, some cases are associated with hepatitis C infection. Management usually involves a watch and wait approach, many may not require treatment for up to 10 years. The mainstay of treatment is splenectomy, performed in the presence of massive splenomegaly or cytopenias associated with either hypersplenism or marrow involvement. The disease, if not caught early is not curable, but prolonged survival is seen with > 50% still alive at 5 years. Interestingly, splenectomy leads to an improvement not only in peripheral cytopenias, but also to a reduction in marrow infiltration [211]. If treatment beyond splenectomy is required, a similar approach is taken as with MALT lymphomas, including treating hepatic C infection if present [265].

Nodal marginal zone lymphomas account for less than 1% of NHL cases. Patients present with disseminated nodal involvement and less than half have marrow involvement at diagnosis. A paraprotein is detectable in about 8% of cases. The estimated 5 year survival is reported to be somewhere between 50% and 70%, with relapses continuing to occur beyond this time, suggesting that it is not curable. At present the number of cases are small, but similar treatments to those for advanced MALT lymphomas, are recommended with a period of observation being appropriate in some [264].

1.3.10 Summary

Non-Hodgkin's lymphoma is a heterogeneous group of malignancies affecting. It has a significant impact with an increasing incidence. Despite recent advances in therapy, a significant number of patients fail to respond or relapse and ultimately succumb to their illness. Therefore new ways of targeting this disease are needed. One system, which could be utilised, is the chemokine system, owing to its central role in the organisation of the adaptive immune system through homing of haematopoietic cells. The next section explores the role of the chemokine system in NHL.

1.4 Chemokines and Lymphoma

Having previously discussed the role that chemokines have in the organisation of the immune system, and the fact that lymphoma is a malignancy of the same, it is logical to examine the role that chemokines and their receptors may have in lymphomas. In fact there is increasing evidence for a significant role for chemokines and their receptors in the pathogenesis of lymphoma, as well as evidence that expression of these can influence outcomes and assist in determining the sub-type of lymphoma. Finally, there is increasing research and interest in looking at ways by which this system can be targeted therapeutically.

1.4.1 Chemokines and Malignancy

Chemokines and their receptors have been studied in a wide range of malignancies. Studies to date show that CXCR4 is the most widely expressed chemokine receptor across a range of tumour types and it is implicated in a number of malignant processes including metastasis, neo-angiogenesis, repression of apoptosis and invasion [264]. It is clear that there are a number of different mechanisms by which chemokines influence, or are influenced by, tumour biology and consequently can have effects on outcomes. A fully detailed discussion is not possible here, but a broad overview of some of these mechanisms will be presented.

Firstly, chemokine and receptor expression may be directly influenced by oncogenes or the consequent dysregulation of transcription factors. One example is the role of β -catenin in breast cancer. It has been shown that abnormal translocation of this protein leads to the activation of a number of transcription factors and leads to the transactivation of CCL2, which has been implicated in the development of metastasis and invasion [86].

Alternatively, dysregulated transcription factors such as is seen in melanoma with NF- κ B leads to up regulation of chemokines such as CXCL1 [266].

Many malignant cells actively recruit leucocytes to the tumour site. These can include any of the cells from the innate or adaptive systems. Foremost amongst these are the tumour-associated macrophages (TAMs) and CCL2 and CCL5 are major attractants for monocyte precursors into tumour sites [267]. TAMs are associated with tumour progression, and are recruited in large numbers in response to chemokines. They are implicated in neoangiogenesis and are thought to have suppressive effects on anti-tumour T cells, thus TAMs are associated with more aggressive disease and poorer outcomes in a wide range of

tumours including breast cancer, melanoma, colon cancer and pancreatic cancer. The production of CCL2 and CCL5 has frequently been detected by both stromal and malignant cells in these tumours [Reviewed in 268]. Chemokines also play a role in the recruitment of neutrophils, dendritic cells, NK cells and tumour infiltrating lymphocytes into tumour sites.

Tumour angiogenesis is central to tumour progression and survival, and chemokines have been shown to have a central role here. Pro-angiogenic chemokines including CXCL5 and CXCL8 act upon the CXCR1 and CXCR2 expressing endothelial cells to promote proliferation and down regulate apoptosis, thereby promoting angiogenesis. The presence of these chemokines has been detected in a number of tumours including, prostate and renal carcinoma, and are associated with tumour angiogenesis and subsequent disease progression [269, 270]. The CXCR4/CXCL12 axis also has a significant role in angiogenesis. CXCR4 is expressed on endothelial cells, and proliferation and cellular migration is induced by CXCL12. However angiogenesis has also been seen to be stimulated via a synergistic action between CXCR4 and VEGF in ovarian tumours [271]. In addition, the CXCR4/CXCL12 axis assists in the migration of endothelial cells, and thus subsequent angiogenesis, to tumour sites and the bone marrow.

As previously described, the CXCR4/CXCL12 axis is integral to the maintenance of stem cells within their bone marrow niche, as well as their involvement in endothelial cell migration, thus explaining the fact that the bone marrow is one of the favoured sites of CXCR4-dependent metastasis in a number of tumours. In contrast, CCR7 is involved in the homing of lymphocytes to the secondary lymphoid organs in response to CCL19 and CCL21. CCR7 expression has been shown to be unregulated in those tumours with lymph node metastases, and is likely to be predictive of the development of lymph node metastases when detected in tumours [Reviewed in 272].

Finally, the atypical chemokine receptors have also been implicated in tumour biology. D6 plays an anti-inflammatory role by sequestering inflammatory chemokines. Two recent papers have suggested that D6 also has a tumour suppressor affect. In both cases murine models were used to induce either skin or colitis associated cancers, with the observation that a greater susceptibility to tumour development and progression was noted in D6^{-/-} mice [269, 273]. In contrast, the atypical receptor CXCR7 seems to act in a tumour promoting fashion. CXCR7 is expressed on transformed but not normal cells and binds to CXCL12 and CXCL11 with great avidity. Its role as a tumour promoter is demonstrated by

the fact that inhibition leads to poorly vascularised and smaller tumours, whilst its expression in malignancies such as prostate and lung cancer is associated with more aggressive disease and a higher risk of recurrence following resection [274].

Thus, chemokines and their receptors have diverse roles in the development and progression of a range of malignancies, and represent viable therapeutic targets.

1.4.2 Chemokines and Lymphoma Development

In contrast to solid tumours, there is evidence to suggest that the chemokine expression found on malignant lymphocytes reflects the physiological expression of the stage of differentiation at which they are ‘trapped’ [Pals et al. 269] see figure 1.13. However, this is not the whole story and chemokines have been directly implicated in the development of lymphomas under chronic inflammatory conditions [275]. As previously discussed chemokines CXCL13 and CCL21 play a central role in the organisation of secondary lymphoid tissues. Studies have shown that inducing ectopic expression of CXCL13 and CCL21 in areas such as the pancreas result in the development of ectopic lymphoid tissue [276, 277]. Can demonstration that, ectopic lymphoid tissue can be induced under experimental conditions, provide an insight into the role of chemokines in the pathogenesis of lymphomas? In the case of those lymphomas associated with chronic antigenic stimulation, such as MALT lymphomas and other B-cell lymphomas, it provides some explanation. For example, lymphoma of the thyroid is uncommon, but when diagnosed the majority of patients have a history of autoimmune thyroid disease [278]. Histological examination of specimens from those with autoimmune thyroid diseases such Hashimoto’s thyroiditis or Grave’s disease reveal the presence of ectopic lymphoid tissue, furthermore it has been demonstrated that CXCR5 and CXCL13 have a major role in the maintenance of this tissue [279]. Whilst, the final trigger for lymphomatous transformation is unclear, what is clear is that chemokines have a role in the pathogenesis of thyroid lymphomas with a greater than 60 fold increase in incidence noted in patients with autoimmune thyroid diseases [280]. Similar patterns are seen in other autoimmune disorders such as Sjögren’s Syndrome and chronic infections including *Helicobacter pylori*.

However, in primarily nodal lymphomas (the majority), the role of chemokines in pathogenesis is less clear. Certainly, chemokine expression has been examined in a number of differing lymphoma subtypes, with particular interest on the microenvironments, although whether the malignant cell creates the microenvironment or vice versa is not all together clear. The lymphoma subtype in which the microenvironment has been best studied is actually Hodgkin’s lymphoma, where <1% of the cells are malignant. The Reed-

Sternberg cells have been shown to release CCL17, a ligand for CCR4, which goes some way into explaining the high numbers of T-cells in the surrounding cellular milieu in Hodgkin's lymphoma.

Some discussion of the microenvironment in the pathogenesis of lymphoma, including the role of chemokines, was discussed earlier during the discussion of lymphoma pathogenesis, yet further points are worth discussing. It is increasingly clear that the microenvironment has a role in the pathogenesis of lymphomas. Such examples include CLL and mantle cell lymphomas (MCL). Mesenchymal stem cells (MSC) are found in the bone marrow and release CXCL12 amongst other cytokines, which has been shown experimentally to lead to the migration of CLL and MCL to these areas. Following migration adhesion molecules such as VLA-4 lead to retention and provide pro-survival signals, including adhesion-dependant drug resistance [281, 282].

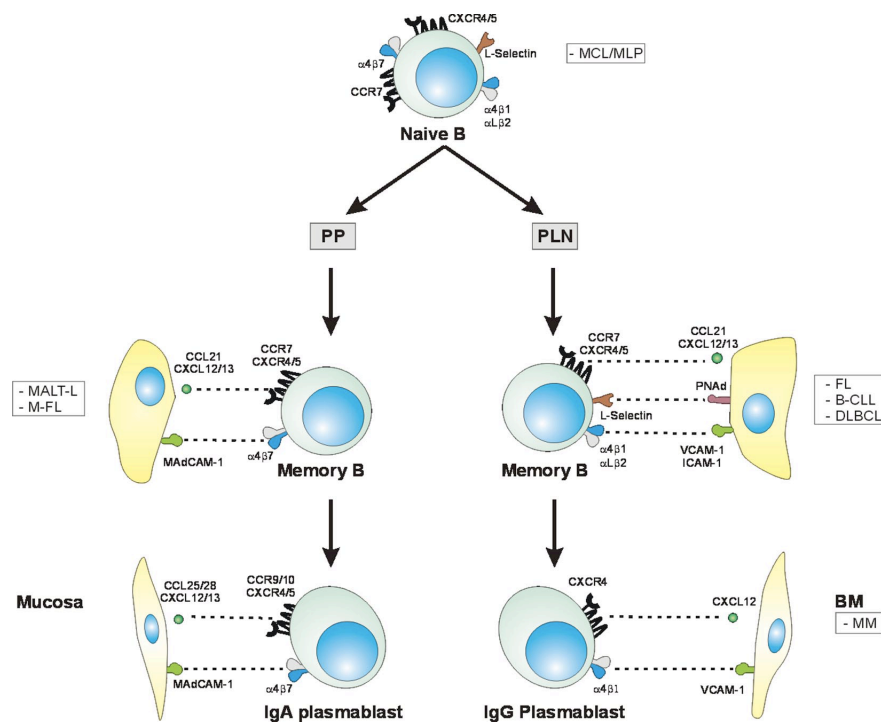


Figure 1.15: Demonstration of chemokine receptor expression at different stages of B-cell differentiation and the corresponding lymphoma sub-types. Taken from Pals, 2007 [283]. PP – Peyer's patches, PLN – peripheral lymph node, BM – bone marrow, MCL – mantle cell lymphoma, MLP – malignant lymphomatous polyposis, MALT-L – mucosa associated lymphoid tissue lymphoma, FL-follicular lymphoma, DLBCL – diffuse large B-cell lymphoma, MM – multiple myeloma.

1.4.3 Lymphoma Subtype and Chemokine Expression

A full discussion of all of the various lymphoma subtypes and the chemokines studies performed with them is out with the scope of this discussion, and only a selection of them will be discussed. A number of the initial studies were performed using lymphoma cell lines, however what follows will primarily relate to studies on primary tissue.

In general CXCR4 and CXCR5 are expressed on the majority of B-cell lymphoma subtypes, and therefore expression alone does not provide a clear differentiation between subtypes [Pals et al 275]. However, CXCR5 and its ligand CXCL13 have been shown to be of value in distinguishing angio-immunoblastic T-cell lymphoma (AITL) from other types of T-cell lymphoma and Hodgkin's lymphoma. AITLs are composed of follicular T helper cells, which secrete CXCL13 [275] and up-regulate CXCR5. This is thought to occur in response to the presentation of EBV viral proteins, leading to T helper cell activation, thereby leading to a positive feedback loop involving B- cells and the malignant follicular T helper cells [284]. The expression of CXCL13 in AITL has now been recognised as part of the distinct immunophenotypic profile and is of diagnostic value [Swerdlow et al 285]. Whilst chemokine receptor expression in most B-cell lymphomas cannot help distinguish between subtypes, or even their normal B-cell counterparts, with heterogeneity demonstrated in studies, some research has shown that there are differences between the responses of malignant and normal B-cells to chemokines. One example is mantle cell lymphoma (MCL), chemokine receptor expression in MCL B-cells and normal CD5+ cells are similar, both expressing CXCR4 and CCR7 amongst other receptors. However, the MCL B-cells demonstrate migration in response to CCL19 whilst their normal counterparts do not [176]. Moreover, chemotaxis in response to CCL19 is enhanced by exposure of the cells to CXCL12 [286]. Whilst these differences may simply reflect differences in the numbers of cell surface receptors, it does suggest that disrupting the CCR7/CCL19 axis will have a detrimental affect on MCL B-cells.

Of course, one group of lymphomas in which chemokine expression is specific is in the cutaneous lymphomas. In cutaneous T-cell lymphomas (CTCL) and Sézary Syndrome (the rare leukaemic form of CTCL) the malignant T-cells co-express the skin homing receptors CCR4 and CCR10 [286].

Finally, expression and the response to ligands of receptors are not the only way in which differences between lymphoma subtypes can be demonstrated. The pattern of chemokine

receptor expression within the cell may also reveal differences. For example, CXCR4, CXCR5 and CCR7 can be detected in the malignant B-cells of primary central nervous system lymphomas. However in contrast to lymphomas with peripheral involvement, these receptors are present in the cytoplasm rather than on the cell surface [287], indicating that they may not respond to their corresponding ligands in the same way.

<i>Receptor</i>	<i>Expression on Lymphocytes</i>	<i>Expression on Lymphomas</i>	<i>Ligands</i>	<i>Predominant sites of homing</i>
<i>Adhesion Molecules</i>				
<i>L-selectin</i>	Naïve T & B cells, central memory T cells	B-CLL, MCL, MZBCL, nodal PTCL	PNAd (MAdCAM-1)	PLN
<i>CLA</i>	Skin homing T-cells	CTCL	E-selectin	Skin
<i>α4β7</i>	Naïve B & T cells, gut-homing T-cells, IgA plasma cells	GI-tract MCL, GI-tract MZBCL, GI-tract FL, EATL	MAdCAM-1 (VCAM-1)	Gut
<i>αEβ7</i>	Intraepithelial cells	GI-tract PTCL, GI-tract MZBCL	E-cadherin	Epithelium
<i>αLβ2 (LFA-1)</i>	Broad expression on B & T cells	Broad expression on B & T cell lymphomas, MM	ICAM-1, ICAM-2	Multiple sites
<i>α4β1 (VLA-4)</i>	Broad expression on B & T cells	Broad expression on B & T cell lymphomas, MM	VCAM-1	Inflammatory sites & bone marrow
<i>Chemokine Receptors</i>				
<i>CCR4</i>	Skin-homing T-cells	CTCL, A-TLL	CCL17, CCL22	Skin
<i>CCR7</i>	Naïve T-cells, central memory T cells	CTCL, CLL, MCL	CCL19, CCL21	PLN
<i>CCR9</i>	Gut homing T cells, intraepithelial T cells, IgA plasma cells	Unknown	CCL25	Intestinal mucosa & crypt epithelium
<i>CCR10</i>	Skin homing T cells, IgA plasma cells	CTCL	CCL27, CCL28	Skin, intestine
<i>CXCR4</i>	Pre-B cells, B cells, plasma cells	Broad expression on B & T cell lymphomas, MM	CXCL12	Secondary lymphoid tissues & BM, migration to germinal centres
<i>CXCR5</i>	Mature B cells	Broad expression on B & T cell lymphomas, MM	CXCL13	Migration to GCs in PLN and Peyer patches

Table 1.9: Adhesion molecule and chemokine receptor expression on lymphoma subtypes and the normal lymphocyte populations along with the anatomical distribution where applicable [Adapted from 288].

1.4.4 Expression and Clinical Stage

There is limited information with regards to the stage of disease and chemokine expression in lymphomas. However one lymphoma in which chemokine receptor expression correlates with disease stages is in CTCL. An intriguing observation has been the reduction in CCR4 expression in those with CTCL as the lymphoma progresses to more advanced stages whilst a corresponding increase in CCR7 expression is noted [275], suggesting that there is a gain in the lymph node homing ability of the cells whilst skin-homing capabilities are diminished.

Of interest, in an associated disease B-cell acute lymphoblastic leukaemia, higher CXCR4 expression has been correlated with the presence of extramedullary disease demonstrating a more advanced disease presentation [289]. This also has implications for prognosis with extramedullary disease being associated with an adverse outcome.

1.4.5 Expression and Prognosis

Again there is limited information on the role of chemokines in the prognosis of non-Hodgkin's lymphoma. As described previously, stromal signatures and chemokines in the microenvironment impact on the prognosis of follicular lymphomas and diffuse large B-cell lymphomas.

However, one of most detailed associations described is the impact of CCR4 expression in Adult T-cell leukaemia lymphoma (ATLL), in which ~88% of cases demonstrate CCR4 expression on the malignant cells [290]. Further analysis has shown that the CCR4⁺ cases have a significantly poorer prognosis than CCR4⁻ cases [291].

Whilst the study did not specifically address prognosis, the role of CXCR3 in the responsiveness to therapy in *Helicobacter pylori* positive cases of gastric MALT lymphomas has been investigated. Yamamoto et al demonstrated that expression of CXCR3 by the malignant cells was associated with an increased risk of non-responsiveness to *Helicobacter pylori* eradication [291]. Therefore it is reasonable to postulate that such cases will require chemotherapy or localized radiotherapy to obtain effective treatment, and testing for CXCR3 expression may be of value in guiding treatment.

1.4.6 Using the Chemokine System as Targeted Therapy

1.4.6.1 General Principles

There is no doubt that the chemokine system is an attractive target for a wide range of diseases including lymphoma. There are a number of ways in which the system could be targeted and two of these have now progressed beyond phase 3 clinical trials into daily clinical use. The most obvious ways include the development of monoclonal antibodies or small molecule antagonists. However, another approach is that of forming a chemokine-cytotoxic ligand. This latter approach could involve conjugation with a radioisotope, cytotoxic agent or even a viral vector. Work has been done in all of these areas, some of which will be explored below.

1.4.6.2 Small Molecule Antagonists of Chemokine Receptors

Currently this is where most of the work has been concentrated. Two chemokine receptor antagonists, plerixafor and maraviroc, are now in clinical use. The first, plerixafor, is a CXCR4 antagonist and was initially developed as an anti-HIV agent. However, it was noted that it led to the release of haematopoietic stem cells into the circulation, and has since been developed and marketed as a new agent to mobilise stem cells prior to harvesting and haematopoietic stem cell transplantation in those who respond poorly to G-CSF. It has been shown to be effective in previously treated patients with myeloma and non-Hodgkin's lymphoma [292]. In addition, stem cells collected following mobilisation with plerixafor have been shown to be as efficient in engrafting as those obtained with G-CSF alone [293]. Furthermore, it has been postulated that plerixafor could be utilised in an attempt to mobilise malignant cells out of protective bone marrow niches and into the circulation where they would be susceptible to cytotoxic agents. However there are concerns that this approach may affect self-renewing stem cells and therefore any agents used should be targeted to the malignant population. Consequently, early clinical studies are underway, using this approach in CLL combined with the administration of rituximab to improve the depth of response.

Maraviroc is an antagonist of CCR5. CCR5 along with CXCR4, acts as a co-receptor with CD4 to allow entry of HIV into cells. A mutation in the receptor, CCR5 $\Delta 32$, is associated with resistance to HIV infection [294] and therefore provided a natural proof-of-principle that inhibiting CCR5 would provide benefit in infected individuals. The MOTIVATE 1 and MOTIVATE 2 trials investigated the use of maraviroc in addition to standard anti-retroviral therapy in those infected with the R5 HIV-1 virus (which predominates in the

earlier stages of infection). The addition of maraviroc demonstrated greater efficacy when compared to placebo in reducing HIV-1 loads and increasing CD4 counts [82] and thus has been added to the armature for the treatment of HIV. Further CCR5 antagonists are in trial or development.

1.4.6.3 Antibody Therapy Targeting the Chemokine System

With the success of monoclonal antibody therapies such as rituximab, there has been much pharmaceutical interest in the development of antibodies for use in a wide range of disorders. The discussion that follows explores the current picture with regards to anti-chemokine receptor therapies in lymphoma.

One of the first reports of the effects of inhibiting chemokine receptors in lymphoma was by Bertolini et al. In their work CXCR4 neutralising antibodies were incubated with Namalwa cells (a human Burkitt lymphoma cell line), prior to injection into NOD/SCID mice and compared with non-incubated cells. In the CXCR4 antibody incubated group, 83% of the mice were alive and disease free >150 days post injection compared to the control group in which all mice died from disease by day 36. Moreover circulating malignant cells were detectable at higher levels in the CXCR4 antibody group at 24 hours [84] in keeping with disruption of the CXCR4/CXCL12 axis required for entry of cells into protective microenvironments.

Monoclonal antibodies against chemokine receptors for the treatment of lymphoproliferative disorders are also in development, one of which has reached clinical trial stage. The first of these is an anti-CCR7 antibody that was developed with the treatment of CLL in mind. CLL cells have high surface expression of CCR7 therefore this is a good and specific target for treatment. Murine *in-vivo* studies have demonstrated complement-mediated toxicity against CLL cells treated with anti-CCR7, with relative sparing of normal T-lymphocytes; however antibody dependent cell-mediated cytotoxicity was low [295]. These results show promise in using monoclonal anti-CCR7 antibodies for this disease, but are yet to enter clinical trials.

Finally, a monoclonal anti-CCR4 antibody therapy has reached the human clinical trials stage. KW-0761 a humanized anti-CCR4 antibody has been used in phase I clinical trials in patients with relapsed ATLL and peripheral T cell lymphomas. This has demonstrated that the treatment is generally well tolerated, with a third of patients demonstrating a response [296]. Phase II trials are awaited.

1.4.6.4 Chemotoxins and Gene Therapy

There has been an increasing amount of work on the conjugation of monoclonal antibodies with cytotoxic agents such as radioisotopes or cytotoxic drugs, in order to deliver targeted treatments. This approach can be taken with chemokines with the development of chemotoxins; chemokines that have been fused with toxic moieties. *In-vivo* studies with a chemotoxin containing CCL17 and a fragment of the *Pseudomonas* exotoxin 38, demonstrated that cutaneous T-cell lymphomas developing in NOD/SCID mice were significantly reduced in size following intra-tumoural injection of this agent [297]. However, the tumours eventually relapsed at which point resistance to further treatment had developed due to reduced surface expression of CCR4 on the tumour cells [298], perhaps indicating that whilst effective, further consolidative therapy would be required to affect a cure.

Finally, a recent case report has indicated that gene therapy may offer a therapeutic tool for those with HIV infection. An HIV-1 positive patient underwent an allogeneic stem cell transplant for acute myeloid leukaemia. His donor had been screened for the presence of the homozygous CCR5 $\Delta 32$ mutation, and the recipient's anti-retroviral therapy was discontinued at the time of the transplant. 20 months following the transplant the patient had no viral rebound, remained off anti-retroviral therapy and was still in remission [298]. Whilst this may initially appear to be a cellular based therapy, it highlights that stem cells could potentially be manipulated to contain the CCR5 $\Delta 32$ mutation, or as in this case, that donors could be genetically screened for the presence of it, prior to use in transplantation. In Summary there are a number of potential ways in which the chemokine system can be targeted to therapeutic effect, some of which have already made it into regular clinical use.

1.5 Adenoviral Vectors

In the previous section, gene therapy was briefly discussed as a potential modality for targeting the chemokine system. Stem cell transplantation is not feasible in the majority of patients, however there are other ways in which gene therapy can be provided, and the use of viral vectors such as adenoviruses and retroviruses have been the focus of research in many institutions. Adenoviral vectors are widely used in gene therapy studies due to their high capacity to transfer genetic material without integrating viral DNA into the host genome. They are also stable *in-vivo*, have a low risk of mutagenesis, and benefit from an understanding gained from decades of study [299]. What follows is an overview of adenoviruses, which were chosen as a potential vector for targeting the chemokine system with gene therapy in this project.

1.5.1 Overview

The adenovirus was first isolated from adenoid tissue in 1953. Since that time over 50 serotypes have been identified and these are divided into six subgroups A-F depending on features such as genetic organization, agglutination, nucleic acid homology and cross-immunoreactivity [300]. Adenoviral vectors (Ad vectors) generally have a low pathogenicity in immunocompetent people, although they are associated with enteric, urological, ocular and respiratory diseases including the common cold. Some subgroups, including A and B, have also been observed to have oncogenic potential in cell culture and animal studies, however, it remains to be clarified whether, these lead to malignancy in humans. Adenoviruses are of great interest as they are able to efficiently transfer genes into a wide variety of cells *in-vivo* and because of these qualities; Ad vectors have been widely employed as gene-delivery vehicles in a variety of applications including gene therapy. Some of these aspects are discussed below.

1.5.2 Structure of the Adenovirus

The adenovirus (figure 1.14) is a non-enveloped, double stranded virus, with a total molecular weight of approximately 150MDa. All of the subtypes have the same capsid structure into which up to 36kbp of DNA can be packed, aided by packaging proteins. The capsid is about 100Å in diameter with a 25-x icosahedral structure. This is composed of three polypeptides, the first, hexon (polypeptide II), forms the major viral antigen and is composed of 12 copies of a trimeric hexon protein. The penton base (polypeptide III) is formed by a complex of 2 proteins creating, the pentameric base. Finally, the fibre (polypeptide IV) is composed of a trimeric protein, which protrudes from the penton base

ending in the C-terminal knob domain. The latter two polypeptides are integral to adenoviral entry into the cell and are discussed below [Reviewed in 301].

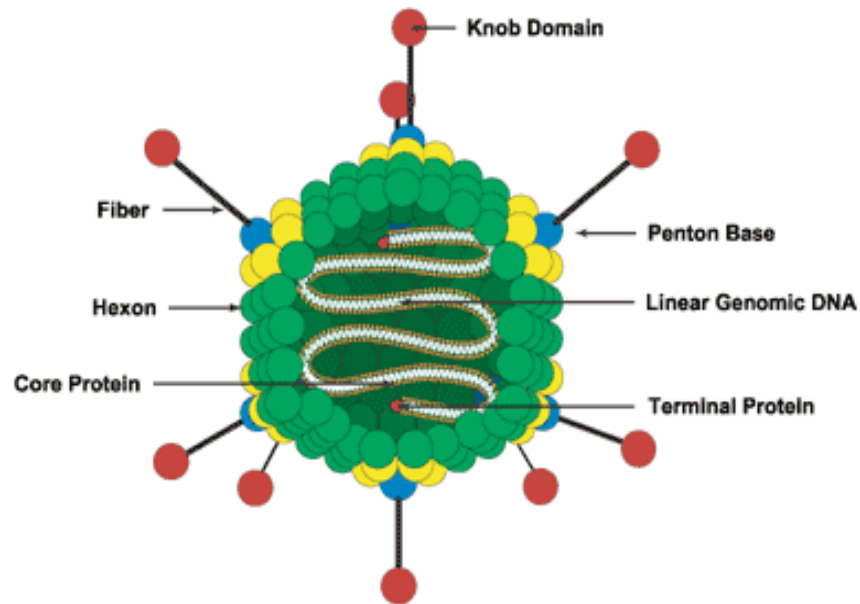


Figure 1.16: Diagrammatic representation of the adenoviral particle, with the major structural components labelled.

1.5.3 Components of Adenoviral DNA and Viral Replication

Within the wild type virus can be found 36kbp of DNA encoding a number of proteins responsible for the transformation of host cells, (i.e. incorporation of viral DNA into host DNA), evasion of host immune defenses and viral replication. The early DNA regions include E1A, E1B, E2, E3 and E4. E1A contains 3 regions leading to the transcriptional activation of the other early viral promoters and also drives transcription of the major late promoters leading to transcription of the structural late viral products forming the capsid [301]. E1A products also act as transcriptional repressors, preventing inhibition of cell-cycle arrest [302]. E1B has a role in infection and transformation, producing 2 proteins one of which has similarities to the anti-apoptotic BCL-2 protein. The second, along with the E4 open reading frame (ORF), forms complexes with the tumor suppressor p53 leading to abrogation of its transcription or even its degradation. These therefore serve to block apoptosis allowing for transformation of the cell [302].

E2 encodes proteins essential for viral DNA replication. Finally, E3 encodes at least 7 proteins that prevent the destruction of the infected cell by evading the host immune system such as preventing TNF induced apoptosis and the killing of cells by cytotoxic lymphocytes through blockade of MHC class I expression on the cell surface [302].

Once within the nucleus, replication occurs dependent upon the initiation primer or terminal protein along with “inverted terminal repeats” (ITRs) at either end of the origin of replication. A common late promoter then guides transcription of the structural elements after splicing of precursor transcripts [303]. The initial events occur 5-6 hours following infection with assembly of virions within the nucleus occurring at approximately 8 hours. 30-40 hours later proteolytic cell lysis results in the release of between 10^4 and 10^5 viral particles [304].

1.5.4 The Coxsackie and Adenovirus Receptor

Adenoviruses primarily gain entry into cells through attachment to the coxsackie-and adenovirus-receptor (CAR) via the knob domain of the virus (see figure 1.15). The mature human CAR is a type-1 transmembrane protein of 365 amino acids, which forms part of the conserved subfamily of the Ig superfamily [304]. The receptor is composed of an extracellular domain consisting of two Ig loops (Ig domain D1 and D2), the transmembrane domain and a variable cytoplasmic tail. The extracellular domain is involved in interaction and binding with the adenovirus as demonstrated by the continued ability of the CAR receptor to function with truncation of its transmembrane or cytoplasmic components. Mutational studies have demonstrated that the CAR receptor binds with residues on the AB, DE loops and β sheet of the adenovirus fiber knob, with the latter able to bind to three molecules of the former [305].

However, although the CAR receptor was initially described due to its association with adenovirus and coxsackie virus B, its physiological role is only just being understood, with a proposed role as an adhesion molecule. It is widely expressed in human tissues with hCAR mRNA being detectable in the liver, kidney, lung, brain, heart, colon, small intestine, testis, prostate and pancreas, with no expression in skeletal muscle (beyond the neonatal period), ovaries, thymus or placenta [306]. Furthermore, it has been difficult to infect haematopoietic cells, particularly lymphocytes, with adenovirus of the C subgroup (the most widely used vehicles in gene therapy), although CAR expression can be detected in 10-15% of CD34+ cells [307]. Expression in tumour cells is variable, probably reflecting their cell of origin.

What regulates CAR expression is unclear. However, CLL cells and peripheral blood lymphocytes can be rendered susceptible to adenoviral infection by activation with

cytokines such as IL-4, IL-2 and CD40L [307]. Whether this relates to up regulation of CAR on the cell surface or is due to other mechanisms, discussed later, remains to be seen. Finally, as mentioned, the physiological role of the CAR receptor is only just being elucidated. It has a clear role in development with maximal CAR expression detected in neonates in a wide range of tissues, including skeletal muscle, and a rapid fall in expression following birth [308]. Murine CAR knock out models have demonstrated a lethal phenotype at approximately day 11 due to multiple cardiac defects [309]. Interestingly, the potential role of CAR in neuronal development has recently been published where the interaction of the CAR Ig domain D2 with a fibronectin fragment including the heparin-binding domain-2 promoted neurite extension, whilst extension did not occur in its absence [309].

Therefore, whilst the precise physiological role of CAR is yet unknown, it is clear that it has a central role in the infectivity of adenoviruses.

1.5.5 Entry of Adenovirus into Cells

As described previously the extra-cellular membrane contains glycosaminoglycans (GAGs), which can bind chemokines and other molecules. However GAGs can also store viral particles such as herpes viruses, human immunodeficiency virus and adenoviruses. Whilst the trapping of adenoviruses in this milieu may reduce infectivity, it also provides a mechanism by which adenoviruses can enter cells [310]. Adenoviruses can enter cells by more than one mechanism, the most efficient of which involves the CAR receptor in all subgroups except B [311].

The first step occurs when the C-terminal knob domain of the fibre protein binds to the amino-terminal V-like Ig domain (D1) of the CAR receptor [312] via residues on loops AB, DE and the β sheet of the fibre protein [305, 306]. The group B adenoviruses have been shown to enter cells via CD46 [311]. Following initial binding, $\alpha_v\beta_3$ or $\alpha_v\beta_5$ integrins (other integrins may also be involved) in the cell membrane act as co-receptors through interaction with the highly conserved RGD motif present in the penton base, with as many as 5 integrins binding at once to form a ring-like structure. This stage is essential for receptor internalization [301]. The clustering of integrins leads to their conformational change resulting in stimulation of the intracellular pathways responsible for the induction of internalization via clathrin-coated pits to endosomes [313]; a system that has been described previously with chemokine/receptor internalization. During this process the capsid is partially disassembled via fiber shedding [314]. As the pH falls, the remaining

capsid is released from the endosomes and transported along microtubules to the perinuclear envelope where further capsid degeneration occurs before the viral DNA is imported into the nucleus [315].

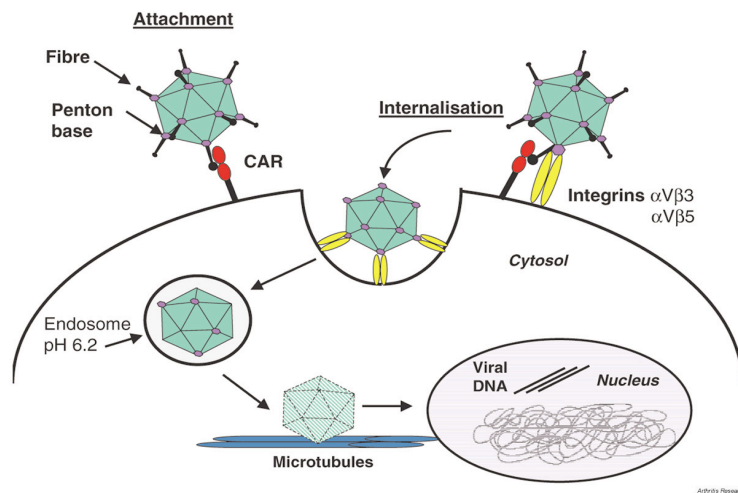


Figure 1.17: An overview adenoviral internalization following attachment to CAR and subsequent integrin mediated endocytosis. The first step entails binding of the fibre knob protein with CAR. Following this α -integrins interact with the RGD motif on the penton base thereby facilitating internalisation by endocytosis and subsequent incorporation into endosomes. The virion is subsequently disassembled allowing incorporation of viral DNA into the nucleus of the host cell. [Taken from 301].

Yet, ablation of the CAR receptor does not prevent adenoviral entry into cells altogether. This has been shown in experiments in which ablation of CAR receptor binding via alterations in the Y477 residue within the CAR binding region of the fibre protein has been engineered. In these studies, adenoviral infection was not abrogated with biodistribution of the virus remaining unchanged including infection of hepatocytes. However, the infectivity of the virus was greatly reduced [316, 317]. It is likely that CAR independent entry of adenovirus into cells is mediated by integrins in most instances. This has recently been demonstrated in a study of adenoviral infection in low CAR expressing cell lines, in which adenoviral infectivity could still be detected and blockade of the CAR receptors by incubation with soluble fiber proteins did not affect this. However antibody blockade of the penton base RGD motif blocked infection, suggesting that it was the interaction with integrins guiding adenoviral entry into the cell. Additional, analysis confirmed that it was indeed $\alpha_v\beta_5$ integrins that were responsible for the attachment and internalization of viral particles [318]. This contradicts earlier studies, which suggested that integrins were only able to promote internalization [319]. Other integrins have also been implicated including $\alpha_M\beta_2$ integrins, which have been shown to mediate adenovirus entry, and thus gene delivery, into haematopoietic cells [313].

Furthermore, other mechanisms have been observed. Amongst these is the ability of the viral fibre knob domain of (adenovirus 5) Ad5 to bind directly to certain vitamin K dependent coagulation zymogens, namely factors; FX, FVII, FIX and protein C, to promote viral entry into hepatocytes and Kupffer cells, in conjunction with complement factor C4BP. This is achieved through the interaction of heparan sulphate on the cell surface and low-density receptor-related protein. Furthermore inhibition of these zymogens with warfarin led to a significant reduction in the infectivity of the virus. Further tests showed that CAR-independent mechanisms were responsible in Kupffer cells [308, 320]. Therefore, it is clear that adenoviral entry into cells is complex with a number of potential mechanisms at play depending upon the adenoviral subtype, cell type and microenvironment with other mechanisms not discussed here also discovered. But what is clear is that entry via attachment with the CAR receptor is the most efficient means of getting the virus into cells.

1.5.6 Adenovirus and Gene Therapy

Adenoviruses have been used in hundreds of clinical trials, including attempts to introduce a functioning transgene for monogenetic disorders and in the treatment of certain malignancies often involving induction of cell death in cancers. To date the majority of clinical trials have been for cancer and although only a minority have reached phase III studies, the treatments in these patients appear to have a low level of toxicity, with 1000's of patients having undergone such treatments [321].

The first generation of adenoviral viral vectors, were developed with the replicative E1 viral DNA being deleted (and sometimes E3) and replaced with the transgene of interest [304](see figure 1.16). In order to replicate the adenovirus, helper cell lines were developed with the necessary replicative elements, the first amongst these being the human embryonic kidney 293 (HEK293) cells [304]. However, these vectors were not efficient enough, proved toxic and were cleared from the circulation quickly due to cytotoxic T-cell mediated immunogenicity. The second generation of vectors had further viral encoding elements removed, namely E2 and E4. However more complex helper-cell lines were required, and whilst transgene expression was improved, there were debates regarding the true reduction in toxicity and immunogenicity. This was highlighted in the only mortality to date directly associated with adenoviral vector therapy, in which a patient receiving therapy for partial ornithine transcarbamylase (OTC) deficiency, died following the

administration of a high titer of a second-generation vector engineered to transfect the gene for OTC into hepatic cells [322].

High-capacity (HC) or “gutless” Ad vectors have since been developed which are devoid of all of the virus coding genes except the internal terminal repeats and packaging signal (ψ), on which replication depends. As a result these HC Ad vectors are able to accommodate up to 36kb of non-viral DNA, leading to a considerable reduction in toxicity and immunogenicity *in-vivo*. Non-coding ‘stuffer’ DNA is incorporated into constructs where necessary to allow for a package-able size of between 28 and 36Kbp [323]. However, without the viral elements required for replication a variety of systems involving plasmids, strains of *E.coli* and helper-cell lines are employed to assist in replication and assembly of these vectors. Further details can be found in chapter 5.

Once the virus has gained entry into the cellular target, transgene expression or cytotoxicity can be elicited in a variety of ways. To drive expression of the transgene, widely expressed promoters can be employed, most commonly the CMV promoter, followed by the gene of interest. If cytotoxicity of malignant cells is the aim, the transgene expressed can encode ‘suicide’ genes causing apoptosis directly or indirectly. These are termed oncolytic viruses. In the latter case, genes such as thymidine kinase or bacterial nitroreductase are inserted. These enzymes then enable the conversion of pro-drugs such as ganciclovir in the case of the former and CB1954, in the case of the latter, into the active metabolites which will then elicit death in these cells, therefore providing a level of specificity [304, 324].

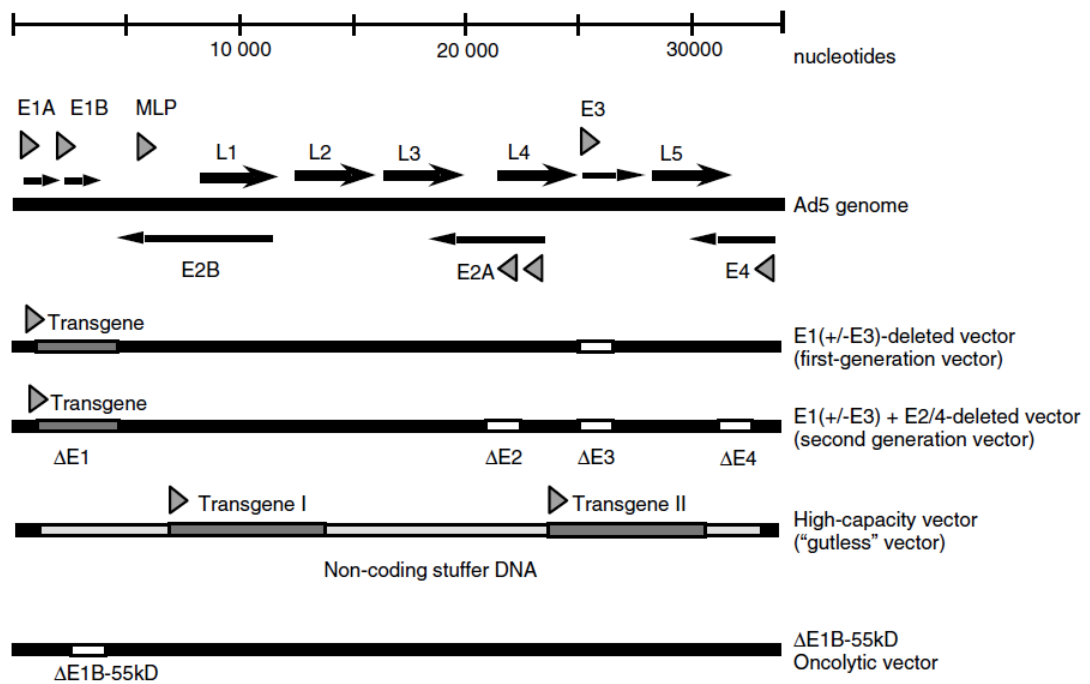


Figure 1.18: Diagram demonstrating the various components of adenoviral genome in the different vector generations. E=early promoters, L=late promoters. [Taken from 325].

1.5.7 Targeting Specific Cells with Adenoviral Vectors

1.5.7.1 Conditionally-Replicating Adenovirus and Tissue-Specific Promoters

Further specificity can be gained by replacing ubiquitous promoters such as the CMV promoters with those that are specific for the target cell in question, i.e. tissue specific promoters, or by the production of conditionally replicating viruses. In the latter case mutations are engineered in the E1B region encoding for those proteins that disable tumour suppressors such as p53. This adds a degree of specificity in that viruses will only be able to replicate in those cells in which p53 is deficient, i.e. tumour cells rather than normal cells. Following replication, cell lysis then occurs with release of the viral particles locally, and potentially systemically, to infect other p53 deficient cells [304].

Tissue specific promoters provide a further level of specificity with a wide range having been used in clinical studies including prostate-specific and bladder urothelial-specific promoters [326]. Another reported promoter is telomerase. This has the advantage of being switched off in most adult somatic cells; although expression remains in germ cells, stem cells, certain long-lived lymphocytes and the majority of tumor cell lines, and it can therefore be argued that it has a wider range of applications in cancer gene therapy.

Telomerase prevents the attrition of telomeres caused by cell divisions and therefore contributes to the immortalisation of malignant cells [327]. This has been shown to be an effective strategy when combined with a ‘suicide’ gene such as bacterial nitroreductase in pre-clinical studies and clinical trial data are now awaited [328]. Another strategy in cancer gene therapy uses the adenovirus vector as a vaccine to enable an immune response to be mounted against telomerase proteins with some promising early clinical trial results [325].

1.5.7.2 Redirection of adenoviral tropism

One problem with adenoviral gene therapy has been the lack of specificity in the biodistribution of the virus. One of the reasons for this is the wide expression of CAR, which consequently limits the application of adenoviral gene therapy due to its wide anatomical expression or due to lack of expression on the cellular target. As such, an approach to this problem is to block endogenous viral tropism whilst simultaneously re-directing it through a receptor on the cell of interest.

There have been a variety of strategies employed to achieve this including chemical modification of the capsid, the use of cross-linked neutralizing antibodies, genetic incorporation of a fibre protein from a different serotype and the genetic incorporation of a peptide ligand into elements of the fibre proteins or penton base. These ways of redirecting the virus essential coat the virus with a different antigens and proteins, thus ‘shrouding’ the virus thereby blocking entry through its natural receptor and redirecting it through the receptor of interest. The term ‘shrouding’ is used later in this thesis to describe this approach, which is used in this project.

The first reports of successful adenoviral tropism redirection were published in 1996. In the first, an adenovirus was constructed with heparin-binding domains incorporated into the C-terminus of the fibre knob, thereby redirecting tropism to heparan-containing receptors on the cell surface [329]. Further experiments have demonstrated that peptides exceeding 50% of the size of the knob domain (>100 amino acid residues) can be incorporated into the fibre without significantly affecting its functional properties [330]. Douglas et al described the use of neutralizing anti-fibre antibodies conjugated with folate to redirect through folate receptors [331].

Chemical modification of the capsid has been described using biotinylation and binding with bifunctional polyethylene glycol (PEG) and polymer coating the virus [332]. This enables the virus to be ‘shrouded’ in a peptide of choice to allow redirection. For example

biotinylation followed by incubation with avidin and then antibodies against c-kit, CD34, IL-2 or CD44 allowed for entry of these vectors into haematopoietic stem cells (c-kit, CD34) or resting and activated T-cells (CD44) or activated T-cells (IL-2), thereby overcoming the issue of gaining entry into these low CAR expressing cells [304].

Finally, modifying the adenovirus by ‘fibre switching’ is another approach. By replacing the fibre of Ad5 with that of Ad35 (Ad5F35), the tropism of the virus is redirected through CD46, which is present on many haematopoietic cells. This approach has been taken to transfect leukaemia and lymphoid cells. In the former case a conditionally replicating Ad5F35 chimera was engineered to express tumor necrosis factor-related apoptosis-inducing ligand (TRAIL), thus inducing apoptosis in the targeted leukaemia cells [333]. Ad5F35 vectors have demonstrated an improved transfection rate in lymphocytes, however, different lymphoid cell lines demonstrated differing levels of transduction, which was more dependant on the intracellular pathways utilized by the virus than on the receptor of entry, indicating a further level of complexity required for the development of gene therapies in lymphoid disorders [334].

Whilst, it has now been clearly demonstrated that adenoviral tropism can be redirected, it should not be forgotten that adenoviruses can enter cells by more than one mechanism, and independently of CAR expression, therefore these approaches may not entirely abrogate the natural tropism of these viruses.

So, despite these advances in adenoviral gene therapy, approval from European and United States authorities for therapeutic administration has yet to be obtained. There are a variety of reasons for this including continued safety concerns, and the lack of results from Phase III clinical trials. Furthermore, as the last study demonstrates the effect of intracellular events on transduction may be unpredictable and require further study. Work is continuing to overcome the many issues with adenoviral gene therapy described above as well as those relating to low efficiencies in transgene expression, the reduction of immunogenicity (in those therapies aimed at continued transgene expression such as in haemophilia A), difficulties in anatomical targeting of the vectors and improving long-term expression of transgenes where needed. Yet, gene therapy remains a promising prospect especially in the field of cancer therapies.

1.6 Aims of Study

There were a number of aims in this project:

- **Investigation of the relationship between chemokine receptor expression and lymphoma sub-type.** Although there is emerging evidence to suggest that there might be such a relationship this was to be investigated further. To do this a system to assess clinical samples from patients with a range of B-cell NHL subtypes for constitutive chemokine receptor expression was required.
- **Correlation between chemokine receptor expression and clinical outcome.** There is limited evidence to support a correlation between chemokine receptor expression in B-cell NHL subtypes and outcome. Therefore following assessment for chemokine receptor expression in B-cell NHL subtypes correlation with clinical outcomes was to be performed.
- **Identification of potential chemokine receptor targets in non-Hodgkin's lymphoma.** It was also hoped that a study of clinical samples would provide information about potential therapeutic targets in NHL.
- **Targeting the chemokine system.** Utilising the chemokine system for targeted therapy was to be explored and experiments attempting to target the chemokine system with cytotoxic agents were performed. CCR7 was identified as a suitable target for these experiments. Initial targeting experiments used radiolabelled CCL19 to assess whether or not cell kill would only be elicited in CCR7⁺ cells.
- **Using gene therapy to target the chemokine system.** The potential to use gene therapy with adenoviral vectors to deliver a 'suicide' gene to targeted cells was explored. However, before using adenoviral vectors containing 'suicide' genes a system to redirect adenoviral tropism through chemokine receptors had to be developed and this was explored in this thesis.
- **Development of a lymphoma mouse model for *in-vivo* targeting experiments.** A lymphoma mouse model was required for *in-vivo* targeting experiments. The aim therefore was to characterise a cell line, which could potentially be used for this purpose.

In summary, it was hoped that this project would provide novel data regarding chemokine receptor expression and its impact on outcomes in NHL, whilst also providing information on potential therapeutic targets. Additionally, it was hoped that approaches to successfully target the chemokine system with cytotoxic agents could be developed.

CHAPTER TWO

MATERIALS AND METHODS

2.1 Materials

2.1.1 Antibodies

Antibodies	Source
Primary Antibodies	
Mouse anti-hCCR4	R&D systems
Mouse anti-hCCR4 - allophycocyanin	R&D systems
Mouse anti- hCCR6	Abcam
Mouse anti-hCCR7	R&D systems
Rat anti-mCCR7-FITC	Abcam
Mouse anti-hCCR9	R&D systems
Mouse anti-hCCR9-allophycocyanin	R&D systems
RatAnti-hCCR10	Abcam
Mouse anti-hCXCR4	R&D systems
Mouse anti-hCXCR4-allophycocyanin	R&D systems
Mouse anti-CD20-phycoerythrin	Becton Dickson
Mouse anti-hexon	Becton Dickson
Mouse anti-hexon	Chemicon
Secondary Antibodies and Detection Reagents	
Viaprobe	Becton Dickson
IgG2A-allophycocyanin (isotope control)	R & D Systems
IgG2B-allophycocyanin (isotype control)	R & D Systems
IgG2B-phycoerythrin (isotype control)	Becton Dickson
Goat anti-mouse IgG-allophycocyanin	R & D Systems
Goat anti-mouse IgG -phycoerythrin	Sigma
Goat anti-rat IgG-phycoerythrin	R&D Systems
Streptavidin-phycoerythrin	Invitrogen

2.1.2 Bacteriology

Item	Supplier
Ampicillin	Sigma-Aldrich
90mm bacteriological Petri dishes	Sterilin
0.1mm Electroporation Cuvettes	Invitrogen
0.2mm Electroporation cuvettes	Invitrogen
Escheria coli BJ5187 cells	Stratagene
Escheria coli Ad-1 BJ5187 cells	Stratagene
Escheria coli DH5a	Invitrogen
ER2925 dam- cells	NEB
Kanamycin	Invitrogen
LB (Luria Burteni) Agar (sterile)	GBRC Central Services
LB broth (sterile)	GBRC Central Services
NZY broth	GBRC Central Services
SOC medium	Invitrogen
Tetracycline	Sigma-Aldrich
XL Blue Supercompetent cells	Stratagene
XL Gold Supercompetent cells	Stratagene

2.1.3 Cell Culture

Item/Reagent	Supplier
Bijoux/ Universal containers	Bibby Sterilin
Blasticidin	Invitrogen
4 well Chamber slide	Nunc
Cryotubes	Nunc
Distilled water (sterile)	GBRC Central Services
DMEM cell culture medium	Invitrogen
Effectene Transfection Kit	Qiagen
Fibronectin	Sigma
Foetal calf serum	Invitrogen
Geneticin	Invitrogen
L-Glutamine 200mM	Invitrogen
HEPES 1M solution	Invitrogen
Penicillin/streptomycin	Invitrogen
Phosphate buffered solution (sterile)	GBRC Central Services
1ml, 5ml, 10ml, 25ml plastic pipettes	Costar
Polyfect Transfection Kit	Qiagen
Puromycin	Sigma-Aldrich
RPMI 1640 cell culture medium	Invitrogen
60mm, 90mm TC dishes	Sterilin
T25, T75, T175 TC flasks	Corning
6 well, 12 well, 24 well TC plates	Corning
96 well TC plates	Corning
TE buffer	Ambion
250ul, 1000ul Tips	Ranin
0.5% Trypsin	Invitrogen

2.1.4 Cell Lines

	Cell Origin	Source
CHO	Chinese hamster ovary	CRG cell bank
Daudi	Human Burkitt lymphoma, EBV positive	Prof. Ruth Jarrett
EL4	Murine Thymic lymphoma	ATCC
HEK.293	Human embryonic kidney	CRG cell bank
Jurkatt	Human T-lymphoblastic lymphoma	CRG cell bank
MOLT-4	Human T-lymphoblastic lymphoma/leukaemia	CRG cell bank
Raji	Human Burkitt lymphoma, EBV positive	Prof. Ruth Jarrett

2.1.5 Chemicals

Chemical	Supplier
Acetic Acid	Sigma
Acetone	Sigma
Agarose (electrophoresis grade)	Invitrogen
Bovine Serum Albumin	Sigma
Bromophenol Blue	Sigma
Chloroform	Fisons Scientific Equipment
Dimethyl sulfoxide (DMSO)	Fisons Scientific Equipment
Ethanol	James Burrough Ltd
Ethidium bromide	Invitrogen
Ethylene diamine tetra acetate disodium salt (EDTA)	Fisons Scientific Equipment
Glycerol	GBRC central services
Hydrochloric acid	Fisons Scientific Equipment
Methanol	Fisons Scientific Equipment
Paraformaldehyde	Sigma
Propan-2-ol	Fisons Scientific Equipment
Sodium acetate	Sigma
Sodium azide	Sigma
Tris-base	Fisons Scientific Equipment
TRIZOL reagent	Invitrogen

2.1.6 Miscellaneous

Item	Supplier
0.2ml Microcentrifuge tubes	Ambion
1KB DNA ladder	Invitrogen
1.5ml Microcentrifuge tubes	Eppendorf
15ml centrifuge tubes	Corning
24 well chemotaxis plate (3mm pore)	Corning
50ml centrifuge tubes	Corning
DEPC treated water	Ambion
Electron Microscopy Cribs	Professor Lawrence Tetley
Glass coverslips	Fisher Scientific Ltd
Glass slides	Fisher Scientific Ltd
Haemocytometer	Fisher Scientific Ltd
Nanovan	Nanoprobes
Poly-L-lysine	Sigma
Polypropylene FACS tubes	Becton Dickson
Sterile 0.2mm acrodisc filters	Gelman Sciences Ltd
Trigene	Medichem International
Vectashield with DAPI	Vector labs
Whatman 3mm filter paper	Whatman International Ltd

2.1.7 Molecular Biology

2.1.7.1 Plasmids

Item	Supplier
pAdEasy-1	Stratagene
pBlueScript KSII(-)	Stratagene
pShuttle-CMV	Stratagene
pShuttle-IRES-hrGFP-1	Stratagene
pShuttle-CMV-LacZ	Stratagene
pCR2.1 TOPO®TA	Invitrogen
pcDNA3.1/V5 His©TOPO®TA	Invitrogen
pEF6/V5-His TOPO®TA	Invitrogen

2.1.7.2 Oligonucleotides

Oligonucleotide Name	Oligonucleotide Sequence
Screening Oligos	
Actin (human and murine)	Forward - tccatcatgaagtgtgacgt Reverse - tactcctgcttgctgatccac
Actin (hamster)	Forward - gtggggcgcgccagggcacca Reverse - ctccttaatgtcacgcacgatttc
Alpha Integrin (human)	Forward - gttgggagattagacagagga Reverse - caaacagccagtagcaaca
Alpha Integrin (murine)	Forward - agtggtttggagcctctgtgag Reverse - cagaaaatccaaaatcgcagcc
hCAR	Forward - agctcctggtgttgcaataagaag Reverse - taagaccaatgagcgctagagcaag
mCAR	Forward - aatgtgaccaacctgcagct Reverse - agcacaagggccagcagcgt
hCCR4	Forward - gatatagcagacaccacctcgatg Reverse - tatgccactgtaaagcccaccaag
hCCR6	Forward - aggtcaggcagttctccaggctat Reverse - tgctgcgcggtagttctggatc
hCCR7	Forward - gtgctggtggtggctctcctgt Reverse - gtaggagcatgccactgaagaagc
mCCR7	Forward - gctcaacctggcctggcagacatcc Reverse - ccacttgatggtgatcaaggcctcc
hCCR9	Forward - atggctgatgactatggctctgaat Reverse - aatgtacctgtccacgctgatgca
hCCR10	Forward - ggtttcctggggccattactctg Reverse - gacggagaccaagtgtgcgcgg
hCXCR4	Forward - aggaaatgggctcaggggactatg Reverse - gatgaaggccaggatgaggacact
hCXCR5	Forward - taccgctaacgctggaaatggac Reverse - gtaggcatggacggcgtggacaat
AdV Flanking Forward	caaggcaaatgtagcaggaggac
AdV Flanking Reverse	cacgtggtgccaacattgatatca
Primers for sequencing	
CDS.hCCR7	Forward - atggacctggggaaacctatgaaa Reverse - ctatggggagaaggtggtggtg
CDS.mCCR7	Forward - atggaccagggaaaccgaggaaa Reverse - ctacggggagaaggttgtggtgt
Acceptor Peptide Insertion	Forward ttcgaggcccagaagatcgagtggcacgagtgatctagata aagaatcgtttgtgtt
	Reverse - ccactcgatcttctgggctcgaagatgctggtcaggcctctt gggcaatgtatga

2.1.7.3 Restriction Enzymes

Enzyme	Recommended Buffer	Supplier
<i>AflII</i>	NEBuffer 2	NEB
<i>ApaI</i>	NEBuffer 4	NEB
<i>BamHI</i>	REact 3	Invitrogen
<i>DpnI</i>	REact 4	Stratagene
<i>EcoRI</i>	REact 3	Invitrogen
<i>EcoRV</i>	REact 2	Invitrogen
<i>HindIII</i>	REact 2	Invitrogen
<i>KpnI</i>	NEBuffer 1	NEB
<i>MluI</i>	NEBuffer	NEB
<i>NaeI</i>	NEBuffer	NEB
<i>NotI</i>	NEBuffer 3	NEB
<i>NruI</i>	NEBuffer 3	NEB
<i>PacI</i>	NEBuffer 1	NEB
<i>PmeI</i>	NEBuffer 4	NEB
<i>PvuI</i>	NEBuffer	NEB
<i>Sall</i>	NEBuffer 3	NEB
<i>SbfI</i>	NEBuffer 4	NEB
<i>SpeI</i>	NEBuffer 2	NEB
<i>XbaI</i>	NEBuffer 2	Invitrogen
<i>XhoI</i>	NEBuffer 2	NEB

2.2 Methods

2.2.1 Obtaining Ethical Committee Approval for use of Patient Samples

In order to comply with the Scottish Human Tissue Authority Act (2006) Ethical approval was required before using clinical samples composed of lymphocyte preparations from affected lymph nodes. An online form was completed via the Central Office for Research Ethics Committees (COREC), via their website www.corecform.org.uk and was submitted to the Regional Ethics Committee. Ethical approval was granted on 17th April 2007.

2.2.2 Tissue Culture

All tissue culture was performed under sterile conditions within a class II biological safety cabinet with laminar flow. The adherent cell lines HEK.293 and CHO were grown in complete medium (1x DMEM with 10% foetal calf serum, 20mM L-Glutamine, penicillin (100IU/ml) and streptomycin (50µg/ml)). Before splitting, the cells were trypsinised using between 1 and 3ml of 0.05% trypsin-EDTA. The cells were then incubated at 37^oC for two minutes. After this the cells were examined microscopically to ensure that they had disassociated from the plastic, the trypsin was then neutralised with 5x volume of complete media, and then the cells were transferred to a 25ml universal container. Cells were spun at 660g for 5 minutes, the supernatant was removed and the cells re-suspended in fresh medium and split according to need, e.g. 1 in 10.

Non-adherent cells lines were split to a concentration of 2×10^5 cells/ml once or twice each week. EL4 cells were grown in 1xDMEM as outlined above. The cell lines; Daudi, Raji, MOLT-4, and Jurkat were grown in RPMI 1640 with 10% FCS, 20mM L-Glutamine, penicillin (100IU/ml) and streptomycin (50µg/ml).

2.2.2.1 Freezing Cells

2×10^6 cells were suspended in 900µl of the appropriate medium for the cell type. 100µl DMSO was then added to the cells (giving a 10% solution of DMSO). The cells were then transferred to cryotubes, before being placed in a "Mr Frosty" containing 250ml of isopropanol. This allows gradual cooling of the samples when the "Mr Frosty" is placed in the -70^oC freezer for 12-16hrs prior to transfer to liquid N₂ tanks for long-term storage

2.2.2.2 Defrosting cells

Cells were taken from liquid N₂ storage and placed into a waterbath at 37°C to thaw. The cells were then placed in a universal container to which 20ml of sterile PBS was added. The cells were then spun down at 660g for 5 minutes and the supernatant discarded. The cell pellet was then re-suspended in 10ml of the appropriate growth medium and transferred to a T25 flask

2.2.2.3 Counting Cells

To count the cells, a Neubauer haemocytometer was used. The cover slip was placed over the grid. 5ml of 0.4% (w/v) trypan blue was then added to 20µl of the cell suspension and the mixture was placed under the cover slip. The cells were then counted, with the number of blue cells noted. The blue cells stained with the trypan blue indicate those cells that are not viable as viable cells do not take up the dye due to intact membranes. Ideally at least 100 cells should be counted within the grid. The cell concentration is then calculated as follows:

$$\frac{\text{Number of cells in central grid}}{\text{Number of squares in central grid}} \times 10^4 = \text{cells/ml}$$

This figure was then multiplied by 1.2 to take into account dilution with the trypan blue solution.

Cell viability was then calculated as follows:

$$\% \text{ viable cells} = \frac{\text{number of viable cells}}{\text{Total number of cells}} \times 100$$

2.2.2.4 Transfection of Cells

2.2.2.4.1 Stable Transfection of HEK.293 and CHO Cells Using Effectene®

The day before transfection 60mm tissue culture plates were set up to contain 2.5x10⁵ cells and 4mls of complete DMEM for each vector to be transfected. An additional plate was set up to act as a control. The plates were examined the following day to ensure that the cells were between 40-80% confluent, prior to proceeding. The transfection was then carried out according to the manufacturers instructions using the Qiagen Effectene® transfection kit.

24 -48 hours following transfection the cells were assessed for protein expression. If stable transfectants were required then the complete medium was replaced with selective medium containing the appropriate antibiotic.

2.2.2.4.2 Transient Transfection of CHO Cells using Polyfect®

Cells were prepared and assessed for transfection as in 2.2.2.4.1 above. Once prepared, the cells were transfected using the Qiagen Polyfect® reagent, according to the manufacturers instructions. After 24-48hours the cells were assessed for protein expression and used as required.

2.2.2.4.3 Transfection of EL4 Cells by Nucleoporation

For each nucleoporation 1×10^6 cells were used per well of a 6 well tissue culture plate. The EL4 cells were nucleoporated using the Amaxa Nucleoporation Kit L, according to the manufacturers instructions. 24 hours after nucleoporation the cells were spun down and re-suspended in selective medium. At this point they were assessed for protein expression if required.

2.2.3 Analysis of Cell Fluorescence by FACS

a) HEK-293, CHO, and Lymphoma Cell Lines for Single Colour Detection

Cells from the experiments were collected into a 5ml polypropylene FACS tube, spun down and then re-suspended in 400 μ l of ice-cold FACS buffer (PBS with 2% FBS). Data acquisition was performed using CellQuest™ software on a Becton Dickson FACScan. Cells were gated using forward and side scatter (see figure 2.1). Negative controls were used such that >95% of the cells fell between 10^0 and 10^1 on the FL2-H (for phycoerythrin) or the FL1-H (for GFP) channels (see figure 2.1). Test results were analysed using 10,000 gated events, whenever possible, per sample. The data collected was analysed using either the CellQuest™ or FlowJo software programmes.

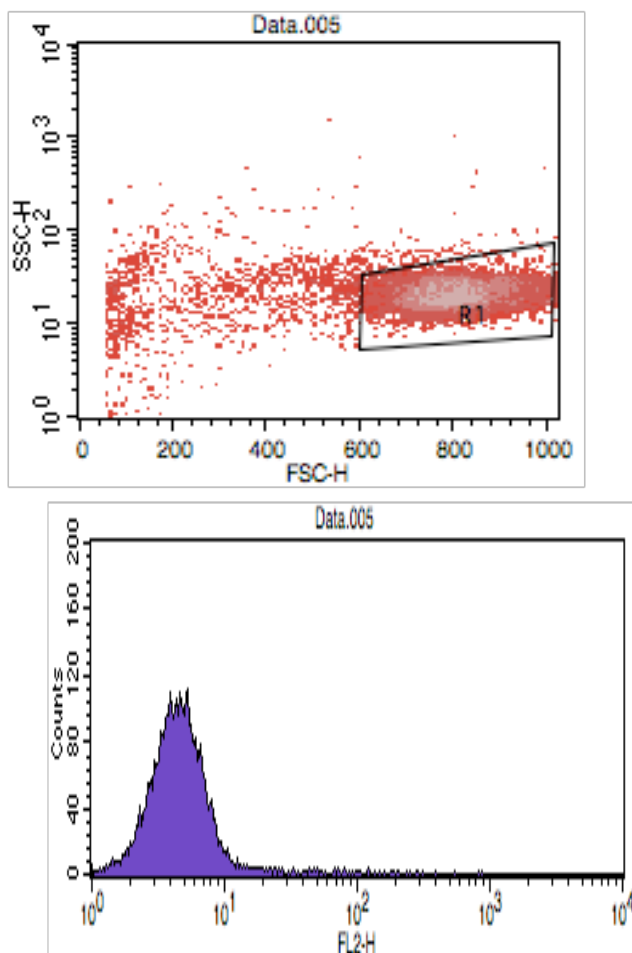


Figure 2.1: Gating for single-colour flow cytometry. Data acquisition of cells was performed using CellQuest™ software on a Becton Dickson FACScan. Cells to be analysed were gated using forward and side scatter as shown in a) demonstrating gating of Raji cells using a dot plot. b) Histogram plot of the same Raji cells used as a negative control, demonstrating that more than 95% of the cells are between 10^0 and 10^1 on the FL2-H gate.

b) Lymphoma cell lines and clinical samples for Two-colour Flow Analysis

After incubation of the cells with the antibodies, 10µl of Viaprobe (Becton Dickson) was added to each cell pellet, and incubated for 10 minutes at 4⁰C before being re-suspended in 400µl of ice-cold FACS buffer. Cells stained with Viaprobe are apoptotic or necrotic and detected on the FL3-H setting (figure 2.2), these were excluded from the final analysis. Forward and side scatter gating of the cells was then performed as before. Two-colour flow using FL2-H (phycoerythrin) and FL4-H (allophycocyanin) gates were then set up using double negative, FL2-H positive, FL4-H positive and double positive controls, with Raji cells as the control cell line. This ensured that any overlap in the light frequencies used was compensated for. Data was acquired using the Becton Dickson FACScan and analysed using either CellQuest™ or FlowJo software (Figure 2.3).

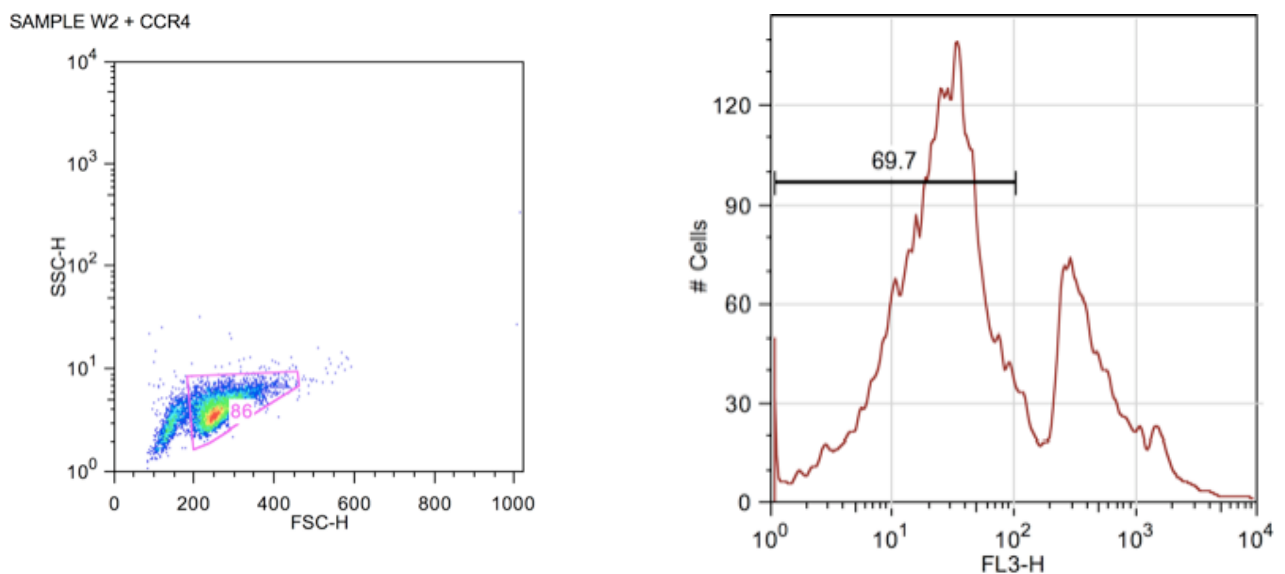


Figure 2.19: Determination of cell viability using ViaProbe. Cells were incubated with 5µl of ViaProbe for 5 minutes prior to analysis using flow cytometry. Cells of the correct size and granularity as determined by forward and side scatter were then gated as shown in a) demonstrating a dot plot with gating of the lymphocyte population to be analysed. Using a histogram plot, cells stained with ViaProbe produced a shift along the FL3-H gate, the peak shifted to the right represented non-viable cells and were excluded from further analysis as shown in b) this demonstrates the viable (FL3-H negative) population accounts for 69.7% of the cells gated in a).

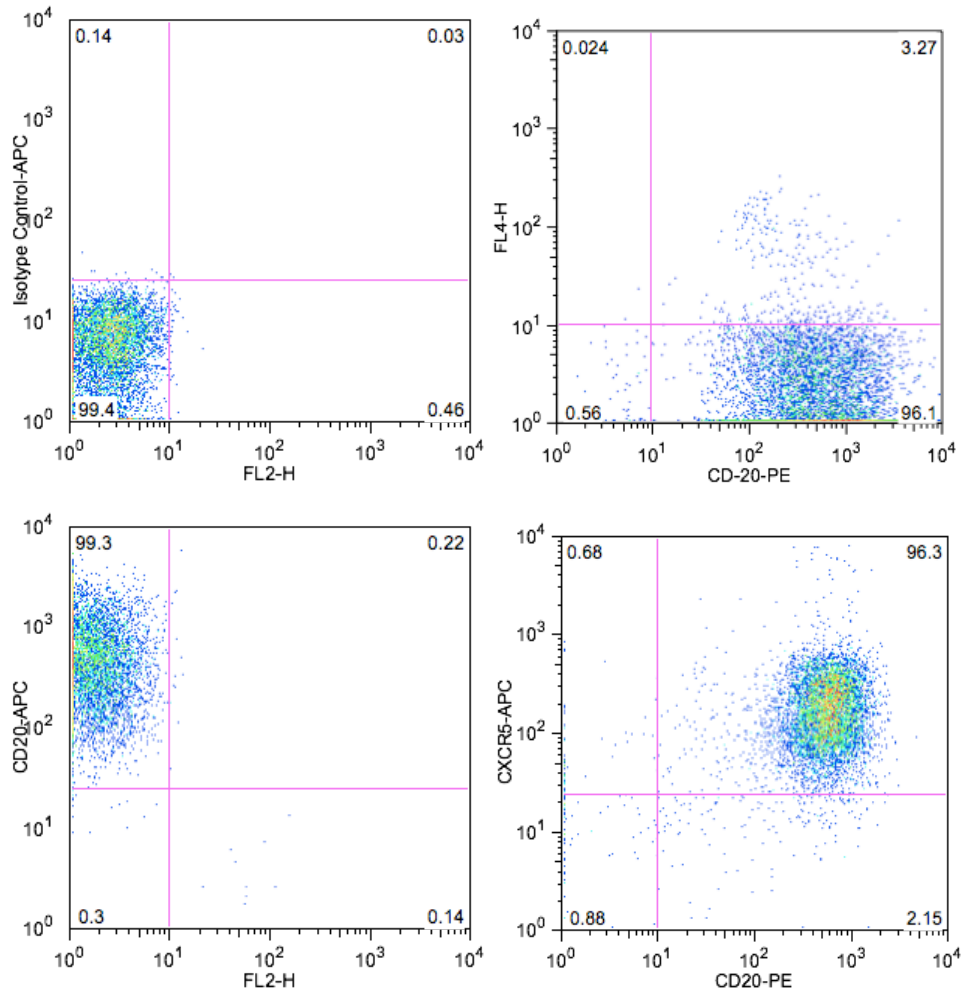


Figure 2.3: Setting up the flow cytometer for 2 colour analysis of lymphocytes. The figure in the top-left shows the negative control, and settings were adjusted to ensure that the cells incubated with isotype controls fell in the bottom left quartile. The figure in the bottom-right demonstrates how the settings were adjusted for compensation ensuring that the cells bound to antibodies conjugated with APC fell to the left of the line. The figure in the top-right demonstrates how the settings were adjusted for compensation ensuring that the cells bound to antibodies conjugated with PE fell below the line. The figure in the bottom right shows how analysis can proceed for double stained cells following compensation.

2.2.4 Molecular Biology

2.2.4.1 Oligonucleotide Synthesis

All oligonucleotides were designed using complete coding sequences obtained through the NCBI nucleotide search engine. Once appropriate sequences for oligonucleotides were identified they were sent to VHBio for synthesis. The oligonucleotides were received as pellets, which were then re-suspended in sterile distilled water and used at the working concentration of 10nM.

2.2.4.2 Nucleic Acid Preparation

2.2.4.2.1 Genomic DNA Extraction

The cells were pelleted by centrifugation at 660g for 5 minutes. The supernatant was discarded and the cells re-suspended in 1ml of PBS and transferred to a 1.5ml microcentrifuge tube. The cells were then centrifuged for 1 minute at 3000rpm using an Eppendorf 5415C microcentrifuge, the supernatant was carefully removed and then 500µl of cell lysis buffer and 5µl of proteinase K were added to the cell pellet. This mixture was then incubated overnight at 55°C. 500µl of isopropanol was added to the mixture and then rotated for 5-10 minutes until the viscosity had disappeared and strands of DNA were visible. This was then spun at 5000rpm in an Eppendorf 5415C microcentrifuge for 5 minutes. The supernatant was removed. 500µl of 70% ethanol was added, being careful not to disturb the pellet (if this occurred the sample was re-spun and the supernatant again discarded), and then carefully removed. 100µl of 1xTE buffer was then added and the sample was incubated at 60°C for 30 minutes to evaporate off any remaining ethanol. The DNA was then stored at 4°C.

2.2.4.2.2 RNA Extraction using Trizol ®

Cells were harvested and centrifuged for 10 minutes at 170g. The cells were then re-suspended in 1ml of Trizol® and transferred to a microcentrifuge tube. These were left to incubate at room temperature for 5-10 minutes. 200µl of chloroform was then added to the cells and the mixture shaken by hand for 15 seconds. The mixture was then centrifuged at 13200rpm for 10 minutes at 4°C in a Fisher Scientific Accuspin Micro 17R refrigerated microcentrifuge. The aqueous phase was carefully removed and transferred to a fresh microcentrifuge tube. RNA was precipitated by adding 500µl of isopropanol to the aqueous phase and incubating at room temperature for 10 minutes. It was then centrifuged

at 13200rpm for 10 minutes at 4°C as above. The supernatant was discarded and the pellet allowed to air dry before being re-suspended in RNAase free water.

2.2.4.2.3 DNAase Treatment of RNA

To remove genomic DNA contamination from the prepared RNA it was treated with DNAase prior to further experiments. To do this a kit from Ambion was used. Briefly, 10µl buffer and 1µl of DNAase was added to the RNA and incubated at 37°C for 30 minutes. 10µl of DNAase inactivator was then added and incubated at room temperature for 5 minutes. The micro-centrifuge tube was flicked intermittently during this time. The RNA mixture was then centrifuged for 1 pulse at 13200rpm in an Eppendorf 5415C microcentrifuge. The supernatant containing the RNA was then removed and placed into a fresh micro-centrifuge tube. The RNA was then stored at -80°C prior to use.

2.2.4.2.4 cDNA Synthesis from RNA

cDNA was obtained by reverse transcription from RNA using the Invitrogen Superscript™ First-Strand Synthesis System for RT-PCR. The manufacturer's instructions were followed, but briefly, 2 microcentrifuge tubes were prepared with the following components: 5µg of the sample RNA, 10µg/ml Oligo (dT) 12-18, 200nM dNTP mix, the volume was then adjusted to 10µl using diethylpyrocarbonate (DEPC) treated water. This was incubated at 65°C for 5 minutes, and then placed on ice for 1 minute. A 9µl mixture of the following components was added at these concentrations: 1 x RT-buffer, 5mM MgCl₂, 10nM DTT and 1ml of RNaseOut™ Recombinant RNase Inhibitor. The samples were then incubated at 42°C for 2 minutes. To one tube (+RT) 1µl (50 units) Superscript™ III Reverse Transcriptase was added with 1µl of DEPC treated water added to the other (-RT control). The samples were then incubated at 42°C for 50 minutes followed by incubation at 70°C for 15 minutes. Following this the samples were stored at -20°C until used for PCR amplification.

2.2.4.3 Polymerase Chain Reaction (PCR)

2.2.4.3.1 Reverse Transcriptase PCR (RT-PCR)

Reddymix™ PCR Master Mix tubes were used in all applications unless otherwise stated. 2-4µl of an oligonucleotide primer mixture (forward and reverse primers) was added to each tube giving a final primer concentration of 10-20µM. When the concentration of the template cDNA was known, 50-100ng of the DNA was added to the appropriate tubes, and

the final volume adjusted to 50 μ l with ddH₂O if required. When the template DNA concentration was unknown (as after cDNA amplification) then 3 μ l of DNA was added to each tube. The tubes were then placed in a thermo-cycler and incubated according to the application as follows:

Screening of cDNA from Lymphoid Cell Lines for Chemokine Receptor Expression:

Step	Temperature	Time	No of Cycles
1	92°C	2 minutes	1
2	92°C	30 seconds	} 35
3	54°C	30 seconds	
4	70°C	3 minutes	
5	70°C	10 minutes	
6	4°C	To end	1

Screening of AdEasy Constructs:

Step	Temperature	Time	No of Cycles
1	92°C	2 minutes	1
2	92°C	30 seconds	} 10
3	52°C	30 seconds	
4	68°C	3 minutes	
5	92°C	30 seconds	
6	55°C	30 seconds	} 20
7	68°C	3minutes	
8	68°C	10 minutes	1
9	4°C	To end	1

2.2.4.3.2 Overlap-extension PCR

Higuchi et al first described this method in 1988. It enables the introduction of a mutation or short peptide sequence at a specific site in the DNA. In this case a short peptide sequence was to be introduced at a specific point. To do this 4 primers were designed. The first 2 primers (flanking primers) were designed to be homologous to regions 1kb 5' and 3'

from the site of interest. The second 2 primers (peptide primers) had the first 24bpb homologous to the 3' and 5' regions beyond to the site of insertion and then the rest of the primer consisted of the sequence required for the peptide to be introduced.

Three PCR reactions were set up using 3µl of cDNA and 1µl of each of the following primer pairs in a ReddyMix™ PCR tube:

- 5' and 3' flanking primers
- 5' flanking and 3' peptide primers
- 3' flanking primer and 5' peptide primer

The PCR programme used for this was the same as that detailed on the previous page for screening of AdEasy constructs.

This produced 3 PCR products. The two 1kb PCR products were then used as template cDNA with the two flanking primers and the PCR reaction was repeated with the above programme. This resulted in a 2kb PCR product. To confirm that the PCR had worked the PCR product was initially digested with the restriction enzyme for the site that had been introduced and then sent for sequencing.

2.2.4.4 Agarose Gel Electrophoresis

A 0.9% gel was used throughout unless otherwise specified. Electrophoresis grade agarose was dissolved in 1 x TAE by heating. The solution was then allowed to cool to 60°C before ethidium bromide was added at a concentration of 0.5mg/ml. This was then poured into gel casts and left to set at room temperature.

DNA loading buffer (40% sucrose, 100mM Tris pH7.5, 1mM EDTA and 0.5mg/ml BγPB) was added to each sample before loading onto the gel. For PCR reactions using Reddy mix tubes the addition of a loading buffer was not required. The samples were then added to the appropriate well of the gel and 5µl of 1kb DNA ladder was added alongside. Unless otherwise indicated the gels were run from the power pack at 100V in TAE buffer until the DNA bands were clearly separated. The gel was then placed on a UV trans-illuminator for visualisation and photography.

2.2.4.5 Restriction Enzyme Digests

A reaction volume of between 20-50µl was used for each digest. Between 5-10 units of the restriction enzyme was used along with the appropriate reaction buffer at 1x concentration.

The mixture was then incubated for 1-2 hours at 37°C. The reaction mixture was then run on a 0.9% agarose gel and the appropriate DNA fragment was cut and gel purified. If the DNA was to be used for a ligation reaction and had undergone digestion with a single restriction enzyme, then dephosphorylation was required to prevent re-ligation. To do this 1 unit of shrimp alkaline phosphatase was added to the DNA and the mixture incubated for 30 minutes at 37°C.

2.2.4.6 Partial Digests

This was performed if two restriction enzyme sites were present in the target DNA and cleavage at only one site was desirable. Four reaction mixtures were set up with 5µl of DNA. A reaction buffer with 50% activity for the appropriate restriction enzyme was chosen and added to the reaction mixture. 5 units of the restriction enzyme was then added to each tube and incubated at room temperature for the following times; 5 minutes, 7.5 minutes, 10 minutes and 12.5 minutes. DNA loading buffer was added to each of the tubes at the appropriate time to inactivate the restriction enzyme. The reaction mixtures were then run on agarose gel until the bands had separated sufficiently to locate the desired DNA fragment.

2.2.4.7 Gel Purification of DNA Fragments and PCR Products

The DNA fragments were cut from agarose gels using a clean scalpel and purified using a Qiagen Qiaquick Gel Extraction Kit according to the manufacturers instructions. The DNA was then eluted from the columns using 20-40µl of distilled water or 1 x TE buffer (pH 8.0). The DNA concentration was then determined by either spectrophotometry and/or by running a 5µl aliquot of DNA alongside a DNA ladder of known concentration.

2.2.4.8 Cloning of PCR Products into TOPO® Vectors

3µl of the PCR product was added to 1µl of vector and 1µl of the salt solution from the TOPO® Vector kit. This mixture was then left to incubate at room temperature for 5-30 minutes. After this time, 3µl of the reaction mixture was used in a transformation reaction (see 2.2.4.1.4). Following this, colonies were picked and overnight cultures set up. Mini-preps were then carried out and the resulting pDNA was assessed to see if the PCR product had been successfully inserted using restriction enzyme digests.

2.2.4.9 Annealing of Oligonucleotides

One pair of oligonucleotides were designed to act as a linker containing specific restriction enzymes sites which enabled the introduction of a new restriction enzyme site into a

vector. 10 μ M (1 μ l) each of the forward and reverse oligonucleotides were placed into a PCR tube. To this 10 μ l of ligation buffer 1 and 2 μ l ligation buffer 2 (from the Roche Rapid Ligation Kit) were added along with 6 μ l of ddH₂O and 1 μ l (10 units) of PNKinase. The reaction mixture was then incubated at 37°C for 20 minutes. The oligonucleotides were then denatured and the kinase deactivated by placing the tube in a water bath at 95°C, the water bath was then switched off and the mixture allowed to cool gradually to room temperature. The annealed oligonucleotide was then ready to be used for ligation into a vector.

2.2.4.10 DNA Ligation using the Roche Rapid Ligation Kit

This was used to insert oligonucleotides or fragments of DNA into vectors. Oligonucleotides were prepared as above. Vectors and DNA fragments were prepared by restriction enzyme digestion to obtain fragments with complimentary ends. If a single enzyme was used to prepare the DNA fragments and plasmids, then the DNA was dephosphorylated as described in 2.2.4.5. The Roche Rapid Ligation Kit was used according to the manufacturer's instructions. The amount of vector and insert used was calculated to give a molar ratio of between 1:1 and 1:3, e.g. 50ng vector and 150ng insert. The ligation product was then used in a transformation reaction as in 2.2.4.14.

2.2.4.11 Site Directed Mutagenesis

The QuickChange® Site-Directed Mutagenesis Kit from Stratagene was used for this according to the manufacturer's instructions. Briefly a control and sample reaction was prepared. The control reaction contained 5 μ l of 10 x reaction buffer, 2 μ l (10ng) pWhitescript control plasmid, 1.25 μ l (125ng) primers #1 and #2, 1 μ l dNTP mix 38.5 μ l ddH₂O giving a total reaction volume of 50 μ l. The sample reaction contained the above reagents with pShuttle.CMV.LacZ instead of the control plasmid and primers designed for site directed mutagenesis instead of primers #1 and #2. To each reaction mixture 1 μ l of Pfu ultra HF DNA polymerase was added and the following PCR programme was then used;

Step	Temperature	Time	No of Cycles
1	95°C	30 seconds	1
2	95°C	30 seconds	
3	55°C	1 minute	} 12-18
4	68°C	1 minute/kb of plasmid length	

After the PCR reaction was completed 1µl of the restriction enzyme *DpnI* was added to each mixture. These were then incubated for 1 hour at 37°C. The mixtures were then transformed using XL-Blue supercompetent cells, using NZY medium as described in 2.2.4.13 below.

2.2.4.12 Preparation of Chemically Competent Cells

Certain strains of *E.coli* used were not chemically competent when obtained. Following calcium chloride treatment the resulting chemically competent cells facilitate the attachment of plasmid DNA to the cell membrane thus allowing for efficient transformation of the *E.coli*. To prepare the cells, they were initially spread onto a LB agar plate. The next day a single colony was picked and placed into 5ml of LB broth for overnight culture. 1ml of the overnight culture was placed into a 100ml of LB broth and incubated at 37°C on an orbital shaker. The optical density (OD) was monitored at 260nm and 280nm, using a Beckman DU 650 spectrophotometer, and when it reached 0.2-0.3 the cells were placed on ice for 10 minutes. The cells were then harvested in 50ml centrifuge tubes at maximum speed at 4°C for 10 minutes in an Eppendorf Centrifuge 5810R. The supernatant was then discarded and the cell pellet re-suspended in 40ml of ice-cold 100mM CaCl₂ and placed on ice for 30 minutes. The cells were then re-pelleted by centrifugation as above. The cell pellet was then re-suspended in 1ml of ice-cold 100mM CaCl₂. They could then be used for transformation or prepared for storage by adding 250ml of sterile 50% glycerol in 100mM CaCl₂.

2.2.4.13 Transformation using Chemically Competent Cells

This method was used to expand stocks of plasmid DNA. Initially 50µl of the appropriate chemically competent *E.coli* strain was placed into a 15ml polypropylene tube. To this 3-5µl of plasmid DNA was added. This mixture was then incubated on ice for 30 minutes. The contents were then 'heat shocked' at 42°C for 40 seconds and placed immediately on

ice again. 250µl of SOC or NZY medium was then added and the tube placed in an orbital shaker and incubated at 37°C for 1 hour. After this between 50 and 250µl of the mixture was spread onto an agar plate containing antibiotics (depending upon which antibiotic resistance gene the plasmid contained). The plates were then incubated overnight. The following day colonies were picked and placed in 5ml of LB broth containing antibiotics for overnight culture before proceeding to minipreps or maxipreps

2.2.4.14 Transformation Using Electrically Competent Cells

This was used for homologous recombination according to the Stratagene AdEasyTM XL Adenoviral Vector System. The *E.coli* strain BJ5183 contains efficient homologous recombination machinery and was used. First the electroporation cuvettes (with a 0.2cm gap) were placed on ice. For each reaction 40µl of BJ5183 cells, 1µg linearised plasmid containing the gene to be inserted and 1µl (100ng) pAdEasy were added to a microcentrifuge tube. These were then transferred to the cuvette and placed into the electroporator set at 200Ω, 2.5kV and 25µF and given one pulse. The cells were then immediately added to 1ml of SOC medium and incubated at 37°C for 1 hour before being spread onto an LB agar plate containing the appropriate antibiotic for selection. The plates were then incubated overnight and the colonies picked for proceeding to minipreps.

2.2.4.15 Plasmid DNA Preparation (Mini/Maxipreps)

Single bacterial colonies were selected and placed in 5ml of LB-medium containing either 50ug/ml ampicillin or 50ug/ml kanamycin. These were incubated overnight at 37°C in a shaker at 225rpm. For minipreps, 1.5ml of the overnight bacterial culture was pelleted by centrifugation at 13200rpm for 10 minutes using an Eppendorf 5415C microcentrifuge. The plasmid DNA was then purified using the QIAprep Spin Miniprep Kit according to the manufacturer's instructions. For larger DNA quantities, 1ml of an overnight culture obtained as described above was placed into 100ml of LB-broth and incubated overnight. This was then purified using the QIAGEN Maxi kit as per the manufacturer's instructions.

2.2.4.16 DNA Sequencing

All DNA preparations were sequenced using the service at AGOWA. The DNA preparations were initially quantified and if of a concentration of 100ng/ml or more were suitable for sequencing. The appropriate primers for sequencing were also sent with the preparations.

2.2.5 In-vitro assays

2.2.5.1 Antibody Staining for Surface Receptor Expression

a) Chemokine receptor antibody staining of HEK-293, CHO and Lymphoma Cells.

Cells were counted and 2.5×10^5 cells obtained for each sample. These were then washed twice in ice-cold FACS buffer re-suspended in 100 μ l of ice-cold FACS buffer and transferred to a clean 1.5ml micro-centrifuge tube. The primary antibody (with or without fluorochrome conjugation) was then added at the appropriate concentration (see table 2.2.1) and incubated at 4 $^{\circ}$ C for 30 minutes. 1ml of ice-cold FACS buffer was then added to each sample, which was then spun at 2000rpm for 5 minutes at 4 $^{\circ}$ C using a Fisher Scientific Accuspin Micro 17R refrigerated microcentrifuge. The supernatant was discarded and then the pellet re-suspended in 400 μ l of ice-cold FACS buffer if the antibody was conjugated to a fluorochrome. If the antibody was not conjugated then the cell pellets were re-suspended in 50 μ l of FACS buffer and a secondary detection antibody conjugated to a fluorochrome was added at the appropriate concentration. These samples were then incubated at 4 $^{\circ}$ C for 30 minutes before being washed with 1ml of FACS buffer and centrifuged at 2000rpm for 5 minutes at 4 $^{\circ}$ C as above. These were then re-suspended in 400 μ l of FACS buffer. All samples were then analysed as in 2.2.3.

b) Chemokine receptor and CD20 antibody staining of Human Lymphoid Cell Lines and Lymphoma Samples.

Cells were incubated with the primary and secondary detection antibodies as above using anti mouse or rat IgG conjugated to APC as the secondary antibody. Before proceeding to FACS analysis the cells were incubated for a third time with anti-CD20-PE. Following the final wash with FACS buffer 5 μ l of Viaprobe was added to the cell pellet and the cells were incubated at 4 $^{\circ}$ C for 10 minutes. The cells were then re-suspended in 400 μ l of FACS buffer and analysed as in 2.2.3. Viaprobe enabled the detection of apoptotic or necrotic cells using FL3-H. FL3-H positive cells were then excluded from the final FACS analysis. In addition lymphoma cell lines were used as negative controls by incubating with isotype antibodies conjugated with fluorochromes.

2.2.5.2 CCL19-Biotin Uptake

Initially a mixture was prepared containing 0.5 μ l biotinylated CCL19 from Almac (formerly Albachem) (at a concentration of 500 μ g/ml), 3 μ l streptavidin-PE and 7.5 μ l PBS per sample. A separate mixture without the CCL19 was also prepared to act as a negative

control. This mixture was incubated in the dark at room temperature for 45 minutes. In the meantime cells were harvested and washed in PBS to ensure that the growth medium had been removed. 2×10^5 cells per sample were then re-suspended in 40 μ l DMEM (with 20mM HEPES at pH 7.3). 10 μ l of the biotin-CCL19 mixture was then added to each sample and the cells incubated in the dark at 37°C for 1 hour. The cells were then moved to ice and washed with 1ml of ice cold FACS buffer, and spun at 2200rpm for 5 minutes in an Eppendorf 5415C microcentrifuge. The supernatant was removed and the cell pellet re-suspended in 400 μ l of FACS buffer and analysed by flow cytometry as in 2.2.3.

2.2.5.3 Radiolabelled Ligand Uptake

All appropriate measures were taken during this experiment to limit exposure to the radiolabelled ligands. Uptake assays were performed using 96-well plates. The radiolabelled ligands ^{125}I -CCL19 and ^{125}I -PM2 (a structural variant of CCL3) were used. These radiolabelled ligands were obtained from Almac. Cells were harvested and washed once with PBS. For each control sample 1×10^4 cells were re-suspended in 100 μ l of standard growth medium and transferred to the wells. Medium containing 1 μ l of 925kBq/ml (specific activity 2200Ci/mmol) of the radio-ligand was prepared. For each sample 1×10^4 cells were re-suspended in 100 μ l of the prepared medium. As additional controls, un-conjugated CCL19 and PM2 were added to cells re-suspended in 100 μ l medium at 1 μ l CCL19 (500 μ g/ml) and 5 μ l PM2 (100 μ g/ml) giving the same concentration of chemokine in all wells. The 96 well plate was then incubated at 37°C for 2, 4, 8 or 12 days and cell proliferation was analysed using the MTT cell proliferation assay outlined below.

2.2.5.4 MTT Proliferation Assay

The Chemicon MTT cell proliferation assay kit was used according to the manufacturer's instructions. Reagent A (50mg MTT) and Reagent B (15ml PBS at pH 7.4) were combined and 10 μ l of this solution was then added to each well of the 96 well plate and mixed well. The plate was then incubated at 37°C for 4 hours, to allow cleavage of the MTT. Wells containing live cells developed black crystals of MTT formazan. 100 μ l reagent C (isopropanol with 0.04M HCl) was then added to each well to develop the colour, dissolving the MTT formazan to give a blue solution. The plate was then read within the hour, using an ELI SA plate reader at a test wavelength of 570nm and a reference wavelength of 630nm and the absorbance recorded. A calibration curve was also developed.

2.2.5.5 Chemotaxis Assays

2.2.5.5.1 Chemotaxis using 24 well HTS Transwell® Plates

Chemotaxis buffer was prepared with either DMEM or RPMI medium containing 20mM HEPES and 1% BSA. The Transwell® plates were prepared by removing the inserts and adding 600µl of chemotaxis buffer to each well with 0, 0.1nM, 1nM, 10nM or 100nM of chemokine. The inserts were then replaced. Then 5×10^5 cells were re-suspended in 100µl of the chemotaxis buffer without chemokine and placed carefully into each of the inserts. The plates were incubated for 3 hours at 37°C. Following incubation, the inserts were removed from the wells and the cells in the medium were counted using a haemocytometer.

2.2.5.5.2 QCM™ Chemotaxis 3µm 96-Well Cell Migration Assay

The assay was performed according to the manufacturer's instructions. In brief, cells were starved, by incubating them in either RPMI, or DMEM without serum for 24 hours. Following this the cells were re-suspended in chemotaxis buffer as outlined above at a concentration of 1×10^5 cells/100µl. Chemotaxis buffer was then prepared with the following concentration of chemokine; 0, 0.1nM, 1nM, 10nM and 100nM, and 150µl of these solutions were added to each well of the feeder tray. The migration chamber was then added and 100µl of the cell suspension added to each well. The cells were then incubated for 3 hours at 37°C. After incubation the migration chamber is removed and the cells from the top side are gently discarded by flipping out the remaining cell suspension. The migration chamber is then placed into a fresh feeder tray containing 150µl of detachment buffer in each well. This is then incubated for at 37°C for 30 minutes. Meanwhile, 75µl from each well of the chemotaxis buffer from the original feeder tray is transferred into a fresh 96 well and after incubation add 75µl of medium from the second feeder tray is added to the same 96 well plate, the second feeder tray is then discarded. The lysis buffer/dye solution is then prepared as per instructions and 50µl of this is added to each of the wells in the remaining 96 well plate. The plate was then incubated for 15 minutes at room temperature in the dark. Following this, 150µl of the solution in each well was transferred to a fresh 96 well plate suitable for luminometry. The plate was then read using a 480/520nm filter set.

2.2.6 Adenovirus Preparation, Modification and Infections

All adenovirus work was performed under sterile conditions within a class II biological safety cabinet with laminar flow. All disposable equipment was soaked in Trigene® for 24 hours to inactivate any live virus before disposal. Approval from the University of Glasgow Genetically Modified Organisms Committee was attained before any work described here was carried out.

2.2.6.1 Expanding Adenoviral Stocks

Initially, 11 x T150 flasks of HEK.293 cells were set up using 25ml of DMEM with 10% FCS and incubated at 37°C. When the cells were approximately 80% confluent the cells in 1 flask were trypsinized and the total number of the cells in the flask calculated. It was then assumed that for the remaining flasks the cell numbers were similar. An adenoviral stock solution of known PFU value was then used to make up a 10ml solution in PBS equating to 1 PFU per cell. The growth medium was removed from the 10 flasks and the cells gently washed with 3mls of PBS. 1ml of the adenovirus solution was then added to each flask and left to incubate at room temperature for 1 hour rocking the flasks occasionally to ensure even coverage. 25mls of DMEM with 2% FCS was then added to each of the flasks, and left to incubate at 37°C for 7-14 days, allowing the adenovirus to form plaques. Once the cells had lifted off the bottom of the flasks and were no longer clumped, the adenovirus was ready to harvest and purify.

2.2.6.2 Purification of Adenovirus using the BD Adeno-XTM Virus Purification Kit

The kit was used as per the manufacturer's instructions. In short, the cells from all 10 flasks were transferred to 2 sterile conical centrifuge tubes. These were then centrifuged for 10 minutes at 1600rpm in a Sorval RC-5B refrigerated superspeed centrifuge. The supernatant was transferred to a fresh T175 flask and kept on ice. The remaining cell pellets were then re-suspended in 5mls of the supernatant and the cells lysed by freeze-thawing 3 times in dry-ice and methanol. The cells were centrifuged again as above and the supernatant added to the T175 flask. The supernatant was then filtered using a bottle-top filter unit and 0.45micron filter, and placed into a fresh T175 flask. Benzonase was then added at 10units/ml to remove any cellular DNA and incubated at 37°C for 30 minutes. The benzonase treated filtrate was then added to an equal volume of 1 x dilution buffer, and using the filter assembly kit provided, passed through the filter at a rate of 20ml/minute. Once all of the filtrate had been passed the entire volume of 1 x wash buffer

(provided in the kit) was passed through the filter (which now held the virus). To elute the adenovirus, 3mls of elution buffer was drawn up in a 5ml syringe. First 1ml of the elution buffer was pushed into the filter with the filtrate collected in a sterile micro-centrifuge tube. The filter was then left to incubate at room temperature for 5 minutes, before flushing through the remaining buffer, and collecting the filtrate in micro-centrifuge tubes. To obtain any remaining adenovirus, 5mls of air was then pushed through the filter. The eluted adenovirus was then centrifuged at 14000rpm for 10 minutes in the Fisher Scientific Accuspin 17R refrigerated microcentrifuge, the supernatant was removed and the remaining adenoviral pellet re-suspended in 50-100 μ l of formulation buffer. The adenovirus was left at room temperature for 30 minutes before being stored at -70°C in a second container for safety.

2.2.6.2 Adenoviral Titre Assay using the BD Adeno-X™ Rapid Titre Kit

This assay enabled a quicker calculation of the adenoviral concentration than the traditional plaque assays giving a titre in IFUs (infection forming units), which is equivalent to PFUs. It was used to calculate the amount of adenovirus obtained following the purification outlined above. The kit was used according to the manufacturer's instructions. In brief, 5×10^5 HEK.293 cells in 1ml of growth medium (DMEM with 10% FCS) were placed in each well of two 12 well plates. Serial dilutions of the stock adenovirus and a control adenovirus of known concentration were then prepared as follows:

Volume of PBS (μ l)	Volume (μ l) & Concentration of adenovirus solution	Final adenovirus Concentration
1000	-	Nil
990	10 of $x 1$	10^{-2}
900	100 of $x 10^{-2}$	10^{-3}
900	100 of $x 10^{-3}$	10^{-4}
900	100 of $x 10^{-4}$	10^{-5}
900	100 of $x 10^{-5}$	10^{-6}
900	100 of $x 10^{-6}$	10^{-7}

100 μ l of the adenoviral solutions were then added to each well of the HEK.293 cells with the lower concentrations being duplicated. The cells were then incubated for 48 hours at 37°C.

The medium from each well was aspirated and the cells were left to air dry for 5 minutes. The cells were then fixed by adding 1ml of ice-cold methanol to each well and incubating at -20°C for 10 minutes. The cells were then washed 3 x with 1ml of PBS + 1% BSA buffer, trying not to disturb the cell layer. 500 μl of mouse anti-hexon antibody (diluted 1:1000 in PBS + 1%BSA) was then added to each well and incubated at 37°C for 1 hour. The cells were washed three times with the buffer, and 500 μl of rat anti-mouse –HRP conjugated antibody (diluted 1:500 with PBS + 1% BSA) was added to each cell. Again the plates were incubated for 1 hour at 37°C . The cells were again washed with the buffer. Following this 500 μl of the DAB working solution was added to each well and the plates were left to incubate at room temperature for 10 minutes. The DAB solution was then removed and 1ml of PBS added to each well. The number of brown cells per field were then counted at x20 objective, a minimum of 3 fields per well were counted.

The adenovirus concentration was then calculated as follows:

$$\text{IFU/ml} = \frac{(\text{infected cells/field}) \times (\text{fields/well})^*}{\text{Volume virus (ml)} \times \text{dilution factor}}$$

For example:

Infected cells/field =13.2

*Fields/well at x20 objective = 573 (for a 12 well plate)

Volume of adenovirus= 0.1ml

Dilution factor = 10^{-6} = 0.000001

$$\text{Therefore the IFU/ml} = \frac{13.2 \times 573}{0.1 \times 0.000001} = 7.56 \times 10^{10} \text{ IFU/ml}$$

2.2.6.3 Shrouding of Adenovirus with Chemokine

This was performed in two parts. Firstly, a NeutrAvidinTM-virus conjugate was prepared by adding 100 μl of NeutrAvidinTM (5mg/ml) to a known quantity of adenovirus in 100 μl PBS. This was incubated at room temperature for 4 hours. The adenovirus-NeutrAvidinTM mixture was then added to a DispoDialyzer with a 100kDa pore size (from Spectrum), and left to dialyse for 1 hour, to remove any un-conjugated NeutrAvidinTM. The adenovirus-

NeutrAvidin™ conjugate was then placed in a fresh micro-centrifuge tube and centrifuged at 14000rpm for 20 minutes in a Fisher Scientific Accuspin Micro 17R refrigerated microcentrifuge. The supernatant was discarded and the pellet re-suspended in 100µl of PBS. The adenovirus-NeutrAvidin™-chemokine conjugate was then prepared by adding 2µl of chemokine (500µg/ml) to the adenovirus and the solution was incubated at room temperature for 2 hours. The solution was then transferred to a fresh DispoDialyzer and dialysed for 1 hour to remove unbound chemokine. The solution was then transferred to a micro-centrifuge tube and centrifuged at 14000rpm for 20 minutes as above. The supernatant was discarded and the adenovirus-NeutrAvidin™-chemokine conjugate (shrouded adenovirus) was re-suspended in formulation buffer (as used in the adenovirus purification protocol in 2.2.6.2) and stored at -70°C.

2.2.6.4 Infection of Mammalian Cells

The method described in 2.2.6.3.1 was used up to the point of incubation for 48 hours. 5×10^5 cells/well were used for all cell lines, and the majority of cases were incubated for 48 hours at 37°C before analysis by one of the method described below. This method was used for infecting cells with the chemokine-shrouded adenovirus.

2.2.6.5 Assessment of Mammalian Cell Infection by Staining for Beta-galactosidase

The Invitrogen β-galactosidase staining kit was used according to the manufacturer's instructions. After incubation with the virus, the cells were washed with PBS. For adherent cells each well was washed with 500µl of PBS. For suspension cells, the cells were transferred to micro-centrifuge tubes, centrifuged for 5 minutes at 2000rpm in the Eppendorf 5415C microcentrifuge, the supernatant removed and the cells re-suspended in 100µl of PBS. The suspension cells were then placed on a poly-L-lysine coated slide and left at room temperature for 45 minutes to enabled adherence to the slide. After washing, the cells were fixed with 500µl (per well or slide) of 1 x fixative solution and left to incubate at room temperature for 10 minutes. The cells were then washed once with PBS. The staining solution was then made up according to manufacturer's instructions. To each sample 500µl of the staining solution was added, and the samples were incubated for up to 2 hours until a blue colour developed. The staining solution was then removed. If 12 well plates had been used for the infections, 1ml of 70% glycerol was added to each well before examination under the microscope. For the slides obtained using slide chambers, the

samples were allowed to air dry and then covered with a cover slip before microscopy. The number of blue cells in each field was then counted. The IFU could then be calculated, if required as in 2.2.6.3 above.

2.2.6.6 Assessment of Mammalian Cell Infection using the Promega Luciferase assay

Cells were incubated with adenoviral vectors containing a luciferase reporter gene in a 96 well plate. Following incubation 1 x lysis buffer was made up as per manufacturer's instructions and 20 μ l was added to each well and the cells were left for a few minutes to lyse. 100 μ l of luciferase assay reagent was added to each well. The 96 well plate was then immediately transferred to a luminometer and the plate was read using a 570/630nm filter set.

2.2.6.7 Assessment of Mammalian Cell Infection by FACS

Cells that had been incubated with the virus were collected, transferred to micro-centrifuge tubes and washed in FACS buffer followed by centrifugation at 2000rpm in an Eppendorf 5415C microcentrifuge. The supernatant was discarded and the cells were re-suspended in 100 μ l of FACS buffer. Mouse-anti-hexon antibody was then added to the cells and they were left to incubate at 4⁰C for 45 minutes. The cells were washed once in 1ml PBS and centrifuged as above. Again the supernatant was discarded and the cells were re-suspended in 50 μ l FACS buffer. This was followed by the addition of anti-mouse-PE antibody (1:50) and incubation at 4⁰C for 45 minutes. The cells were again washed with 1ml of FACS buffer as above, and the cell pellet was re-suspended in 400 μ l of FACS buffer and analysed as in 2.2.5.2.3.

2.2.6.8 Preparation of Adenovirus for Visualisation by Electron Microscope

Initially, carbon cribs were prepared by coating in poly-L-lysine. This was done by, placing 1 drop of 0.01% poly-L-lysine solution onto each crib, and incubating them at room temperature for 30 minutes. The cribs were then rinsed by placing them on drops of distilled water three times for 5 minutes. They were then left to air dry. 20 μ l drops of a solution containing the adenovirus to be examined were placed onto parafilm. The carbon cribs were then placed onto these drops 'shiny' face up, and left to adhere to the adenovirus for 15-20 minutes. The cribs were then rinsed with PBS as outlined above with the distilled water. Excess fluid was removed by blotting with filter paper after the third

rinse. The cribs were then placed on a 20µl drop of 2.5% glutaraldehyde for 10-15 minutes. The cribs were then rinsed with drops of distilled water as above. The cribs were then transferred to drops of Nano-van for 30 seconds. The cribs were then held in forceps to dry. Once dry, they could be placed in a crib holder before examination under the electron microscope.

If the virus was to be labelled with gold, the cribs were first placed on drops of 0.1M glycine, to quench the glutaraldehyde, for 20 minutes. They were then placed on drops of biotin-gold and left for 15-20 minutes. This was then followed by 3 rinses with distilled water before being stained with the Nano-van.

2.2.7 In-vivo Assays

2.2.7.1 Maintenance of Mice

Mice were housed in a pathogen free environment within the animal facility at the University of Glasgow. They were fed and watered *ad libitum*. The procedures outlined below were in accordance with United Kingdom Home Office guidelines, with the appropriate personal and project licences. An approved schedule one technique was used to kill the mice.

2.2.7.2 Infection of Mice with Adenovirus

Enough “Shrouded” and non-“shrouded” virus was prepared in sterile PBS at the concentration of 1×10^8 IFU/200µl for 12 mice. 6 mice were injected via the tail vein with the shrouded virus and 6 mice with the non-shrouded virus. This was performed by, staff members of the University of Glasgow, animal facility. Three mice from each group were then sacrificed at 48 hours and 96 hours. The inguinal lymph nodes, spleen, gut, lungs, kidneys and heart were then collected from each mouse. Sacrificing of the mice, and subsequent dissection of the mouse tissues, was performed by Prof. Gerard Graham.

2.2.7.3 Assessment of Virus Infection in Mouse Tissues

2.2.7.3.1 Cryopreservation of Mouse Tissues and Preparation of Slides

Each of the collected tissues were embedded in a tissue freezing medium then stored at -70°C. Once the tissues had been frozen, slides were prepared using a cryostat. The slides were then stored at -70°C.

2.2.7.3.2 β -galactosidase Staining of Mouse Tissues

The slides containing the mouse tissues were allowed to thaw on ice. They were then fixed by incubation in a solution of 0.5% glutaraldehyde and 4% formalin for 10 minutes. This was followed by washing in PBS for 1 minute, and, if required, placed in a solution of haematoxylin for a few seconds followed by thorough rinsing. The slides were then stained for β -galactosidase expression as outlined in 2.2.6.6 above and the slides examined under light microscopy.

2.2.8 Statistical Analysis

All statistical analysis was performed using the Microsoft Excel or Graph Pad Prism 4 software package.

CHAPTER THREE

ANALYSIS OF CHEMOKINE RECEPTOR EXPRESSION IN NON-HODGKIN'S LYMPHOMA

3.1 Introduction

As described in the introduction there is some evidence to suggest that there is a relationship between the subtype of non-Hodgkin's lymphoma and chemokine receptor expression [335]. One of the primary aims of this project was to examine this hypothesis further, thus potentially aiding in the diagnosis and classification of lymphomas.

Constitutive chemokine receptors, rather than inflammatory chemokine receptors, were studied because expression is more restricted to particular cell types and they have a more predictable anatomical distribution [275]. Any co-existent inflammatory processes, and consequent up regulation of inflammatory chemokines, in the affected lymph node tissues such as infection or tissue injury from preliminary investigations such as fine needle aspiration, were also less likely to confound any results obtained. Such studies may also provide more specific targets for certain subtypes or enable more accurate prognostic information to be obtained. In order to examine whether or not there are any differences in chemokine receptor expression between subtypes of NHL primary tissues from patients with a variety of NHL subtypes were obtained. The primary tissues consisted of lymphocyte preparations from the affected lymph nodes of the patients with NHL.

However, before testing patient samples, an accurate method for determining chemokine receptor expression on the surface of lymphocytes was needed to ensure that the patient samples were utilised to their full potential. This method was developed and optimised using selected lymphoma cell lines, in which chemokine receptor expression was initially verified by a variety of methods, before being used as controls in the set up of testing of clinical samples.

This chapter describes the system and results pertaining to chemokine receptor expression obtained initially with lymphoma cell lines, and subsequently on testing of patient samples. Finally, chemokine receptor expression on clinical samples was correlated with clinical presentation and outcomes and the results from this are presented.

3.2 Use of Cell Lines to Verify Oligonucleotides for the Detection of Chemokine Receptors

3.2.1 Identifying Cell Lines to be used

Before commencing antibody testing, cell lines expressing the receptors of interest were needed and the presence or absence of RNA for these receptors was examined first.

Oligonucleotides were designed to identify the presence of RNA for the human constitutive chemokine receptors: CCR4, CCR6, CCR7, CCR9, CCR10, CXCR4 and CXCR5. In the case of CXCR5 two splice variants, termed CXCR5a and CXCR5b in this thesis, were identified and thus two primer pairs were designed for this receptor.

To identify cell lines expressing the constitutive chemokine receptors CCR4, CCR6, CCR7, CCR9, CCR10, CXCR4 and CXCR5 a literature search was performed. Raji (human B-cell Burkitt lymphoma) cells were identified as expressing CCR7 and CCR10 with Daudi (human B-cell Burkitt lymphoma) cells identified as also expressing CCR10 along with CCR6 [136]; both cell lines express CXCR4 and CXCR5 [336]. MOLT-4 (human T-cell leukaemia/lymphoma) cells express CCR9 [336]. Finally, KU-812 (human basophilic) cells were identified as endogenously expressing CCR4 [337].

3.2.2 RT-PCR Results on Cell Lines

Using the primers for the constitutive chemokine receptors shown in section 2.1.7.2, RT-PCR was performed on the cell lines described above with the exception of the KU-812 cells. This showed that CCR4 was expressed in Daudi and MOLT-4 cells despite a lack of literature at the time to support CCR4 expression in these cells. In the case of the Daudi cells, the levels of CCR4 RNA were low, and so not clearly evident in figure 3.1.

However, cloning of the PCR product subsequently confirmed its presence in Daudi cells, and interestingly, Daudi cells are now recommended by manufacturers such as Thermo Fisher Scientific and Imgenex, as positive controls for their anti-CCR4 antibodies. As expected, CCR6 was expressed in the Daudi cells but was also apparent at a low level in both the MOLT-4 and Raji cells. CCR7 was expressed in Raji cells and Daudi cells, but only very weakly in MOLT-4 cells. CCR9 was demonstrated in MOLT-4 as expected but was also seen in Raji and Daudi cells. CXCR4 and CXCR5 were expressed in all three cell lines described above, with both splice variants of CXCR5 being detected in Raji and Daudi cells (CXCRb not shown) and only CXCR5b detected in MOLT-4 cells.

However, CCR10 expression was not seen in any of the cell lines despite reports in the literature to the contrary [338]. Therefore a cell line, which had previously been developed

within the laboratory to express human CCR10, L1.2.hCCR10 cells, were used as the positive control to demonstrate that the CCR10 primers were functional. Of note, although it appears in the gels that CCR10 is expressed in all three cell lines, this PCR product was the incorrect size and when sent for sequencing did not correspond to CCR10. The results of RT-PCR are shown in figures 3.1 and 3.2 and summarised in table 3.1.

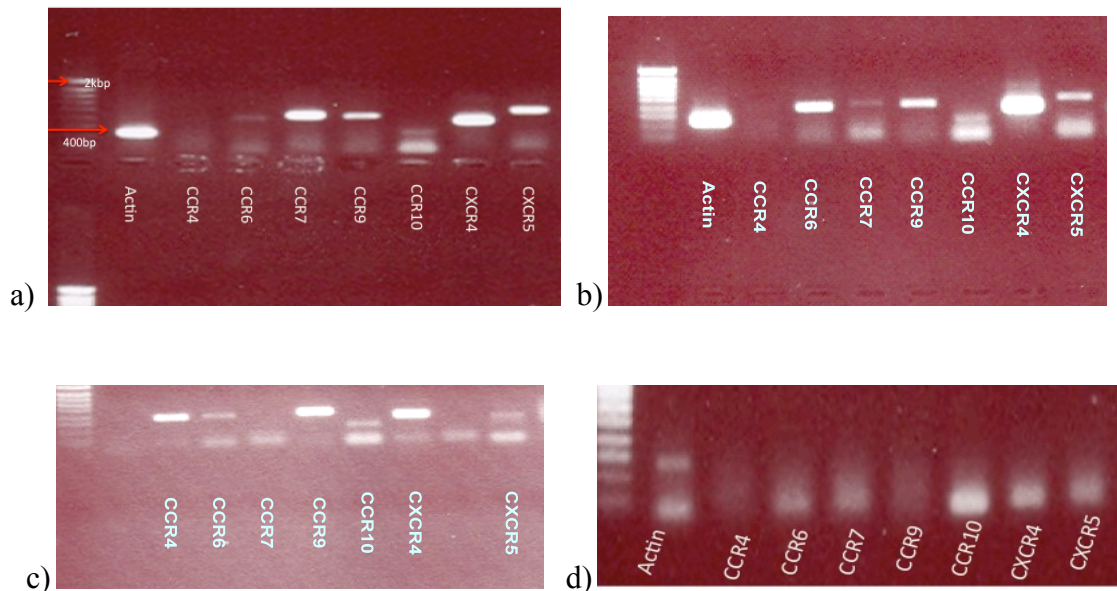


Figure 3.1: Expression of constitutive chemokine receptor expression in human lymphoma cell lines. a) Raji cells b) Daudi Cells, c) MOLT-4 cells, d) minus RT control. RNA was prepared from the cell lines using Trizol®, DNAase treated and cDNA was synthesised ± reverse transcriptase. Primers for actin and the chemokine receptors CCR4, CCR6, CCR7, CCR9, CCR10, CXCR4, CXCR5a and CXCR5b were then used for amplification of cDNA using the PCR programme in 2.2.4.3. The PCR products were then run on a 1% agarose gel containing ethidium bromide. The arrows on figure a) indicate the size of the PCR product obtained with actin and demonstrate the 2kbp mark on the DNA ladder.

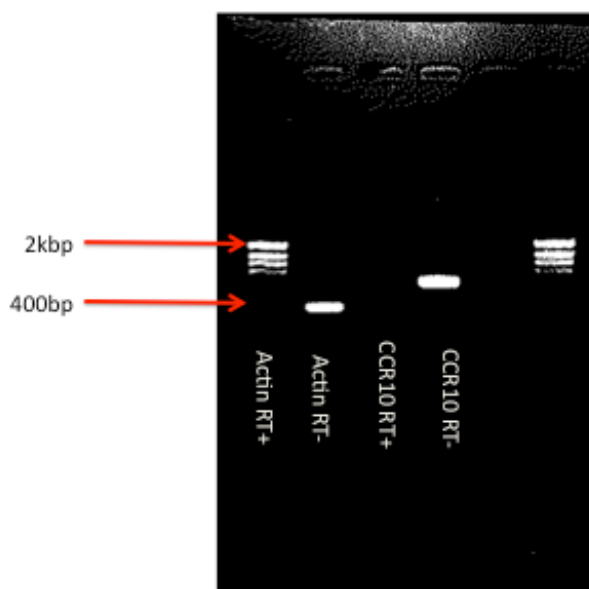


Figure 3.2: Confirmation of hCCR10 RNA expression in L1.2.hCCR10 cells. RNA was prepared from L1.2.hCCR10 cells using Trizol®, DNAase treated and cDNA was prepared using \pm reverse transcriptase. Primers for actin and CCR10 were used for amplification of cDNA using the PCR programme in 2.2.4.3. The PCR products were then run on a 1% agarose gel containing ethidium bromide. The arrows indicate the size of the PCR product obtained with actin (400bp) and demonstrate the 2kbp mark on the DNA ladder.

	<i>DAUDI</i>	<i>MOLT-4</i>	<i>RAJI</i>
CCR4	+/-	+	-
CCR6	+	+	-
CCR7	+	-	+
CCR9	+	+	+
CCR10	-	-	-
CXCR4	+	+	+
CXCR5a	+	-	+
CXCR5b	+	+	+

Table 3.1: Expression of constitutive chemokine receptor RNA in Raji, Daudi and MOLT-4 cells. RNA was prepared from the cell lines using Trizol®, DNAase treated and cDNA was prepared with or without reverse transcriptase. Primers for chemokine receptors CCR4, CCR6, CCR7, CCR9, CCR10, CXCR4, CXCR5a and CXCR5b were used to amplify cDNA using the PCR programme in 2.2.4.3. PCR products were run on a 1% agarose gel containing ethidium bromide and the expression chemokine receptor RNA was recorded for each cell line. + positive, - negative, +/- weak positive.

3.2.3 Topocloning and Sequencing to Verify the Chemokine Receptor Primers

All of the RT-PCR products obtained in 3.2.2 above were cloned into the pCR2.1TOPO® TA vector and subsequently sent for sequencing. For each primer pair, sequencing confirmed that the RT-PCR product obtained corresponded with the appropriate chemokine receptor.

3.3 Testing of Chemokine Receptor Antibodies Using Cell Lines

Having characterised chemokine receptor expression at the transcript level in MOLT-4, Raji and Daudi cells, testing of chemokine receptor antibodies on the cell lines using single colour flow cytometry was performed. Once the antibodies had been verified in this way, they could then be used for further optimisation of a system to analyse the clinical samples.

Antibodies to CCR4, CCR6, CCR7, CCR9, CCR10, CXCR4 and CXCR5 (known to bind both splice variants) were obtained and used at concentrations recommended by the manufacturer. Following incubation with the primary chemokine receptor antibody the cells were incubated with a secondary antibody, (anti-IgG- phycoerythrin (PE) or anti-IgG-allophycocyanin (APC)) and were then subsequently analysed by single colour flow cytometry as detailed in section 2.2.3a. This analysis confirmed that Raji cells have surface expression of CCR7, CCR9, CXCR4 and CXCR5, Daudi cells have surface expression of all of the chemokine receptors studied except CCR10 and that MOLT-4 cells have surface expression of CCR4, CCR6, CCR9, CXCR4 and CXCR5. Finally, the CCR10 antibodies were verified using L1.2.hCCR10 cells and this confirmed surface expression of this receptor. Figure 3.3 shows a selection of the results obtained, indicating that a positive control for each of the chemokine receptors had been identified prior to the testing of clinical samples.

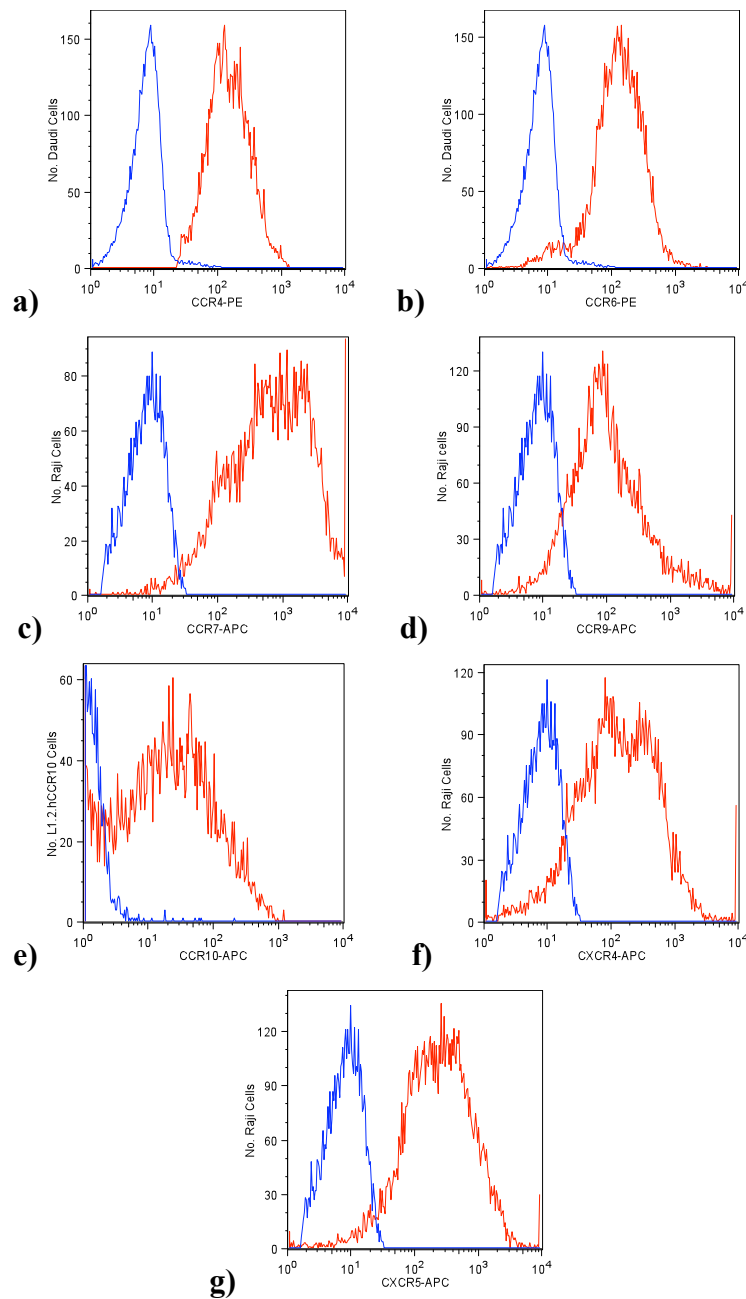


Figure 3.3: Results of single colour flow cytometry on Raji, Daudi or L1.2hCCR10 cells with chemokine receptor antibodies. a) Daudi cells and CCR4 antibody, b) Daudi cells and CCR6 antibody, c) Raji cells and CCR7 antibody, d) Raji cells and CCR9 antibody, e) L1.2.hCCR10 and CCR10 antibody, f) Raji cells and CXCR4 antibodies and g) Raji cells and CXCR5 antibodies. The cells were incubated with the appropriate primary chemokine receptor antibody or FACS buffer alone, followed by incubation with a secondary antibody conjugated with PE or APC or an isotype control conjugated with PE or APC. The cells were then analysed using flow cytometry. In each case the blue line represents the isotype (negative) control and the red line expression of the chemokine receptor analysed.

Once the primary antibodies had been verified in this manner, two-colour flow cytometry was optimised prior to the testing of clinical samples. The mature B-cell marker, CD20, was chosen to identify the B-cells (and therefore malignant cells) in the clinical samples obtained from patients with B-cell NHL. Incubating the clinical samples with CD20 and the chemokine receptor antibodies would then allow analysis of the degree of chemokine receptor expression on B-cells from the patient samples. In order to set up two-colour flow Raji cells were used. The same first steps used for single flow cytometry were used however in this instance the secondary antibody was conjugated with APC, and was followed by incubation of the Raji cells with an anti-CD20 antibody directly conjugated with PE. Following incubation with the anti-CD20 antibody and the chemokine receptor antibody the Raji cells were incubated with ViaProbe to ensure that only viable cells were analysed. ViaProbe binds to necrotic or apoptosing cells and so in analysing the data, cells demonstrating binding with this probe were excluded. Figures 2.1 and 2.2 and in the methods section demonstrate the process of gating on viable cells and setting up 2-colour flow cytometry.

3.4 Testing of Patient Samples

Once the antibodies had been successfully verified as being suitable for use in this study, the next step was to proceed with the testing of patient samples for chemokine receptor expression. This would enable the collection of data to determine firstly, if there was a variation in receptor expression with differing subtypes, and subsequently enable correlation with clinical data such as mortality and disease stage at presentation. Patient samples were obtained from frozen stocks maintained by Prof. Ruth Jarrett's research group at the Leukaemia Research Laboratory within the Glasgow Veterinary School. The non-Hodgkin's lymphoma subtype samples obtained were as follows; diffuse large B-cell lymphoma (DLBCL) - 17 cases; follicular lymphoma - 16 cases; mantle cell lymphoma (MCL) - 17 cases; chronic lymphocytic leukaemia/small lymphocytic lymphoma (CLL/SLL) - 24 cases; MALT lymphoma - 10 cases and Burkitt's lymphoma - 9 cases. Each sample was thawed and then washed once with PBS prior to dividing into 8 aliquots of equal size. Each aliquot contained at least 2×10^5 cells, and 7 of these underwent the incubation steps as described in 2.2.3b of the methods section, whilst the 8th sample was used as a negative control and incubated with an isotype control. Each sample was then analysed for viability and only viable cells were gated for further analysis. The mean overall viability for the clinical samples was 69.89% (95% CI: 62.63-77.16%). For each sample analysed, the total number of CD20 positive (or in the case of CLL/SLL CD19

positive as, this subtype has a lower level of expression of CD20 [336]) cells were recorded, along with the number of cells demonstrating dual expression for both CD20 and the chemokine receptor, these figures were then used to calculate the percentage of B-cells expressing the chemokine receptor of interest.

3.4.1 Comparison of Chemokine Receptor Expression within Each NHL Subtype.

Within each lymphoma subtype there were notable differences in constitutive chemokine receptor expression. The median percentage of B-cells expressing the receptor of interest with the 95% confidence intervals in brackets will be used to outline the results outlined for the 6 NHL sub-types which follow.

i) **Follicular lymphoma** cases had a median age at presentation of 55 (37-72) years with a male: female ratio of 1:1.75, representative of demographic data in the literature for follicular lymphoma [176]. Follicular lymphoma represented the NHL sub-type with the lowest expression of chemokine receptors. In the follicular lymphoma cases the mean percentage of B-cells expressing each of the chemokine receptors were as follows (with 95% confidence intervals in brackets; CCR4 11.84% (10.0-27.0), CCR6 10.35% (3.2-17.4), CCR7 25.54% (14.5-36.6), CCR9 13.04% (6.5-19.6), CCR10 0.18% (0.04-0.3), CXCR4 52.17% (39.9-64.4) and CXCR5 84.5% (67.3-101.7). Having lower levels of CCR6 and CCR9 when compared to the other NHL sub-types can be explained by the anatomical distribution of this lymphoma with predominantly nodal and bone marrow disease being typical [176] and CCR6 and CCR9 expression is predominantly associated with gut and mucosal tissues [176]. However, what is surprising is the lower expression of CXCR4 than that demonstrated by other NHL subtypes, which cannot be readily explained, especially with its predilection for bone marrow. The results above are shown in figure 3.4.

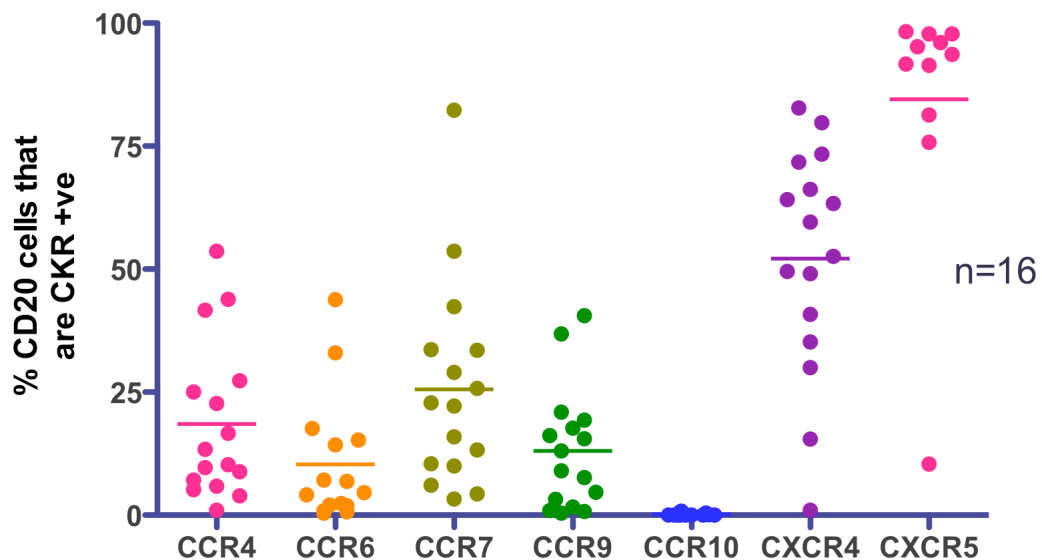


Figure 3.4: Distribution of chemokine receptor expression in 16 follicular lymphoma cases. The horizontal lines indicate the mean expression of the chemokine receptor studied. Lymphocyte suspensions from lymph node tissues were obtained from patients diagnosed with follicular lymphoma. These were then divided into 8 aliquots. Each aliquot was incubated with a primary antibody for one of CCR4, CCR6, CCR7, CCR9, CCR10, CXCR4, CXCR5 or FACS buffer only. The cells were then incubated with a secondary antibody (or isotype control if only incubated with FACS buffer) conjugated with APC. Following this, all cells (except the isotype control) were incubated with anti-CD20-PE, following which the cells were analysed by 2-colour flow cytometry.

ii) **Diffuse large B cell lymphoma** cases also had a representative demographic with the median age at presentation being 64 (21-80) years and a male: female ratio of 1:1.(75) [339]. The DLBCL cases had a more varied expression of receptors (see figure 3.5), with CCR10 detected at the lowest levels and CXCR5 at the highest. The results for the mean percentage of B-cells with detectable receptor expression were as follows; CCR4 61.59% (47.7-75.5), CCR6 27.34% (17.2-37.5), CCR7 60.89% (47.2-74.6), CCR9 38.87% (28.0-49.8), CCR10 1.57% (-1.0-4.1), CXCR4 78.26% (68.2-88.3) and CXCR5 96.01% (93.9-98.1). The most surprising result was a high % of CCR4 expression, a receptor, which is usually expressed on Th2 and Treg cells along with skin homing T-cells [176]. Certainly, CCR4 expression has not previously been widely reported in B-cell lymphomas other than in a single case report [340], and reports have been restricted to CCR4 expression in T-cell lymphomas and Hodgkin's disease [341].

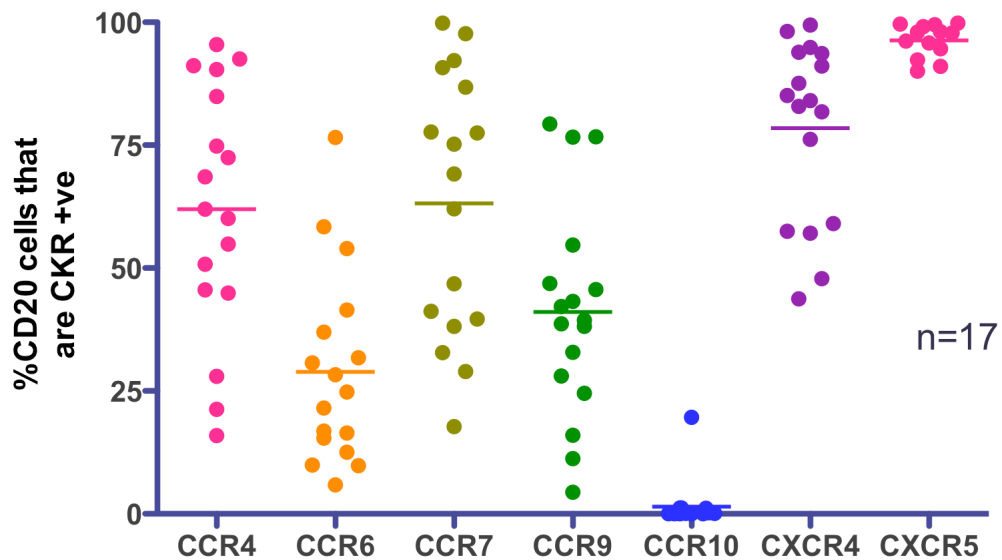


Figure 3.5: Distribution of chemokine receptor expression in 17 diffuse large B-cell lymphoma cases. The horizontal lines indicate the mean expression of the chemokine receptor studied. Lymphocyte suspensions from lymph node tissues were obtained from patients diagnosed with diffuse large B-cell lymphoma. These were then divided into 8 aliquots. Each aliquot was incubated with a primary antibody for one of CCR4, CCR6, CCR7, CCR9, CCR10, CXCR4, CXCR5 or FACS buffer only. The cells were then incubated with a secondary antibody (or isotype control if only exposed to FACS buffer) conjugated with APC. Following this, all cells (except the isotype control) were incubated with anti-CD20-PE, following which the cells were analysed by 2-colour flow cytometry.

iii) **Mantle cell lymphoma** cases demonstrated some interesting findings. Again the demographic were representative with male predominance (male: female ratio 2:1) and a median age at presentation of 63 (46-86) years [291]. As with DLBCL, there was variety between the mean expressions of the different receptors (see figure 3.6) these were as follows; CCR4 56.67% (42.0-71.3), CCR6 24.09% (9.2-38.9), CCR7 91.03% (80.5-101.6), CCR9 35.34% (19.0-51.7), CCR10 0.16% (-0.0-0.3), CXCR4 95.33% (92.1-98.5) and CXCR5 93.89% (85.2-102.6). As with DLBCL, there was marked expression of CCR4, with MCL cases demonstrating the highest mean expression of this receptor. The other striking feature of these cases is the high expression of CCR7. However rather than being a new finding, this supports findings already reported in the literature [176]. Moreover, it emphasises the potential role of this receptor as a therapeutic target.

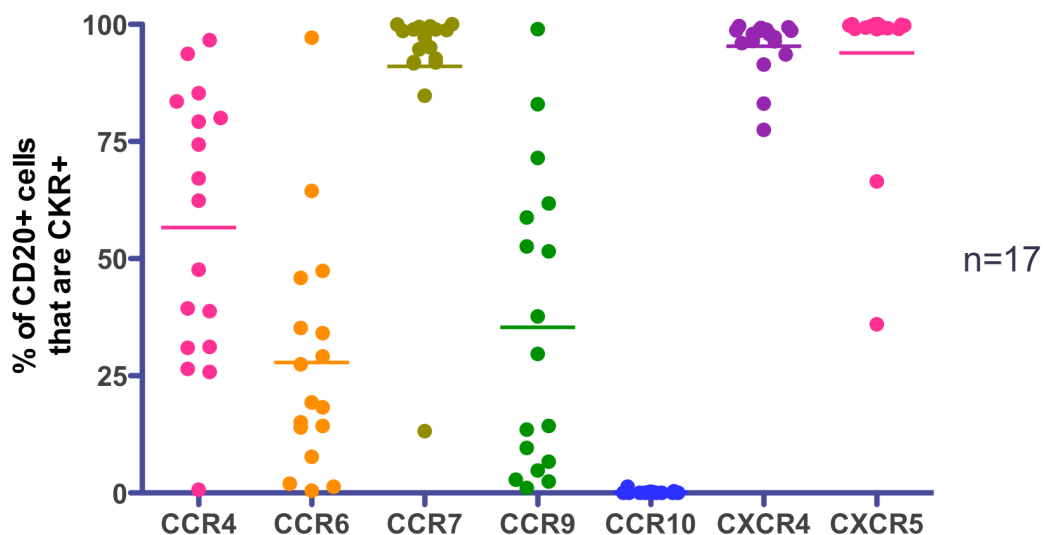


Figure 3.6: Distribution of chemokine receptor expression in 17 mantle cell lymphoma cases. The horizontal lines indicate the mean expression of the chemokine receptor studied. Lymphocyte suspensions from lymph node tissues were obtained from patients diagnosed with mantle cell lymphoma. These were then divided into 8 aliquots. Each aliquot was incubated with a primary antibody for one of CCR4, CCR6, CCR7, CCR9, CCR10, CXCR4, CXCR5 or FACS buffer only. The cells were then incubated with a secondary antibody (or isotype control if only exposed to FACS buffer) conjugated with APC. Following this, all cells were incubated with anti-CD20-PE (except the isotype control), after which the cells were analysed by 2-colour flow cytometry.

iv) The **Burkitt's lymphoma** cases were unusual in that all the cases occurred in male patients with a median age of 35 (0-82) years, reflecting the higher incidence in the younger age groups. However, Burkitt's lymphoma does have a higher incidence in males than females [286]. Again there was a variation in chemokine receptor expression within the B-cell population with the mean results obtained as follows; CCR4 56.89% (38.0-75.8), CCR6 27.85% (14.9-40.8), CCR7 52.94% (27.8-75.1), CCR9 39.10% (20.5-57.7), CCR10 1.93% (-0.6-4.5), CXCR4 97.63% (94.0-101.3) and CXCR5 98.58% (97.3-99.8). These figures are shown graphically in figure 3.7. It is interesting to note that the sample from the oldest patient (82 years) demonstrated the lowest level of expression for all of the chemokine receptors an observation that was not seen with any of the other NHL subtypes. Again there was notable expression of CCR4 in these cases, although there were no other significant findings or differences from the other lymphoma subtypes. Despite the literature previously discussed pertaining to CCR10 expression in Burkitt's lymphoma cell lines, CCR10 was not significantly expressed in any of the 9 cases studied. It is of course possible that there are differences in chemokine receptor expression between the endemic cases of Burkitt's lymphoma (which Daudi and Raji cell lines represent) and sporadic cases of Burkitt's lymphoma reported here. Although of course, CCR10 expression was not demonstrable at either the RNA or protein level in Daudi and Raji cells during this study.

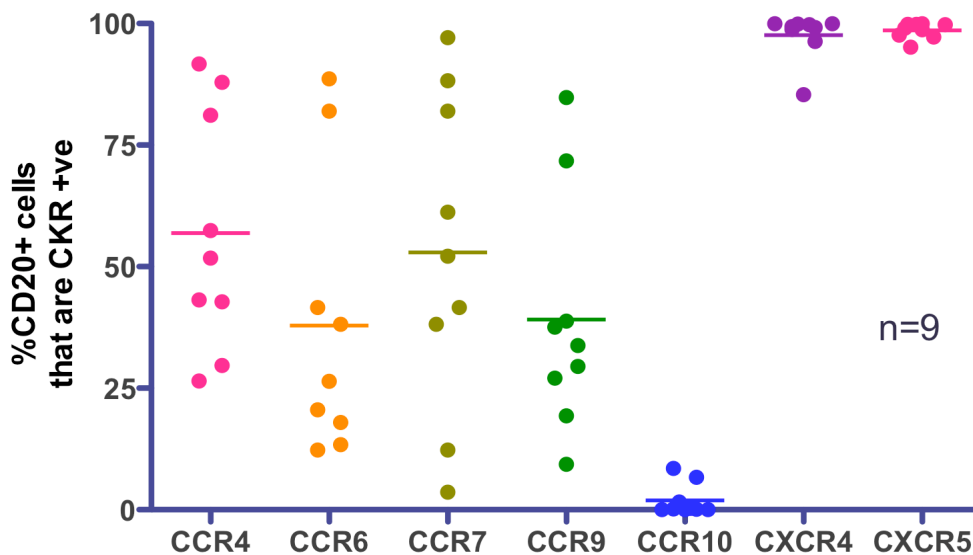


Figure 3.7: Distribution of chemokine receptor expression in 9 Burkitt's lymphoma cases. The horizontal lines indicate the mean expression of the chemokine receptor studied. Lymphocyte suspensions from lymph node tissues obtained from patients diagnosed with Burkitt's lymphoma. These were then divided into 8 aliquots. Each aliquot was incubated with a primary antibody for one of CCR4, CCR6, CCR7, CCR9, CCR10, CXCR4, CXCR5 or FACS buffer only. The cells were then incubated with a secondary antibody (or isotype control if only exposed to FACS buffer) conjugated with APC. Following this, all cells were incubated with anti-CD20-PE (except the isotype control), after which the cells were analysed by 2-colour flow cytometry.

v) The **MALT lymphoma** cases were also consistent with the known demographic data for this subtype with a median age of 65 (44-78) years and a female predominance with a male:female ratio of 4:1 [176]. Again there were differences with chemokine receptor expression (see figure 3.8) and the mean percentage of B-cells expressing the chemokine receptors analysed were as follows; CCR4 51.13% (40.3-61.9), CCR6 38.84% (19.4-58.2), CCR7 57.37% (36.6-78.1), CCR9 50.63% (25.7-75.6), CCR10 1.62% (0.1-3.1), CXCR4 90.66% (84.7-96.6) and CXCR5 95.72% (91.2-100.2). The MALT lymphoma cases represented the highest expression of both CCR6 and CCR9. This, however, would be expected as these lymphomas involve the mucosal tissues, most commonly the gut, with CCR6 and CCR9 demonstrating tropism for these anatomical sites [151, 176]. Interestingly, yet again, CCR4 expression was seen. Expression of the remaining chemokine receptors demonstrated no differences on comparison with the other NHL subtypes.

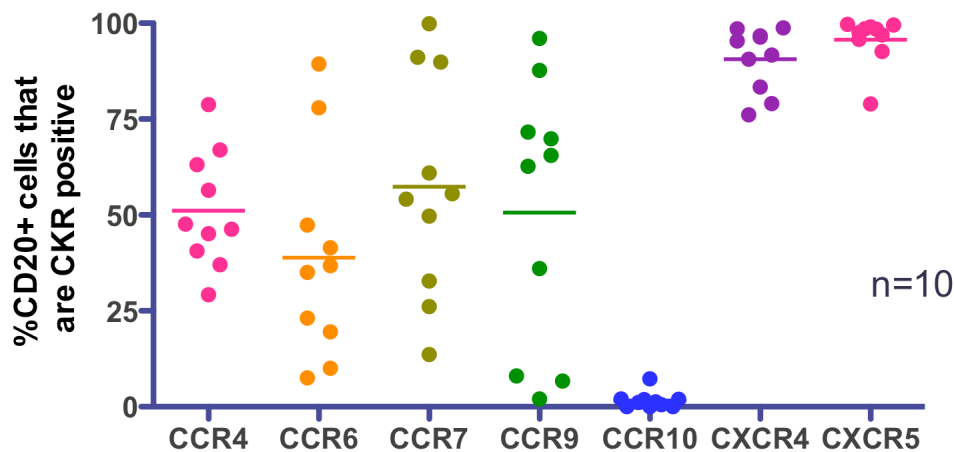


Figure 3.8: Distribution of chemokine receptor expression in MALT lymphoma cases. The horizontal lines indicate the mean expression of the chemokine receptor studied. Lymphocyte suspensions from lymph node tissues were obtained from patients diagnosed with MALT lymphoma. These were then divided into 8 aliquots. Each aliquot was incubated with a primary antibody for one of CCR4, CCR6, CCR7, CCR9, CCR10, CXCR4, CXCR5 or FACS buffer only. The cells were then incubated with a secondary antibody (or isotype control if only exposed to FACS buffer) conjugated with APC. Following this, all cells were incubated with anti-CD20-PE (except the isotype control), after which the cells were analysed by 2-colour flow cytometry.

vi) The median age at presentation of the **chronic lymphocytic leukaemia/small lymphocytic lymphoma** cases was 65 (15-89) years with an equal sex distribution, again consistent with published demographic data in CLL/SLL patients [342]. The mean chemokine receptor expression on the B-cells, as identified by CD19 expression, from these cases were as follows; CCR4 24.90% (16.1-33.7), CCR6 9.50% (0.9-18.0), CCR7 95.83% (91.4-100.3), CCR9 32.22% (21.3-43.2), CCR10 0.12% (-0.1-0.3), CXCR4 76.81% (68.3-85.4) and CXCR5 94.82% (91.7-97.4) (see figure 3.9). In general chemokine receptor expression was comparatively lower in CLL/SLL cases when compared to other subtypes (comparable to those levels found in follicular lymphoma). However there was one notable exception in that CCR7 expression in these cells was higher than with any other subtype [176]. This is akin to the CCR7 levels in mantle cell lymphoma cases, and thus demonstrating that CCR7 is an ideal target for CLL/SLL.

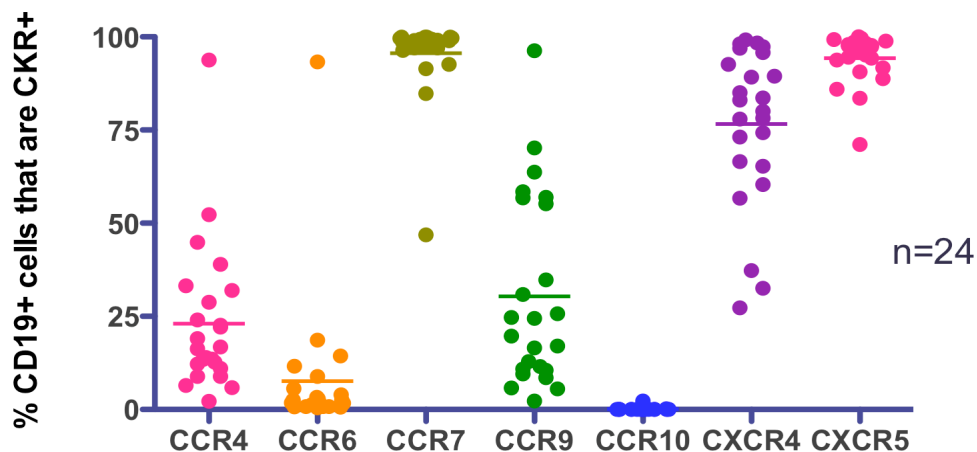


Figure 3.9: Distribution of chemokine receptor expression in 24 CLL/SLL. The horizontal lines indicate the mean expression of the chemokine receptor studied. Lymphocyte suspensions from lymph node tissues from patients diagnosed with CLL/SLL were obtained. These were then divided into 8 aliquots. Each aliquot was incubated with a primary antibody for one of CCR4, CCR6, CCR7, CCR9, CCR10, CXCR4, CXCR5 or FACS buffer only. The cells were then incubated with a secondary antibody (or isotype control if only exposed to FACS buffer) conjugated with APC. Following this, all cells were incubated with anti-CD19-PE (except the isotype control), after which the cells were analysed by 2-colour flow cytometry.

Whilst it would have been ideal to test against normal B-lymphocytes this was not done for a variety of reasons. It is difficult to compare malignant B-cells with normal B-cells as different lymphoma sub-types represent different stages of B-cell differentiation and it is not easy to isolate these B-cell subpopulations. B-cell populations in normal lymph node would potentially, but not necessarily, encompass all of these stages. Peripheral blood or bone marrow lymphocytes would have been incomparable due to the differences in chemokine receptor profiles in normal lymphocytes at these sites. Finally, plenty of literature is available to determine expected chemokine expression on the normal B-cell population at the various stages of B-cell differentiation, and information on this can be found in the discussion in chapter 7.

A summary of the results described in this section can be found in table 3.2 below.

	<i>% of B-cells Expressing the Chemokine Receptor</i>					
	<i>DLBCL</i> <i>n=16</i>	<i>FL</i> <i>n=16</i>	<i>MCL</i> <i>n=17</i>	<i>BL</i> <i>n=9</i>	<i>MALT</i> <i>n=10</i>	<i>CLL/SLL</i> <i>n=25</i>
<i>CCR4</i>	61.59 ± 6.52	11.84 ± 3.98	56.67 ± 6.92	56.89 ± 8.20	51.13 ± 4.77	24.90 ± 4.27
<i>CCR6</i>	27.34 ± 4.75	10.35 ± 3.11	24.09 ± 6.56	27.85 ± 6.12	38.84 ± 8.58	9.50 ± 4.13
<i>CCR7</i>	60.89 ± 6.44	25.54 ± 5.20	91.03 ± 4.97	52.94 ± 10.89	57.37 ± 9.18	95.83 ± 2.16
<i>CCR9</i>	38.87 ± 5.12	13.04 ± 3.07	35.34 ± 7.70	39.10 ± 8.07	50.63 ± 11.02	32.22 ± 5.30
<i>CCR10</i>	1.57 ± 1.21	0.18 ± 0.07	0.16 ± 0.08	1.93 ± 1.09	1.62 ± 0.68	0.12 ± 0.09
<i>CXCR4</i>	78.26 ± 4.71	52.17 ± 5.75	95.33 ± 1.49	97.63 ± 1.58	90.66 ± 2.62	76.81 ± 4.14
<i>CXCR5</i>	96.01 ± 0.96	84.5 ± 7.72	93.89 ± 4.11	98.58 ± 0.55	95.72 ± 1.98	94.52 ± 1.37

Table 3.2: Summary of mean chemokine receptor expression across different NHL subtypes. Each point shows the mean % of B-cells expressing the chemokine receptor ± standard error of the mean (SEM). Lymphocyte suspensions obtained from lymph node samples from patients with follicular lymphoma, DLBCL, MCL, Burkitt's lymphoma, MALT lymphoma and CLL/SLL were incubated with chemokine receptor antibodies, followed by incubation with secondary antibodies conjugated with APC and finally anti-CD20-PE or anti-CD19-PE. 2-colour flow cytometry was then used to analysis the percentage of B-cells expressing the different chemokine receptors.

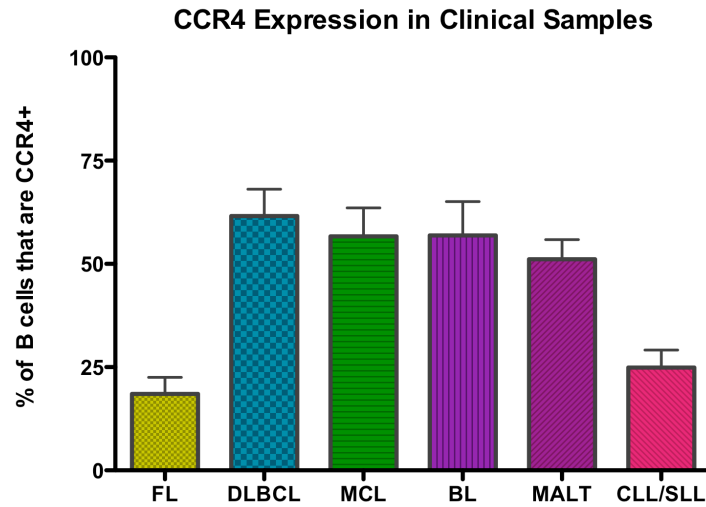
3.4.2 Comparison of Constitutive Chemokine Receptor Expression Between Lymphoma Subtypes

As well as noting the chemokine receptor expression in individual NHL subtypes, analyses were performed to see if there were any significant differences between the subtypes and chemokine receptor expression. Expression of a number of chemokine receptors showed significant differences across the NHL subtypes whilst with the remainder no significant differences were detected. These differences are discussed in this section. All statistical analyses between chemokine receptor expressions in the different NHL subtypes were performed using the un-paired student's t-test.

3.4.2.1 CCR4 Expression

Expression of CCR4 varied across the different NHL subtypes with the higher grade lymphomas (DLBCL, Burkitt's lymphoma and MCL), having significantly higher expression than the more indolent lymphomas (follicular lymphoma and CLL/SLL) (see figure 3.10). In all comparisons between follicular lymphoma and DLBCL, Burkitt's lymphoma and MCL, the difference in CCR4 expression was significant with $p < 0.0001$ in all cases. The difference in expression between CLL/SLL cases and DLBCL, Burkitt's lymphoma and MCL was also highly significant with p-values of $p < 0.0001$, $p = 0.0008$ and $p = 0.0002$ respectively. As mentioned earlier, the expression of CCR4 in B-cell lymphomas has not previously been reported beyond a single case report, and thus it is difficult to explain these differences. However, the MALT lymphoma, cases also demonstrated higher CCR4 expression, and was significantly higher than that seen in both follicular lymphoma and CLL/SLL cases (p-values; < 0.0001 and 0.0012 respectively). Whilst expression of CCR4 in the MALT lymphoma cases was lower than with DLBCL, Burkitt's lymphoma and MCL, this was not significant with p-values of $p = 0.2619$, $p = 0.5418$ and $p = 0.5788$ respectively. Of course, whilst MALT lymphomas tend to be indolent, the fact that in the clinical cases examined here, nodal, rather than the more typical extra-nodal disease was present; they may not be wholly representative of this lymphoma subtype. Yet, higher CCR4 in MALT lymphomas may be explained by the fact it is of mucosal origin and that that up regulation of CCR4 in mucosal tissues has been observed in response to inflammatory stimuli such as allergens [296]. Moreover CCR4 and its ligands have been implicated in the homing of T-cells to the gastric mucosa during *Helicobacter pylori* infection [343] (a known aetiological agent in MALT lymphomas). Whether a similar response is also seen in B-cells is an interesting question. Of course it is also possible that inflammation explains the higher CCR4 expression in the DLBCL, Burkitt's lymphoma

and MCL cases, as these lymphomas often have a higher inflammatory component than the more indolent forms.



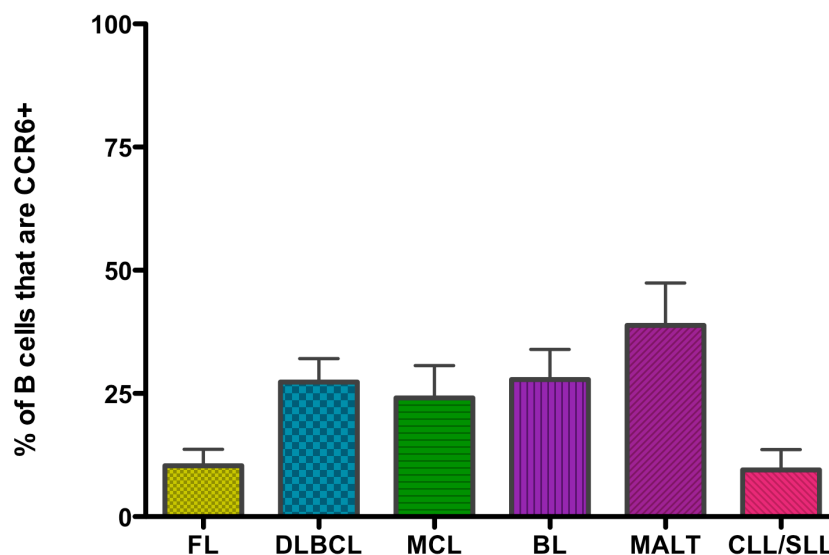
	DLBCL	MCL	BL	MALT	CLL/SLL
FL	p<0.0001	p<0.0001	p<0.0001	p<0.0001	ns
DLBCL	-	ns	ns	ns	p<0.0001
MCL		-	ns	ns	p=0.0002
BL			-	ns	p=0.0008
MALT				-	p=0.0012
CLL/SLL					-

Figure 3.10: Comparison of CCR4 expression between the lymphoma subtypes.

Lymphocytes obtained from lymph node tissues taken from patients with follicular lymphoma (FL), DLBCL, MCL, Burkitt's lymphoma (BL), MALT lymphoma and CLL/SLL. Each sample was incubated with anti-CCR4. This was followed by incubation with a secondary antibody conjugated with APC and finally incubation with anti-CD20-PE or anti-CD19-PE. 2-colour flow cytometry was then used to assess what proportion of B-cells expressed CCR4. The error bars represent the standard error of the mean. The table summarises the comparisons performed between the lymphoma sub-types, the analysis was performed using the unpaired t-test.

3.4.2.2 CCR6 Expression

The differences in CCR6 expression between the lymphoma subtypes was less striking than those seen with CCR4 expression (see figure 3.11) although, again there was significantly lower expression in follicular lymphoma cases when compared to DLBCL ($p=0.0071$), Burkitt's lymphoma ($p=0.0217$) and MALT lymphoma ($p=0.0017$). CLL/SLL cases also demonstrated lower expression of CCR6 when compared to DLBCL ($p=0.0083$), Burkitt's lymphoma ($p=0.0136$) and MALT lymphoma ($p=0.0015$). MCL cases did not demonstrate any significant difference in expression of CCR6 when compared to the other subtypes including follicular lymphoma and CLL/SLL. Unsurprisingly, the highest expression of CCR6 was seen in the MALT lymphoma cases. However this difference in expression was not significant when compared to any of the subtypes other than follicular lymphoma and CLL/SLL as described above, perhaps this may be explained by the fact that the tissue from these cases comprised of affected lymph nodes, and that CCR6 had been down regulated thus enabling homing of the malignant lymphocytes to the nodes.



	DLBCL	MCL	BL	MALT	CLL/SLL
FL	p=0.0071	ns	p=0.0217	p=0.0017	ns
DLBCL	-	ns	ns	ns	p=0.0083
MCL		-	ns	ns	p=0.0002
BL			-	ns	p=0.0136
MALT				-	p=0.0015
CLL/SLL					-

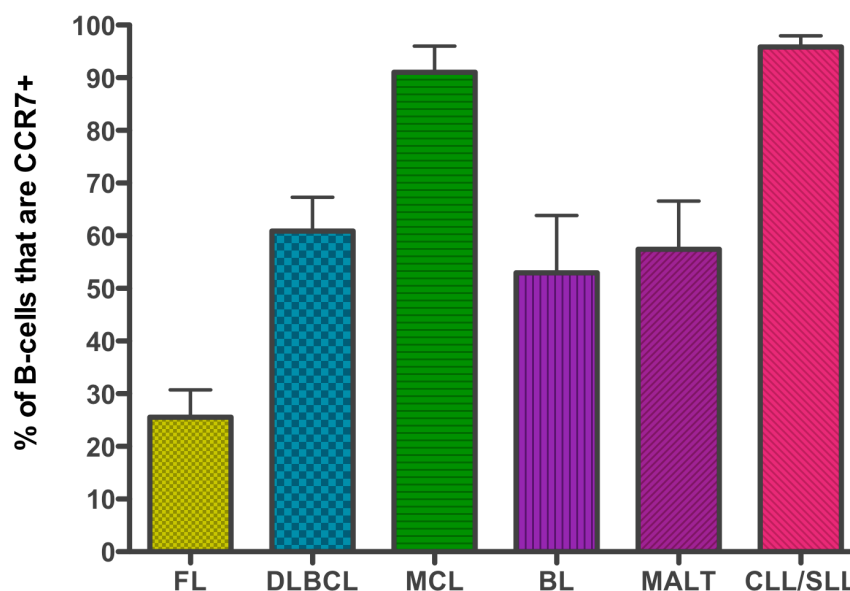
Figure 3.11: Comparison of CCR6 expression between the lymphoma subtypes.

Lymphocytes obtained from lymph node tissues taken from patients with FL, DLBCL, MCL, BL, MALT lymphoma and CLL/SLL. Each sample was incubated with anti-CCR6. This was followed by incubation with a secondary antibody conjugated with APC and finally incubation with anti-CD20-PE or anti-CD19-PE. 2-colour flow cytometry was then used to assess what proportion of B-cells expressed CCR6. The error bars represent the standard error of the mean. The table summarises the comparisons performed between the lymphoma sub-types, the analysis was performed using the unpaired t-test.

3.4.2.3 CCR7 Expression

There was a wide variation in CCR7 expression across the NHL subtypes as shown in figure 3.12. Yet again the lowest expression was noted in the follicular lymphoma cases with significantly lower expression of CCR7 in this subtype when compared to all of the other with the FL vs. DLBCL $p=0.0002$, FL vs. MCL $p<0.0001$, FL vs. Burkitt's lymphoma $p=0.0171$, FL vs. MALT lymphoma $p=0.0033$ and FL vs. CLL/SLL $p<0.0001$. However in this instance rather than having lower expression, CLL/SLL had significantly higher expression of CCR7 when compared to follicular lymphoma, DLBCL, Burkitt's lymphoma, and MALT lymphoma with a p-value in all of these comparisons of $p<0.0001$. A similarly high expression of CCR7 was also seen in MCL with MCL vs. FL $p<0.0001$, MCL vs. DLBCL $p=0.0008$, MCL vs. Burkitt's lymphoma $p=0.0012$ and MCL vs. MALT lymphoma $p=0.0016$. As discussed in the previous section, high CCR7 expression in MCL and CLL/SLL has been demonstrated in a number of studies, although comparison of CCR7 with other lymphoma subtypes is not widely reported. It is possible that the very high CCR7 expression seen in the MCL and CLL/SLL cases reflects the fact that these cells are found in the mantle zone of the lymph node where the B and T cell interactions occur and are mediated by CCR7 [344]. However, with expression of CCR7 exceeding 50% in all subtypes analysed (other than follicular lymphoma), exploration of targeted therapy against CCR7 would not be unreasonable in NHL.

In contrast, the lower expression of CCR7 in follicular lymphoma may also be explained by the stage of differentiation of the B cells, as the normal counterpart of the follicular lymphoma cells are entering a stage of differentiation when CCR7 expression is down regulated [143].

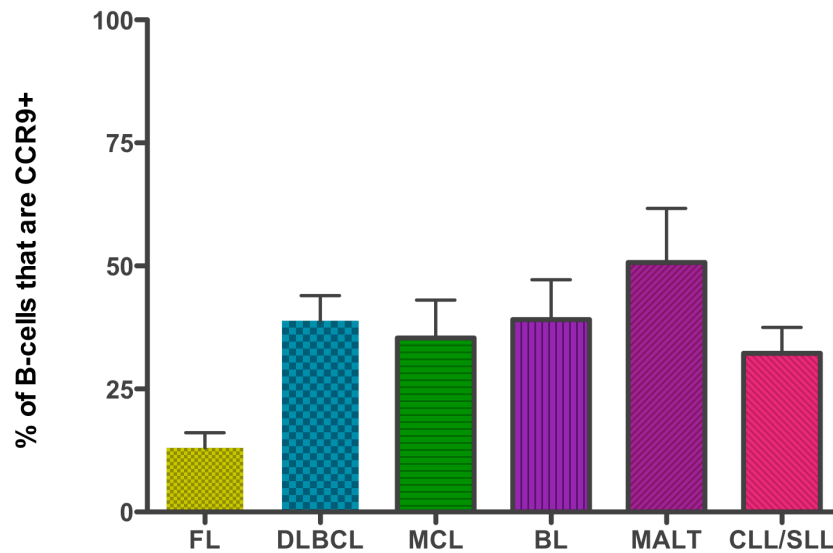


	DLBCL	MCL	BL	MALT	CLL/SLL
FL	p=0.0002	p<0.0001	p=0.0171	p=0.0033	p<0.0001
DLBCL	-	P=0.0008	ns	ns	p<0.0001
MCL		-	p=0.0012	p=0.0016	p<0.0001
BL			-	ns	p<0.0001
MALT				-	p<0.0001
CLL/SLL					-

Figure 3.12: Comparison of CCR7 expression between the lymphoma subtypes. Lymphocytes obtained from lymph node tissues taken from patients with FL, DLBCL, MCL, BL, MALT lymphoma and CLL/SLL. Each sample was incubated with anti-CCR7. This was followed by incubation with a secondary antibody conjugated with APC and finally incubation with anti-CD20-PE or anti-CD19-PE. 2-colour flow cytometry was then used to assess what proportion of B-cells expressed CCR7. The error bars represent the standard error of the mean. The table summarises the comparisons performed between the lymphoma sub-types, the analysis was performed using the unpaired t-test.

3.4.2.4 CCR9 Expression

There were differences in CCR9 expression between the different subtypes (see figure 3.13), however in this instance the only significant difference demonstrable was between follicular lymphoma and the other 5 subtypes, again with lower expression seen, the results were as follows, FL vs. DLBCL $p=0.0002$, FL vs. MCL $p=0.0132$, FL vs. Burkitt's lymphoma $p=0.0015$, FL vs. MALT lymphoma $p=0.0006$ and FL vs. CLL/SLL $p=0.01$. Although MALT lymphoma had the highest median expression of CCR9, as with CCR6, this was not significant, and the previous observation regarding lymph node tissue may apply here too. It was also a little surprising that the MCL cases had lower CCR9 expression as this lymphoma has a high incidence of gut involvement [143], with many clinicians advocating colonoscopy and biopsy as part of the staging procedure. Moreover $\alpha 4\beta 7$ integrins, which are co-expressed with CCR9 in gut homing lymphocytes, have been detected in those cases of MCL with gut involvement [244]. Although, of course the same argument regarding nodal vs. extra-nodal tissue could be used here, and widespread nodal involvement is far more common than with MALT lymphomas [345].



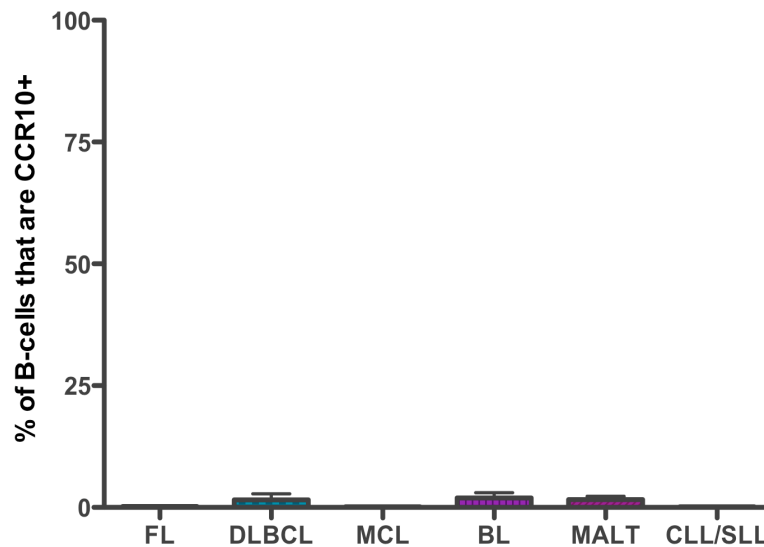
	DLBCL	MCL	BL	MALT	CLL/SLL
FL	p=0.0002	p=0.0132	p=0.015	p=0.0006	P=0.01
DLBCL	-	ns	ns	ns	ns
MCL		-	ns	ns	ns
BL			-	ns	ns
MALT				-	ns
CLL/SLL					-

Figure 3.13: Comparison of CCR9 expression between the lymphoma subtypes.

Lymphocytes obtained from lymph node tissues taken from patients with FL-follicular lymphoma, DLBCL, MCL –mantle cell lymphoma, BL-Burkitt's lymphoma, MALT lymphoma and CLL/SLL. Each sample was incubated with anti-CCR9. This was followed by incubation with a secondary antibody conjugated with APC and finally incubation with anti-CD20-PE or anti-CD-19-PE. 2-colour flow cytometry was then used to assess what proportion of B-cells expressed CCR9. The error bars represent the standard error of the mean. The table summarises the comparisons performed between the lymphoma sub-types, the analysis was performed using the unpaired t-test.

3.4.2.5 CCR10 Expression

CCR10 expression in all of the lymphoma subtypes was low, with less than 0.5% of cells expressing this receptor overall (see figure 3.14). Although CCR10 has been detected in the endemic Burkitt's lymphoma cell lines in published studies (although not verified in this study) [176], the absence of expression is not entirely surprising considering that this receptor is involved predominantly in the homing of lymphocytes to the skin [336], and the lymphocytes analysed here were all derived from lymph nodes, furthermore lymphoma subtypes studied here have a low incidence of cutaneous involvement [136].



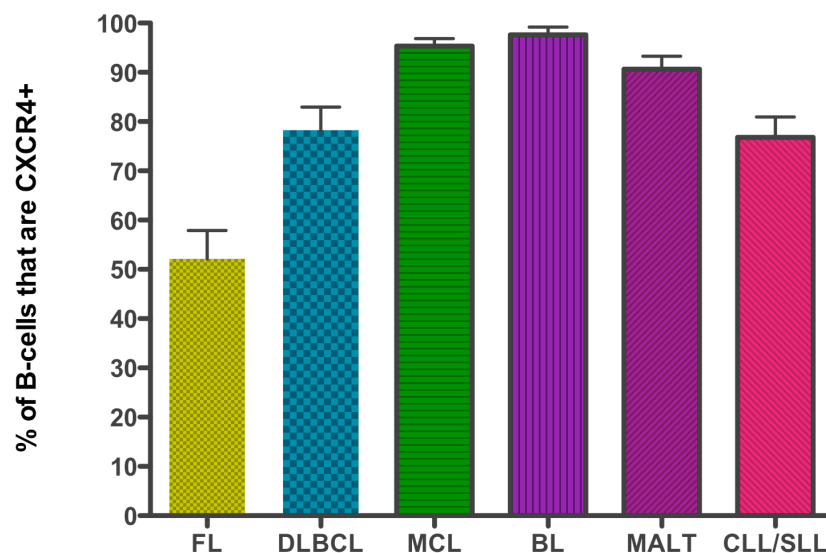
	DLBCL	MCL	BL	MALT	CLL/SLL
FL	ns	ns	ns	ns	ns
DLBCL	-	ns	ns	ns	ns
MCL		-	ns	ns	ns
BL			-	ns	ns
MALT				-	ns
CLL/SLL					-

Figure 3.14: Comparison of CCR10 expression between the lymphoma subtypes.

Lymphocytes obtained from lymph node tissues taken from patients with FL, DLBCL, MCL, BL, MALT lymphoma and CLL/SLL. Each sample was incubated with anti-CCR10. This was followed by incubation with a secondary antibody conjugated with APC and finally incubation with anti-CD20-PE or anti-CD19-PE. 2-colour flow cytometry was then used to assess what proportion of B-cells expressed CCR10. The error bars represent the standard error of the mean. The table summarises the comparisons performed between the lymphoma sub-types, the analysis was performed using the unpaired t-test.

3.4.2.6 CXCR4 Expression

Once again follicular lymphoma cases represented the group with the lowest receptor expression, with CXCR4 expression being significantly lower in comparisons with other subtypes although CXCR4 expression was generally high (see figure 3.15). The results of the comparative studies with follicular lymphoma were as follows; FL vs. DLBCL $p=0.0014$, FL vs. MCL $p<0.0001$, FL vs. Burkitt's lymphoma $p<0.0001$, FL vs. MALT lymphoma $p<0.0001$, FL vs. CLL/SLL $p=0.0010$. There were no significant differences in CXCR4 expression between the other lymphoma subtypes. CXCR4 has been noted in B-cells at all stages of differentiation, with expression occurring in the earliest stages of lymphocyte development and persisting to the latter stages [176], therefore the lower expression of this chemokine receptor on follicular lymphoma cells cannot be readily explained.



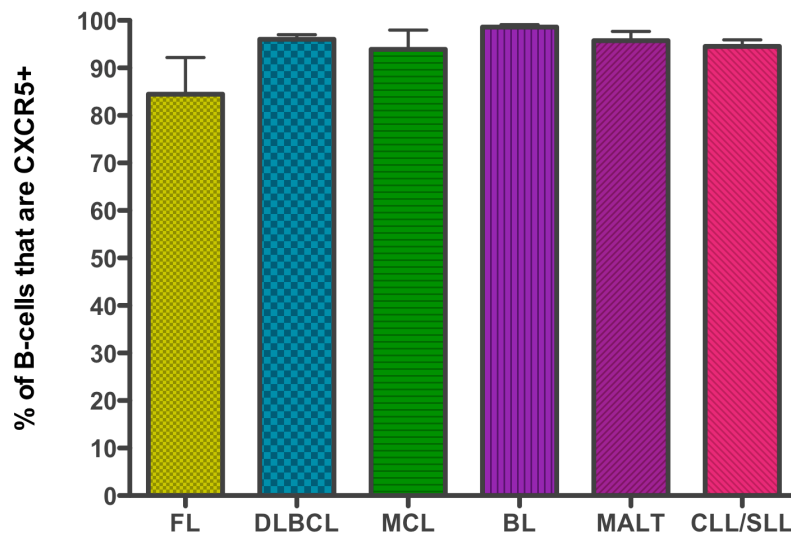
	DLBCL	MCL	BL	MALT	CLL/SLL
FL	$p=0.0014$	$p<0.0001$	$p<0.0001$	$p<0.0001$	$P=0.001$
DLBCL	-	ns	ns	ns	ns
MCL		-	ns	ns	ns
BL			-	ns	ns
MALT				-	ns
CLL/SLL					-

Figure 3.15: Comparison of CXCR4 expression between the lymphoma subtypes.

Lymphocytes obtained from lymph node tissues taken from patients with FL, DLBCL, MCL, BL, MALT lymphoma and CLL/SLL. Each sample was incubated with anti-CXCR4. This was followed by incubation with a secondary antibody conjugated with APC and finally incubation with anti-CD20-PE or anti-CD19-PE. 2-colour flow cytometry was then used to assess what proportion of B-cells expressed CXCR4. The error bars represent the standard error of the mean. The table summarises the comparisons performed between the lymphoma sub-types, the analysis was performed using the unpaired t-test.

3.4.2.7 CXCR5 Expression

As with CCR10, there were no significant differences between the lymphoma subtypes with regards to CXCR5 expression (see figure 3.16). However, in contrast to CCR10, CXCR5 expression was universally high, which corresponds to the fact that CXCR5 expression is found on B-cells at virtually all stages of development (albeit at varying levels) [143] and is considered by many as a B-cell marker. Once again lower expression was seen in the follicular lymphoma cases, but this was not significant with more than 80% of cells expressing the receptor.



	FL	DLBCL	MCL	BL	MALT	CLL/SLL
FL	-	ns	ns	ns	ns	ns
DLBCL		-	ns	ns	ns	ns
MCL			-	ns	ns	ns
BL				-	ns	ns
MALT					-	ns
CLL/SLL						-

Figure 3.16: Comparison of CXCR5 expression between the lymphoma subtypes.

Lymphocytes obtained from lymph node tissues taken from patients with FL, DLBCL, MCL, BL, MALT lymphoma and CLL/SLL. Each sample was incubated with anti-CXCR5. This was followed by incubation with a secondary antibody conjugated with APC and finally incubation with anti-CD20-PE or anti-CD19-PE. 2-colour flow cytometry was then used to assess what proportion of B-cells expressed CXCR5. The error bars represent the standard error of the mean. The table summarises the comparisons performed between the lymphoma sub-types, the analysis was performed using the unpaired t-test.

3.5 Correlation of Constitutive Chemokine Receptor Expression with Clinical Outcome

As discussed in the introduction there have been studies demonstrating that expression of certain chemokine receptors are associated with differences in prognosis and clinical presentation. Following analysis of the chemokine receptor expression on the clinical samples, the differences in CCR4 expression were the most surprising, and subsequently of most interest. Expression of the other constitutive chemokine receptors in the different NHL subtypes could be explained by correlation with chemokine receptor expression of their normal B-cell counterpart or by the natural tropism of the lymphoma. As has previously been discussed, CCR4 expression is associated with an adverse prognosis in T-cell lymphomas, such as adult T-cell leukaemia/lymphoma [143]. Therefore it would be of interest to see if the same held true for the B-cell lymphomas studied here, and therefore the association between CCR4 expression and outcome was examined. In order to do this patient data correlating with the samples analysed previously were collected from established databases, the Scottish & Newcastle Lymphoma Group (SNLG) and West of Scotland Lymphoma Group (WOSLG). Prior to entry in these databases, consent had been obtained from all patients allowing their clinical information to be released to researchers in the field of lymphoma. Only clinical details for diffuse large B-cell lymphoma, follicular lymphoma and mantle cell lymphoma were analysed. The reasons for this were three fold; firstly the number of cases of Burkitt's lymphoma was too low to be of value in this study and was unlikely to be representative of this lymphoma subtype as all patients in this group were male. Secondly, MALT lymphomas were excluded from clinical correlation, as by definition if there is nodal involvement, these are already an unusual subtype of this lymphoma, which is usually associated only with mucosal involvement. Finally, the majority of CLL/SLL cases were not followed up as part of either database. This is because although CLL/SLL is considered by current WHO guidelines to be a single disease entity, clinically CLL and SLL present in a very different manner with the leukaemic presentation being more common and therefore, these cases would not have been entered into either database on many occasions.

3.5.1 Correlation Between CCR4 Expression and Clinical Course

3.5.1.1 Overall Survival and CCR4 Expression

When looking at the correlation between CCR4 expression and outcome in the three, lymphoma subtypes, the only significant difference was in those patients with DLBCL (see figure 3.17a). For the purposes of this analysis CCR4 expression was considered to be high in an individual patient if the percentage of B-cells expressing CCR4 in their sample was higher than the median observed from the above studies for that lymphoma sub-type. In the case of DLBCL the median % of B-cells expressing CCR4 was 61.1%, with 8 patients in the high CCR4 expression group and 7 in the low CCR4 expression group. Analysis was performed using the log-rank (Mantel-Cox) test. The Kaplan-Meier charts below show the overall survival in the patient groups for DLBCL, mantle cell lymphoma and follicular lymphoma. Figure 3.17a clearly demonstrates a significant ($p=0.004$) survival advantage in those patients with a higher than median expression of CCR4, with all 4 deaths occurring in the low CCR4 expressing cohort. Furthermore, median survival for the high CCR4 expressing group had not been reached. However the median survival for the low expressing CCR4 group was only 22 months. This is contrary to previous studies looking at CCR4 expression and outcome in T-cell lymphoma [291] and Hodgkin's lymphoma [291] where high expression of CCR4 correlated with a poorer clinical outcome.

In contrast, when assessing the outcome in mantle cell lymphoma patients where the median % of CCR4 expressing B-cells was 62.4%, the median survival for those 6 patients with high expression of CCR4 (20.4 months) was lower than for the 8 patients with low CCR4 expression (46 months), suggesting that higher CCR4 expression adversely affected outcome, but this difference was not statistically significant ($p=0.2545$). The Kaplan Meier chart for this is shown in figure 3.17b. Finally, the differences between high and low CCR4 expression in follicular lymphoma cases were not significant ($p=0.1737$) either with the median % of CCR4 expression being 11.8%, the median survival was not reached in either arm, with the high expressing group containing 6 patients and the low expressing group containing 7 patients (figure 3.17c). Although it is interesting to note that all deaths occurred in the high CCR4 expression arm. The fact that median survival was not reached in either arm and that differences in survival were not significant between low and high CCR4 expressing patients was perhaps not surprising considering that follicular cases have lower overall CCR4 expression and that the disease has a more indolent course with a median survival beyond 10 years from diagnosis [340].

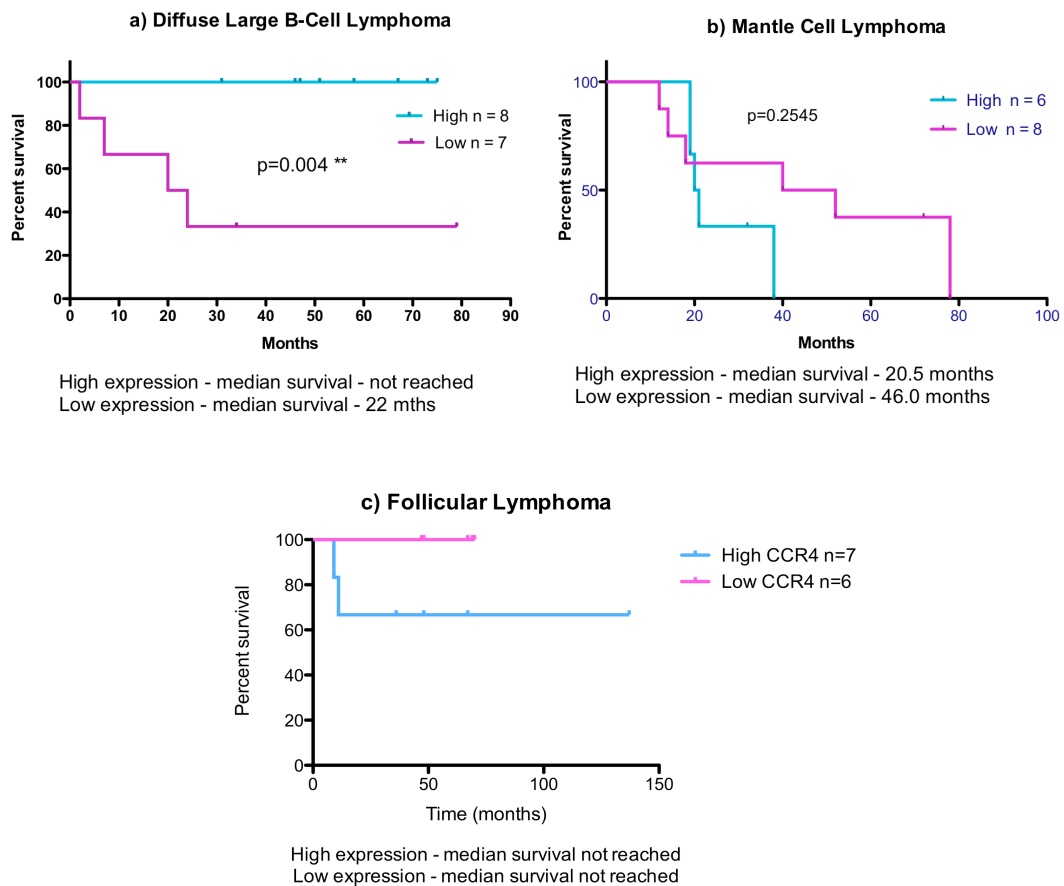


Figure 3.17: Kaplan-Meier charts comparing survival between NHL patients with high or low levels of CCR4 expression on B-cells. a) Diffuse large B-cell lymphoma cases, b) Mantle cell lymphoma cases, c) Follicular lymphoma cases. Survival data was obtained on those patients whose samples were analysed in section 3.4 from the SNLG and WOSLG; this data was then used to create these survival graphs. Patients were considered as having high CCR4 expression if the percentage of B-cell expressing CCR4 in their samples was greater than the median for that NHL group. Statistical analysis was performed using the log-rank (Mantel-Cox) test.

3.5.1.2 Stage of Lymphoma at Presentation and CCR4 Expression

If this is explored further, it can be shown that, with diffuse large B-cell lymphoma, clinically more advanced stage disease appears to be seen more frequently in those with low CCR4 expression. No significant differences could be detected however, due to the very small patient group, but the results are shown graphically in figure 3.18, which show higher numbers of patients with most advanced stage of disease (Stage IV) seen in the low CCR4 expression group compared to the high CCR4 expressing group (3 vs. 1). No obvious differences in stage at clinical presentation was seen in those patients with mantle cell lymphoma and the level of CCR4 expression, with all patients presenting in the advanced stages (stage III and IV). Unfortunately, too few of the follicular lymphoma cases had initial staging information available and no conclusions could be made about the relationship between CCR4 expression and clinical stage at presentation.

No conclusions can be made with regards to CCR4 expression and the clinical stage of disease in DLBCL, MCL or follicular lymphoma. However, although the numbers are small, there is an indication that CCR4 expression may correlate with prognosis in DLBCL with higher expression appearing to confer a good prognosis. In contrast there was a non-significant trend towards to more adverse outcomes in MCL and follicular lymphoma. Further discussion of these observations can be found in chapter 7.

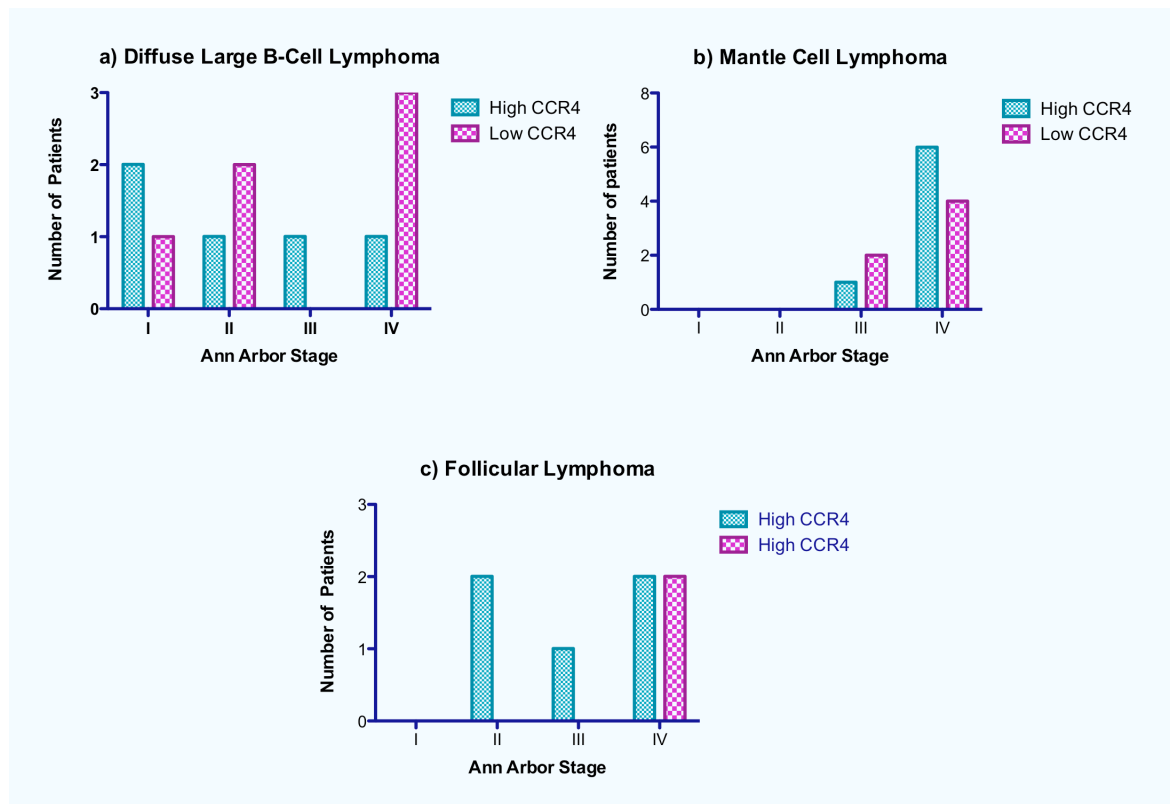


Figure 3.18: Correlation between clinical stage and CCR4 expression in patients with DLBCL, MCL or follicular lymphoma. Clinical data relating to the stage of disease at presentation was obtained on those patients whose samples were analysed in section 3.4 from the SNLG and WOSLG, this data was then used to analyse whether or not there was a relationship with stage at presentation and the level of CCR4 expression. Patients were considered as having high CCR4 expression if the percentage of B-cell expressing CCR4 in their samples was greater than the median for that NHL group. No obvious relationship was demonstrated, however, data on the clinical stage at presentation was not recorded for all patients.

3.6 Summary

Further discussion of the results outlined in this chapter can be found in chapter 7.

However the following summary points can be made with regards to the studies described.

1. Constitutive chemokine receptor expression has been characterised in MOLT-4, Daudi and Raji cells by using RT-PCR and flow cytometry studies.
2. A relationship between constitutive chemokine receptor expression and non-Hodgkin's lymphoma subtype has been shown.
3. CCR4 expression is significantly higher in higher grade lymphoma sub-types when compared to more indolent lymphoma sub-types, with the exception of MALT lymphomas.
4. There appears to be a correlation between high CCR4 expression and a favourable outcome in patients with DLBCL. This is not seen in cases of MCL or follicular lymphoma with a non-significant trend to poorer outcomes.
5. A trend towards more advanced disease is seen in those patients with low CCR4 expression and DLBCL. However, the number of cases was too low to draw any firm conclusions.
6. No obvious relationship was noted between disease stage and CCR4 expression in MCL or follicular lymphoma.

CHAPTER FOUR

IN-VITRO STUDIES OF CCR7

4.1 Introduction

Having characterised chemokine receptor expression on a selection of non-Hodgkin's lymphoma (NHL) subtypes, the second aspect of this project was to examine how the chemokine system could be targeted to provide a therapeutic strategy in NHL. However, before doing this a suitable chemokine receptor and in-vitro model was required in order to provide a proof-of-principle for subsequent targeting strategies that may be employed. In this case CCR7 was the chemokine receptor chosen. CCR7 was chosen for a number of reasons; firstly, it is the second most commonly expressed receptor in cancers following CXCR4 [176]. However unlike CXCR4 it has a more restrictive pattern of expression in normal tissues, namely naïve T cells, central memory T-cells, [86], dendritic cells, thymocytes and naïve B-cells [346]. Another reason for choosing CCR7 as a target is its integral role in the homing of lymphocytes to secondary lymphoid organs (the most common sites of dissemination in lymphomas). This is highlighted by studies in CCR7^{-/-} mice in which gross abnormalities in the structural organisation of secondary lymphoid organs are observed. Furthermore, these abnormalities correlate with dysfunctional immune responses including delayed antibody responses [347]. Additionally, CCR7 has clearly been demonstrated to be involved in the development of nodal metastases in other malignancies, demonstrating that this target could have therapeutic potential across a range of tumour types [88].

In order to test CCR7, cell lines expressing this receptor were required for study. Cell lines were engineered to express hCCR7 so that cells with high expression of the receptor could be studied. In addition, Raji cells were chosen as a cell line known to endogenously express hCCR7. Results from experiments using Raji cells would be more likely to resemble those expected from studies on primary lymphoma tissue samples or from *in-vivo* lymphoma studies, than engineered cell lines. Finally, although CCR7 responds to two ligands, CCL19 and CCL21, the experiments that follow used CCL19. This was a deliberate choice as although CCR7 responses to CCL21 are up to 100 fold more potent, only CCL19 is internalised following receptor binding [348]. This is important as many of the methods explored for targeting and killing CCR7 positive cells require internalisation

of the ligand bound to a cytotoxic agent such as ^{125}I (described in this chapter), adenovirus (described in chapter 5) or chemotoxins. This chapter outlines the development of an hCCR7 expressing cell line, along with functional assays on these and Raji cells, and finally the results obtained from one approach to target CCR7 cells and induce cytotoxicity.

4.2 Constructs and Cell Lines

The PCR-based strategy outlined in sections 2.2.4.3.1 and 2.2.4.8 was used to develop the pcDNA3.1-hCCR7 vector (Figure 4.1). This was used to develop a human CCR7 (hCCR7) expressing cell line. Human embryonic kidney cells (HEK 293) cells were used to engineer a cell line with high levels of hCCR7. In brief, primers were developed to obtain a PCR product encompassing the complete coding sequence of hCCR7. cDNA from Raji cells was synthesised using reverse transcriptase, this was subsequently used for RT-PCR using the primers detailed above. Following verification by sequencing, the PCR product obtained after RT-PCR was inserted into the pcDNA3.1/V5 His⁶TOPO³TA vector using Hind III and EcoR V restriction enzyme sites, now termed pcDNA3.1.hCCR7 (figure 4.1). This plasmid was then transfected into HEK-293 cells using Effectene[®] (2.2.2.4.1). Stable transfectants were obtained by selection with G418 (neomycin) (0.8mg/ml) added to the culture medium. The resulting pool of transfectants was then sub-cloned in order to obtain a pool of high hCCR7 expressing cells. These cells were analysed for hCCR7 expression in the two ways as described below.

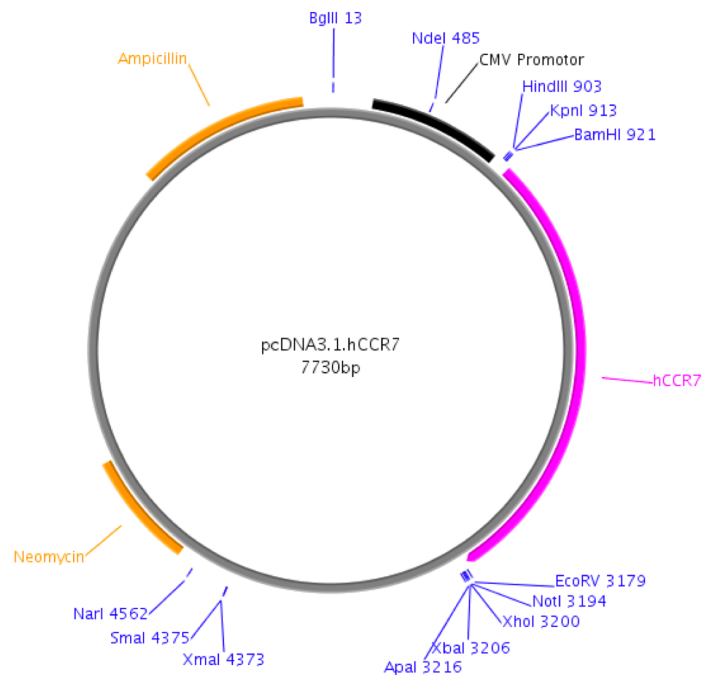


Figure 4.1: pcDNA3.1.hCCR7 used to engineer hCCR7 expressing cell lines. Primers were developed to enable amplification of the complete coding sequence for hCCR7 by PCR. This was then cloned into the pcDNA3.1/V5 His@TOPO@TA using *HindIII* and *EcoRV* restriction enzyme sites. The resulting construct is outlined above.

4.2.1 Assessment of hCCR7 Expression by Flow Cytometry

Once adequate numbers of stably transfected cells were obtained through G418 selection, they were harvested and examined for expression of hCCR7 using an anti-hCCR7 antibody. Single-colour flow cytometry as described in 2.2.3 was then used to analyse the expression of hCCR7 following incubation with anti-hCCR7 antibody and a secondary antibody conjugated to the fluorochrome phycoerythrin (PE). Un-transfected HEK293 cells were used as a negative control. The results of flow cytometry on the sub-pool with the highest CCR7 expression (HEK.hCCR7.1) are shown in figure 4.2. This demonstrates successful transfection of HEK293 cells with hCCR7, as evidenced by a shift in fluorescence to the right along the FL2-H gate in figure 4.2b as compared to figure 4.2a, which represents untransfected HEK 293 cells. However, in the dot plot (figure 4.2b) and the overlay histogram (figure 4.2c), it can be seen that there are 2 distinct populations within the transfected cells expressing hCCR7 at different levels. All of these cells are

subsequently referred to as HEK.hCCR7 cells and the two populations were maintained as a pool in medium containing G418.

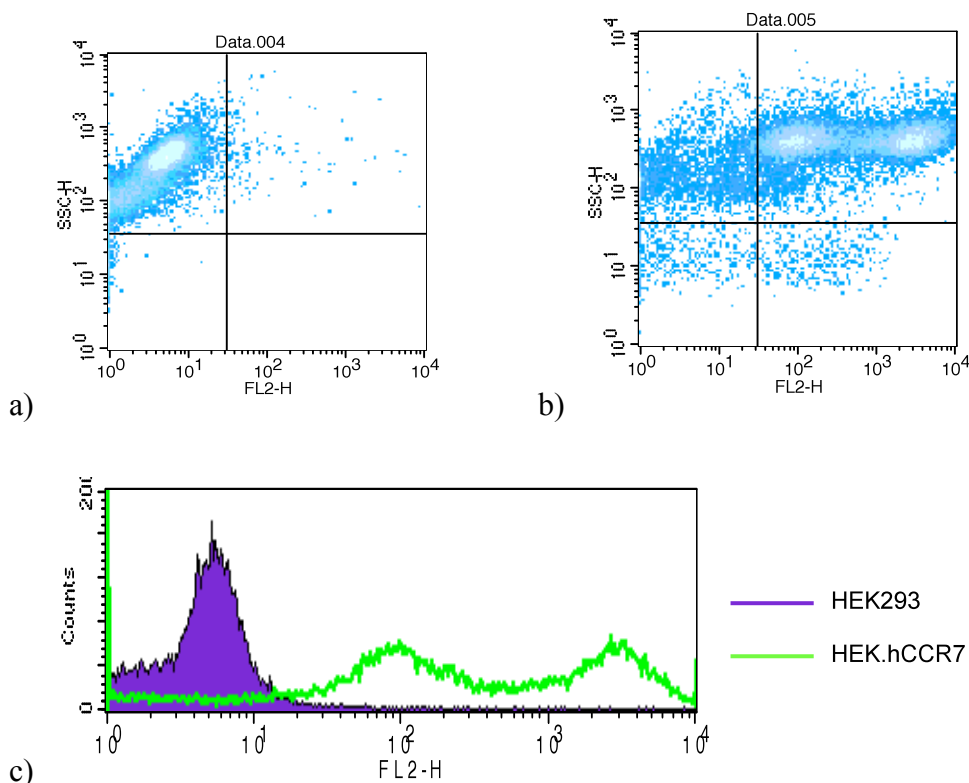


Figure 4.2: hCCR7 surface expression in HEK293.hCCR7 cells. a) Untransfected HEK293 cells incubated with anti-hCCR7 antibody, b) HEK.hCCR7 cells incubated with anti-hCCR7 antibody c) Overlay histogram confirming expression of hCCR7 by HEK.hCCR7 cells. Note 2 peaks of hCCR7⁺ indicating a pool of HEK.hCCR7 cells. HEK293 cells were transfected with pcDNA3.1.hCCR7 using Effectene® (section 2.2.2.4.1) and incubated in a selective media containing G418. The cells were then analysed for hCCR7 expression using single colour flow cytometry. This data is representative of the results obtained from this analysis on at least 3 occasions.

4.2.2 Functional assessment of hCCR7 Expression by biotin-CCL19

Uptake

Although the HEK.hCCR7 cells demonstrated good surface expression of hCCR7, the functional competence of this receptor had to be formally demonstrated. In order to do this, analysis of the ability of the cells to take up one of the ligands for CCR7, CCL19, was analysed. For this, CCL19 with biotinylation at the C-terminus of the protein was used, enabling binding of streptavidin-PE, whilst leaving the N-terminus free to interact with its cognate receptor. This method is described in section 2.2.5.2, and similar experiments performed in the laboratory using confocal microscopy, have demonstrated that the biotin-CCL19/streptavidin-PE complex is internalised by cells expressing CCR7 (Iain Comerford, PhD thesis, 2005). Following incubation of the cells at 37⁰C for one hour, in the dark, with

biotin-CCL19 and streptavidin-PE, up take of the complex was detected using single-colour flow cytometry, The results of the biotin-CCL19 uptake studies are shown in figures 4.3 and 4.4. Figure 4.3 is a graphical representation of the mean fluorescent intensity obtained following analysis of two pools of the hCCR7 transfected cells, HEK.hCCR7.1 and HEK.hCCR7.2, compared with HEK293 cells. This shows that with increasing concentrations of the biotin-CCL19, increased uptake of the chemokine is noted in the hCCR7+ cells, with the HEK.hCCR7.1 pool having the highest degree of uptake, this correlated with higher hCCR7 expression in the HEK.hCCR7 cells as determined by flow cytometry analysis using anti-hCCR7 antibodies. Subsequent analysis, including the results shown in figure 4.2 and 4.4 were performed using the HEK.hCCR7.1 pool, now referred to as HEK.hCCR7 cells. The dot plots also demonstrate that the hCCR7 receptors are functional and are able to bind to, and internalise, CCL19 (figure 4.4b) with a shift to the right along the FL2-H gate noted in comparison to the negative control (4.4a). Again it can be seen that there are two populations within these cells, corresponding with the two populations observed in the previous section. CCL19 is therefore a useful tool in assessing the ability of the receptor to internalise on binding with its cognate ligand.

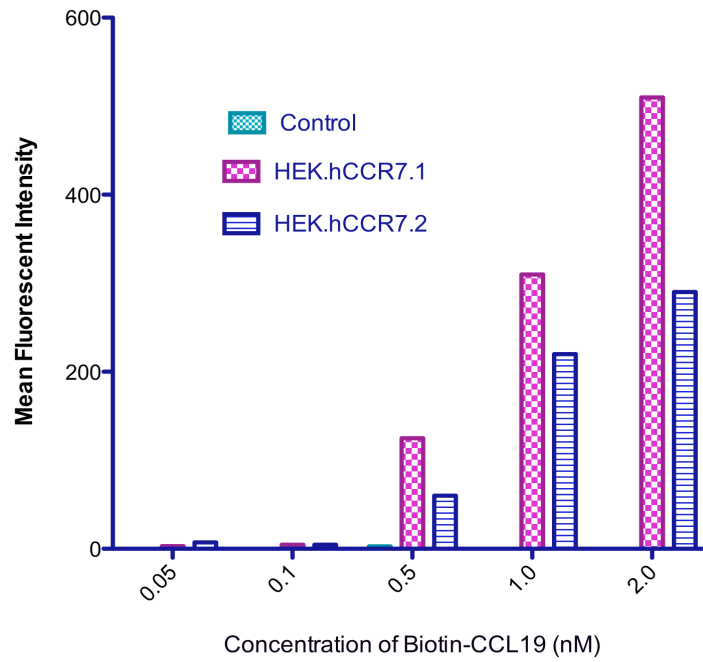


Figure 4.3: Biotin-CCL19 uptake by pools of HEK.hCCR7 cells. Cells were incubated with biotin-CCL19 and streptavidin-PE for 1hr at 37°C using different concentrations of CCL19. Following this biotin-CCL19 binding/uptake by the cells was analysed using single-colour flow cytometry. Results from the negative control sample, HEK 293 cells, can just be observed at the 0.5nM concentration point on the graph. This experiment was performed in triplicate on one occasion.

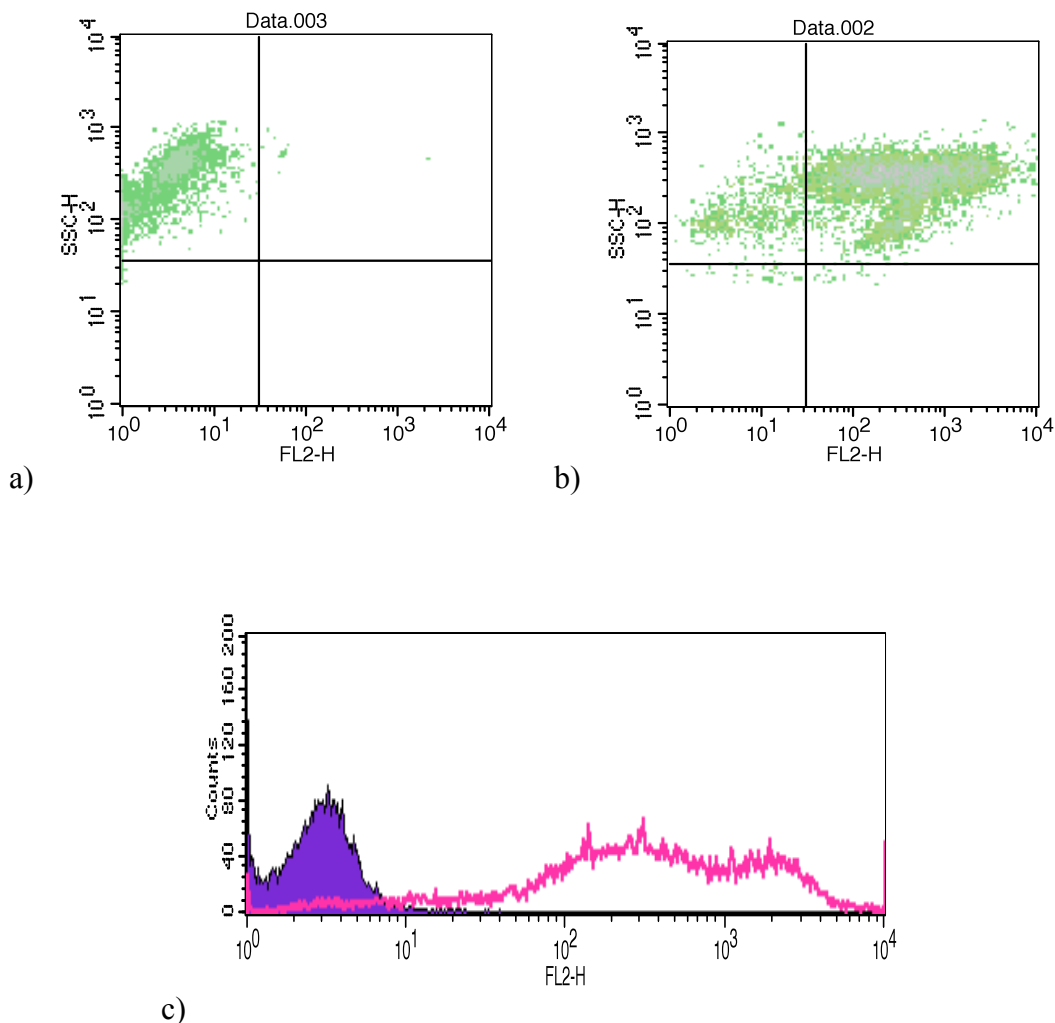


Figure 4.4: Biotin-CCL19 uptake by HEK.hCCR7 cells. a) Un-transfected HEK293 cells incubated with biotin-CCL19 and streptavidin-PE, b) HEK.hCCR7 cells incubated with biotin-CCL19 and streptavidin-PE c) Overlay demonstrating that the HEK293-hCCR7 (pink line) cells take up biotin-CCL19 with lack of uptake by HEK293 cells (purple curve). Cells were incubated with biotin-CCL19 and streptavidin-PE for 1hr at 37°C using different concentrations of CCL19. Following this biotin-CCL19 binding/uptake by the cells was analysed using single-colour flow cytometry. The mean fluorescent intensity was calculated from the population of cells contained within the upper right quadrant in figure b). This data is representative of results obtained from this experiment and represents single data points.

4.3 Functional Analysis of CCR7 in Raji Cells

As described in the introduction to this chapter, in addition to studying hCCR7 in cells engineered to express it, it was also the aim to study the function of hCCR7 in cells with endogenous expression. In Chapter 3, it was demonstrated that Raji cells express hCCR7 at both the transcriptional and protein level and further assays were then undertaken to elucidate whether or not the expressed receptor was functional. This is important because, as seen in some studies on normal and malignant B cells, expression of CCR7 does not always equate with function [119]. This may be due to a number of reasons including the concentration of receptors on the cell surface, the concentration of the ligand in the microenvironment, the presence of stimulatory or inhibitory substances and other microenvironmental factors. By knowing if expression translated into function, it could be determined whether or not the Raji cells were suitable to be used as an *in-vitro* lymphoma model for targeted cellular toxicity. The functional aspects of hCCR7 in Raji cells were tested in two ways; these are outlined below.

4.3.1 Biotin-CCL19 Uptake in Raji Cells

The biotin-CCL19 uptake assay was used to assess whether or not CCR7 on Raji cells were capable of internalising this ligand. The same method was used for this assay as for the HEK.hCCR7 cells described in section 4.2.2. using a biotin-CCL19 at a concentration of 0.5nM. In this case, the negative control consisted of Raji cells incubated with streptavidin-PE and PBS only. Following incubation, again at 37⁰C for 1 hour, the cells were analysed using single colour flow cytometry. The results are shown in figures 4.5a-d. These show that there is increased fluorescence detected in the Raji cells incubated with the biotin-CCL19 (figure 4.5b), with a shift to the right along the FL2-H gate as compared to those not exposed to biotin-CCL19, with no shift detected (figure 4.5a). Figure 4.5c shows the overlay histogram with blue peak shifted to the right, representing Raji cells incubated with biotin-CCL19, whilst the red peak representing those cells not exposed to the biotin-CCL19 does not show any shift. Furthermore, figure 4.5d demonstrates the mean fluorescent intensity (MFI) obtained during the analysis. There was a significantly higher MFI ($p=0.0005$) detected in the Raji cells, incubated with the biotin-CCL19, with a MFI of 178.63 (95% confidence interval: 106.4-245.96) when compared to the Raji cells incubated with the streptavidin-PE only with a MFI of 5.67 (95% confidence interval: -3.97-19.03). These data therefore demonstrate that CCR7 on Raji cells is able to bind to, and internalise, CCL19. It could be assumed that all binding of CCL19 was due to the endogenously expressed hCCR7. However another explanation could be that the Raji cells also express

the atypical receptor CCX-CKR. CCX-CKR also binds to and internalises CCL19, although to date no signalling events have been detected as a consequence [286]. Therefore it is possible that not all of the biotin-CCL19 is being internalised by CCR7 but rather through this atypical receptor too. This is addressed in the next section.

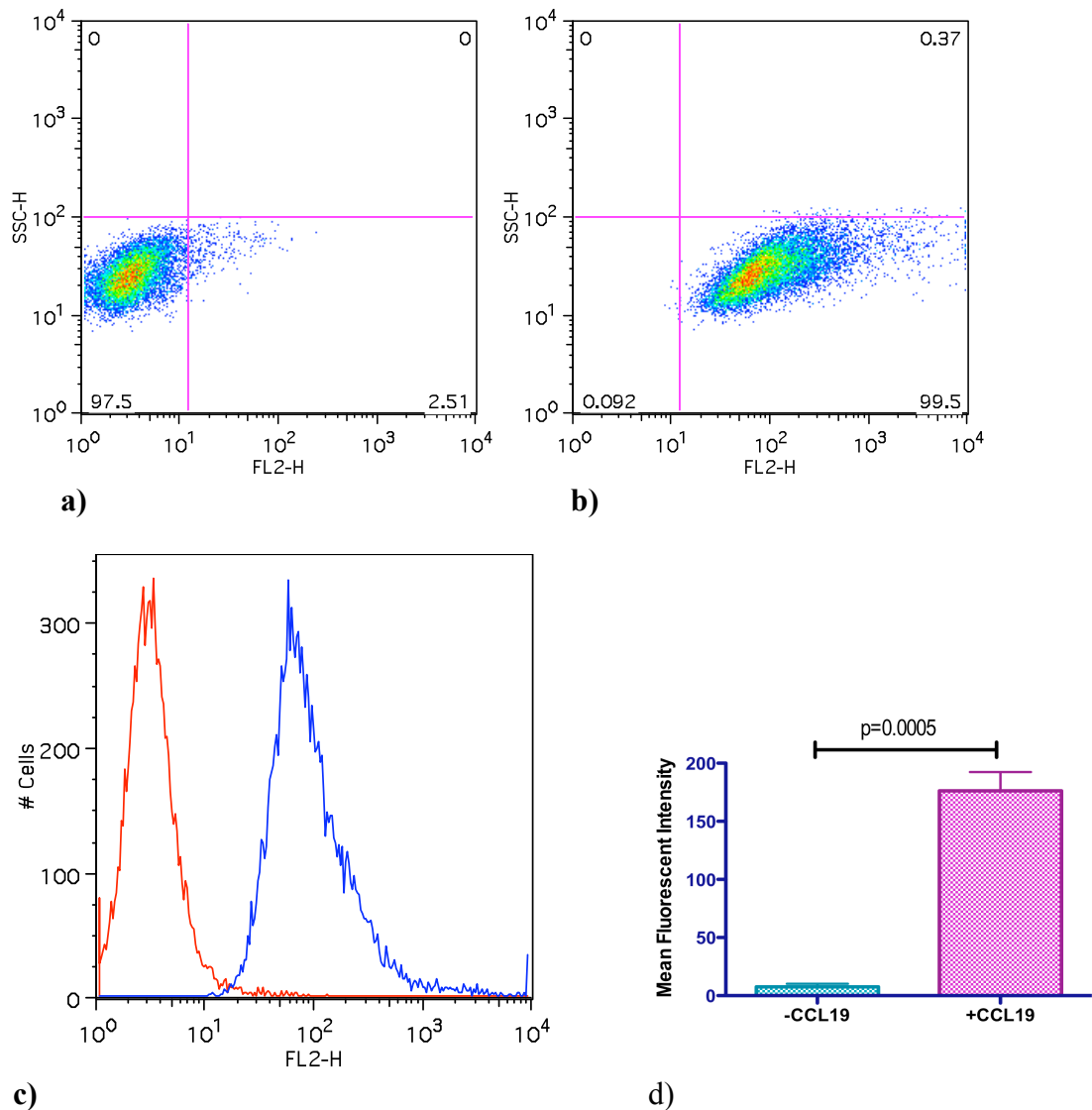


Figure 4.5: Biotin-CCL19 uptake in Raji cells. Cells were incubated with biotin-CCL19 and streptavidin-PE or streptavidin-PE alone, for 1hr at 37°C. Following this biotin-CCL19 uptake by the cells was analysed using single-colour flow cytometry. a) Raji cells incubated with streptavidin-PE alone, b) Raji cells incubated with the biotin-CCL19-streptavidin-PE complex, c) Overlay histogram plot comparing Raji cells incubated with biotin-CCL19 (blue peak) or streptavidin-PE alone (red peak), d) Graph showing a significant difference in mean fluorescent intensity between Raji cells incubated with or without biotin-CCL19. The samples were set up in triplicate and the results in the graph experiment represent the results obtained on a single occasion. MFI for the positive cells was calculated from the population seen in the lower right quadrant in figure b).

4.3.2. Chemotaxis Assays on Raji cells

CCX-CKR is an atypical receptor that to date has not demonstrated any intracellular signalling following internalisation of CCL19 [349], and thus does not support chemotaxis. In retrospect it would have been interesting to assess Raji cells for expression of CCX-CKR, however this was not done. Yet, studies were performed to assess whether or not CCR7 expression on Raji cells was sufficient to induce chemotaxis. If chemotaxis could be induced in Raji cells following exposure to CCL19, it could be concluded that biotin-CCL19 uptake was, at least in part, due to binding to CCR7. The following assays were performed to assess the ability of CCL19 to induce chemotaxis.

4.3.2.1 Chemotaxis Assay using Transwell® Plates.

The method described in section 2.2.5.5.1 was employed. 1×10^5 cells were added to the insert of each well containing varying concentrations of either CCL19 or CXCL12. Negative controls consisted of wells containing no chemokine. CXCL12, the ligand for CXCR4 was used as a positive control as CXCR4 is known to be highly expressed on B-cells and has been consistently demonstrated to induce chemotaxis in both normal and malignant B cells, furthermore CXCR4 expression had been confirmed on Raji cells as shown in section 3.4.1. Following incubation, the cells that had passed through the chemotaxis chamber into the medium below were counted and a migration index calculated as follows:

$$\frac{\text{Number of cells migrating to chemokine}}{\text{Number of cells migrating without chemokine}} = \text{Migration Index}$$

The results of this are shown in figure 4.6. This demonstrates that both CCL19 and CXCL12 induce chemotaxis in the Raji cells, confirming that the endogenously expressed CCR7 and CXCR4 on these cells are functional. The highest migration index was obtained at a chemokine concentration of 100nM with each ligand, with a migration index of 29 ± 7.51 following exposure to CCL19 and 33 ± 5.86 following exposure to CXCL12. It is possible that higher levels of chemotaxis could be achieved at higher concentrations of chemokine although it is just as likely that the degree of chemotaxis would fall due to receptor desensitisation. There was however, some concern during the experiment that not all of the cells passing through the wells were being counted and that chemotaxis was being under reported, so an alternative method for assessing chemotaxis was sought. This is outlined in the next experiment.

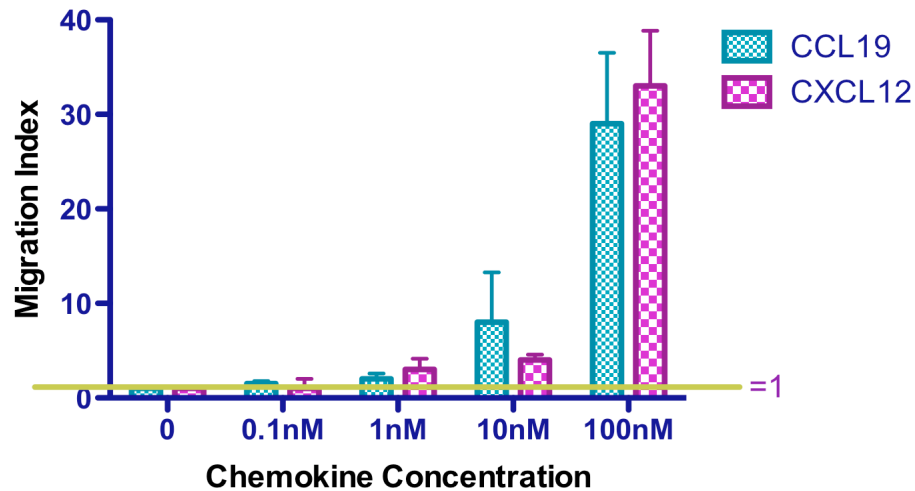


Figure 4.6: Chemotaxis of Raji cells using Transwell® chemotaxis plates. Chemotaxis buffer containing different concentrations of CCL19 or CXCL12 was added to each well of a Transwell® plate. The inserts were added, and into each of these Raji cells were placed. Following incubation at 37°C for 3 hours, the number of Raji cells passing through the chemotaxis chamber into the buffer below was counted. A migration index was calculated as outlined in section 4.3.2.1, with migration index of greater than 1 indicating that migration has occurred. Analysis at each chemokine concentration was performed in triplicate and the error bars represent the standard error of the mean. Each sample was set up in triplicate, and the experiment was performed once.

4.3.2.2 Chemotaxis of Raji Cells using the QCM™ Chemotaxis Assay

This method was chosen, as it does not rely on using the haemocytometer to assess the number of cells that have passed through the chemotaxis chamber. Instead it uses a fluorescent dye that can bind to any nucleic acid that has been released following cell lysis. This is reported to give a more accurate measurement of chemotaxis as, cells which may have been attached to the base of the plates or the bottom of the chemotaxis filter are lysed through the process and included in the analysis; these are often missed with manual cell counting methods. Following cell lysis a plate reader using a 480/520nm filter set is used to determine the degree of fluorescence, which, in turn correlates with the number of cells in the lysate. The method was followed as described in section 2.2.5.5.2. Only CCL19 was used in this assay as it had already been established that the Raji cells migrated in response to this ligand. Prior to performing the experiment a calibration curve was set up, in which known quantities of cells were added to the bottom of the chambers followed by cell lysis and analysis of the degree of fluorescence. This calibration curve is shown in figure 4.7 and demonstrates that there is a good correlation between fluorescence (RFU) and cell numbers as determined by linear regression analysis with a correlation co-efficient of $r^2=0.9455$. This was then used to determine the number of Raji cells that had undergone chemotaxis following exposure to CCL19. The results of the Chemotaxis assay using the

QCMTM method are shown in Figure 4.8. These mirror the results obtained from the Transwell® Chemotaxis assay, however the migration indices obtained were lower with a migration index of 3.71 ± 1.86 at a CCL19 concentration of 100nM. However, further optimisation of this method would have been performed, if time and resources were available, as has the potential to be a valuable assay because more samples can be compared, with fewer cell numbers, which would make this assay ideal for the analysis of primary lymphoma samples from patients, in which only a limited amount of tissue is available.

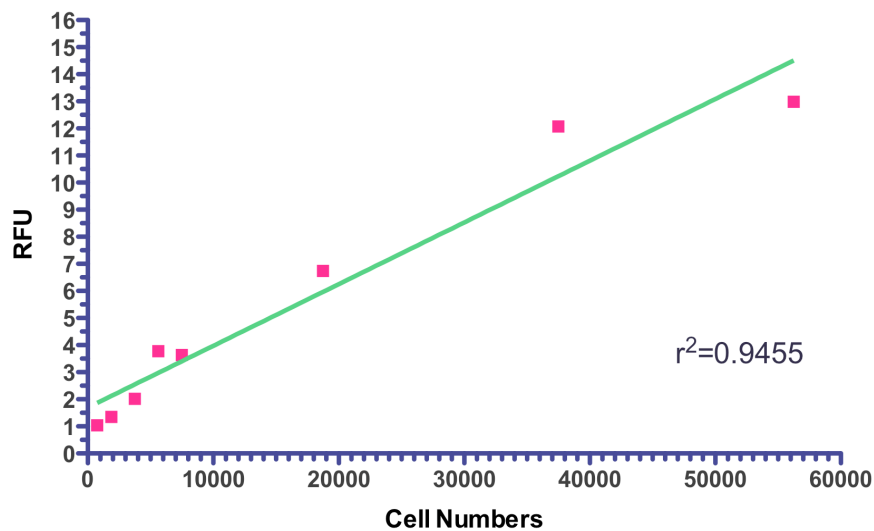


Figure 4.7: Calibration curve for QCMTM Chemotaxis Assay using Raji cells. Different quantities of Raji cells were added to wells of a 96 well luminometry plate. To each well lysis buffer/dye solution from the QCMTM kit was added and the plate incubated at room temperature for 15minutes. The plate was then read using a 480/520nm filter set and the RFU recorded for each well. Each point on the calibration curve represents the mean RFU obtained from 3 wells containing the same number of cells, and indicates that there is a good correlation between RFU and cell number.

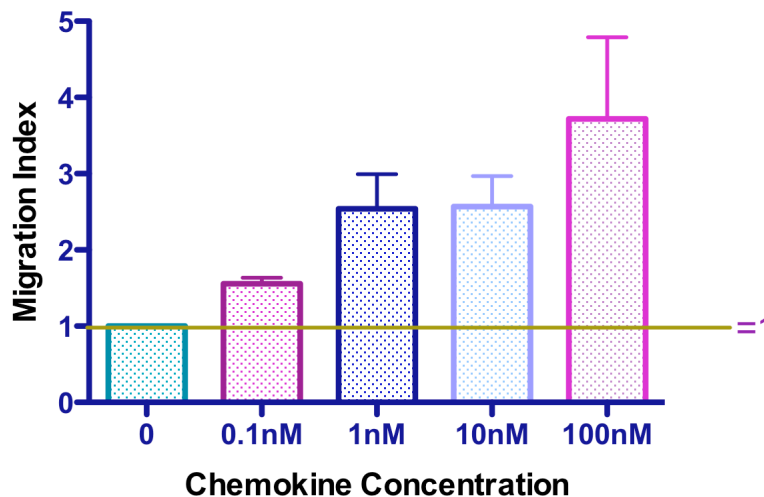


Figure 4.8: QCM™ Chemotaxis assay using Raji cells. Chemotaxis buffer containing a known concentration of CCL19 was added to each well of a 96 well feeder plate. Inserts were added, and Raji cells were added to each of the 96 inserts. Following the steps outlined in 2.2.5.5.2, the cells were incubated with lysis buffer/ dye solution for 15 minutes and transferred to a 96 well luminometry plate for reading using a 480/520nm filter set. A migration index of >1 indicates that migration has occurred. Analysis at each chemokine concentration was performed in triplicate and the error bars represent the standard error of the mean. This procedure was performed once.

The results from both of the chemotaxis assays demonstrate that CCR7 expression on Raji cells was sufficient to induce chemotaxis. Furthermore, the chemotaxis assays confirm that at least a proportion of biotin-CCL19 uptake demonstrated in section 4.3.1 was due to binding with CCR7 rather than with CCX-CKR. Of course, biotin-CCL19 binding to CCX-CKR may still have been occurring. However, demonstration that Raji cells are able to bind to, and potentially internalise, CCL19 meant that the Raji cells could be used for cell targeting experiments using cytotoxic agents.

4.4 Cell killing by exposure to a radio-labelled chemokine

There are a number of ways in which the chemokine system can be targeted to elicit cell death. One example in clinical trials is the anti-CCR4 antibody, which induces antibody dependant cell-mediated cytotoxicity (ADCC) [349]. Further possibilities include the use of chemotoxins, in which the active portion of a chemokine is fused with toxic agents such as *Pseudomonas* exotoxin 38 [297], or as described here by using a chemokine conjugated to a active radioisotope such as Iodine-125 (¹²⁵I). The latter approach is already used in clinical practice with radiolabelled antibodies used in the treatment of lymphomas, such as Iodine-131 labelled anti-CD20 antibodies [298].

In this experiment chemokines labelled with ^{125}I were used. This radio-isotope has a relatively long-half life of approximately 59 days, meaning that it was suitable for experiments requiring incubation over a period of days or weeks. ^{125}I is a gamma emitter with low emission to cells out with those containing the isotope, although sufficient radiation may be delivered to be cytotoxic to surrounding tissues [350]. The aim here was to test whether a chemokine labelled with the radio-isotope ^{125}I , would lead to enhanced killing of cells expressing the cognate chemokine receptor compared to the receptor-negative cells. On day one of the experiment a calibration curve for the MTT cell assay was prepared using known quantities of HEK293 cells. The MTT assay is a method by which viable cell numbers within a small volume of medium can be quantified whilst enabling maximum protection for the operator with regards to radio-isotope exposure. Following addition of the reagents live cells develop black crystals of MTT formazan, after addition of a developing reagent the crystals dissolve to form a blue coloured solution, the absorbance of which is measured using a 570/630nm filter set. The calibration curve is shown in figure 4.9 demonstrating good correlation with absorbance and cell numbers with a correlation co-efficient of $r^2=0.9931$.

On day 1 four 96 well plates were set up as follows: 3 wells with HEK293 cells in medium only, 3 wells with HEK.hCCR7 cells in 100 μl medium containing 0.5 μg of CCL19/100 μl , 3 wells with HEK.hD6 in 100 μl medium containing 0.5 μg of PM2, 3 wells with HEK293 in 100 μl medium containing 1 μl of PM2- ^{125}I conjugate (925kBq/ml, specific activity 2200Ci/mmol and 10 $\mu\text{g}/\text{ml}$ PM2), 3 wells with HEK.hCCR7 cells in 100 μl medium containing 1 μl of CCL19- ^{125}I conjugate (925kBq/ml, specific activity 2200Ci/mmol and 10 $\mu\text{g}/\text{ml}$ CCL19) and 3 wells with HEK.hD6 in medium containing 925kBq/ml of PM2- ^{125}I conjugate as detailed above. HEK.hD6 cells were used as a positive control as D6 is an atypical receptor that is capable of efficiently internalising chemokines [351] and so should be susceptible to killing with the PM2- ^{125}I conjugate. PM2, is a truncated form of CCL3, known to bind to and be internalised by D6. The cells were then incubated for 2, 4, 8 or 12 days at 37 $^{\circ}\text{C}$ with the growth medium containing the chemokine or chemokine- ^{125}I conjugate where appropriate, being replaced with fresh stock on day 6.

The cells were then harvested on the appropriate day and the MTT cell assay performed to assess the number of remaining cells. The results of this are shown in figure 4.10.

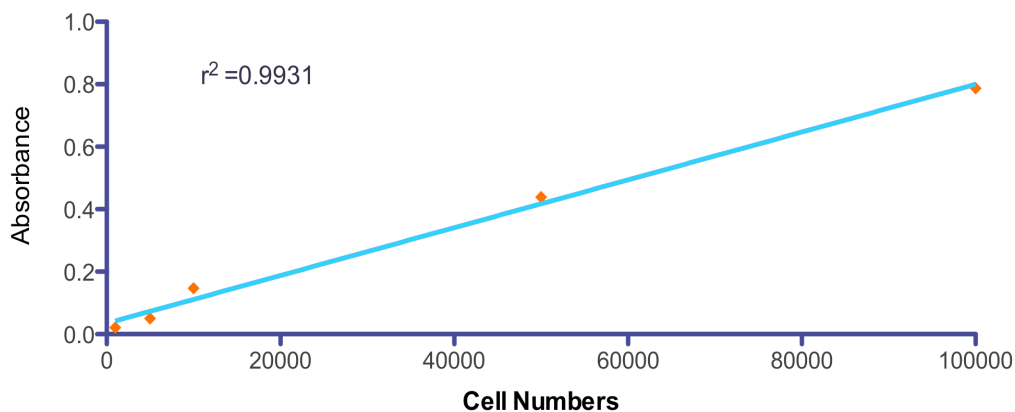


Figure 4.9: Calibration curve for the MTT Cell assay. A known quantity of HEK293 cells was added to individual wells within a 96 well plate. The reagents from the MTT kit were then added to each well as outlined in section 2.2.5.4 and read using 570/630nm filters. Each point on the calibration curve represents the mean absorbance obtained from 3 wells containing the same number of HEK293 cells, and indicates good correlation between absorbance and cell number.

On day 2, those cells, which had not been exposed to the radiolabelled ligands, had proliferated, with higher numbers of cells noted. In comparison those cells, which had been exposed to ^{125}I , did not show any increase in cells numbers, with cells numbers unchanged when compared to day 1 suggesting that cell kill had occurred. Comparison between the cell numbers in those wells containing radiolabelled ligand with those that did not demonstrated a significant difference ($p < 0.0001$ using student t-test). However, comparison between HEK293, HEK.hCCR7 and HEK.hD6 cells exposed to radiolabelled chemokine did not reveal any significant differences between the cell numbers suggesting non-specific cell killing.

On day 4, the highest cells numbers were again recorded in those chambers with no radioisotope exposure. However, on this occasion, there were significant differences between HEK293, HEK.hD6 and HEK.hCCR7 cells exposed to ^{125}I . The HEK.hCCR7 cell numbers were significantly lower when compared to both HEK.hD6 and HEK293 cells numbers with p-values of $p = 0.0028$ and $p = 0.0031$ respectively. This suggested an increased level of cell kill of CCR7⁺ cells by CCL19- ^{125}I , and thus potentially targeted cell kill had been achieved.

On day 8 although there were fewer HEK.hCCR7 cells in the well exposed to CCL19- ^{125}I compared to the cell numbers in the HEK293 and HEK.hD6 wells exposed to PM2 ^{125}I , the differences were no longer significant, and cell numbers in all 3 groups had started to increase indicating that cell killing had slowed. Of note, the cell numbers in each of the wells with no radioisotope exposure were lower. The likely explanation for this relates to

events on day 6. When changing the medium on this day, there was such a degree of proliferation that the cells had lifted off the bottom of the wells and the majority of them were removed with the old medium, as such the results on these days reflect gross underestimations of cell proliferation. This also explains the findings in these chambers on day 12.

On day 12 the lowest numbers of cells were seen in the wells that did not contain ^{125}I . No further increases in cell numbers were seen in the wells containing HEK293, HEK.hCCR7 or HEK.hD6 exposed to chemokine ^{125}I indicating that cell kill had occurred. However although the well containing HEK.hD6 cells and PM2 ^{125}I was the only one to show a fall in cell number, comparison with cell numbers in the wells containing HEK293 and HEK.hCCR7 cells and ^{125}I did not show any significant differences suggesting that cell kill was again non-specific.

The results of this study can be seen graphically in figures 4.10 and 4.11.

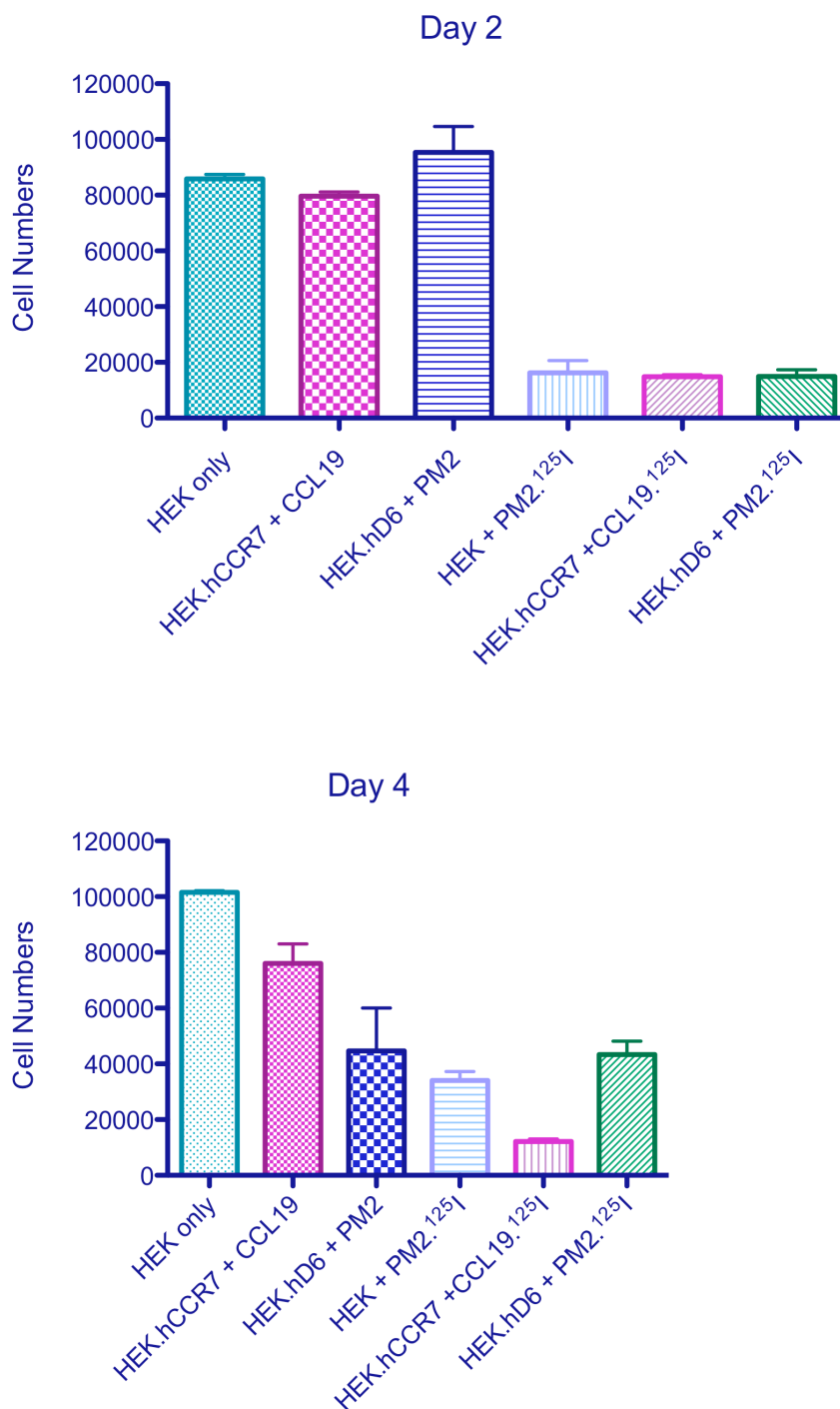


Figure 4.10: Comparison of cell numbers at day 2 and 4 between wells exposed or not exposed to radiolabelled chemokine. Cells were incubated with medium alone, or medium containing PM2 or CCL19 with or without radiolabelling with ¹²⁵I for 2, 4, 8, or 12 days. Following incubation the cell numbers were determined using the MTT assay (section 2.2.5.4). These graphs show the cell numbers obtained using the MTT cell proliferation assay after incubation at 2 and 4, data from days 8 and 12 are not shown as the experiment was invalidated due to loss of the control cells. Each incubation was performed in triplicate and the error bars in the graphs represent the standard error of the mean.

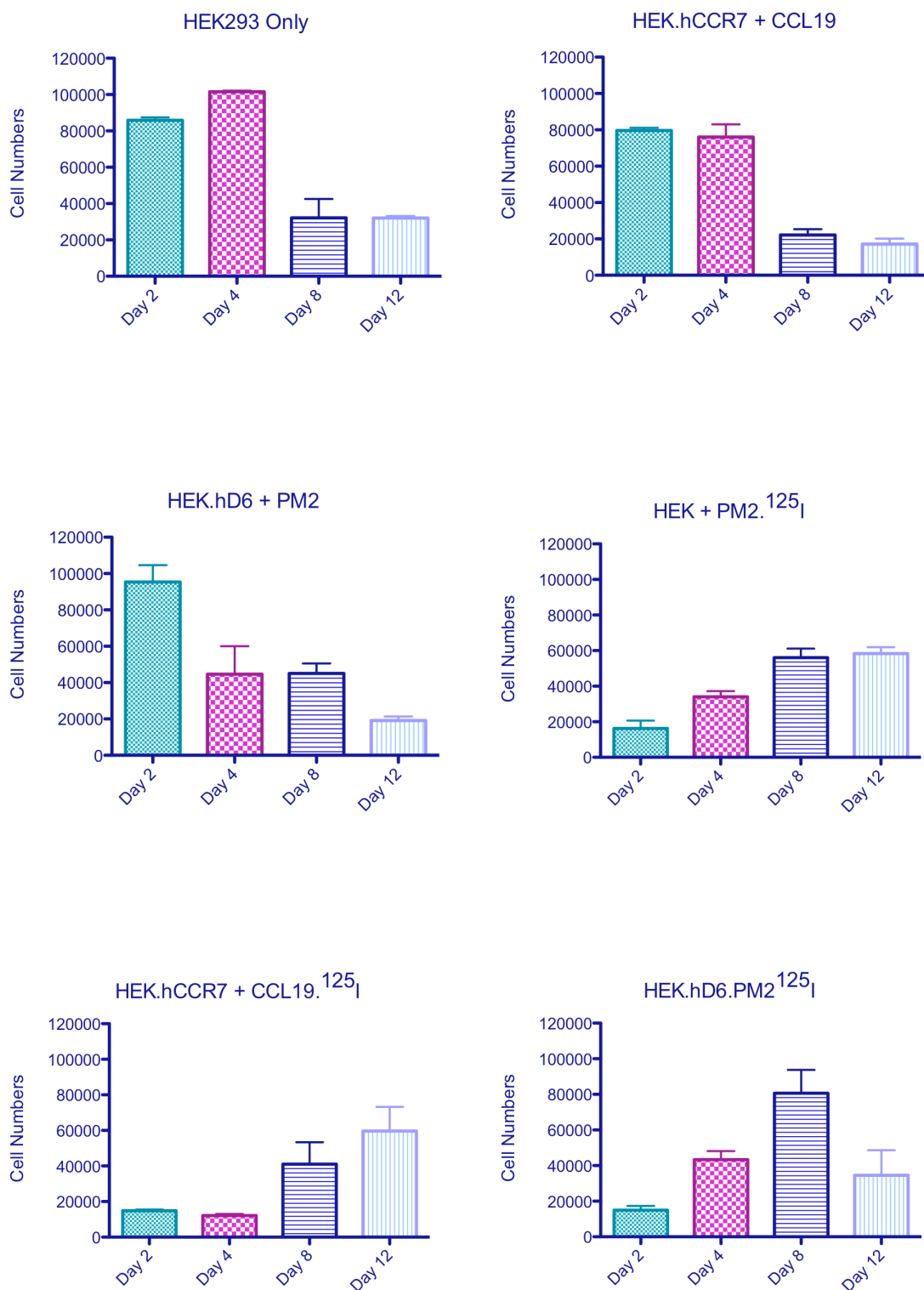


Figure 4.11: Cell numbers following 2, 4, 8 or 12 days incubation with radiolabelled chemokine. Cells were incubated with medium alone, or medium containing PM2 or CCL19 with or without radiolabelling with ¹²⁵I for 2, 4, 8, or 12 days. Following incubation the cell numbers were determined using the MTT assay (section 2.2.5.4). These graphs show the cell numbers obtained using the MMT cell proliferation assay after incubation at 2, 4, 8, and 12 days. Each incubation was performed in triplicate and the error bars in the graphs represent the standard error of the mean.

Firm conclusions about the ability to utilise the chemokine receptors to induce targeted cell death using radiolabelled chemokines cannot be drawn from the results of this initial experiment. Nonspecific killing of cells was occurring as evidenced by the fact that at 3 of the 4 time points, there were no significant differences in cell numbers between ^{125}I exposed wells containing HEK293, HEKhCCR7 or HEK.hD6 cells. Further studies are required to optimise the experiment further. This would include using lower concentrations of the radioisotope, to see if there really was an appreciable difference between cytotoxicity and receptor expression as suggested with the day 4 results, by aiming to avoid non-specific cell kill. Additionally, HEK293 cells expressing the atypical chemokine receptor CCX-CKR might be a more appropriate positive control than D6 transfected HEK cells. The reason for this is that CCX-CKR also binds, and internalises, CCL19 [126], and so any differences between the level of decay of the PM2- ^{125}I and the CCL19- ^{125}I , as a result of the timing of the conjugation and potential differences in the degree of cytotoxicity would be negated.

The results discussed in sections 4.2 to 4.3 of this chapter enabled progression onto further experiments discussed in chapters 5 and 6.

4.5 Summary

In summary, this chapter had demonstrated the following:

1. Stable HEK.hCCR7 cells have been successfully created that express good levels of hCCR7 and are capable of taking up one of its ligands, CCL19.
2. Raji cells not only endogenously express hCCR7 but the receptor is also functional as shown by the capability of these cells to bind to CCL19.
3. Functionality of hCCR7 is also demonstrated by the ability of Raji cells to migrate in response to CCL19.
4. The results obtained with the use of radiolabelled chemokines to target the chemokine system were not conclusive and further optimisation of the experiments would be required before confirming this as an effective approach.

CHAPTER FIVE

REDIRECTION OF ADENOVIRAL TROPISM THROUGH CHEMOKINE RECEPTORS

5.1 Introduction

As detailed in the previous chapter, there are a number of ways in which the chemokine system can be targeted to elicit cell death. The use of radiolabelled chemokines was described in section 4.4, although further work is required to see if this is a suitable approach. In this chapter, the potential use of cytolytic gene therapy will be explored, one example of which includes the transduction of suicide genes such as thymidine kinase, which if expressed will lead to cell death following exposure of cells to ganciclovir [127]. The potential advantage of using gene therapy, in this case by utilising adenoviral vectors, is that the targeting can be more specific with additional degrees of specificity being included in the system, such that intracellular as well as extracellular variables can be taken advantage of.

For example, the engineering of a vector to incorporate a telomerase promoter to regulate expression of the 'suicide' gene ensures that the gene is only expressed in those cells expressing telomerase, namely malignant cells as well as germ cells, stem cells and certain long-lived lymphocytes. This approach has been utilised to transfect cells with an adenoviral vector containing the 'suicide' gene, bacterial nitroreductase, for potential use in clinical cancer trials [132].

However, whilst the intracellular characteristics of the target cell can be hijacked leading to self-destruction, more specific targeting can be achieved by trying to control the cell population being transfected in the first place. In the case of adenoviral vectors, this means redirecting the natural tropism of the vector such that it will enter through an alternate receptor, in this case a chemokine receptor. As described in chapter 1, adenovirus 2 (Ad2) and adenovirus 5 (Ad5) are the two adenoviral serotypes used most frequently in gene therapy due to their low pathogenicity and lack of oncogenic potential [325]. These serotypes enter the cell following interaction of the viral knob protein with the coxsackie-adenovirus receptor (CAR) on the cell surface [304]. Work has been published detailing a number of different methods by which adenoviral tropism has been successfully redirected.

Such examples include ‘fibre switching’ where the fibre protein from a different adenoviral serotype such as Ad35 replaces that of Ad2 or Ad5, which then redirects the virus through CD46 [306]; or the incorporation of peptides including elements of heparin binding domains redirecting binding to heparan sulphate, into the fibre knob protein [334]; or the use of anti-fibre antibodies conjugated to a ligand, such as folate, redirecting the virus through the folate receptor [330]. Finally, chemical conjugation of the adenovirus with a ligand is an alternative approach.

There have been a variety of chemical ‘linkers’ used, to attach proteins to be fibre knob, including biotinylation. Viruses that had first been biotinylated and then incubated with avidin were then subsequently incubated with antibodies to elements such as IL-2 have also led to successful redirection into haematopoietic cells which do not normally express CAR [332]. This final approach was chosen for attempting redirection through chemokine receptors. A reason for this was that if the adenovirus could be efficiently biotinylated, and then conjugated with avidin, then the system could be used with a variety of different chemokines depending upon the cell population to be targeted. However, the difficulty with chemokines is that the N-terminus of the chemokine is required to interact with its cognate chemokine receptor, whilst the viral fibre knob protein interacts with CAR via its C-terminus. So, in order to re-direct adenoviral vectors through chemokine receptors, a system by which the N-terminus of the chemokine could remain free to interact with its receptor was required. It is also worth noting that, following binding with CAR, adenoviral particles are internalised via endocytosis into clathrin-coated pits as occurs following chemokine receptor-ligand binding. Thus the method of internalisation of the virus should not, in theory, be affected by entry through the chemokine receptor [333]. This chapter outlines the experiments performed attempting to re-direct viral tropism through chemokine receptors.

5.2 Infection of HEK293 and HEK.hCCR7 Cells Following Chemical shrouding of Adenovirus with Chemokine

In order to achieve chemical conjugation of the adenovirus with chemokine, and thus redirection of adenoviral tropism, the method outlined in 2.2.6.4 was used and is shown diagrammatically in figure 5.1. This method of chemically coating the virus is referred to as shrouding the virus from now onwards. EZ-Linked Maleimide Activated NeutrAvidin™ Protein provides a free sulfhydryl (-SH) group that allows conjugation to proteins and other molecules containing this group whilst still allowing for binding to biotin. The adenoviral fiber knob protein in Ad5 and Ad2 serotypes has been shown to contain free

sulfhydryl groups [311]. The viral vector used initially was a ‘high capacity, gutless’ adenovirus 5 containing a CMV promoter and LacZ reporter gene (Ad5.CMV.LacZ), thus enabling the detection of successful infection through the detection of LacZ expression. Following incubation of the virus with NeutrAvidin™, the mixture was dialysed using a dialysis membrane with a pore size of 100kDa, in order to remove any un-bound NeutrAvidin™. Following centrifugation and re-suspension of the Ad5.CMV.LacZ vector, shrouding of the virus was attempted using biotinylated chemokines again with a final dialysis stage to remove unbound chemokine. The biotinylated chemokines have the N-terminus unaltered thereby allowing for interaction with the cognate receptor.

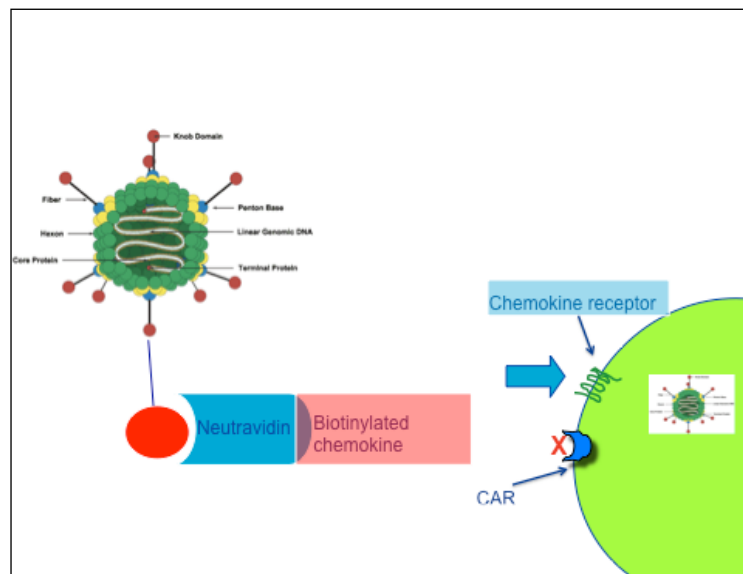


Figure 5.20: Outline of strategy to redirect adenoviral tropism. Initially the Ad5.CMV.LacZ vector was incubated with NeutrAvidin™ in order to conjugate the fibre knob protein with this protein. The Ad5.CMV.LacZ-NeutrAvidin™ conjugate was then incubated with biotinylated chemokine to enable chemokine shrouding of the virus. The shrouded virus is therefore blocked from entering the cell through CAR, and redirected through the chemokine receptor.

Initially 6.6×10^8 infection forming units (ifu)/ml of Ad5.CMV.LacZ were incubated for 1 hour with 0.5mg/ml of the NeutrAvidin™ protein, before shrouding with biotin-CCL19. Following conjugation 12-well plates were set up for viral infection using 5×10^5 HEK293 or HEK.hCCR7 cells in each well. 100µl of Ad5.CMV.LacZ at a concentration of 6.6×10^4 or 6.6×10^5 ifu/ml giving final viral titres of 6.6×10^3 or 6.6×10^4 ifu per well. This equates to a multiplicity of infection (MOI) of 0.0132 or 0.132 ifu/cell. After 48 hours the cells were analysed for LacZ expression by staining for β -galactosidase, as detailed in 2.2.6.6, with LacZ positive cells appearing blue. The degree of infection was then determined by microscopic examination of the plates and by counting the number of blue cells per field at x20 objective. The infection was then calculated as follows:

$$\text{IFU/ml} = \frac{(\text{infected cells/field}) \times (\text{fields/well})}{\text{Volume virus (ml)} \times \text{dilution factor}}$$

A sample calculation can be found in section 2.2.6.3.

The initial results are shown in Figures 5.2 and 5.3. The first figure shows the difference in the rates of infection between the CCR7⁺ and CCR7⁻ cells at the two viral concentrations. Using a titre of 6.6×10^3 ifu/well, the rates of infection were as follows: CCR7⁺ cells; $2.21 (\pm 0.16) \times 10^8$ ifu/ml vs. CCR7⁻ cells; $1.38 (\pm 0.2) \times 10^8$ ifu/ml, these difference were significantly different with $p=0.0023$ (using an unpaired t-test). The same was seen at a the higher viral titre of 6.6×10^4 ifu/well with the results as follows; CCR7⁺ cells; $4.06 (\pm 0.54) \times 10^8$ ifu/ml vs. CCR7⁻ cells; $1.6 (\pm 0.27) \times 10^8$ ifu/ml and again the degree of infection was significantly higher in the CCR7⁺ cells with $p=0.0002$. These results are also shown in figure 5.3 in which it is clear that there are a higher number of LacZ positive (blue) cells in the CCR7⁺ population as compared to the CCR7⁻ population.

However, there was a high degree of background infection. There were a couple of potential reasons for this. Firstly, there may have been incomplete shrouding of the adenovirus with the chemokine allowing entry into the HEK293 and HEK.hCCR7 cells via the CAR receptor. Secondly, as described in section 1.5.4, adenovirus can also enter the cells via alpha integrins on the surface in a CAR independent fashion, albeit at a lower rate, via the RGD motif on the base of the viral shaft protein. This could also be responsible for, or at least contribute to, the degree of background infection. However it is reported that entry via this method is 10 fold lower and this was not the case in this instance, suggesting that this is not the only explanation and that the first was more likely. Yet, what was clear even with these preliminary results was that the adenovirus could be successfully redirected through the chemokine receptor by CCL19.

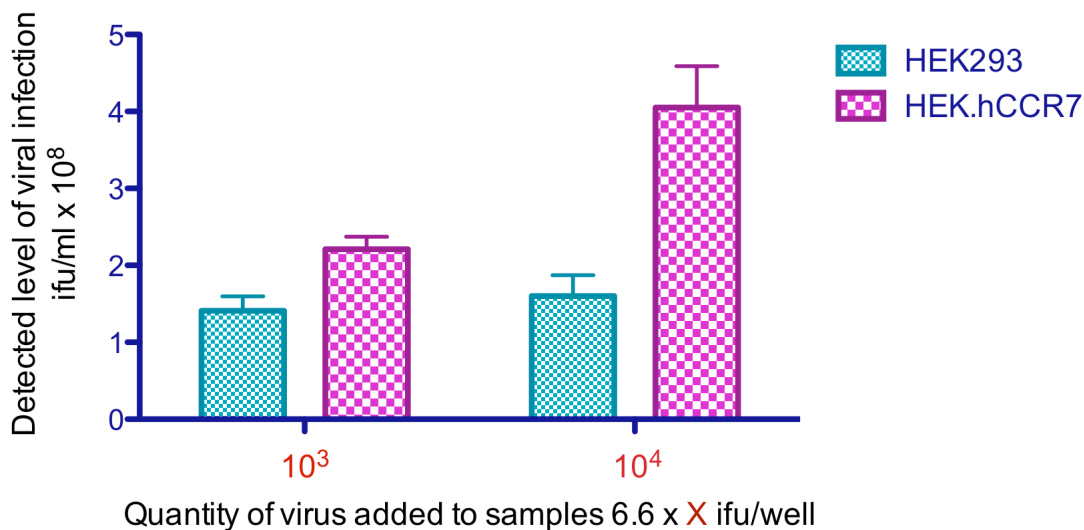
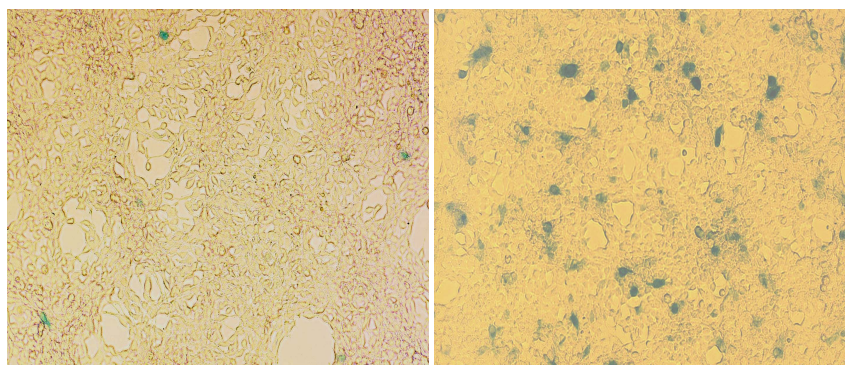


Figure 5.21: Infection of HEK293 and HEK.hCCR7 cells with Ad5.CMV.LacZ shrouded with biotin-CCL19. Ad5.CMV.LacZ shrouded with CCL19 was added to HEK293 and HEK.hCCR7 cells at two different concentrations, and then incubated for 48 hours at 37°C. The cells were then assessed for LacZ expression by staining for β -galactosidase as detailed in 2.2.6.5 indicating successful transfection of the reporter gene. The positive cells were then counted using a 20x objective lens. The viral titre (ifu/ml) for each infection was then calculated as in 2.2.6.2. Each bar on the graph represents 30 microscopic fields counted across nine wells containing the same cell type and viral concentration. These results represent data collected from experiments repeated on three separate occasions (3 wells counted at each time). The error bars represent the standard error of the mean (SEM).



HEK293

HEK.hCCR7

Figure 5.22: Analysis of Ad5.CMV.LacZ infection in HEK293 and HEK.hCCR7 cells. Cells were incubated with Ad5.CMV.LacZ shrouded with CCL19 for 48 hours. After this staining for β -galactosidase was performed to assess LacZ expression, and therefore successful infection by the adenovirus. These images (taken at 20x objective) demonstrate a higher rate of infection in HEK.hCCR7 cells as indicated by a higher number of LacZ positive (blue) cells.

5.3 Infection of CHO and CHO.hCCR5 Cells with Adenovirus shrouded with CCL3.

Whilst the initial attempts to redirect the adenovirus through hCCR7 gave results indicating that the approach described above was effective, the degree of background infection was such that further refinement of the experiments were required to demonstrate, with a higher degree of certainty, that adenoviral redirection was occurring. Chinese Hamster Ovary cells (CHO) were identified as a cell line that expresses neither CAR nor alpha integrins. RT-PCR was performed using primers for CAR and alpha integrins on RNA extracted from CHO and HEK293 cells. The RT-PCR results for CAR expression in HEK293 and CHO cells are shown in Figure 5.4, confirming the absence of CAR expression in CHO cells. Data confirming the presence of alpha-integrins in HEK293 and their absence in CHO cells are not shown. Therefore, in the absence of CAR and α -integrin, the only way in which the chemokine-shrouded adenovirus could enter the chemokine receptor expressing CHO cells would be through the chemokine receptor. The infection experiments were then repeated on CHO cells as described in section 5.2 with stable CHO transfectants expressing hCCR5 (CHO.hCCR5) that had previously been developed in Professor Graham's laboratory. This time the Ad5.CMV.LacZ particles were shrouded in one of the ligands for hCCR5, CCL3. The results from this CCR5-redirection infection are shown in Figure 5.5. As would be expected, the background infection rate in the CHO cells was greatly reduced. In fact the overall rates of infection were 3 logs lower when compared to the HEK293 infection studies. The CHO.hCCR5 cells showed infection rates of $13.4 (\pm 1.46) \times 10^5$ ifu/ml cells which was significantly higher ($p < 0.0001$) than those obtained with CHO cells with rates of $1.3 (\pm 0.28) \times 10^5$ ifu/ml following infection with CCL3 shrouded adenovirus again indicating that chemokine shrouding allowed the Ad5.CMV.LacZ to be successfully directed through the cognate chemokine receptor.

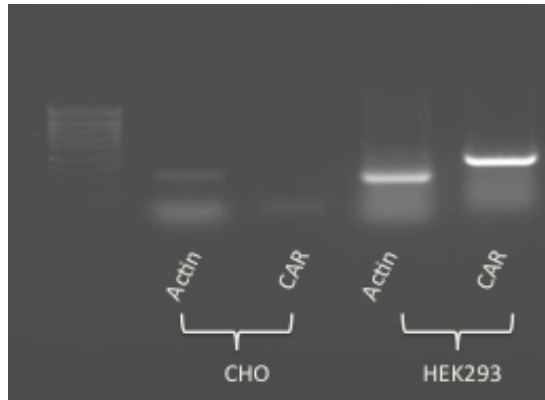


Figure 5.23: CAR expression in CHO and HEK293 cells. RNA was prepared from the CHO and HEK293 cells using Trizol®, these were DNAase treated and cDNA was prepared using reverse transcriptase. Primers for actin (human or hamster) and CAR were then used to amplify cDNA using the PCR programme in 2.2.4.3. The PCR products were then run on a 1% agarose gel containing ethidium bromide.

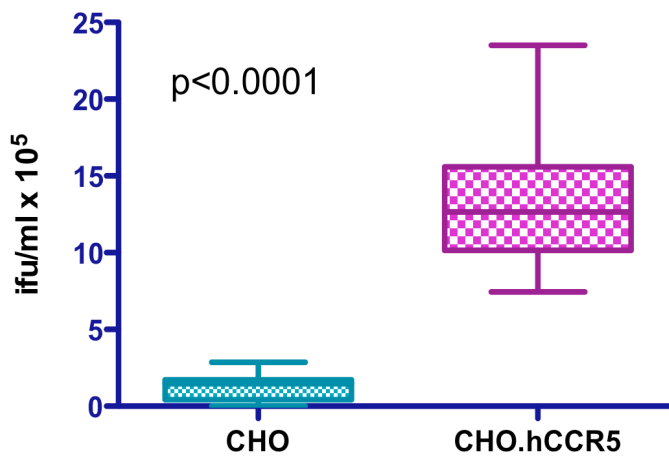


Figure 5.24: Infection of CHO and CHO.hCCR5 cells with Ad5.CMV.LacZ shrouded with biotin-CCL3. Ad5.CMV.LacZ shrouded with CCL3 was added to CHO and CHO.hCCR5 cells at a concentration of 6.6×10^4 ifu/well, and incubated for 48 hours at 37°C. The cells were assessed for LacZ expression and the ifu/ml titres for each sample were calculated as before. Each bar on the graph represents 30 microscopic fields counted across three wells containing the same cell type and viral concentration. This experiment was repeated twice. The error bars represent the SEM.

5.4 Optimisation of Infection Rates

Now that it had been shown that adenoviral tropism could be successfully redirected through chemokine receptors, the next step was to try to optimise the method in order to obtain higher infection rates in the cell lines used. This would ensure the most efficient use of the vector and have implications later when proceeding to targeted cytolytic therapy.

5.4.1 Effect of Incubation Time with NeutrAvidin™ on the Rate of Infection

The first step was to determine whether or not the length of time the adenovirus was incubated with NeutrAvidin™ prior to chemokine conjugation, which had previously been 1 hour, altered infection rates. Infections were performed, as before, but with virus that had been incubated with NeutrAvidin™ for 1, 2, or 4 hours prior to incubation with chemokine. In this experiment CHO.hCCR5 cells were infected with Ad5.CMV.LacZ shrouded in CCL3 in order to reduce the rate of background infection and make conclusions regarding efficiency of infection clearer. The results are shown in Figure 5.6. The highest infection rates were obtained with 4 hours incubation. For all experiments following this an incubation time of 4 hours was used.

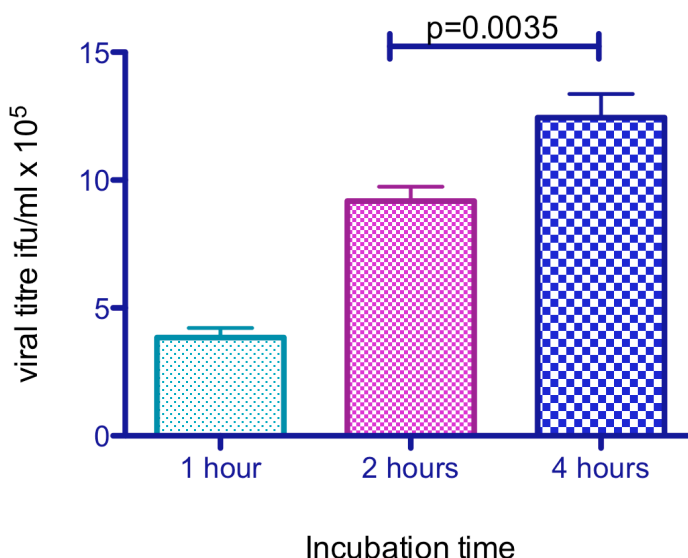


Figure 5.25: Infection rates with different durations of Ad5.CMV.LacZ incubation with NeutrAvidin™. Ad5.CMV.LacZ was incubated with NeutrAvidin™ 0.5mg/ml for 1, 2 or 4 hours. The resulting conjugates were then shrouded with the CCL3 prior to infection of CHO.hCCR5 cells with 6.6×10^4 ifu/well. Following infection and incubation for 48 hours, the cells were analysed for LacZ expression and the ifu/ml titre calculated for each time point. Each bar on the graph represents 40 microscopic fields counted across three wells containing virus incubated with NeutrAvidin™ for the same length of time. This analysis was performed on one occasion. The error bars represent the SEM.

5.4.2 Effect of Incubation Time with Chemokine on the Rate of Infection

Once the optimum NeutrAvidinTM incubation time had been determined, the optimum incubation time with chemokine was determined in the same way, again with CHO.hCCR5 and CCL3 and with incubation times of 1, and 4. As with NeutrAvidinTM, the optimum incubation time was 4 hours (see figure 5.7). An incubation time of 4 hours with the chemokine was used from this time onwards.

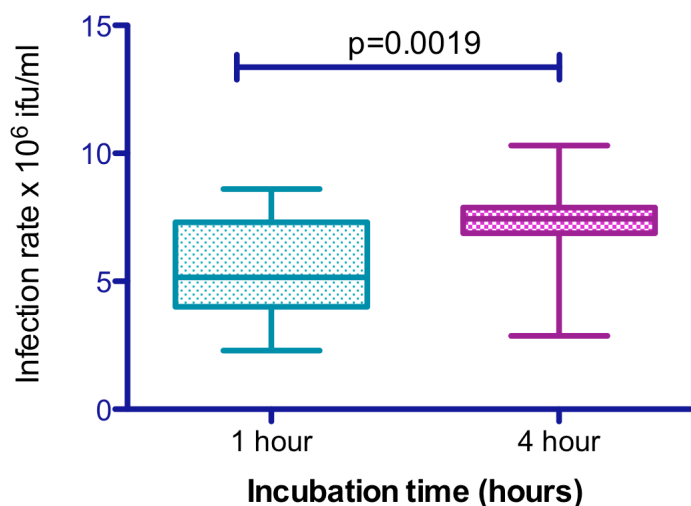


Figure 5.26: Infection rates with different incubation times with CCL3. Ad5.CMV.LacZ conjugated with NeutrAvidinTM after 4 hours incubation was incubated with biotin-CCL3 for 1 and 4 hours. Following this CHO.hCCR5 cells were infected with the shrouded virus from the different time points with a viral load of 6.6×10^4 ifu/well. Subsequently infection rates were assessed using β -galactosidase staining as before following 48 hours incubation. Each bar on the graph represents 40 microscopic fields counted across three wells containing virus incubated with CCL3 for the same length of time. This analysis was performed on one occasion. The error bars represent the SEM.

5.4.3 Effect of NeutrAvidinTM concentration on infection rates

The previous experiments had been performed using NeutrAvidinTM at a concentration of 0.5mg/ml during the incubation step. The experiments were repeated, this time using 4 hours incubation time and with NeutrAvidinTM concentrations of 0.25, 0.5, 0.75 and 1.0mg/ml. HEK293 cells with or without hCCR7 expression were used for these experiments.

The results demonstrated that the optimum NeutrAvidinTM concentration for infection was obtained at concentration of 0.75mg/ml. Again at each concentration there were significant differences in the rate of infection between CCR7⁺ and CCR7⁻ cells with p-values of CCR7⁺ vs. CCR7⁻ of p=0.0002, p=0.0003, p=0.0003 and p<0.0001 at 0.25 mg/ml, 0.5

mg/ml, 0.75mg/ml and 1.0mg/ml NeutrAvidin™ concentrations respectively. The data for this is shown in Figures 5.8 and 5.9 with figure 5.9 clearly demonstrating the variations in infections rates as evidenced by differences in numbers of LacZ positive cells between the different NeutrAvidin™ concentrations. It was surprising that a lower infection rate was obtained with the highest NeutrAvidin™ concentration of 1.0mg/ml; one possible explanation for this is that the Ad5.CMV.LacZ particles start to clump together, thereby preventing entry into cells via either the CAR or chemokine receptor. From this point on a NeutrAvidin™ concentration of 0.75mg/ml was used in chemokine shrouding experiments.

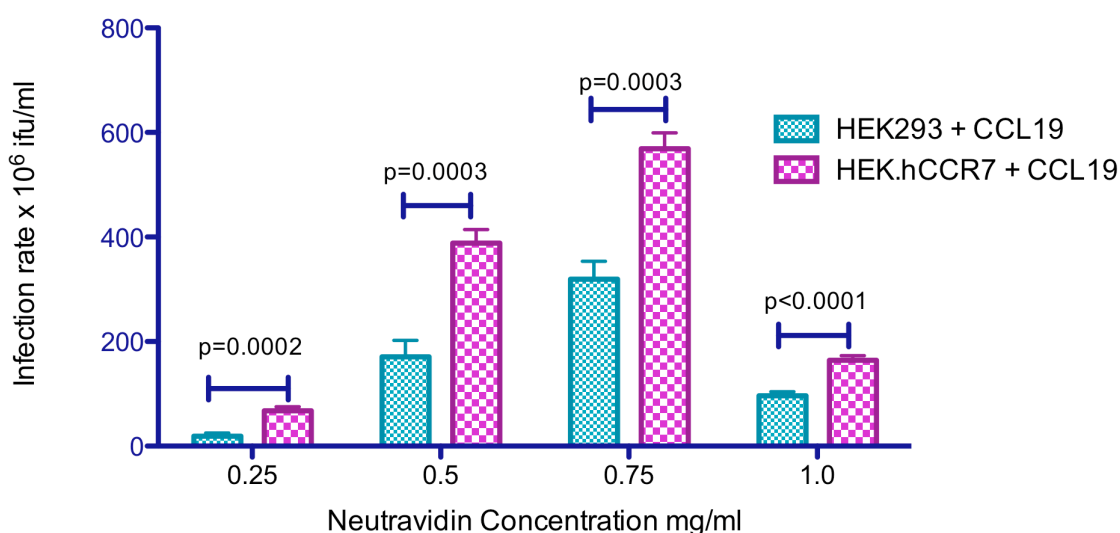


Figure 5.27: Effect of NeutrAvidin™ concentration on Ad5.CMV.LacZ infection rates. Ad5.CMV.LacZ was incubated with NeutrAvidin™ at concentrations of 0.25mg/ml, 0.5mg/ml, 0.75mg/ml and 1.0mg/ml for 4 hours. The Ad5.CMV.LacZ-NeutrAvidin™ conjugates were shrouded with CCL19 and used to infect HEK.293 and HEK.hCCR7 cells with 6.6×10^4 ifu/well. Analysis of infection by assessment of LacZ expression was performed as before after 48 hours incubation. For each NeutrAvidin™ conjugate cells were counted in 30 fields across 3 wells, represented by the bars in the graph. This analysis was performed on one occasion. The error bars represent the SEM.

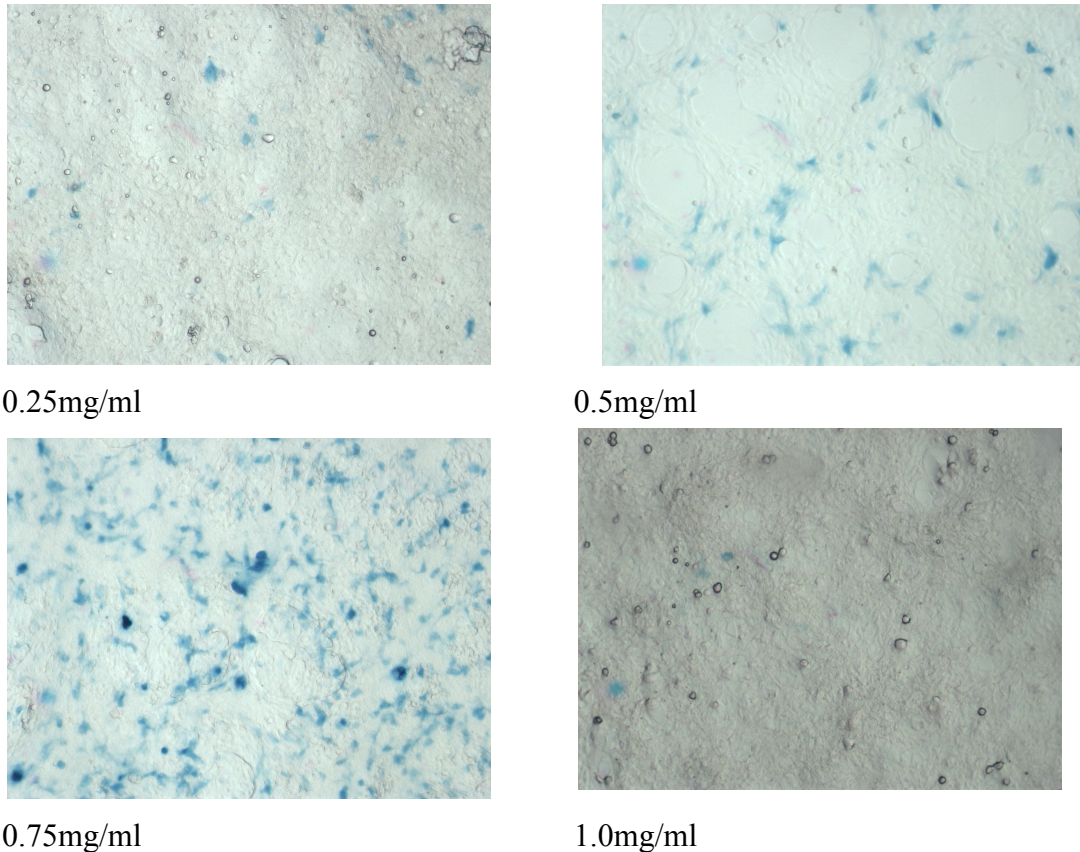


Figure 5.28: HEK.hCCR7 cells infected with Ad5.CMV.LacZ incubated with NeutrAvidin™ at different concentrations. Ad5.CMV.LacZ was incubated with NeutrAvidin™ at concentrations of 0.25mg/ml, 0.5mg/ml, 0.75mg/ml and 1.0mg/ml for 4 hours. The Ad5.CMV.LacZ-NeutrAvidin™ conjugates were shrouded with CCL19 and used to infect HEK.hCCR7 cells with viral particles at 6.6×10^4 ifu/well. Analysis of infection was performed after 48 hours incubation by assessment of LacZ expression with positive cells staining blue.

5.5 Infection of Raji Cells with Adenovirus shrouded in CCL19

Now that it had been demonstrated that adenovirus could be successfully redirected through cells engineered to express CCR7 or CCR5, the next step was to demonstrate that it could be re-directed through CCR7 in cells that express the receptor endogenously. In the previous chapter it was demonstrated that Raji cells not only endogenously express CCR7, but that the receptor is functional in these cells. Before starting infection experiments in this cell line, the expression of CAR was also determined. Normally, CAR is expressed in all mammalian cells except stem cells, haematopoietic cells and many muscle cells. There is however some literature suggesting that malignant lymphoma cell lines do express the CAR receptor [352], albeit at a lower level than in other tissues, and this was certainly found to be the case with Raji cells as shown in figure 5.10.

However, as lymphoma is the tumour type that is being explored in this thesis, infection of a lymphoma cell line was important thus the study progressed with Raji cells. Raji cells express functional CCR7 receptors and thus the infection experiments were performed

using CCL19 to shroud and to attempt redirection of the virus. Raji cell suspensions containing 5×10^5 cell in 500 μ l were infected with CCL19 shrouded Ad5.CMV.LacZ adenovirus at a MOI of 0.132 ifu/cell. Control samples were set up in parallel, with Ad5.CMV.LacZ that had not been shrouded with CCL19, at the same viral concentrations. The cells were incubated for 48 hours. Following incubation, the cells were washed once with PBS and then transferred to a poly-L-lysine coated microscope slide to adhere for 45 minutes. The cells were then assessed for LacZ expression, as described previously. The results are shown in figure 5.11 and figure 5.12. Figure 5.11 shows images of the infected Raji cells, clearly demonstrating a higher degree of infection in those cells exposed to the CCL19 shrouded adenovirus.

There was a significantly ($p=0.0097$), increased rate infection in Raji cells with the CCL19 shrouded Ad5.CMV.LacZ (mean; $22.3 (\pm 8.4) \times 10^6$ ifu/ml) compared to the non-shrouded virus (mean: $1.09 (\pm 0.18) \times 10^6$ ifu/ml), reflecting a greater than twentyfold difference. These results again clearly demonstrate that Ad5.CMV.LacZ can be successfully redirected through chemokine receptors.

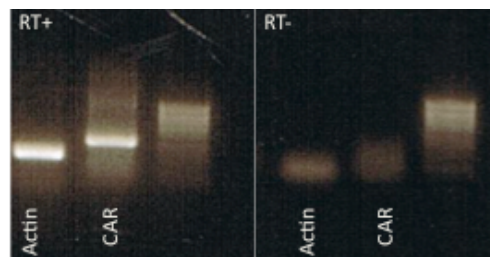


Figure 5.29: CAR expression in Raji Cells. RNA was prepared from Raji cells using Trizol®, these were DNAase treated and cDNA was prepared using reverse transcriptase (with a RT-control). Primers for actin and CAR were used to amplify cDNA using the PCR programme in 2.2.4.3. The PCR products were then run on a 1% agarose gel containing ethidium bromide. For comparison the actin PCR product is 400bp.

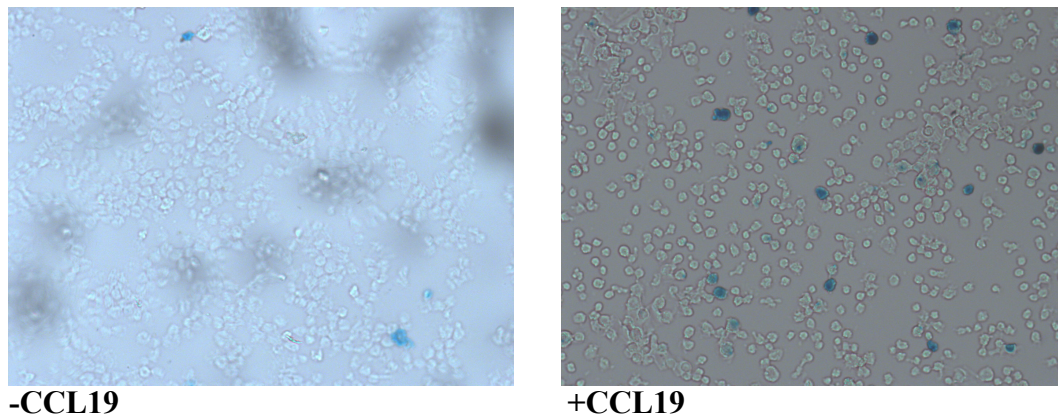


Figure 5.30: Raji cells infected with Ad5.CMV.LacZ shrouded with CCL19. Raji cells were infected with Ad5.CMV.LacZ with or without shrouding with CCL19 at 6.6×10^4 ifu/well. Following incubation for 48 hours, the cells were transferred to poly-L-lysine coated cells and left to adhere for 45 minutes. They were then assessed for LacZ expression by staining for β -galactosidase (blue cells). These figures demonstrate enhanced infection with CCL19-shrouded virus (right figure) compared to non-CCL19-shrouded virus.

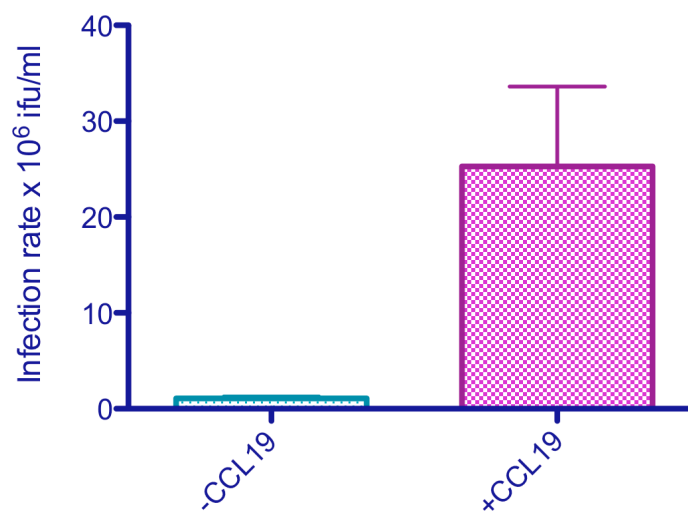


Figure 5.31: Infection of Raji cells with CCL19 shrouded Ad5.CMV.LacZ. 6.6×10^4 ifu/well of Ad5.CMV.LacZ with or without CCL19-shrouding were added to Raji cells and incubated for 48 hours. Cells were then placed on poly-L-lysine coated slides to enable adherence. Infection with Ad5.CMV.LacZ was then assessed as before, and the ifu/ml titres were calculated following counting of LacZ positive cells in 30 fields across 3 slides. This procedure was repeated in triplicate three times, and the results above reflect the data obtained from each of these experiments. The error bars represent the SEM.

5.6 Increasing the Specificity of Cell Targeting using Different Promoters

It has been shown that it is possible to improve the specificity of cell targeting for malignant cells further by using hTERT and hTR promoters, which are telomerase promoters predominantly expressed in germ cells and malignant cells [325, 353](Bilsland, 2003). At a later stage, once redirection of adenovirus through chemokine receptors had been optimised, it was considered that using these promoters would add a valuable additional level of specificity when constructing the oncolytic virus for targeted therapy. Yet, before proceeding, it was important to determine if the telomerase promoter was present in HEK293 cells, as these cells would be ideal for use in initial *in-vitro* proof-of-principle studies, to target the chemokine receptor positive cells.

5.6.1 Comparison of infection rates in HEK293 and A2780 cells following infection with Ad5.hTERT.Luc

Infection experiments were repeated on HEK293 and the human ovarian cancer cell line A2780 (which is known to express hTERT and hTR). However, on this occasion the adenovirus used were Ad5.hTERT.Luc, Ad5.hTR.Luc and Ad5.SV40.Luc obtained from Alan Bilsland. These vectors contain hTERT, hTR or SV40 promoters, the latter promoter acting as a positive control, as it should promote transcription in most cell types. Luc encodes the reporter gene luciferase, present in each of the 3 vectors. After 48 hours incubation of HEK293 and A2780 cells with the virus, a luciferase assay was performed on the cells using the Promega Luciferase Assay kit according to the manufacturer's instructions outlined in section 2.2.6.6. The results of this experiment are shown in figure 5.13. There were higher luciferase expression levels with all three viruses in the HEK293 cells when compared to expression in the A2780 cells, indicating that the telomerase promoters could be used to efficiently initiate reporter gene expression in HEK293 cells.

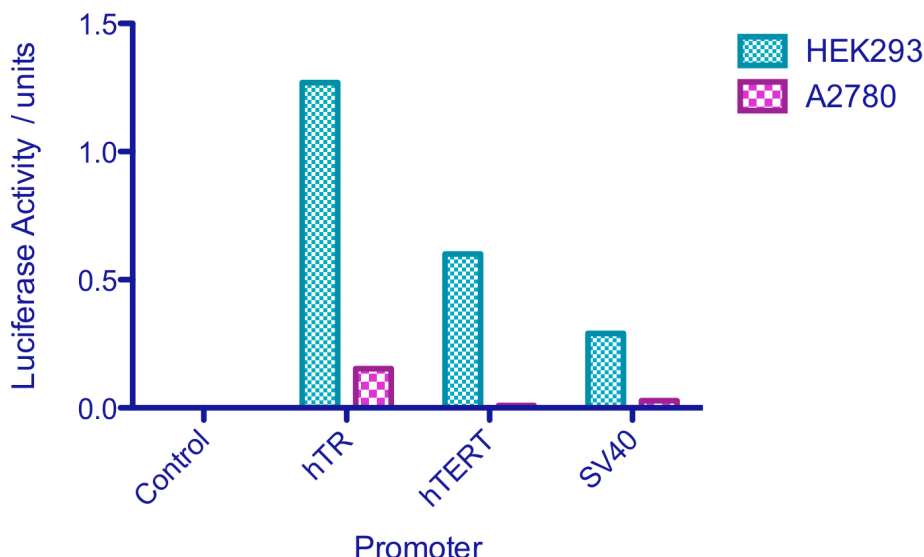


Figure 5.32: Infection of HEK293 and A2780 cells with Ad5.hTR.Luc, Ad5.hTERT.Luc and Ad5.SV40.Luc. HEK293 and A2780 cells were infected with the above viral vectors, without prior shrouding with chemokine. Following 48 hours incubation, infection was assessed using the Promega luciferase assay kit (section 2.2.6.6). This experiment was repeated once only, with each sample set up in triplicate. There is clearly more efficient infection of HEK293 cells compared to A2780 cells.

5.6.2 Comparison of Infection in HEK293 and HEK.hCCR7 Cells with Ad5.hTR.Luc shrouded with CCL19

The above experiment was repeated, however this time HEK293 and HEK.hCCR7 cells were infected with Ad5.hTR.Luc with or without shrouding with CCL19 as described previously. Ad5.hTR.Luc was chosen as this had resulted in the highest rate of infection in the previous experiment. After infection, the cells were analysed for luciferase activity. The highest luciferase activity and hence infection rate was obtained with HEK.hCCR7 cells incubated with CCL19 shrouded virus, although on this occasion this was not significantly different to the infection rate obtained in HEK293 cells incubated with the CCL19 shrouded virus ($p=0.0597$).

However it was interesting to note that infection rates were higher using the CCL19 shrouded virus than with the non-shrouded virus. Comparing HEK.hCCR7 cells incubated with CCL19 shrouded virus with HEK.hCCR7 cells incubated with non-shrouded virus, showed a significantly higher rate of infection in the former group ($p \leq 0.001$) as indicated by the higher rate of reporter gene activity. The difference between infection rates in HEK293 cells exposed to the two virus groups was not significant ($p=0.1829$). One

explanation for this observation might be that infection through CCR7 is more efficient than CAR. However, the most likely explanation is that the virus is able to enter the cell by both CCR7 and CAR dependent mechanisms, and so the increased rates of infection simply reflect the fact that more receptors are available to the virus. The results are shown graphically in figure 5.14.

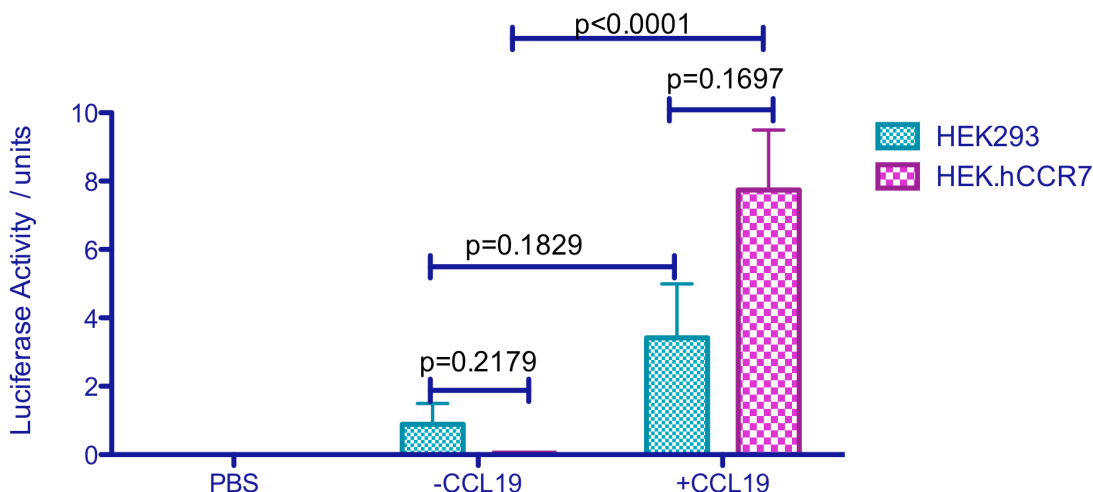


Figure 5.33: Infection of HEK.hCCR7 cells with CCL19 shrouded Ad5.hTR.Luc. HEK293 and HEK.hCCR7 cells were incubated with Ad5.hTR.Luc with (+CCL19) or without (-CCL19) shrouding with CCL19 at 6.6×10^4 ifu/well. After 48 hours infection of cells was assessed using the Promega luciferase assay kit. Each bar represents analysis of three samples containing the same cells and viral vectors, with the error bars representing the SEM. This experiment was performed once.

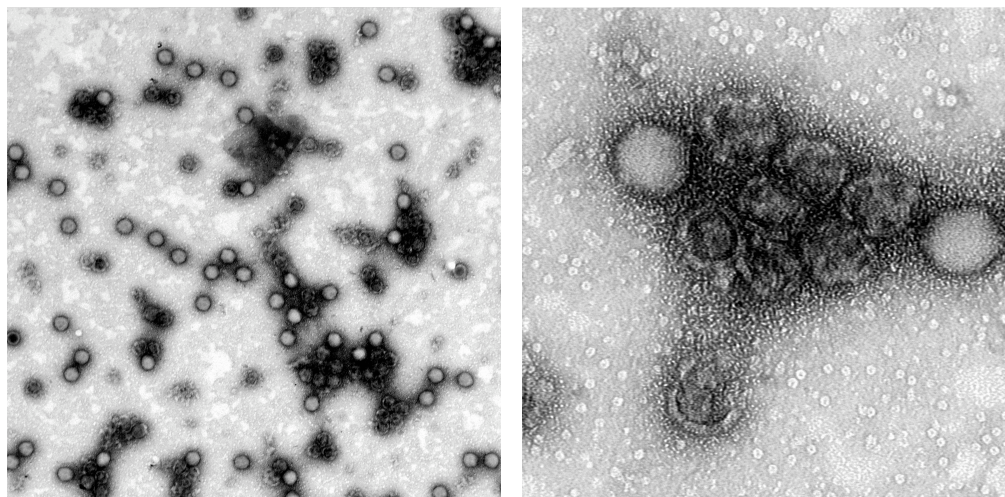
5.7 Assessment of NeutrAvidin™ binding to adenovirus using electron microscopy.

As discussed previously, one potential reason for the degree of background infection seen in these experiments is incomplete binding of the NeutrAvidin™ to the viral knob proteins. Each adenovirus has 12 viral knobs to which one molecule of the NeutrAvidin™ can attach, and each molecule of NeutrAvidin™ will bind one molecule of biotin. To investigate the possibility of incomplete binding, electron microscopy was employed. By using biotin-gold, conjugation could be visualised using electron microscopy for detection of the gold particles. Any biotin-gold binding to NeutrAvidin™ conjugated to the viral knob protein would then be readily visualised and the degree of viral shrouding assessed. ‘Cribs’ for electron microscopy were prepared as discussed in section 2.2.6.8, in which

adenovirus, that had undergone NeutrAvidinTM conjugation, was settled onto the ‘cribs’ followed by the addition of biotin-gold. Adenovirus that had not undergone conjugation with NeutrAvidinTM was used as a negative control. The images obtained from the negative controls are shown in figure 5.15.

The images in figure 5.16 represent those viral particles that had undergone incubation with NeutrAvidinTM. If the chemical conjugation had been 100% successful, then there should be 12 gold particles visible per virus, however, as can be seen, only a small proportion of the viral knob proteins appear to have been shrouded by the NeutrAvidinTM with only a few gold particles seen per virus. This strengthens the hypothesis postulated earlier that incomplete conjugation of the virus with NeutrAvidinTM and by extension incomplete shrouding with CCL19 or CCL3, was responsible, at least in part, for the high degree of background adenoviral infection observed in previous experiments.

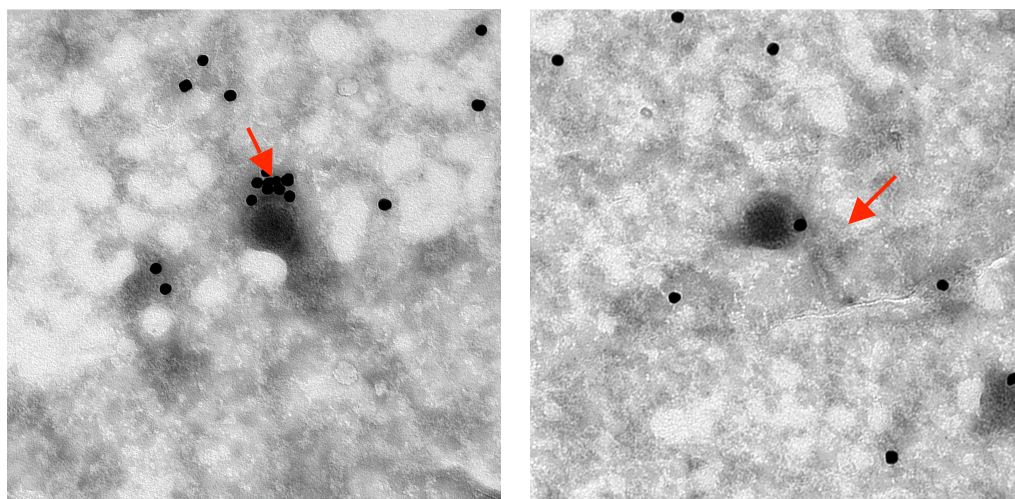
However, despite this, overall the experiments show a significant increase in CCR7 and CCR5 dependent infection rates with only this partial degree of shrouding, and so if a more efficient way of shrouding the virus could be found then redirection of the adenoviral tropism through the chemokine receptors should be even more efficient. The rest of this chapter describes the way in which this could potentially be achieved.



x 8000

x 25000

Figure 5.34: Electron micrograph of non-labelled adenovirus. Adenoviral particles were prepared for electron microscopy using 'cribs' as described in section 2.2.6.8. Images were taken at x8000 and x25000 magnifications.



x 12500

x12500

Figure 5.35: Ad5.CMV.LacZ-NeutrAvidin™ conjugates incubated with biotin gold. Ad5.CMV.LacZ-NeutrAvidin™ conjugates were incubated with biotin-gold, following which the virus was prepared for electron microscopy as described in 2.2.6.8. Images were taken at x12500 magnification. Gold particles can be seen as black dots on the image as indicated by the red arrows indicating that only a small proportion of the adenoviral fibre knobs have bound to NeutrAvidin™. If all viral knob proteins had been conjugated with NeutrAvidin™ then 12 gold particles per viral particle would be observed.

5.8 Modification of the adenoviral knob protein

As mentioned above more efficient shrouding of the adenovirus with the chemokine is required to diminish the background infection. One strategy is to increase the degree of NeutrAvidin™ binding by enhancing biotinylation of the adenovirus. Acceptor peptides (AP) are small 15 amino acid peptides that are biotinylated by the *Escherichia coli* enzyme biotin ligase [325]. Biotin ligase has previously been used to successfully biotinylate AP tagged proteins in-vitro [354]. This being the case it was thought that if this AP could be incorporated into the viral knob, then this would allow for more efficient shrouding of the virus via biotinylation. One potential problem with this is that incorporation of a peptide into the viral knob may affect its function and the ability of the adenovirus to be endocytosed by the cell. However, it has been shown that peptides up to 40 amino acids long can be incorporated into the viral knob protein without significantly affecting its ability to infect cells via the CAR receptor and endocytosis [354]. So it was thought that the above approach would be feasible. The steps taken to incorporate the AP into the viral knob protein are described in the following sections and the approach is showed diagrammatically in figure 5.17.

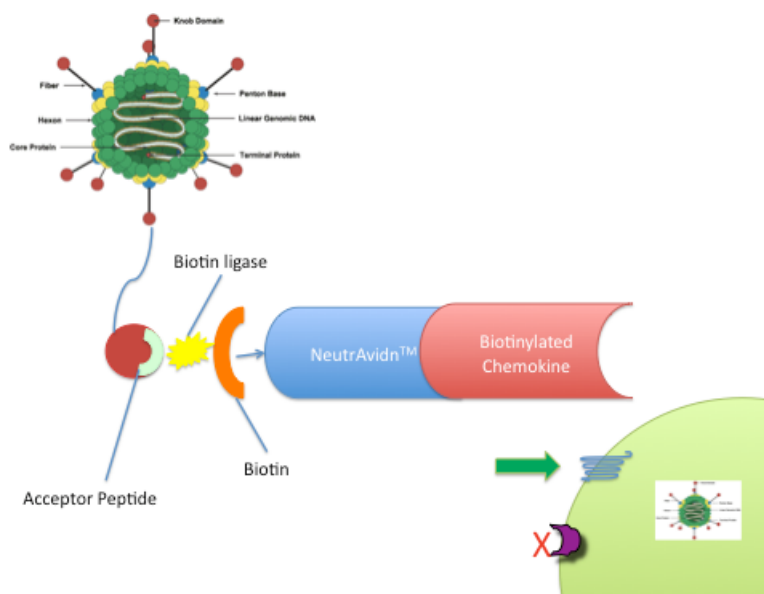


Figure 5.36: Strategy to improve efficiency of adenovirus shrouding with chemokines. The acceptor peptide can be biotinylated by the enzyme biotin ligase [331]. By inserting the acceptor peptide into the fibre knob protein biotinylation of the virus could be achieved and thus more efficient conjugation with NeutrAvidin™. This would result in improved shrouding of the virus with chemokine and potentially enhance adenoviral infection through the chemokine receptor.

5.8.1 Construction of a Vector for Homologous Recombination with the pAdEasy Vector

The most effective way of incorporating genes into the adenoviral vector is through a system of homologous recombination. The AdEasy™ Adenoviral system from Stratagene was employed for this purpose. The diagram in figure 5.18, below, demonstrates how this system works; essentially a vector containing the gene of interest is engineered with 2 flanking sequences homologous to the adenovirus sequence in which the gene is to be inserted. The vector also contains a gene to allow for selection, such as the kanamycin resistance gene, flanked by unique restriction enzyme sites to allow removal of this gene at the final stages.

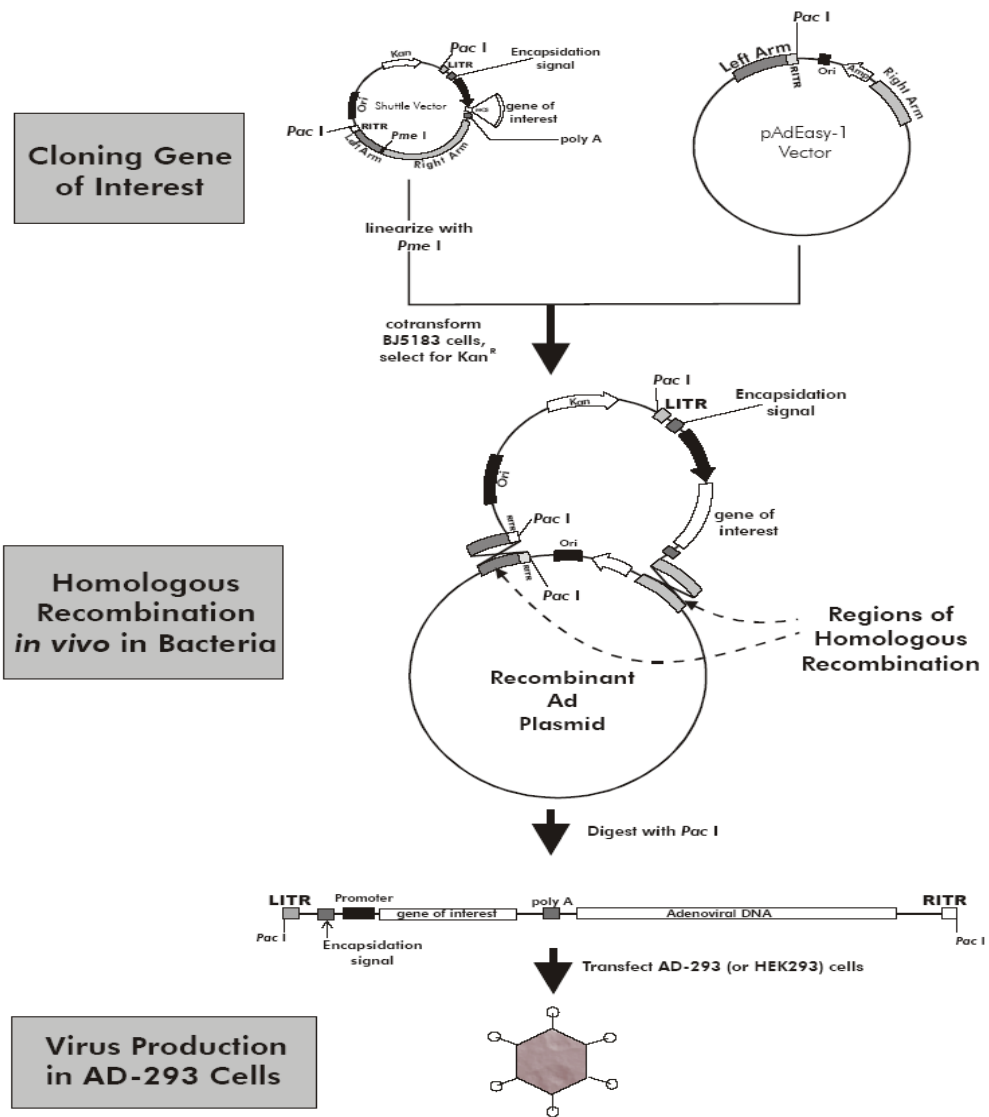


Figure 5.37: Homologous recombination using the Stratagene AdEasy™ Adenoviral System. In order to engineer an adenoviral vector containing the acceptor peptide a system of homologous recombination was attempted. However, in place of the shuttle vector detailed in the above diagram, a vector containing 2 arms homologous to the adenoviral fibre knob protein gene sequence was engineered containing the acceptor peptide and a unique *Xba*I site (see figure 5.21). Figure taken from the Stratagene AdEasy™ Adenoviral System manual.

The ultimate aim of this part of the project was to insert the acceptor peptide sequence onto the end of the viral fibre knob, and the intended vector for development is shown in figure 5.19. The first step was to design primers to obtain two 1kbp fragments of the adenovirus sequence using RT-PCR described in section 2.2.4.3.1, on either side of the end of the sequence of the viral knob protein, the first fragment contained the last 1kbp of the fibre knob protein sequence, with the second fragment containing 1kbp immediately downstream of the fibre knob protein sequence. These fragments were used initially as a template to engineer the vector construct to incorporate the acceptor peptide sequence and subsequently, they would provide regions for homologous recombination enabling the insertion of the acceptor peptide into the fibre knob protein sequence. Once these fragments had been obtained they were used as the template for overlapping-extension PCR, as in section 2.2.4.3.2 and figure 5.20 to introduce both the acceptor peptide sequence, and a unique *XbaI* restriction enzyme site, onto the end of the sequence for the viral knob. *XbaI* was chosen as examination of the pAdEasy vector sequence did not demonstrate the presence of any *XbaI* sites, and this could then be used as a surrogate restriction marker for confirmation of insertion of the acceptor peptide sequence. The primers used for this are outlined in 2.1.7.2 of the methods section. The sequence for the acceptor peptide itself is shown below.

GGC CTG AAC GAC ATC TTC GAG GCC CAG AAG ATC GAG TGG CAC GAG TGA
Gly Leu Asn Asp Ile Phe Glu Ala Gln Lys Ile Glu Trp His Glu Stop

The insertion of the acceptor peptide sequence and *XbaI* site onto the end of the fibre knob protein sequence was successfully achieved as demonstrated by figure 5.21. This figure shows the 2kb (lane 1) product obtained by overlap-extension PCR, which was then digested with *XbaI*, showing that 1kb fragments are obtained and indicating successful incorporation of the acceptor peptide sequence.

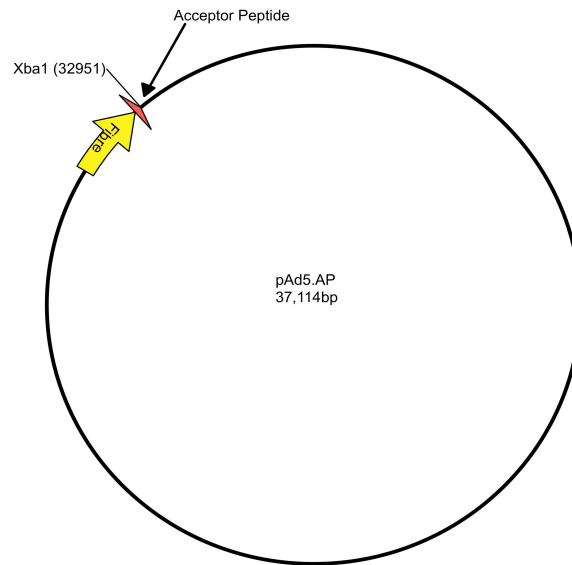


Figure 5.38: Map of adenoviral vector containing the acceptor peptide. Note the positioning of the acceptor peptide at the end of the fibre knob protein sequence, followed by the unique *Xba*I site.

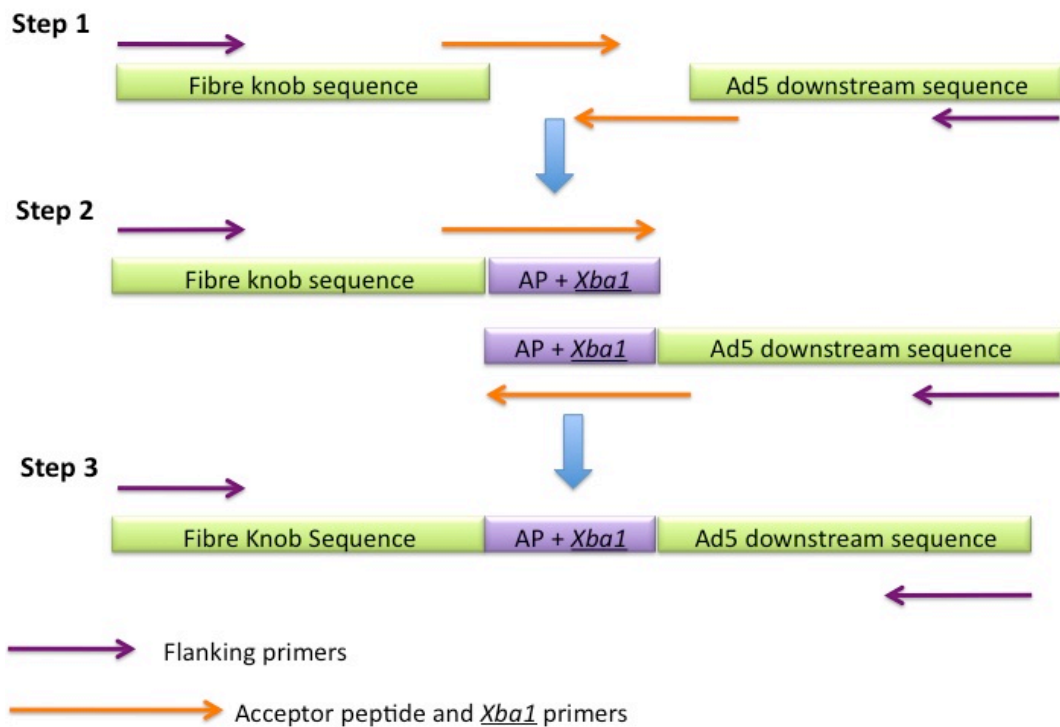


Figure 5.39: Overlap extension PCR. Step 1: 2 fragments of DNA (template DNA) are amplified incorporating the gene sequence into which the acceptor peptide and *Xba1* sequences are to be inserted. Flanking primers and extension primers (containing the acceptor peptide and *Xba1* sequences as well as areas homologous to the template DNA) and PCR is set up as in section 2.2.4.3.2. Step 2: The extension primers add the sequence to be inserted onto the ends of the template DNA during the early stages of PCR. Step 3: The flanking primers enable amplification of the entire construct consisting of the two DNA template fragments, acceptor peptide and *Xba1* site.

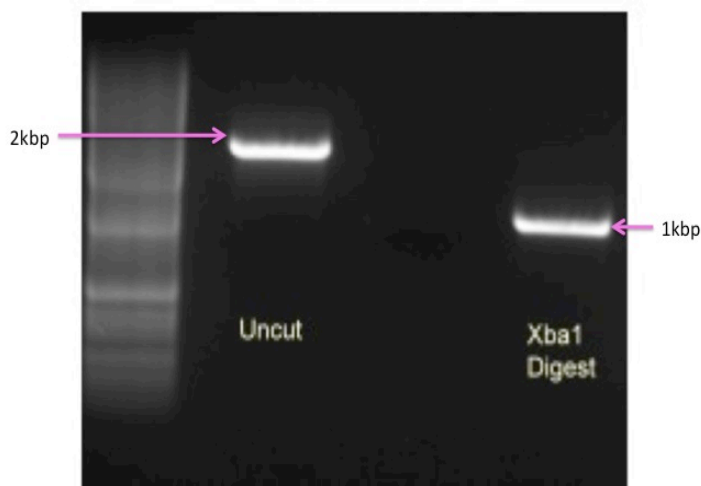


Figure 5.40: *Xba*1 digest of overlap extension PCR product. Two 1kbp fragments consisting of a) last 1kbp of adenoviral fibre knob protein sequence and b) 1kbp immediately downstream of fibre knob protein sequence, were used in overlap extension PCR overlap with flanking primers and primers containing the sequence for the acceptor peptide and a *Xba*1 site (see figure 5.20). To confirm that the 2kbp product (lane 1) obtained contained the acceptor peptide sequence an *Xba*1 digest was done on the PCR product and then run on a 1% agarose gel containing ethidium bromide. The gel image above confirms the successful incorporation of the acceptor peptide onto the end of the fibre knob protein sequence with 1kbp fragments (lane 2) obtained after *Xba*1 digest.

This 2kbp product was then inserted into the pCR2.1 TOPO vectors as described in 2.2.4.8, and the resulting vector (now termed pCR2.1.Ad5.AP shown in figure 5.22a) was sent for sequencing to ensure that the acceptor peptide sequence was in the correct place. In the meantime pBluescript vector was used to obtain the tetracycline sequence flanked by two *Xba*1 sites. The plan was to insert the tetracycline sequence into the *Xba*1 site at the end of the acceptor peptide sequence of the pCR2.1.Ad5.AP using simple ligation techniques as described in 2.2.4.10. However, after digesting with *Xba*1, no fragments were seen with the pCR2.1.Ad5.AP suggesting that ligation was unsuccessful or that the *Xba*1 digestion was not working.

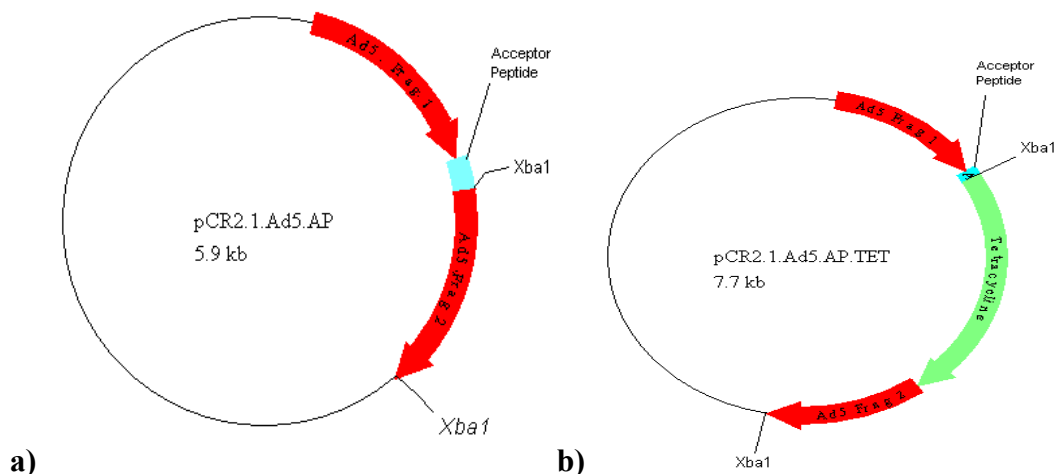


Figure 5.41: Vectors created for homologous recombination with pAdEasy. Both vectors incorporate the acceptor peptide and an *Xba1* site at the end of the fibre knob protein sequence a) pCR2.1.Ad5.AP without tetracycline selectable marker b) pCR2.1.Ad5.AP.Tet with a tetracycline selectable marker.

Consequently, the sequence surrounding the *Xba1* site was examined more carefully, and it was discovered that the primer developed to incorporate the acceptor peptide contained a methylation site encompassing the *Xba1* site. DNA adenine methyltransferase (DAM) is a bacterial enzyme that recognises and subsequently methylates the sequence 5'GATC 3', which if incorporated or partially incorporated into a restriction enzyme site, renders it resistant to cleavage. Therefore, as it appeared the digestion was not working because of methylation, a DAM negative strain of *E. coli* was identified and the pCR2.1.Ad5.AP vector was transformed using the DAM⁻ ER2925 *E. coli* strain from NEB. The vectors produced in this way were then digested with *Xba1* successfully as the *Xba1* site was no longer methylated. Yet, before proceeding with the ligation of the tetracycline sequence, another problem had to be addressed. The pCR2.1 TOPO vector also contains an *Xba1* site downstream of the Ad5.AP insertion, therefore a simple *Xba1* digest would lead to the removal of the 2nd flanking arm of the Ad5 sequence (see figure 5.22a and b). To counteract this problem a partial digest was performed as in section 2.2.4.6 and the 2kb fragment was identified and gel purified prior to ligation with the tetracycline gene sequence to produce the vector termed pCR2.1.Ad5.AP.TET (figure 5.22b). The tetracycline gene was used as a selectable marker to ensure that colonies obtained following tetracycline exposure contained the construct of interest. These colonies were then analysed using digestion with *BamHI* to identify a 4kb and a 2kb product indicating successful ligation. The flanking primers initially used to obtain the 2kb viral fragment were then used on potential colonies to detect the correct size insert of the Ad5.AP and tetracycline gene combined. This gave the expected 3.6kb fragment size, which also

demonstrated the correct band sizes with *Xba*I digest (Figure 5.23) and this was then sent for sequencing. Sequencing confirmed the correct placement of the AP and tetracycline genes within the construct. This construct is termed pCR2.1.Ad5.AP.Tet shown in figure 5.22b. The vector was then propagated by transformation into ER2925 *E.coli* and subsequent plasmid DNA preparation as described in section 2.2.4.16. The DNA concentration of the vector was then quantified using spectrophotometry to measure optical absorbance at 260 and 280nm.

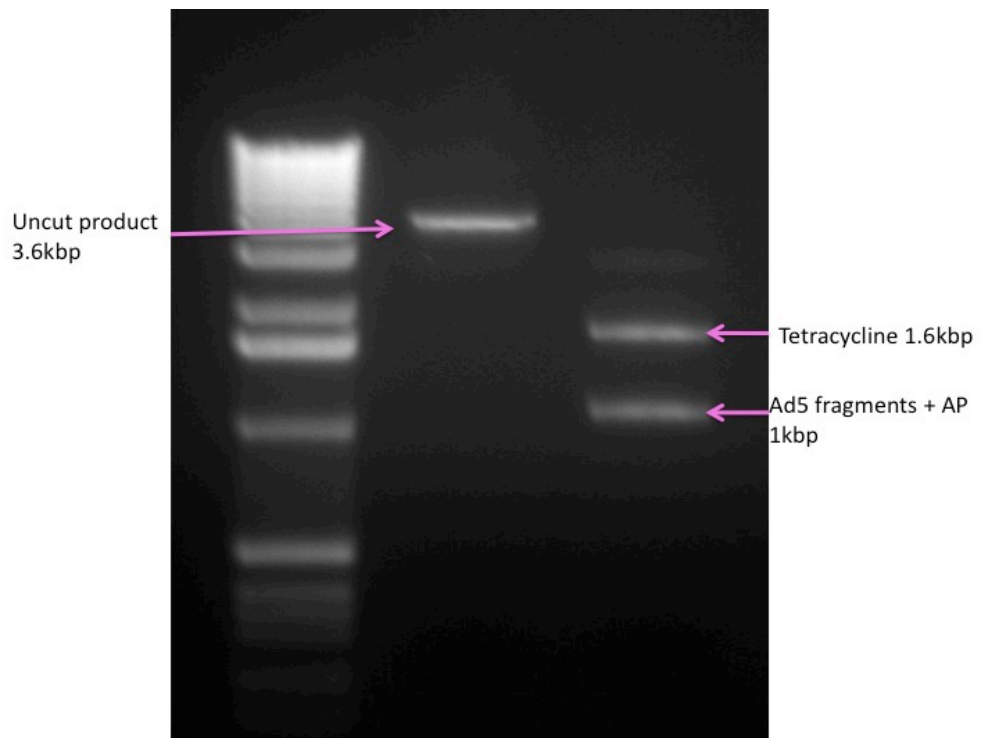


Figure 5.42: *Xba*I digest on RT-PCR product from pCR2.1.Ad5.AP.Tet construct. To confirm that the pCR2.1.Ad5.AP.Tet construct contained the acceptor peptide gene sequence and the tetracycline resistance gene at the correct site, the adenovirus flanking primers were used to amplify the sequence of interest using the PCR programme outlined in 2.2.4.3. The resulting product was 3.6kb as predicted a digest with *Xba*I produced 2 fragments consisting of the 1.6kb tetracycline resistance gene and the 1kb adenovirus gene segments.

5.8.2 Homologous Recombination with pAdEasy and pCR2.1.Ad5.AP.Tet.

The method outlined in the Stratagene pAdEasy Adenoviral System manual was followed in order to engineer an adenoviral vector placing the sequence for the AP at the end of the fibre knob protein using the construct created in section 5.8.1. Essentially, 2µg of pCR2.1.Ad5.AP.Tet was linearised using *NotI* and run on an agarose gel. This was gel purified and then dephosphorylated, and again gel purified prior to final DNA quantification using spectrometry. The concentration was then adjusted to 1µg/µl. 1µl each of the linearised plasmid and the pAdEasy vector were then added to 40µl of BJ5183 cells in an electroporation cuvette (0.2cm) and electroporated at 200Ω, 2.5Kv and 25µF. One ml of LB broth was then added and the cells transferred to a 14ml Falcon tube for transformation. They were plated onto tetracycline containing plates. DNA from the colonies obtained was then prepared using the modified DNA preparation protocol as described in methods section 2.2.4.16. The DNA samples were then analysed by restriction enzyme mapping using *AscI* and *HindIII* to confirm homologous recombination. However the expected fragment sizes were not seen despite repeated electroporation and selection of numerous colonies. To investigate this further, the pAdEasy vector sequence was examined in more detail; it unfortunately transpired that the origin of replication (*ori*) sequence of the pAdEasy vector actually contained a large portion of the tetracycline resistance gene.

To determine whether this portion of the tetracycline resistance gene was sufficient to confer resistance to cells transfected with the pAdEasy vector, the vector was transformed into BJ5183 cells and plated onto agar plates containing tetracycline. Colonies were able to grow, confirming that the pAdEasy vector provided tetracycline resistance to transfected cells. It was as therefore concluded that firstly, tetracycline could not be used as a selectable marker and that secondly one reason for the unexpected restriction enzyme maps was that potentially random recombination events were occurring between the *ori* sequence and the Ad5.AP.Tet construct. Therefore an alternative strategy was required.

5.8.3 Development of pCR2.1.Ad5.AP.Kan

Now that it was clear that tetracycline could not be used as a selectable marker an alternative was sought. Kanamycin was subsequently chosen as a selectable marker for insertion into the constructs used to incorporate the AP into the fibre knob protein as,

examination of the pAdEasy vector did not reveal any sequence homologous to that of the kanamycin resistance gene, and so random recombination events were unlikely to result.

As the pCR2.1.Ad5.AP vector had already been constructed the insertion of the kanamycin gene was relatively straightforward. A pBlueScript vector containing the kanamycin resistance gene sequence flanked by *Xba*I sites had been developed previously in the laboratory. The kanamycin gene sequence was therefore digested using *Xba*I and ligated into the *Xba*I partial digest product of pCR2.1.Ad5.AP and transformed using DAM⁻ *E.coli* as previously described. RT-PCR using the flanking primers was then used to screen the colonies as before. A 4.3kb fragment was obtained indicating successful insertion of the kanamycin resistance sequence into pCR2.1.Ad5.AP. Analysis by restriction enzyme mapping was also performed using *Eco*RI to give the predicted 1, 3.3 and 3.9kbp fragments and an *Xba*I digest giving 2.3kbp and 1kbp fragments. The size of the kanamycin resistance sequence is 2.3kb. Analysis demonstrated the correct sizes and the resulting vector termed pCR2.1.Ad5.AP.Kan shown in figure 5.23, was then ready for use in homologous recombination.

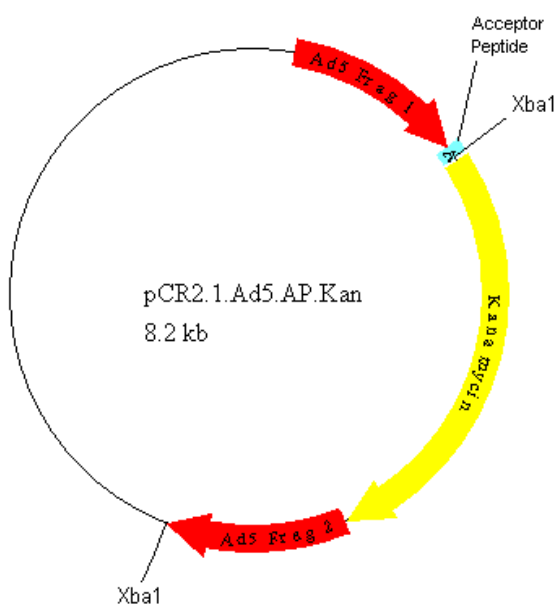


Figure 5.43: Vector map of pCR2.1.Ad5.AP.Kan. This replaced pCR2.1.Ad5.AP.Tet for attempts at homologous recombination with pAdEasy to introduce the acceptor peptide sequence onto the end of the adenoviral fibre knob protein sequence. Examination of the pAdEasy sequence did not reveal any areas homologous to any part of the kanamycin gene sequence.

5.8.4 Homologous Recombination with pAdEasy and pCR2.1.Ad5.AP.Kan

The method, as outlined above, was used for homologous recombination but using *ScaI* to linearise the plasmid rather than *NotI*. After transformation the preparations were spread onto agar plates containing both ampicillin and kanamycin to select for colonies containing the insert and the pAdEasy vector. Analysis of the resulting colonies with restriction enzyme mapping using *EcoRI* would have been expected to yield fragments of the following sizes:

1238bp, 7637bp, 4546bp, 2052bp, 2623bp, 4880bp, 1011bp, 11544bp.

However, this map was not obtained. The colonies obtained were also screened using the flanking primers as before, but no PCR products were obtained. The electroporation was subsequently repeated using the 4.3kb PCR product obtained when using the flanking primers on the pCR2.1.Ad5.AP.kan vectors. These products would consist solely of the construct with 2 homologous arms separated by the Acceptor peptide sequence, the *XbaI* sites and the kanamycin resistance gene. By using these products it was hoped that any unexpected recombination events with other areas of the pCR2.1 vector, in particular the other kanamycin resistance gene cassette, would not occur. However, again, no suitable colonies were obtained and restriction enzyme mapping revealed unexpected fragment sizes. It was thought that it was possible that, recombination events between the newly formed vectors continued, and that this explained the unexpected results. Therefore an alternative strategy was again required.

5.8.5 Sub-cloning to obtain pAdEasy.AP

This method involves a series of restriction enzyme digests followed by ligation to obtain the vector construct. The first step was to identify unique restriction enzyme sites within the pAdEasy vector, which would enable a fragment incorporating the entire homologous region used in the pCR2.1.Ad5.AP vector to be inserted. *PacI* and *SpeI* sites were identified which after a double digest with these enzymes produced a fragment of 6.8kb in size incorporating the entire homologous region. The next step was to design an oligonucleotide incorporating the sequence for these restriction enzyme sites as a linker and to ligate this into a pBlueScript KSII vector as detailed in methods sections 2.2.4.9 and 10. The oligonucleotide used for this was as follows:

CGC/G/ACTAGT/CATGC/TTAATTAA/C

Once the linker had been successfully incorporated into the pBlueScriptKSII vector, the *PacI/SpeI* fragment from the pAdEasy vector was ligated into this giving a pBluescript.SpeI.PacI.Frag vector. Two unique restriction enzyme sites (*KpnI* and *ApaI*) were then identified in the Ad5 homologous regions contained within the pCR2.1.Ad5.AP.Kan vector (see figure 5.25). The fragment resulting from digestion with these two enzymes was ligated into the pBlueScript.SpeI.PacI.Frag which had also undergone digestion with *KpnI* and *ApaI*, thereby incorporating the acceptor peptide, *XbaI* site and kanamycin resistance gene into the 6.8kb pAdEasy fragment at the correct site. Once this had been achieved, the resulting vector, pBluescript.SpeI.PacI.Frag.AP, was created. This vector and the pAdEasy vector were then digested with *SpeI* and *PacI*, and the new fragment containing the acceptor peptide, *XbaI* site and kanamycin gene resistance sequence was then ligated into pAdEasy. The final step had to be repeated a number of times. However eventually the final ligation resulted in colonies producing two constructs of the correct size, which were candidates for further analysis. The DNA preparation demonstrating these 2 colonies is shown in figure 5.26.

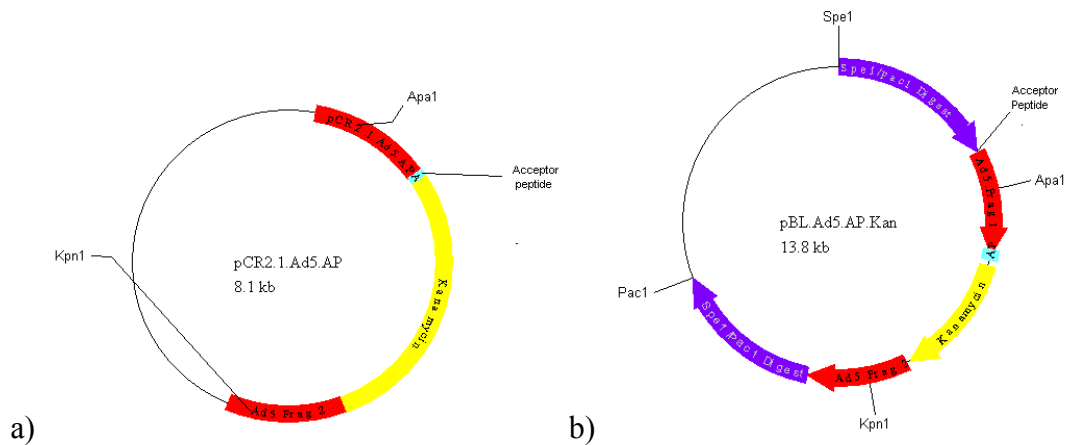


Figure 5.44: Vector maps of pCR2.1.Ad5.AP.Kan and pBL.Ad5.AP.Kan. These demonstrate the *ApaI* and *KpnI* sites in pCR2.1.Ad5.AP.Kan and the *ApaI*, *KpnI*, *SpeI* and *PacI* sites in pBluescript.Ad5.AP.Kan used for the subcloning strategy employed to engineer pAdEasy.AP.

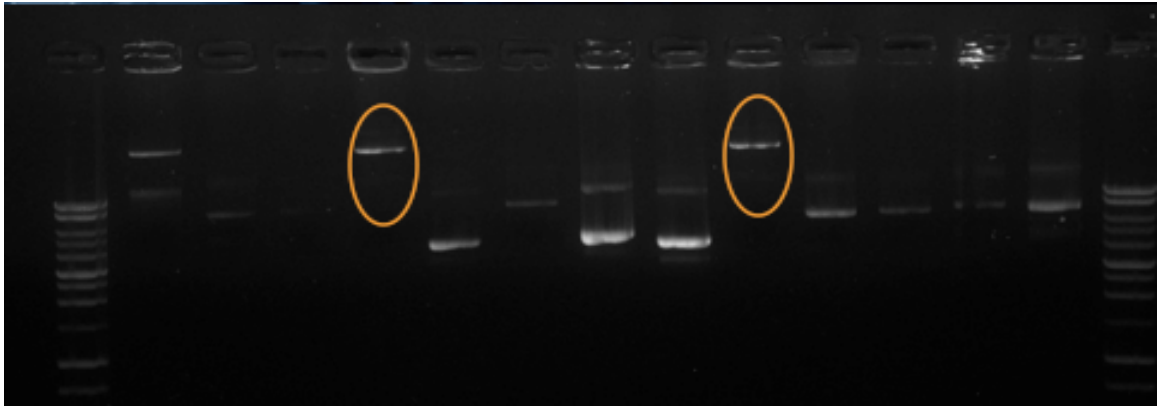


Figure 5.45: DNA preparation of ligation with pAdEasy and pBluescript.Spe1.Pac1.Frag.AP fragments. The final step in the subcloning strategy was to ligate *Spe1/Pac1* digests of pAdEasy with *Spe1/Pac1* digest of pBluescript.Spe1.Pac1.Frag.AP to create pAdEasy.AP. This ligation was then transformed as in 2.2.4.13 following which mini-preparations of plasmid DNA (see 2.2.4.16) were prepared. These DNA preparations were then run on a 1% agarose gel with ethidium bromide. Two plasmid preparations were identified as potentially representing pAdEasy.AP these are highlighted in orange.

These colonies were then further analysed by using the original adenovirus flanking primers to obtain a PCR product 4.3kb in size, consistent with the 2 homologous Ad5 regions and the kanamycin resistance gene. This was then digested with *Xba1* to confirm that an *Xba1* site was present along with the kanamycin resistance gene in the pAdEasy vector. This yielded the expected fragment sizes of 2.3kb corresponding to the kanamycin resistance sequence and 1kb fragments corresponding to the homologous arms used initially. This is shown in figure 5.27. The construct, pAdEasy.AP, was then sent for sequencing, which confirmed the correct sequence of the acceptor peptide, *Xba1* site and surrounding adenovirus sequence.

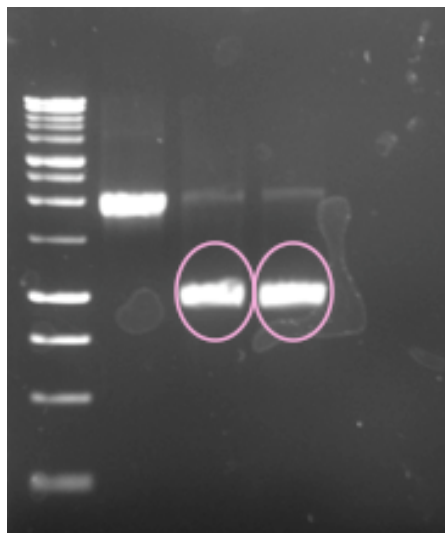


Figure 5.46: *Xba*I digest on RT-PCR product from pAdEasy.AP construct. The adenovirus flanking primers were added to the DNA preparation obtained in figure 5.26, in order to amplify the construct containing the acceptor peptide sequence. A 2kbp PCR product was obtained which was then digested with *Xba*I. This resulted in a 1kbp product confirming the presence of an *Xba*I and therefore the acceptor peptide sequence. This was later confirmed by sequencing.

5.9 Incorporation of a reporter gene into pAdEasy.AP

The pAdEasy.AP construct would be capable of producing virions following transfection into HEK.293 cells, however subsequent infection experiments would require the expression of a reporter gene to enable assessment of infection. Therefore, the pAdEasy.AP vector was used to develop two additional vectors, one with LacZ and the other with GFP as reporter genes. This was simply achieved by using the pAdEasy Adenoviral system and the pShuttle vectors commercially available for use with the system as shown in figure 5.28. Basically, the vectors pShuttle.CMV.LacZ and pShuttle.CMV.IRES.GFP obtained from Stratagene were used as described in 5.8.2, to attempt homologous recombination with pAdEasy.AP. In both cases this was successful and the vectors pAdEasy.AP.GFP and pAdEasy.AP.LacZ were produced. Once these vectors had been produced, the plan was to transfect these into HEK.293 cells in order to produce adenoviral particles containing the acceptor peptide at the end of the fibre knob protein. However this was not possible because of time constraints.

Once produced, these vectors would be biotinylated using biotin ligase, followed by incubation with NeutrAvidin™. The first step would then be to study the efficiency of conjugation with NeutrAvidin™ by electron microscopy study as described in section 5.7. If improved NeutrAvidin™ conjugation was confirmed, this would be followed by repeating the infection experiments outlined in this chapter with chemokine ‘shrouded’

adenovirus to assess firstly, the degree of infection obtained in the chemokine receptor positive cells, and secondly whether or not the background level of infection had been reduced.

Subsequently, these adenoviral vectors would be modified further to contain cytolytic genes such as thymidine kinase in order to study targeted oncolytic strategies.

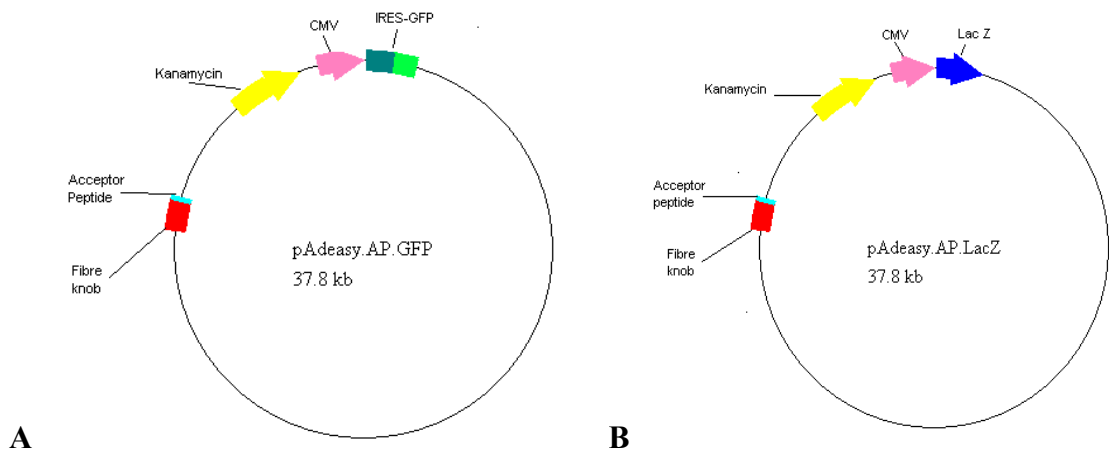


Figure 5.47: Vector maps of pAdEasy.AP.GFP and pAdEasy.AP.LacZ. These would be used to transfect HEK293 cells in order to produce adenoviral particles for, further infection experiments following biotinylation and shrouding with chemokine.

5.10 Summary

This chapter has demonstrated the following:

1. Adenoviral tropism can be re-directed through chemokine receptors, using simple biochemical shrouding of the virus with NeutrAvidin™ and biotinylated chemokines in CHO and HEK.293 cells that have been transfected in order to express CCR5 and CCR7.
2. In HEK.293 cells there is a high degree of background staining. One reason for this is incomplete shrouding of the adenovirus using the biochemical method. This was demonstrated using electron microscopy. It is also possible however, that some of the background staining was due to entry of the adenovirus using alpha integrins on the cell surface.
3. Optimisation experiments enabled a more efficient infection rate demonstrating optimum infection rates at an incubation time of 4 hours with the NeutrAvidin™ at a concentration of 0.75mg/ml.
4. Infection of Raji cells, which were shown to endogenously express CCR7, resulted in preferential infection with the CCL19 ‘shrouded’ adenovirus, again demonstrating that adenoviral tropism could be re-directed through chemokine receptors.
5. Further optimisation of this system was sought by introducing an acceptor peptide into the fibre knob protein sequence of the adenovirus. This should enable more efficient shrouding of the adenovirus by effectively biotinylating the virus using biotin ligase.
6. Vectors consisting of pAdEasy with the acceptor peptide, and either the LacZ or GFP reporter gene were created, but unfortunately time constraints prevented the final translation of these into adenovirus particles.

CHAPTER SIX

EL4 CELLS AS AN *IN-VIVO* NON-HODGKIN'S LYMPHOMA MOUSE MODEL

6.1 Introduction

The development of an *in-vivo* model is an integral step in the development of targeted therapies for lymphoma. The next aim of this project was to develop a lymphoma mouse model for *in-vivo* studies to assess whether or not the cytotoxic therapies developed affected the targeted, chemokine receptor expressing, cell populations without causing non-specific toxicity to other tissues and cell populations. To do this a cell line was looked for which could establish easily measurable tumour bulk in mice, without lethality, so that any response to the targeted therapy could be objectively measured. EL4 cells were identified as potentially fulfilling this role.

EL4 cells are an ascitic T-cell lymphoma cell line derived from the C57/BL6 mouse following inoculation with 9:10 dimethyl-1:2 benzantracene [354]. Injection of 1×10^5 cells into the flank of a C57/BL6 mouse has been noted to lead to the development of a measurable tumour in 7-10 days, whilst injection of 1×10^6 cells lead to measurable tumour development with metastasis [355]. As well as fulfilling the requirement of being able to induce measurable tumours, these cells had the advantage of being developed in a standard strain, C57/BL6 of laboratory mice. EL4 cells have been used extensively over the years in a variety of studies, and are therefore readily available and well characterised. For these reasons EL4 cells were chosen as a potential *in-vivo* mouse model for the adenovirus infection experiments and subsequent targeting of lymphoma cells.

However, before proceeding with *in-vivo* studies further characterisation of the cell line was required, in particular its expression of CCR7, and this will be outlined in this chapter along with early *in-vivo* adenovirus infection experiments.

6.2 Assessment of mCCR7 Expression in EL4 Cells

The first step in characterising the EL4 cells was to determine whether or not they expressed CCR7. This was done in two ways.

6.2.1 Assessment of Murine CCR7 Expression by RT-PCR

Primers were developed for the detection of murine CCR7 (mCCR7) and are shown in section 2.1.7.2 of the methods section. RT-PCR was performed with these primers, using the primers for mouse actin as a positive control. The results are shown in figure 6.1, and demonstrate that mCCR7 is expressed at the RNA level in EL4 cells.

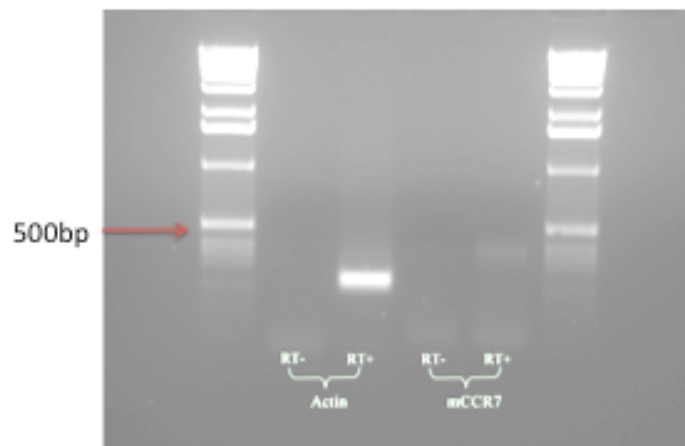


Figure 6.1: mCCR7 expression in EL4 cells. RNA was prepared from EL4 cells these were DNAase treated and cDNA was prepared using +/- reverse transcriptase. Primers for actin and mCCR7 were used to amplify cDNA using the PCR programme in 2.2.4.3. PCR products were then run on a 1% agarose gel containing ethidium bromide.

6.2.2 Assessment of mCCR7 Expression in EL4 cells using Flow Cytometry

An anti-mCCR7 antibody from AbCam with, and without, conjugation with FITC were used for the experiments assessing mCCR7 expression. Initially, the unconjugated antibody was incubated with the EL4 cells and subsequently incubated with a secondary antibody conjugated with PE, as previously described. Following this, flow cytometry was used to assess the expression of mCCR7 on the surface of EL4 cells. In figure 6.2 it can be seen that the EL4 cells express mCCR7 at the protein level as demonstrated by an increase MFI on flow cytometry.

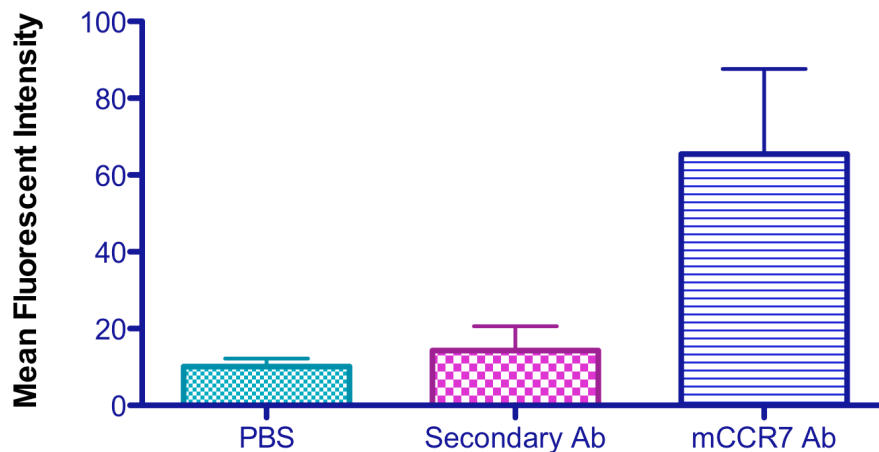


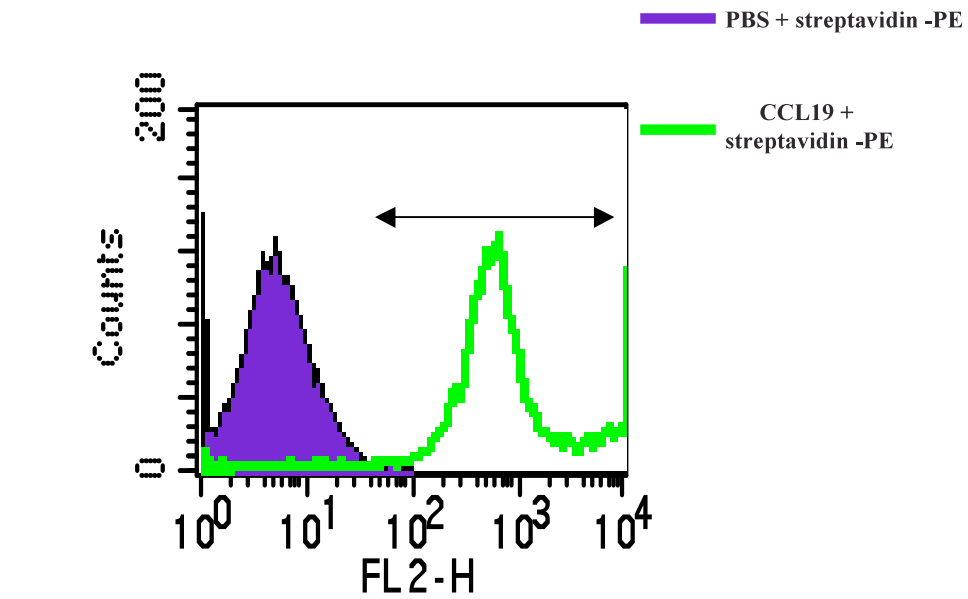
Figure 6.2: Surface mCCR7 expression in EL4 cells. EL4 cells were incubated with anti-CCR7 antibody followed by incubation with a secondary antibody conjugated with PE. EL4 cells incubated with PBS or secondary antibody alone were used as negative controls. Analysis of surface mCCR7 was performed using single colour flow cytometry. Each bar represents 3 test samples and the error bars show the SEM.

6.3 Assessment of functional mCCR7 expression EL4 cells

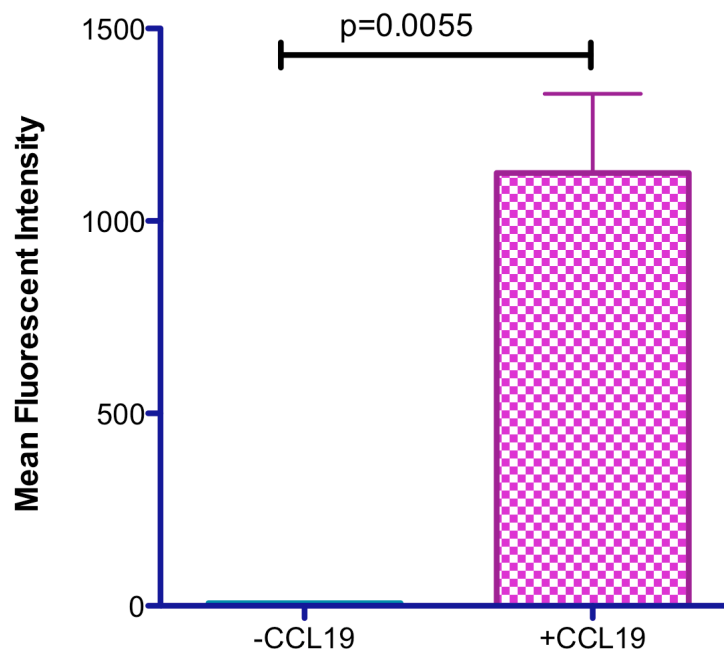
Having confirmed that EL4 cells express mCCR7, it was important to ensure that this expressed receptor was functional. As with the Raji cell line, this was done in 2 ways.

6.3.1 Biotin-CCL19 Uptake by EL4 Cells

The method described in 2.2.5.2 was used again for this cell line. Only one negative control was possible as these cells had been shown to express mCCR7. This control was streptavidin-PE with PBS, but without the CCL19. The results are shown in figure 6.3a and b. In figure 6.3a, the green line representing the EL4 cells exposed to biotin-CCL19 shows a clear shift to the right along the FL2-H gate, when compared to the cells that were not exposed (purple peak), thus demonstrating that the EL4 cells had bound the biotin-CCL19. This is shown quantitatively in figure 6.3b, in which the uptake of biotin-CCL19 by the EL4 cells is shown by the high MFI of those cells incubated with biotin-CCL19 (mean MFI: 1125 ± 205.2) compared to those that were not (mean MFI: 7.14 ± 0.43). These results not only show that EL4 cells bind to, and potentially internalise, biotin-CCL19, but that they do so at a higher level than seen previously with the HEK.hCCR7 or the endogenously hCCR7 expressing Raji cells.



a)



b)

Figure 6.3: Biotin-CCL19 uptake by EL4 cells. Cells were incubated with biotin-CCL19 and streptavidin-PE or streptavidin-alone, for 1hr at 37°C. Following this biotin-CCL19 uptake by the cells was analysed using single-colour flow cytometry. a) Overlay histogram plot comparing EL4 cells incubated with biotin-CCL19 (green peak) or streptavidin-PE alone (purple peak) b) Graph showing a significant difference in mean fluorescent intensity between EL4 cells incubated with or without biotin-CCL19, the population used to calculate the MFI for the positive cells is demonstrated by the arrowed marker in a). Each sample was repeated in triplicate and on three occasions. The error bars indicate the SEM.

6.3.2 Chemotaxis Assay with EL4 Cells using CCL19

Whilst it is clear that EL4 cells are able to bind to CCL19, as previously discussed in chapter 4, it could not be assumed that this leads to intra-cellular signalling, as the atypical receptor CCX-CKR can also bind to and internalise CCL19. Therefore, the Transwell® chemotaxis assays (methods section 2.2.5.5.1) were performed as discussed in section 4.4.2.1. CCL19 and CXCL12 were again used the latter acting as a positive control. The results of this are shown in figure 6.4. They clearly show that chemotaxis was induced in EL4 cells in the presence of CCL19, with a tailing off of response with the higher CCL19 concentration of 100nM. The peak CXCL12 concentration inducing chemotaxis is not deducible from these results, although there is significantly more chemotaxis in response to CXCL12 at 100nM than with CCL19 at the same concentration ($p=0.0229$). However, although these results confirmed that the mCCR7 was functional, the degree of chemotaxis was less than would have been expected considering the high degree of biotin-CCL19 binding. When comparing the migration indexes obtained with Raji and EL4 cells, the former had a tenfold higher rate of migration. The most likely explanation for this discrepancy will be discussed later in this chapter.

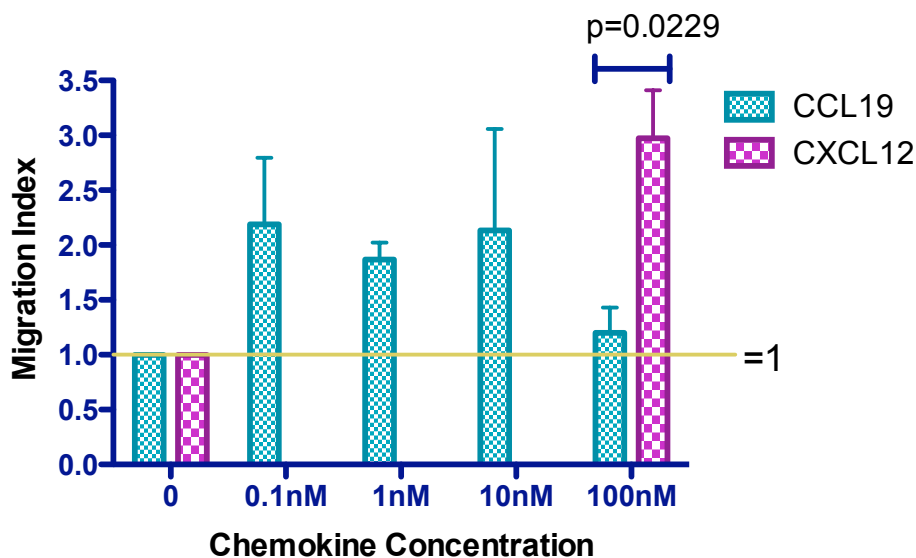


Figure 6.4: Migration of EL4 cells in response to CCL19 and CXCL12. Chemotaxis buffer containing different concentrations of CCL19 or CXCL12 was added to each well of a Transwell® plate. Inserts were added, and into each of these EL4 cells were placed. Following incubation at 37°C for 3 hours, the number of EL4 cells passing through the chemotaxis chamber. A migration index was calculated as outlined in section 4.3.2.1. A migration index of greater than 1 indicates that chemotaxis has occurred. Analysis at each chemokine concentration was performed in triplicate and the error bars represent the SEM. This experiment was performed once only.

6.4 Adenoviral Infection of EL4 Cells

Despite the low level of chemotaxis induced in the EL4 cells, the decision was made to examine redirection of the adenovirus through CCR7 in EL4 cells and subsequent infection. However, before proceeding with this, RT-PCR was performed looking at the expression of the CAR receptor and α_v -integrins in EL4 cells. This was done in order to assess the likelihood of significant background infection in these cells as adenovirus enters cells predominantly through binding with CAR although it can enter cells using α_v -integrins alone (although at a much lower rate. Figure 6.5 clearly demonstrates the absence of detectable RNA for these proteins both CAR and α_v -integrins. The question arises, looking at the figure, as to whether or not the primers for CAR and α_v -integrins were working, however repeat RT-PCR showed consistent results and, as will be demonstrated later in this chapter, the same primers confirmed the presence of these transcripts in a range of mouse tissues. The lack of CAR and α_v -integrin expression provided further confirmation that EL4 cells were an ideal cell line to further optimise successful chemokine dependent redirection of adenoviral tropism through CCR7 as background infection rates were likely to be low.

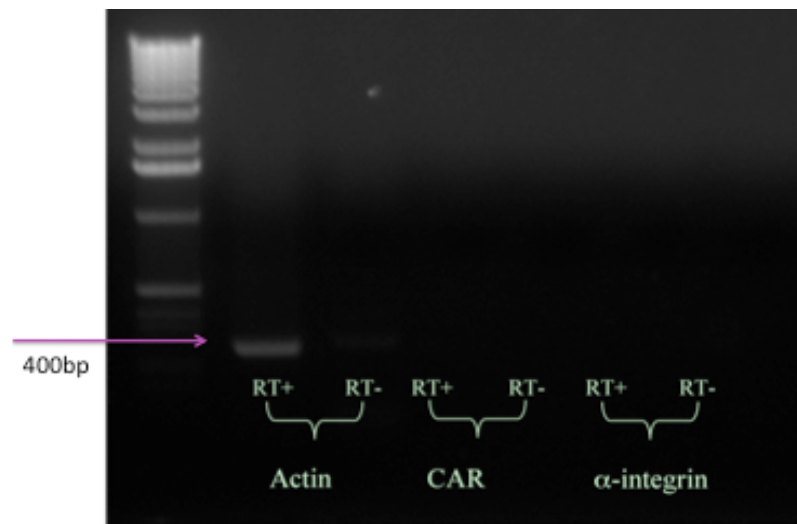


Figure 6.5: CAR and α_v -integrin expression in EL4 cells. RNA was prepared from EL4 cells these were DNAase treated and cDNA was prepared using +/- reverse transcriptase. Primers for actin, CAR and α_v -integrin and were used to amplify cDNA using the PCR programme in 2.2.4.3. PCR products were then run on a 1% agarose gel containing ethidium bromide.

6.4.1 Initial Infection Experiments with Chemically shrouded Adenovirus.

The EL4 cells were incubated with CCL19 shrouded adenovirus as previously described with Raji cells in section 5.6. The cells were incubated for 48 hours and then assessed for the rate of infection using β -galactosidase detection. Unfortunately, no infection was detected in any of the EL4 cells despite repeated attempts with longer incubation times and with an increased MOI of 2 ifu/cell. At this point it was thought that this could be due to one of three reasons. Firstly, if the adenovirus was getting into the cells, was there a problem with the transduced expression of LacZ? There has been some suggestion that the CMV promoter is less efficient in malignant cell lines and haematopoietic cells and that an alternative such as elongation factor 1 α (EF1 α) may improve the efficiency of gene expression [356](Teschendorf, 2002). Secondly, although mCCR7 expression had been detected, was the surface expression too low to enable sufficient uptake of the virus and to enable LacZ expression? However, it should be borne in mind that only one viral particle is needed to enter the cell and lead to transfection, and here a MOI of 2 ifu/cell was used in EL4 infection experiments. Finally, was there some other mechanism by which transfection was being affected? All of these issues were investigated.

6.4.2 Alternate Methods of Detecting Adenoviral Infection

6.4.2.1 Determination of the Optimum Anti-hexon Antibody Concentration

To determine whether or not the cells were infected by the adenovirus, an alternative method of infection was sought. In this case adenoviral antibodies were employed. An anti-hexon antibody was chosen that could be used in flow cytometry analysis. However, before this antibody could be used it was necessary to optimise its use with a cell line which is readily infected by the virus. For this purpose the HEK293 cell line was used. The cells were infected with adenovirus as previously described in method section 2.2.6.4 using different quantities of adenovirus so that a variety of adenoviral infection rates could be assessed using this method. Following 48 hours incubation the HEK293 cells were counted and 2.5×10^5 cells were transferred to a microcentrifuge tube. These cells were incubated with anti-hexon antibody at different concentrations followed by incubation with a secondary antibody at the same concentration for each sample (the secondary antibody used here was a rat anti-mouse IgG conjugated to PE at a concentration of 1:250). Following this, single-colour flow cytometry was performed and the results assessed.

These results are shown in figure 6.6 below. They demonstrate that the optimum concentration of the anti-hexon antibody was 1:100 when analysed with cells incubated with an initial viral titre of 3.5×10^7 ifu/ml, although detection of adenoviral infection at lower starting viral titres was less clear in discriminating between anti-hexon-body concentrations. From this point on an anti-hexon antibody concentration of 1:100 was used in experiments.

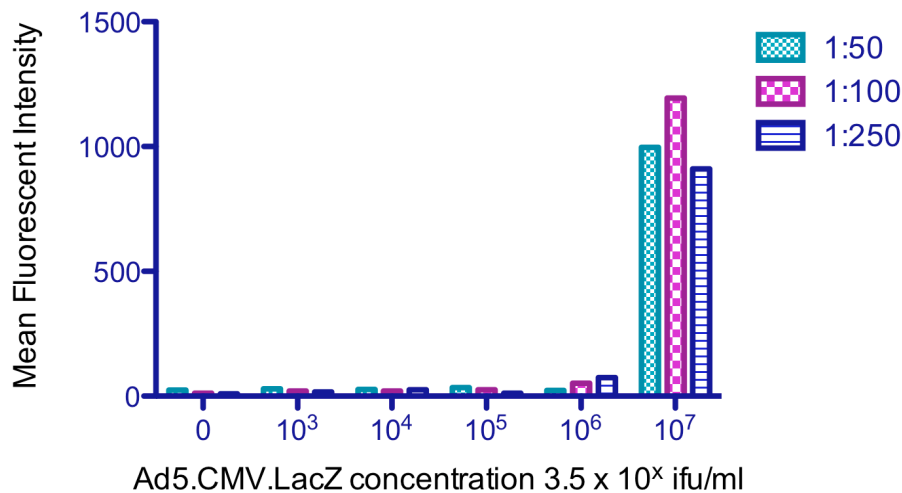


Figure 6.6: Determination of anti-hexon antibody concentrations for use in adenoviral experiments. HEK293 cells were infected with different quantities of Ad5.CMV.LacZ as shown above and incubated for 48 hours. Each sample was repeated in triplicate. The cells were then washed and incubated with anti-hexon antibody at different concentrations, following which they were incubated with a secondary antibody conjugated with PE. The cells were then assessed by single colour flow cytometry to determine the optimum anti-hexon antibody concentration. In this case this was an antibody concentration of 1:100 was identified as giving the best results, which was used for subsequent infection experiments.

6.4.4.2 Detection of Adenoviral Infection in EL4 Cells using Flow Cytometry

The EL4 cells were incubated with the CCR19 shrouded adenovirus as previously described. Following incubation, the cells were incubated with the anti-hexon antibody and secondary antibody-PE and analysed by flow cytometry. Again, no discernible infection was noted and therefore further investigation as to the cause of this was initiated

6.5 Effect of Increasing mCCR7 Expression on the rate of Infection

As no infection was detected using the flow cytometry method, it was felt that the problem was potentially due to insufficient expression of mCCR7 on the cell surface. Therefore next step was to attempt to increase mCCR7 expression in the EL4 cells.

6.5.1 Development of pEF6.mCCR7 and Transfection into EL4 Cells

In order to increase mCCR7 expression vector containing the complete gene sequence for mCCR7 was created using the methods described in sections 2.2.4.3.1 and 2.2.4.8. The primers used are shown in section 2.1.7.2. In this case a vector incorporating the EF1 α promoter, pEF6/V5-His TOPO $\text{\textcircled{R}}$ TA, was employed. This was because of a previous suggestion that the CMV promoter was less efficient in malignant cells than this promoter. The vector used for transfection in the EL4 cells, pEF6.mCCR7 is shown in figure 6.7.

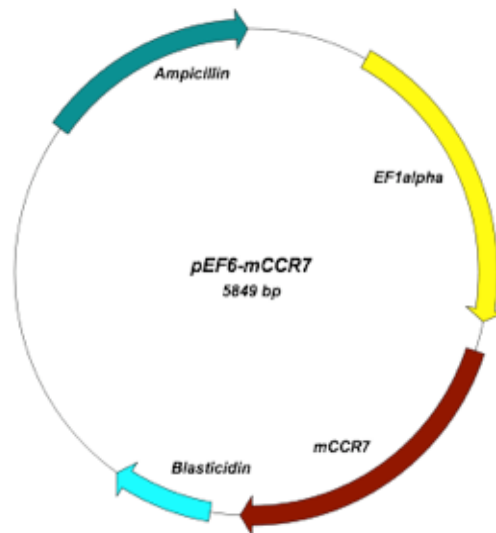


Figure 6.7: Vector map of pEF6.mCCR7. This plasmid was used to transfect EL4 cells in order to increase surface expression of mCCR7.

To transfect the EL4 cells, the Amaxa electroporation system was used as described in 2.2.2.4.3 using pEF6.mCCR7. Following transfection, cells were selected depending on their resistance to blasticidin. These cells were then subcloned and analysed for mCCR7 expression using single colour flow cytometry following incubation with anti-mCCR7-FITC antibody. The results of this analysis are shown in figure 6.8. The plots in 6.8 compare mCCR7 surface expression on EL4 cells that have not been transfected with three different pools of mCCR7 transfected EL4 cells termed EL4.mCCR7.1, EL4.mCCR7.2 and EL4.mCCR7.3. These show that there has been a greater shift along the FL1-H gate in

all three pools, indicating higher expression of mCCR7 in these compared to the EL4 cells. It is also worth noting that in each population of cells that there were two peaks demonstrating low and high mCCR7 expressing subpopulations. Once it had been confirmed that there were populations of cells demonstrating increased mCCR7 expression analysis was carried out to assess CCR7 function in these cells.

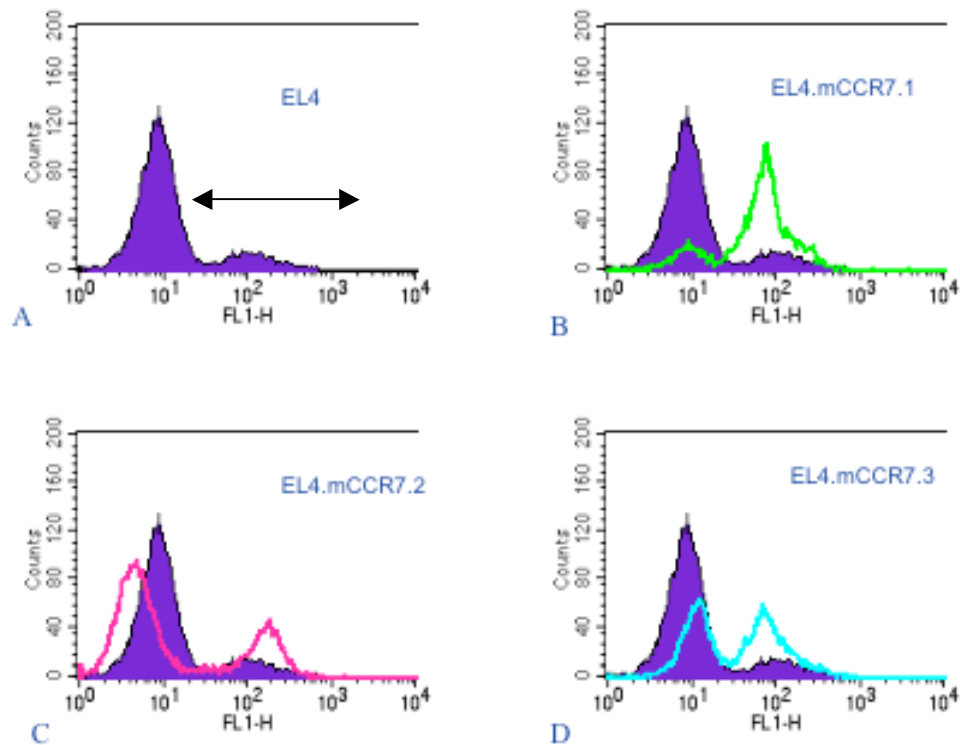


Figure 6.8: mCCR7 expression in pools of EL4.mCCR7 cells. a) Represents EL4 cells that have not been transfected and this curve is used as a comparison in graphs b), c) and d) representing 3 pools of the mCCR7 transfected EL4 cells. EL4 cells were transfected with pEF6.mCCR7 by electroporation as detailed in section 2.2.2.4.3. Following selection in blasticidin, pools were selected for analysis of mCCR7 expression. The cells were incubated with anti-mCCR7-FITC. Cells were then analysed using single-colour flow cytometry. All positive cells as indicated by the marker in figure a) were used to calculate mean fluorescent intensity.

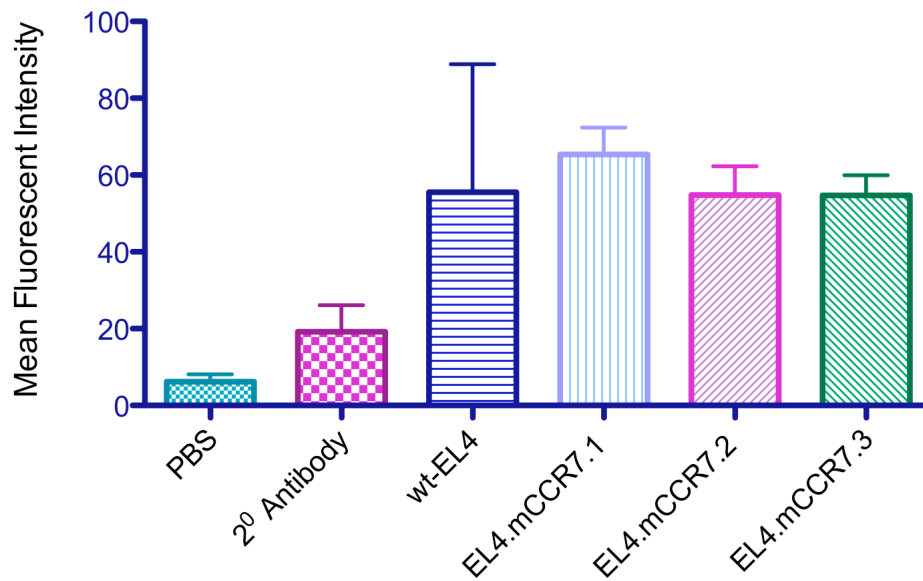


Figure 6.9: Expression of mCCR7 in pools of EL4.mCCR7 cells. EL4 cells were transfected with pEF6.mCCR7 by electroporation as detailed in section 2.2.2.4.3. Following selection in blasticidin, pools were selected for analysis of mCCR7 expression. The cells were incubated with anti-mCCR7-FITC antibody. Cells were then analysed using single-colour flow cytometry. This experiment was repeated twice, with triplicate samples.

6.5.2 Functional Analysis of EL4 Cells with Increased mCCR7 Expression

6.5.2.1 Biotinylated-CCL19 Uptake in EL4.mCCR7 Cells

As before, in addition to confirming mCCR7 expression in the EL4.mCCR7 pools, it was important to establish that the CCR7 was functional. In the first instance the three clones were studied for biotin-CCL19 internalisation in comparison with EL4 cells. Untransfected EL4 cells were used as a control for this analysis in addition to cells that had not been exposed to biotin-CCL19. The results of this study are shown in figures 6.10 and 6.11. Figure 6.10 demonstrates a higher degree of biotin-CCL19 in all three EL4.mCCR7 pools, as evidenced by a greater shift to the right along the FL2-H gate. Again dual populations are seen. Furthermore, figure 6.11 clearly demonstrates the increased CCL19 uptake in those cells with higher mCCR7 expression, with the highest mean MFI obtained from clone EL4.mCCR7.2 with an MFI of 2523.99 compared to that obtained in EL4 cells which was MFI-1480.59 and to a MFI of 6.71 in cells exposed to streptavidin-PE only.

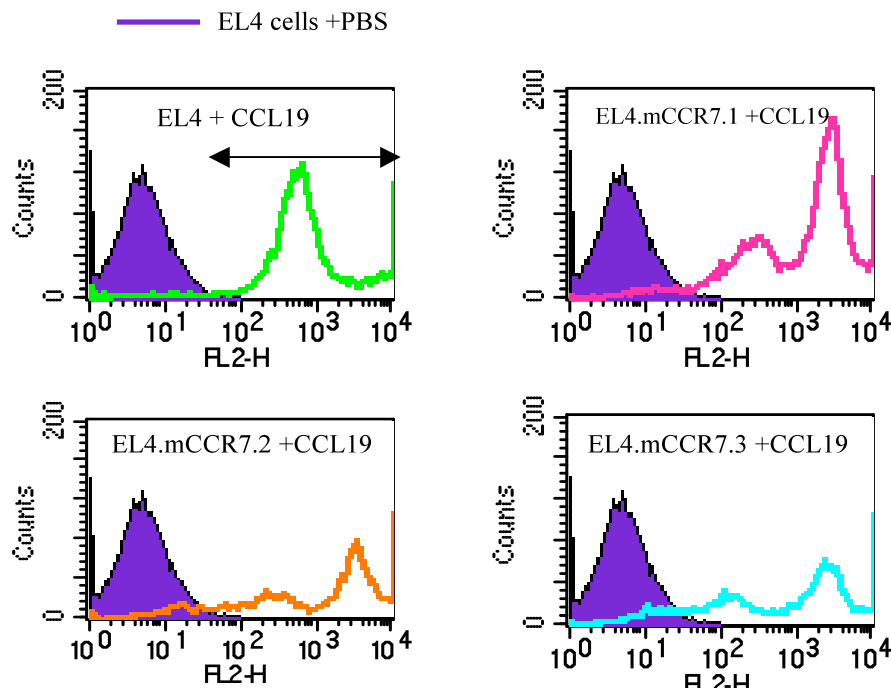


Figure 6.10: Biotin-CCL19 uptake in EL4.mCCR7 pools. Histogram plots demonstrating increased CCL19 uptake in the EL4.mCCR7 pools. The purple peaks represent EL4 cells with streptavidin-PE only, the green line represents untransfected EL4 cells, pink represents EL4.mCCR7.1 cells, orange represents EL4.mCCR7.2 cells and blue represents EL4.mCCR7.3 cells. Cells were incubated with biotin-CCL19 and streptavidin-PE or streptavidin-alone, for 1hr at 37°C. Following this biotin-CCL19 uptake by the cells was analysed using single-colour flow cytometry. All positive cells as indicated in figure a) were used to calculate the mean fluorescent intensity.

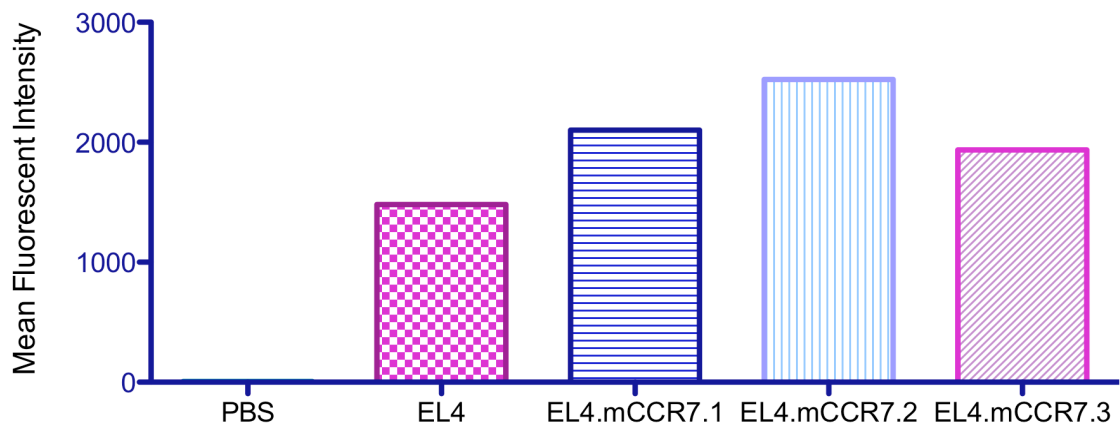


Figure 6.11: Uptake of biotin-CCL19 by EL4.mCCR7 cells. Cells were incubated with biotin-CCL19 and streptavidin-PE or streptavidin-alone, for 1hr at 37°C. Following this biotin-CCL19 uptake by the cells was analysed using single-colour flow cytometry. The graph shows the MFI obtained with each cell population following biotin-CCL19 uptake. Note the highest degree of uptake was seen in EL4.mCCR7.2 cells. This experiment was only performed once due to loss of the transfected cell populations.

6.5.2.2 Migration of EL4 and EL4.mCCR7 cells towards CCL19

Following analysis of the EL4.mCCR7 pools, pool EL4.mCCR7.2 was chosen for future experiments due to the highest level of biotin-CCL19 uptake and will now be referred to as EL4.mCCR7 cells. The same method using the QCMTM chemotaxis assay as described with the Raji cells in 4.3.2.2 was used to assess the ability of the EL4 and EL4.mCCR7 cells to migrate in response to CCL19. This was chosen as the number of EL4.mCCR7 cells available was too low for use in the Transwell® assay. However, before commencing with the assay a calibration curve was developed using known cell numbers as described with Raji cells in 4.3.2.2. The results of this are shown in figure 6.12, and clearly demonstrate a linear relationship between cell number and RFU. Once this was established, a chemotaxis assay was performed using EL4 and EL4.mCCR7 cells at CCL19 concentrations of 0, 0.1, 1.0, 10 and 100nM. The RFU levels obtained on analysis were then used to calculate cell numbers and subsequently the migration index. The results of this are shown in figure 6.13. This confirms that EL4 cells do migrate in response to CCL19 exposure and, as would be expected, chemotaxis is more marked in the EL4.mCCR7 cells, although the difference in the migration indices were not significant between the two EL4 populations. These results again demonstrate that increased mCCR7 expression by transfection, does correlate with enhanced function in these cells.

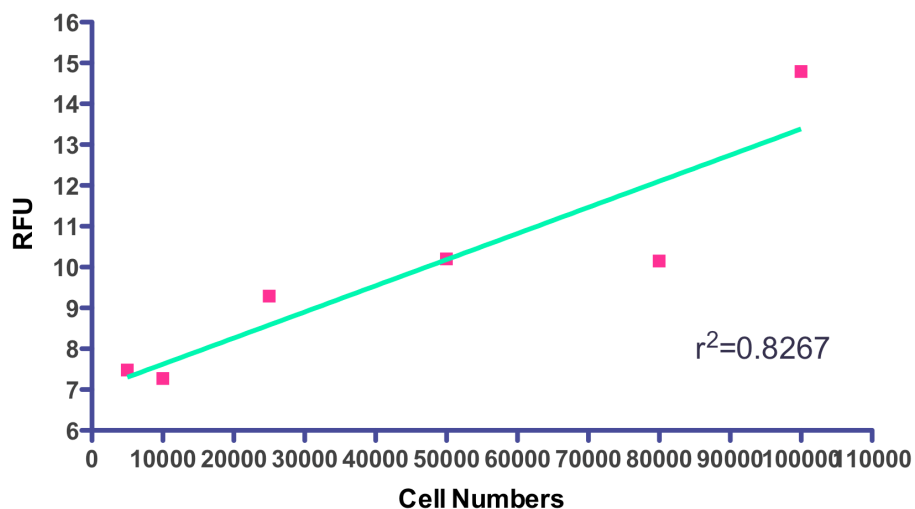


Figure 6.12: QCMTM Calibration curve using EL4 cells. Known quantities of EL4 cells were added to wells of a 96 well luminometry plate. Lysis buffer/dye solution from the QCMTM kit was added to the cells and the plate incubated for 15 minutes at room temperature. The plate was then read using a 480/520nm filter set and RFU recorded for each well. Each point on the calibration curve represents the mean RFU obtained from 3 wells containing the same number of cells, indicating a good correlation between RFU and cell number.

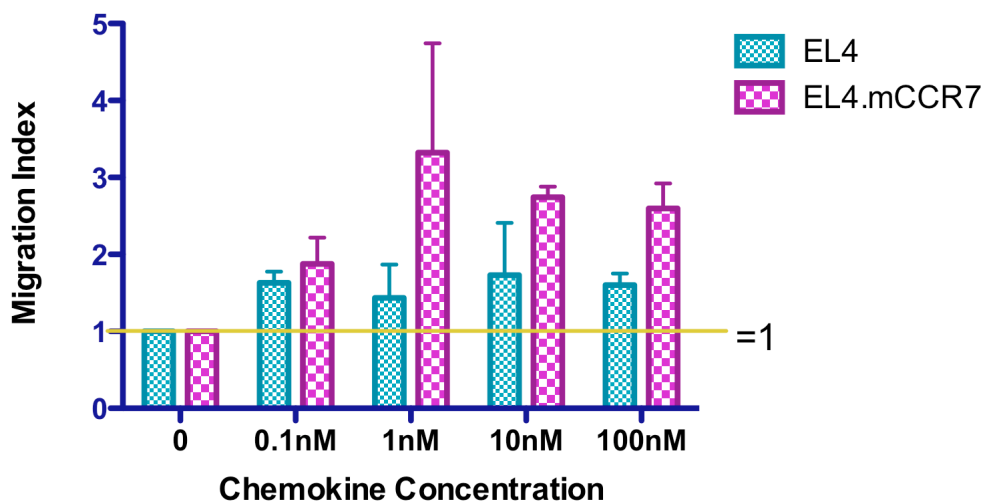
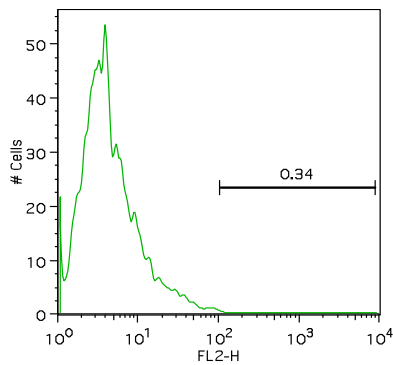


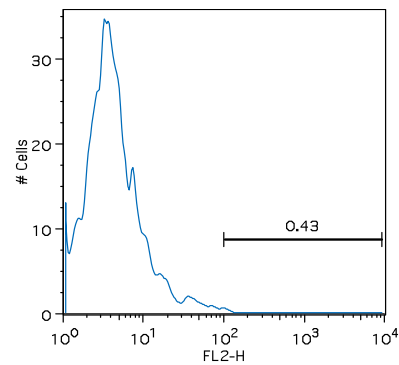
Figure 6.13: Migration of EL4 and EL4.mCCR7 cells towards CCL19. Chemotaxis buffer containing different concentrations of CCL19 was added to a 96 well feeder plate. EL4 cells were then added to each insert. Following incubation the cells were incubated with lysis buffer/ dye solution for 15 minutes before transferring to a 96 well luminometry plate for reading at 480/520nm. A migration index of >1 indicates that migration has occurred. This experiment was performed once with analysis at each chemokine concentration was performed in triplicate. The y axis figures relate to the mean value with the error bars representing the SEM.

6.5.3 Adenoviral Infection in EL4 and EL4.mCCR7 Cells

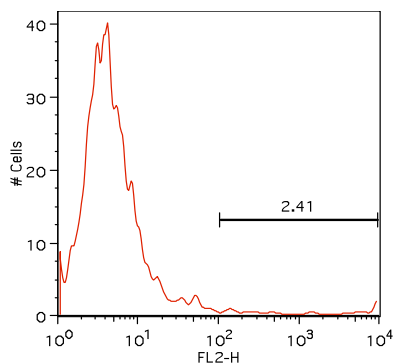
Adenoviral infections were again set up in EL4 cells as well as EL4.mCCR7 cells at a MOI of 2 ifu/cell. Following incubation with the CCL19 shrouded virus, the cells were incubated with the anti-hexon antibody and analysed using single colour flow cytometry. Whilst, the results were not significantly different, they did show infection of a small population of EL4.mCCR7 cells (2.41%). A smaller population of EL4 cells (0.43%) were positive by flow cytometry, however this was equivalent to those cells with no viral exposure (0.34%) and was therefore considered to be due to background artifact. The results are represented in the histograms in figure 6.14.



a) EL4 +PBS



b) EL4 + CCL19 shrouded Ad5.CMV.LacZ



c) EL4.mCCR7 + CCL19 shrouded Ad5.CMV.LacZ.

Figure 6.14: Detection of Ad5.CMV.LacZ infection in EL4 cells using anti-hexon antibody.

EL4 cells were incubated for 48 hours with CCL19 shrouded Ad5.CMV.LacZ at a MOI of 2 ifu/cell. The cells were then washed and incubated with anti-hexon antibody followed by incubation with a secondary antibody-PE conjugate. Single-colour flow cytometry was then used to determine if any infection of EL4 cells had occurred. In EL4.mCCR7 cells a small population (2.41%) of cells were positive by flow cytometry indicated a small population of infected cells.

6.6 Investigating Other Causes of Sub-optimal Infection of EL4 Cells

One other possible reason for the sub-optimal infection of EL4 cells may relate to the expression of another chemokine receptor for which CCL19 is a ligand. To date, the only other receptor identified as binding CCL19 is the atypical chemokine receptor CCX-CKR [357]. Work within the chemokine research group had shown that CCX-CKR binds, and leads to the internalisation of, CCL19. However, it did not lead to any detectable downstream signalling, and it appears that the ligand is passed into lysosomes where it is destroyed [127]. The questions here were firstly, do EL4 cells express CCX-CKR? Secondly, if it is present, does the expression of CCX-CKR inhibit the ability of adenovirus to infect the cell in some way? The following experiments will outline the steps taken to investigate this possibility.

6.6.1 Expression of CCX-CKR in EL4 Cells

Unfortunately there are no commercially available antibodies suitable for the detection of CCX-CKR either by Western blot or flow cytometry analysis. Therefore, RT-PCR was performed to see if CCX-CKR was expressed at the RNA level. Primers for murine CCX-CKR had already been developed within the laboratory and were used. The results are shown in figure 6.15 and show that CCX-CKR is strongly expressed at the RNA level. Functionally, biotinylated CCL19 uptake had been previously used, however because EL4 cells also express CCR7, it was difficult to determine which receptor contributed most to the CCL19 uptake at this stage.

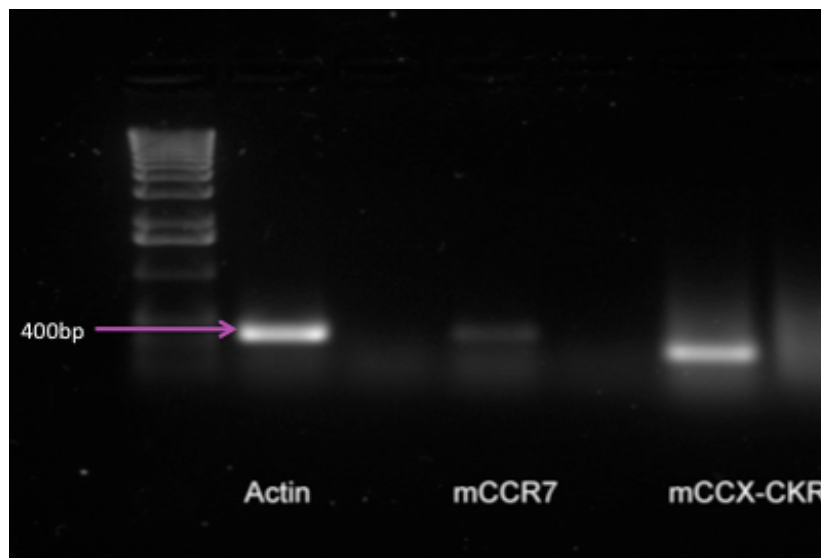


Figure 6.15: Expression of mCCR7 and mCCX-CKR in EL4 cells by RT-PCR. Lanes 2, 4 and 6 represent the RT- controls. RNA was extracted from EL4 cells, DNAase treated and cDNA synthesised +/- reverse transcriptase. Primers for actin, mCCR7 and mCCX-CKR were then added to the cDNA and the PCR programme in 2.2.4.3.1 was used. PCR products were run on a 1% agarose gel containing ethidium bromide.

6.6.2 Development of CCX-CKR Expressing Cell Lines

One way of determining whether or not CCX-CKR limited the ability of the adenovirus to infect cells was to develop cell lines expressing this receptor, but which were negative for CCR7. Within the laboratory, vectors for CCX-CKR as well as HEK293 cells transfected with CCX-CKR were available. However, in view of the high degree of background infection experienced with HEK293 cells it was thought prudent to also develop a cell line expressing CCX-CKR which was negative for the CAR receptor. As before, CHO cells were selected for this purpose. As a comparison HEK293 cells and CHO cells transfected

with CCR7 were used as positive controls. CHO cells were transfected with either pcDNA3.1.hCCR7 (detailed in section 4.2) or pcDNA3.1.hCCX-CKR.HA (developed previously in the laboratory) as described in method section 2.2.2.4.2. The transfected cells were then analysed for expression of CCR7 or CCX-CKR using anti-CCR7 antibodies in the case of the former, and biotinylated CCL19 uptake studies in the case of the latter. These analyses confirmed the presence of both of these receptors in the cell lines and can be seen in figure 6.16. Clone CHO.hCCX-CKR.1 had the highest degree of CCL19-binding as so was chosen for future experiments. These cells are referred to as CHO.hCCX-CKR cells for the remainder of the thesis. The second graph shown in figure 6.16 confirms successful transfection of the CHO cells with hCCR7, with the highest level of expression found in the first clone tested. This clone will be referred to as CHO.hCCR7 for the remainder of the thesis.

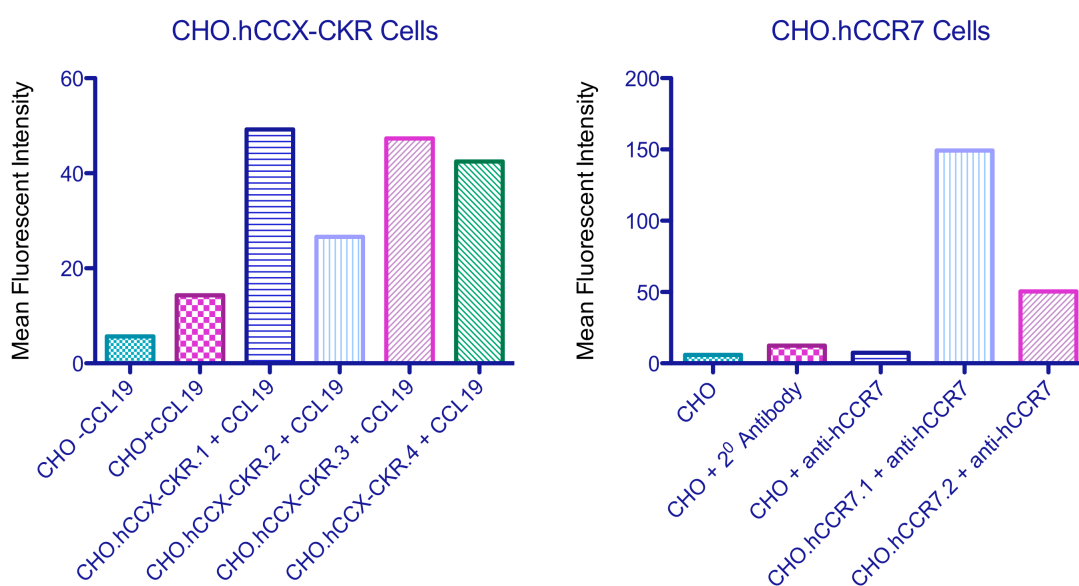


Figure 6.16: Analysis of hCCX-CKR and hCCR7 expression in transfected CHO cells. CHO cells were transfected with either pcDNA3.1.hCCR7 or pcDNA3.1.hCCX-CKR.HA. Following incubation in selective media with G418 pools of cells were assessed for a) expression of hCCR7 by incubation with anti-hCCR7 and a PE-conjugated secondary antibody, or b) expression of CCX-CKR by incubation with biotin-CCL19/streptavidin-PE; followed by analysis using single-colour flow cytometry. The left hand graph shows increased biotin-CCL19 binding by the 4 pools of CHO cell lines transfected with pcDNA3.1.hCCX-CKR.HA (CHO.hCCX-CKR.1-4). The right hand graph demonstrates surface hCCR7 on the CHO cells transfected with pcDNA3.1.hCCR7 (CHO.hCCR7.1 and 2). This analysis was performed once.

6.6.3 Infection with Adenovirus shrouded with CCL19 in Cells Expressing CCX-CKR or CCR7

Infection experiments with adenovirus shrouded with CCL19 were set up in HEK293 cells and in CHO cells expressing either CCR7 or CCX-CKR. Following incubation, the cells were analysed for the presence of adenoviral infection using the anti-hexon antibody, and single colour flow cytometry and by staining for β -galactosidase. The results are shown in figures 6.17 to 6.19. The histograms in figure 6.18 clearly demonstrate that adenovirus infection is occurring at a greater rate in both the HEK.hCCR7 and HEK.hCCX-CKR cells with a greater shift along the FL2-H axis when compared to HEK293 cells. This was confirmed by assessment of LacZ expression, which was performed to confirm the flow cytometry findings. The images in figure 6.17 and the histogram in figure 6.19 demonstrates the same results with CHO.CCX-CKR and CHO.hCCR7 cells as with HEK cells, albeit at a lower level of infection. Surprisingly, it appeared that the cells expressing CCX-CKR receptors had a higher degree of adenoviral infection when compared to cells expressing CCR7. However, it is not possible to draw the conclusion that CCX-CKR facilitates higher rates of infection when compared to CCR7, as the number of receptors per cell were not analysed prior to the experiments. Yet, what is apparent is that CCX-CKR does not appear to inhibit the ability of the adenovirus to infect cells nor does it limit the expression of any reporter genes. Thus further investigation into the cause of the low degree of adenoviral infection in the EL4 cells was required.

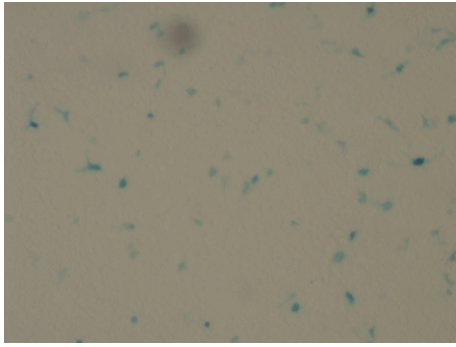
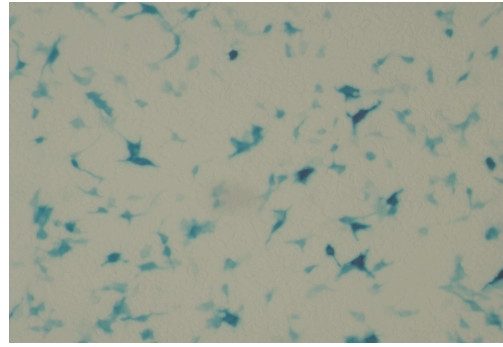
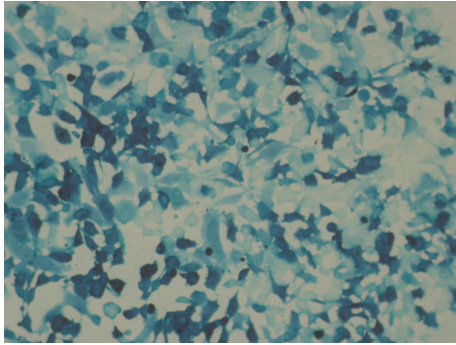
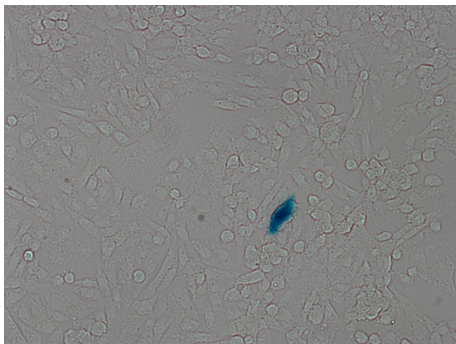
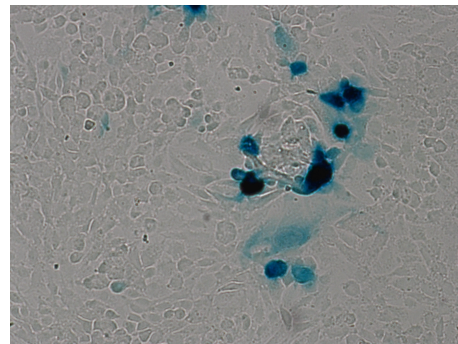
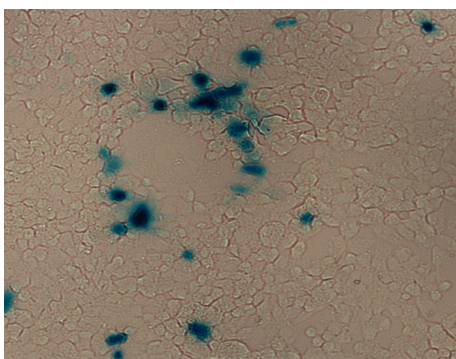
**a) HEK293****b) HEK.hCCR7****c) HEK.CCX-CKR****d) CHO****e) CHO.hCCR7****f) CHO.CCX-CKR**

Figure 6.17: Infection of CHO and HEK293 cells expressing hCCR7 or hCCX-CKR. HEK293, HEK.hCCR7, HEK.hCCX-CKR, CHO, CHO.hCCR7 and CHO.hCCX-CKR cells were infected with CCL19 shrouded Ad5.CMV.LacZ and incubated for 48 hours. Following incubation cells were assessed for infection by staining for β -galactosidase. These micrographs were taken at x20 objective.

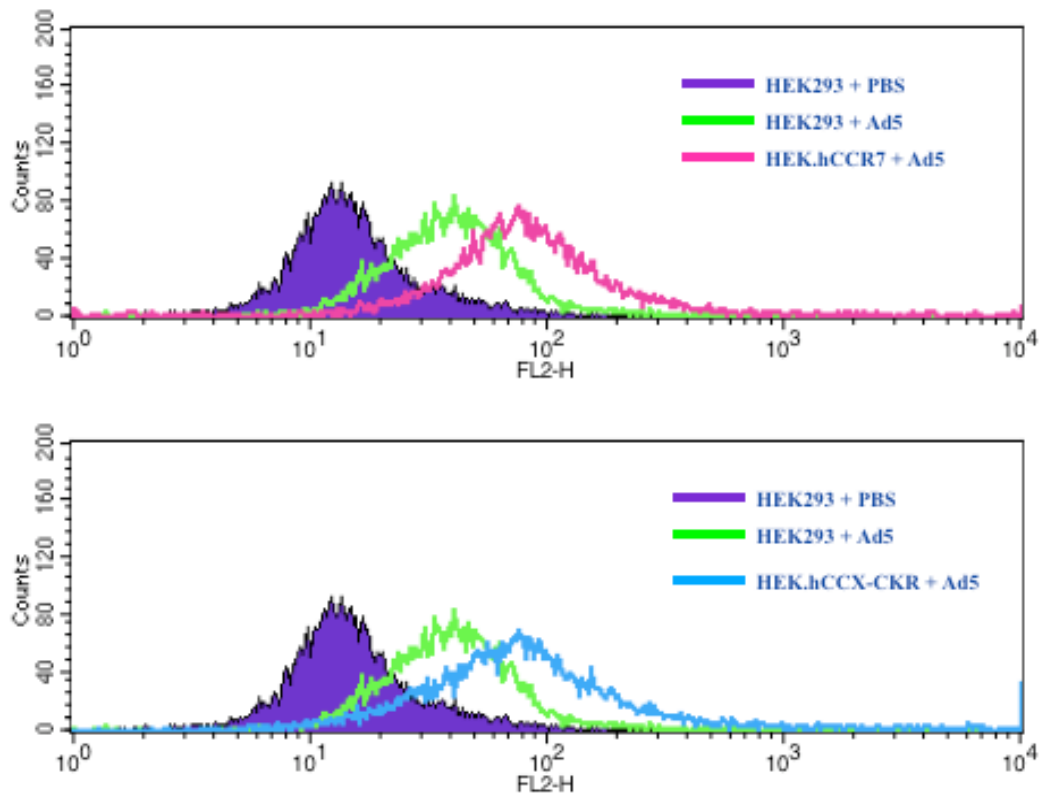


Figure 6.18: Adenoviral infection of HEK.hCCR7 and HEK.hCCX-CKR cells. HEK293, HEK.hCCR7 and HEK.hCCX-CKR cells were incubated with CCL19 shrouded Ad5.CMV.LacZ or PBS alone for 48 hours. Following incubation the cells were washed and then incubated with anti-hexon antibody followed by incubation with a PE-conjugated secondary antibody. Cells were then assessed for Ad5 infection using single-colour flow cytometry. The histogram plots demonstrate increased detection of Ad5 hexons in HEK.hCCR7 and HEK.hCCX-CKR cells compared to HEK293 cells indicating higher rates of infection.

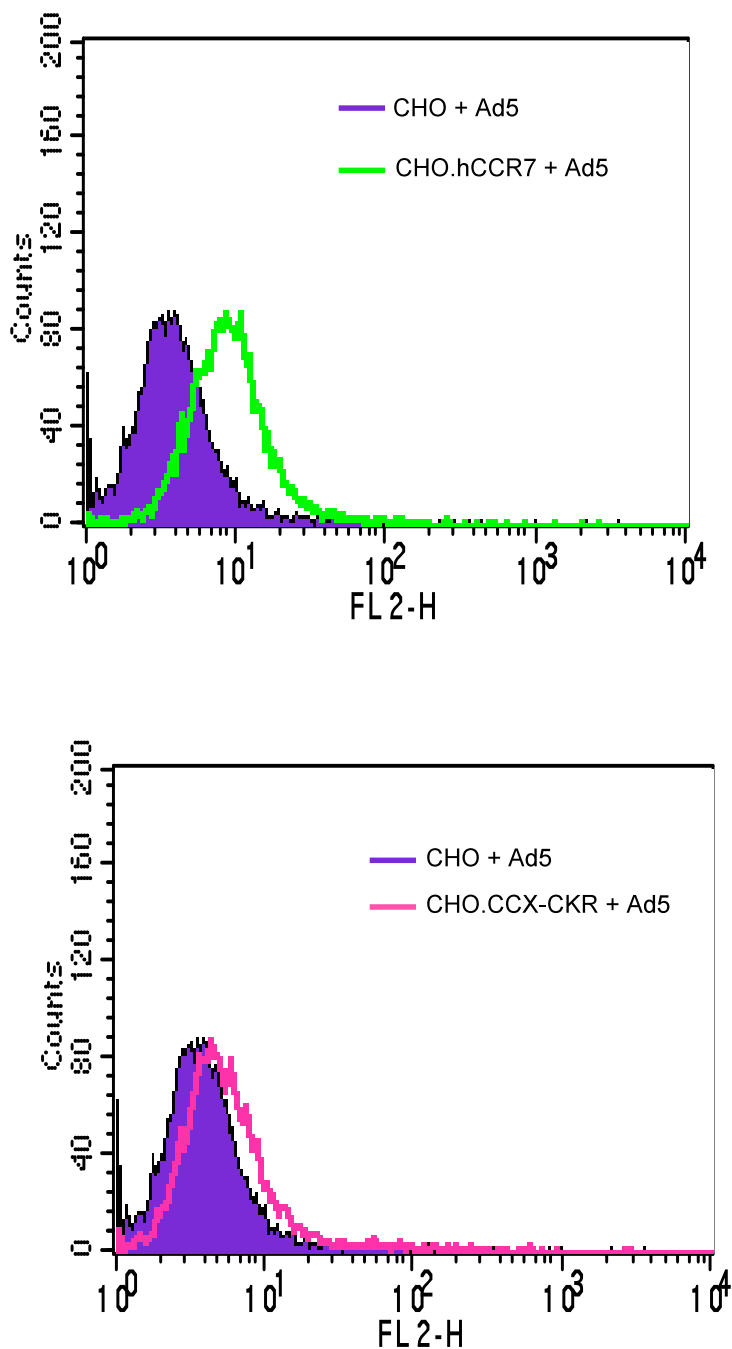


Figure 6.19: Adenoviral infection of CHO.hCCR7 and CHO.hCCX-CKR cells. CHO, CHO.hCCR7 and CHO.hCCX-CKR cells were infected with CCL19 shrouded Ad5.CMV.LacZ and incubated for 48 hours. Following incubation cells were washed and incubated with anti-hexon antibody followed by incubation with a PE-conjugated secondary antibody. Cells were assessed for Ad5 infection using single-colour flow cytometry. The histogram plots demonstrate detection of Ad5 hexons in CHO.hCCR7 and CHO.hCCX-CKR but not in CHO cells indicating Ad5 infection occurred in both hCCR7⁺ and hCCX-CKR⁺ cells.

6.7 Optimising the Infection of EL4 Cells Further

At this point, there was concern that it would not be possible to use the EL4 cells as an adenoviral transducible lymphoma mouse model. However, before searching for an alternative cell line a literature search was performed to investigate whether or not these cells had been successfully infected with adenovirus in the past. Leon et al had used EL4 cells as a CAR negative cell line to assess the efficiency of transfection with the CAR receptor, and analysed the ability of the adenovirus to infect the EL4 cells through this transfected receptor [127]. The vector used for transfection of EL4 cells with the CAR receptor also contained the reporter gene for GFP. A variety of different promoters including CMV were used as well as different MOIs. They demonstrated that EL4 cells were able to be successfully infected with the adenovirus and express GFP once CAR expression had been successfully introduced to the cell. However significant results were only obtained once the MOI reached 200 ifu/cell. Up until this point, the infection experiments in this project had been using a MOI of 2 ifu per cell. It was therefore felt worthwhile to repeat the experiments using the higher MOI.

6.7.1 Infection of EL4 cells with a higher MOI

EL4 cells were infected with adenovirus shrouded in CCL19 as previously described, but this time a MOI of 200 ifu per cell was used compared to an MOI of 0.132 or 2 ifu/ml in previous experiments described in this thesis. As a higher MOI was used in these experiments it was decided to attempt infection of untransfected EL4 cells first. The adenovirus infection was again assessed using single colour flow cytometry following incubation with the anti-hexon antibody. Remarkably, increasing the MOI lead to detectable infection in 14.84% of the EL4 cells exposed to adenovirus shrouded with CCL19 and these results are shown in figure 6.20. Although there was a trend towards increased detection of anti-hexon antibodies in the EL4 cells exposed to CCL19 shrouded adenovirus, this did not reach statistical significance, yet showed promise for future work. Work with EL4 cells would therefore continue as they maintained their potential for use in a lymphoma mouse model.

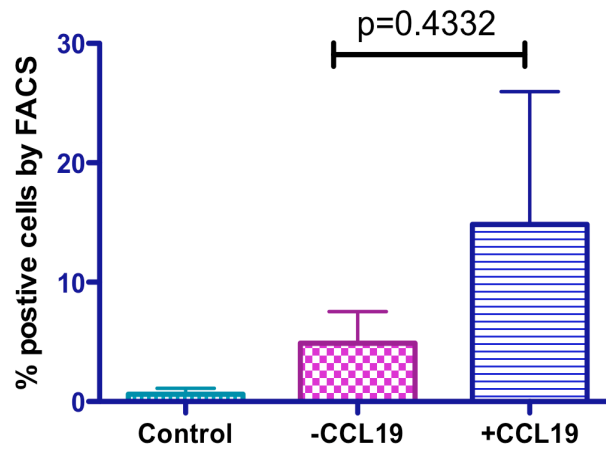


Figure 6.20: Infection of EL4 cells with CCL19 shrouded Ad5.CMV.LacZ at MOI of 200. EL4 cells were incubated with Ad5.CMV.LacZ with or without CCL19 shrouding for 48 hours. The cells were then washed and incubated with anti-hexon antibody followed by incubation with a PE-conjugated secondary antibody. Infection of EL4 cells was then assessed using single-colour flow cytometry. Each sample was run in triplicate and the error bars represent the SEM.

6.7.2 Development of an Adenoviral Vector using EF1- α as a Promoter

As previously discussed, one other potential reason for the inability to detect Lac Z in EL4 cells is the low efficiency of the CMV promoter to induce gene expression in haematopoietic cells. The EF1- α promoter is reported to increase the efficiency of transcription of reporter genes in haematopoietic cells [358], and as such the use of this promoter in subsequent infection experiments may improve results. In addition, it has been shown that infection of EL4 cells with adenoviral vectors containing the GFP reporter gene can be successfully detected by examination for expression of GFP by flow cytometry.

Therefore the next aim was to develop an adenoviral vector containing EF1- α as the promoter and GFP as the reporter gene. In order to do this, the AdEasy adenoviral vector system was employed again. The first step in this was to develop a pShuttle vector containing EF1- α instead of the CMV promoter. A pShuttle vector was obtained from Stratagene, which contained IRES.GFP and the CMV promoter. No vector was commercially available containing the EF-1 α promoter, and therefore it was necessary to replace the CMV promoter with the EF-1 α promoter using subcloning techniques. Suitable restriction enzyme sites were searched for but subsequently it was necessary to introduce a novel restriction enzyme site into the pShuttle vector in order to facilitate the subcloning strategy. Two restriction enzyme sites, *KpnI* and *NruI*, were identified in the pEF6/V5-His TOPO®TA, obtained from Invitrogen, enabling a DNA fragment incorporating the gene sequence for EF1 α to be obtained following digestion with these two enzymes. A *KpnI* restriction enzyme site was identified in the pShuttle vector at an appropriate site after the CMV promoter sequence however an *NruI* sequence was not identified at any point in the pShuttle vector. For this reason, site directed mutagenesis was used to introduce an *NruI* site upstream of the CMV promoter. The method for this is described in section 2.2.4.11 and an *NruI* site was successfully introduced into the correct position. Following restriction enzyme digestion with *NruI* and *KpnI* of the pEF6/V5-His TOPO®TA, a product of 4.1KB was obtained containing the EF1 α sequence. This was then ligated into with the modified pShuttle vector now containing the *NruI* restriction enzyme site that had been digested with *NruI* and *KpnI* thereby removing the DNA containing the sequence for the CMV promoter. This produced the pShuttle vector shown in figure 6.21. The pShuttle vector was then utilised for homologous recombination using BJ5187 cells as previously described. Homologous recombination was successful and the vector pAdeasy.EF6.IRES.GFP, was created. The next step would have been to transfect this

vector into HEK.293 cells in order to produce viral particles, however time restrictions prevented this.

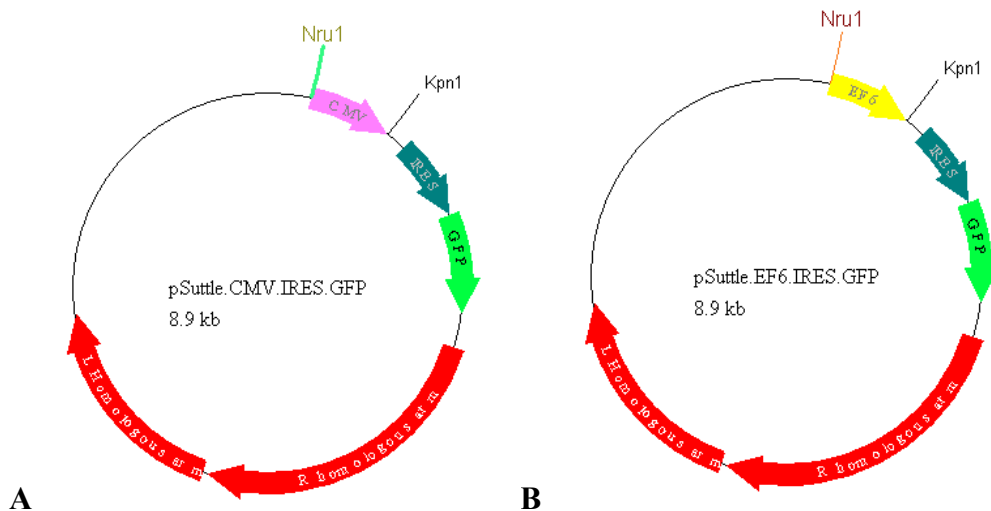


Figure 6.21: Vector maps of pShuttle.CMV.IRES.GFP and pShuttle.EF6.IRES.GFP. The first vector was obtained from Stratagene and an *Nru1* site was introduced as indicated, using site directed mutagenesis. This allowed for replacement of the CMV promoter with the EF6 (EF-1 α) promoter from the pEF6/V5-His TOPO@TA vector using subcloning techniques and the *Nru1* and *Kpn1* restriction sites as indicated above, to create pShuttle.EF6.IRES.GFP.

6.8 Expression of CAR, α_v -integrin and CCX-CKR in Murine Tissues and Cells

Now that early experiments had demonstrated the possibility of redirecting adenoviral tropism through the chemokine receptors in EL4 cells, the next step was to assess the expression of the CAR receptor, α_v -integrin and CCX-CKR in a variety of murine tissues and leukocytes. Examination of CAR and α_v -integrins expression would provide information regarding the natural tropism of the adenovirus in tissues and cell populations within the mouse, therefore predicting where non-shrouded adenoviral particles were likely to be detected after infection and thus provide a comparison for those mice infected adenovirus shrouded with CCL19. Successful redirection of adenoviral tropism through CCX-CKR has been clearly demonstrated with resulting expression of the transfected reporter gene, LacZ. Thus knowing the distribution of CCX-CKR in mouse leukocytes and tissues, would enable prediction of the likely distribution of redirected adenovirus following infection with CCL19 shrouded virus and predict for potential toxicities using this virus to deliver cytolytic therapy.

It is already known that CCX-CKR is present in most tissues, although it is particularly strongly expressed in the heart, lung and brain [357], and this work was not repeated. CCR7 is expressed predominantly on naïve B and T cells, subsets of memory T cells and dendritic cells, however further analysis of CCX-CKR expression across a range of haematopoietic cells was required and the results of RT-PCR for CCX-CKR (using primers already developed in the laboratory) on haematopoietic cells is shown in figure 6.23. Analysis of CAR and α_v -integrin expression was performed using RT-PCR and the primers used in earlier in this chapter. The results of these studies are shown in figures 6.22. A summary of these findings is shown in table 6.1. Essentially they show that transcripts for CAR can be detected in RNA from the brain, heart, kidney, liver and lung and at a lower level in the spleen and thymus confirming the previously published findings as discussed in section 1.5. Alpha-integrin transcripts are present in all of these tissues too, with highest levels seen in the brain and kidney. With regards to expression in haematopoietic cells, CAR transcripts were detected in the bone marrow as a whole, but the only haematopoietic cells that were positive were Lin-Sca⁺ precursors. For α -integrin expression, again the bone marrow and Lin-Sca⁺ RNA contained transcripts for this, but in addition macrophages were also positive for α -integrin expression at the transcription level. The results of RT-PCR for CAR and α -integrin expression in these cells, again confirms the published findings demonstrating low or absent expression in haematopoietic cells.

There was limited expression of CCX-CKR in haematopoietic cells, with only lymphocytes from lymph nodes and mast cells expressing this receptor at the transcript level. These results, in addition to those published by Townsend et al (348), indicate that it may be difficult to determine successful redirection of adenoviral tropism following shrouding with CCL19. However subtle differences may be observed particularly on examination of lymph node tissue, which should not be infected by the un-shrouded virus.



Figure 6.22: Expression of CAR and α_v -integrin in murine tissues and leukocytes. RNA was extracted from a range of murine tissues and leukocytes as detailed above, followed by DNAase treatment. cDNA was synthesised using +/- reverse transcriptase. Primers for actin, CAR and α_v -integrin were then used as in 2.2.4.3. PCR products were run on a 1% agarose gel containing ethidium bromide. In each case the first PCR product is actin (as positive control and 400bp in size), the second product is α -integrin and the third CAR.

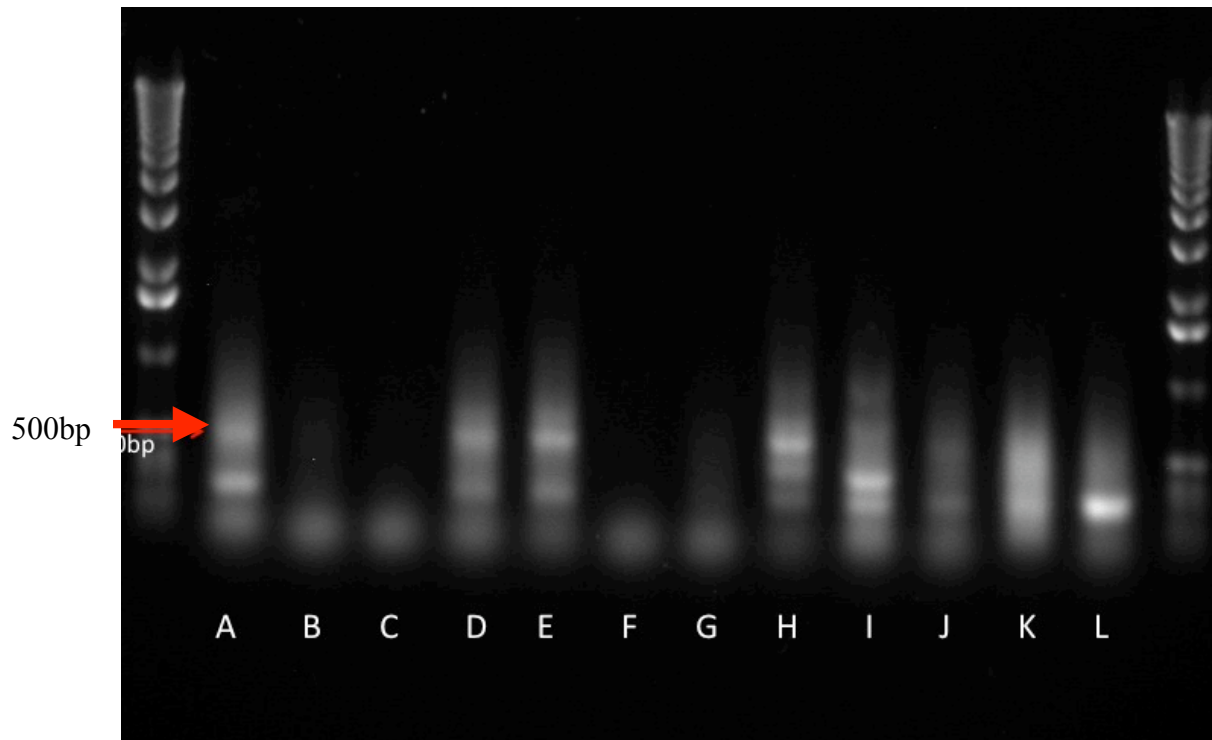


Figure 6.23: Expression of CCX-CKR in mouse tissues and leukocytes. RNA was extracted from a range of murine tissues and leukocytes as follows: A- bone marrow, B- lymph node, C- dendritic cells, D- Lymph node B-cells, E- Lymph node T-cells, F- Splenic B-cells, G- Splenic T-cells, H – mast cells, I- macrophages, J- polymorphonuclear cells, K-Lin-Sca⁺ precursors, L- Lin-Sca⁻ precursors. The RNA was DNAase treated and cDNA synthesised using +/- reverse transcriptase. Primers for mCCX-CKR were then used as in 2.2.4.3. PCR products were run on a 1% agarose gel containing ethidium bromide. There is no actin control shown in this figure as this analysis was performed at the same time as the RT-PCR shown in figure 6.22. The red arrow indicates the CCX-CKR transcript that is 500bp in size. The RNA samples and primers for murine CCX-CKR were obtained from Clive McKimmie.

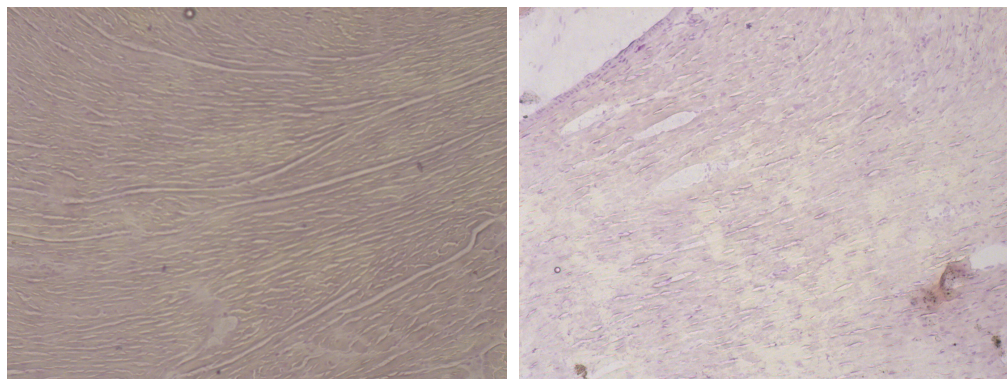
	<i>α-integrin</i>	<i>CAR</i>	<i>CCX-CKR</i>
<i>Tissue</i>			
<i>Bone Marrow</i>	-	+	+
<i>Brain</i>	+	+	++
<i>Heart</i>	-	+	++
<i>Kidney</i>	+	+	+
<i>Liver</i>	wk +	+	+
<i>Lung</i>	wk +	+	++
<i>Lymph Node</i>	-	-	-
<i>Spleen</i>	wk +	wk+	
<i>Thymus</i>	wk+	+	
<i>Haematopoietic cell</i>			
<i>Dendritic cells</i>	-	-	-
<i>Lymph Node B-cells</i>	-	-	+
<i>Lymph Node T-cells</i>	-	-	+
<i>Splenic B-cells</i>	-	-	-
<i>Splenic T-cells</i>	-	-	-
<i>Mast cells</i>	-	-	+
<i>Macrophages</i>	+	-	-
<i>Polymorphonuclear Cells</i>	-	-	-
<i>Lin⁻Sca⁺</i>	-	+	-
<i>Lin⁻Sca⁻</i>	-	-	-

Table 6.10: Expression of CAR, α_v -integrins and CCX-CKR in mouse tissues and leukocytes. RNA was extracted from a range of murine tissues and leukocytes as detailed above, followed by DNAase treatment. cDNA was synthesised using +/- reverse transcriptase. Primers for CAR, α_v -integrin and CCX-CKR were then used as in 2.2.4.3. PCR products were run on a 1% agarose gel containing ethidium bromide. Information on CCX-CKR expression in brain, heart, kidney, liver, lung, spleen and thymus was obtained from the paper by Townsen et al [349].

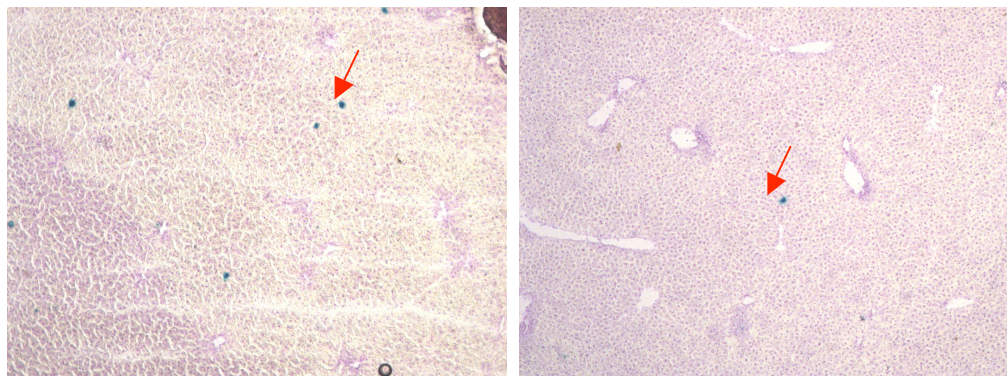
6.9 Infection of C57/BL6 Mice with Adenovirus Shrouded in CCL19

In order to assess whether the adenoviral tropism could be redirected through chemokine receptors *in-vivo*, infection of two groups of C57/BL6 mice were infected with Ad5.CMV.LacZ with or without shrouding with CCL19. Twelve female mice were selected at six weeks old and each mouse was injected with 6.6×10^8 viral particles in 100 μ L of PBS using via the tail vein. Six mice were injected with adenovirus that had undergone shrouding with CCL19 and the remaining six were injected with adenovirus that had not been 'shrouded' with CCL19. After 48 hours, three mice from each group were culled according to schedule 1 techniques. The remaining mice were culled at 96 hours. From each mouse the inguinal lymph nodes, spleen, liver, gut, lungs, kidney and heart were harvested. These were then placed in a cryopreservative and stored at -70°C . In order to assess the degree of infection in each of the mouse tissues a cryostat was used to create sections suitable for microscopy. This is described in methods section 2.2.7.4.1. Each sample was then assessed for infection using as indicated by expression of LacZ by staining for β -galactosidase.

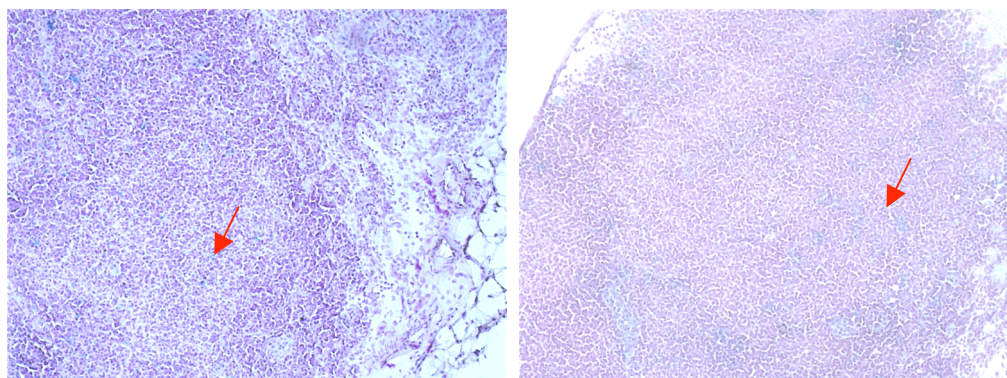
Initial analysis showed that there was possibly increased infection in the inguinal lymph nodes in those mice, which, had been exposed to the shrouded virus as opposed to those that had been exposed to the un-shrouded virus, suggesting *in-vivo* redirection of adenoviral tropism. However this did not appear to be consistent in all mice examined and differences in β -galactosidase staining were subtle. Yet, there did appear to be a reduced rate of infection in the liver of those mice exposed to the shrouded virus when compared to the mice exposed to the un-shrouded virus. No significant differences in infection were shown seen upon with analysis of the lungs, kidney, spleen, heart or gut. Figures 6.24a-f, demonstrate these findings. This early experiment shows that it may be possible to redirect adenoviral tropism *in vivo* as well as *in vitro* although further work is required.



a) Heart - CCL19 (x10 magnification) b) Heart + CCL19 (x10)



c) Liver – CCL19 (x10) d) Liver + CCL19 (x10)



e) Lymph Node – CCL19 (x10) f) Lymph Node + CCL19 (x10)

Figure 6.24: Infection of C57/BI6 Mice with CCL19 shrouded Ad5.CMV.LacZ. Mice were injected in the tail vein with equal quantities of Ad5.CMV.LacZ with or without CCL19 shrouding (6 in each group). After 48 or 96 hours mice were culled. Slides were prepared from lymph node, spleen, lung, gut, heart, kidney and liver. The slides were then assessed for infection using β -galactosidase staining. The differences between the two groups were subtle. These images demonstrate the lack of LacZ expression in heart tissues, increased LacZ expression in hepatic tissue in mice infection with non-shrouded virus compared to those infected with CCL19 shrouded virus and increased β -galactosidase staining in the lymph nodes of mice infected with the CCL19 shrouded virus compared to those infected with non-shrouded virus. The red arrows indicate positive cells.

6.10 Summary

The results in this chapter demonstrate the following points.

1. EL4 cells express mCCR7 at both the RNA and protein level as demonstrated by RT-PCR and single colour flow cytometry.
2. mCCR7 expression in EL4 correlates with function as demonstrated by the ability of EL4 cells to migrate towards CCL19 and to bind biotinylated CCL19.
3. Infection of the EL4 cells with adenovirus shrouded with CCL19 was unsuccessful using a MOI of 2 ifu per cell, however increasing the MOI to 200 ifu per cell led to detectable infection in the EL4 cells, although the degree of infection did not reach statistical significance.
4. Increasing mCCR7 expression in EL4 cells lead to enhanced chemotaxis and biotinylated CCL19 uptake. Initial experiments also suggested that increased mCCR7 expression also correlated with improved infection with the shrouded adenovirus, even at a MOI of 2 ifu per cell.
5. CAR receptor, α_v -integrin and CCX-CKR expression in a range of murine tissues and cells was characterised enabling some prediction as to which cell types and tissues were likely to be infected with the adenovirus with or without CCL19 shrouding.
6. Initial in-vivo experiments exploring the possibility of redirecting viral tropism through chemokine receptors suggested that there were possible differences in the rates of infections in different tissues, with those tissues expressing CCR7, with lymph nodes, showing higher degrees of infection when exposed to the adenovirus shrouded in CCL19. In addition, the liver that does not express CCR7, showed a lower degree of infection in those mice exposed to the shrouded virus as opposed to those exposed to the non-shrouded virus.

CHAPTER SEVEN

DISCUSSION

7.1 Non-Hodgkin's Lymphoma and Chemokine Receptor Expression

The results obtained from the analysis of clinical samples, outlined in chapter 3, demonstrated differences between non-Hodgkin's lymphoma (NHL) subtypes and chemokine receptor expression. With the exception of CCR4 expression, which is discussed further below, the results were consistent, on the whole, with published data.

As discussed in sections 1.3 and 1.4 of the introduction, the malignant lymphocytes in the various types of NHL appear to correlate with B-cells at a particular stage of B-cell development, as such, chemokine receptor expression on these lymphocytes reflect this. For example, the postulated normal B-cell counterpart for mantle cell lymphoma (MCL) is a CD5⁺ pre-germinal centre (GC) B-cell. Comparison of gene expression of CCR7, CXCR4 and CXCR5 between mantle cell lymphoma cells and CD5⁺ pre-GC B-cells has shown no obvious differences [349]. Therefore, it has been suggested that lymphoma dissemination reflects the physiological rather than pathological properties of the malignant lymphocytes.

In discussion of the receptors more specifically, CXCR4 and CXCR5 were expressed at consistently high levels across the samples. This is unsurprising as CXCR5 has been noted to be a marker of mature B-cells and has been detected regularly in B-cell lymphomas [359], whilst CXCR4 is expressed at varying stages of B-cell differentiation including in mature B-cells [360]. Despite this there were some results observed on testing of the clinical samples, which, appeared contrary to these earlier published data.

For example, in this thesis it has been noted that the average percentage of B cells expressing chemokine receptors in follicular lymphoma cases was lower in general than with all of the other subtypes studied. Initially, this appeared difficult to explain, however germinal centre cells have been noted to show a low level of migration in response to chemokines [361] and furthermore down regulation of CXCR4, CXCR5 and CCR7 has been observed in germinal centre cells on comparison with other B-cells subsets [362]. More recently, further analysis of GC B-cells has added to these data.

Within lymph node follicles the dark zone is a CXCL12 rich area predominantly comprised of centroblasts, whilst the light zone is a CXCL13 rich area comprised of centrocytes, the latter cell type being the normal B-cell counterpart of follicular lymphoma [359]. Analysis of CXCR4 expression on these two B-cell subsets has revealed that CXCR4 expression is detectable on centroblasts whilst down regulated or absent on centrocytes [176]. These observations would certainly help to explain the lower levels of chemokine receptor expression noted in the follicular lymphoma samples, discussed in chapter 3.

With regards to expression of CCR6, the highest level of expression was seen in MALT lymphoma cases. MALT lymphomas represent post-GC marginal zone B-cells [363]. CCR6 expression is gained in B lymphocytes following migration out of the bone marrow [176] and regulates mucosal and humoral immunity particularly in the small intestine [364]. Therefore the higher, although not significantly so, level of expression in the MALT lymphoma cases was to be expected. Certainly, this is in accordance with published findings, with 20-28% of normal B-cells from this subset noted to express CCR6 in one study [365] with up to 90% of these B-cells expressing CCR6 in another [362]. What is perhaps a little unusual on first inspection is the lower level of CCR6 expression detected in the MCL cases. As has already been discussed MCL has a strong association with gut involvement and so a higher level of expression would be expected. Certainly CCR6 has been reported as being able to distinguish MCL, MALT and marginal zone lymphomas from others [366]. However, this has not been a consistent finding with lymphocytes from cases of MCL in another study being observed to show down regulation of CCR6 on comparison with their normal B-cell counterpart [342]. Furthermore, loss of CCR6 expression has been reported in other B-cell lymphomas such as CLL/SLL and follicular lymphoma [367].

A discussion regarding CCR9 expression in the subtypes of lymphoma is presented in section 3.5.2.4, with lower than expected expression noted in MCL and, although not significant, the highest level of expression being seen in MALT lymphomas. As already noted both MALT lymphoma and MCL have a high propensity to gut involvement, with CCR9 known to regulate homing towards the gut higher expression of this receptor in these NHL types would be expected. There is little remaining in the literature to expand this discussion further.

In all NHL subtypes analysed less than 1% of B-cells expressed CCR10. CCR10 is implicated in the homing of T-cells to the skin and mucosal surfaces [364]. However, the lack of CCR10 expressed observed in Burkitt's lymphoma primary cells and cell line samples was contrary to the previously published data [366]. Moreover, whilst CCR10 is implicated in the recruitment of cells to mucosal surfaces, it has been shown that memory B-cells do not express this receptor, although plasmablasts have been shown to express it [336]. Unfortunately there are little data available relating to CCR10 expression in less mature B-cells, but it is possible that CCR10 expression only occurs following differentiation to plasmablasts, if this is the case the lack of CCR10 expression in the clinical samples analysed would be expected.

Further discussion relating to CCR4 and CCR7 expression can be found later in this chapter.

7.2 Chemokine Receptor Expression and Function: Differences Between Normal B-cells and Malignant B-cells

Whilst expression of chemokine receptors may not enable easy differentiation between malignant lymphocytes or even their normal B-cell counterparts, other subtle aspects of chemokines and their receptors do distinguish them.

Differences in the degree of expression of various chemokine receptors between malignant and normal lymphocytes have been observed. For example expression of CXCR4, CXCR5 and CCR7 in patients with CLL/SLL appears to be increased when compared to comparable normal B-cell populations. Moreover the higher the expression of these receptors was associated with more advanced lymph node involvement [368, 369]. Higher expression of CXCR4 and CXCR5 has also been noted in other B-cell lymphoproliferative diseases such as nodal follicular lymphoma (although again lower expression than MCL and CLL/SLL) and mantle cell lymphoma [359]. However, in one study no such differences were detected between CXCR4 and CXCR5 expression in normal B cells and B cell lymphoproliferative disorders. However, in this instance unlike the other reports, the only normal control used was peripheral blood B-lymphocytes, whilst the test samples were obtained from a range of sources including lymph node, bone marrow and peripheral blood, and as such this may have affected the results obtained [359].

Similar differences have been noted with CCR7 expression, and these will be explored later in this discussion.

With the differences in the intensity of expression noted, it would be logical to explore whether these differences equate to differences in responses to chemokines. Again, this has been examined. As discussed in section 1.4.3, MCL cells have been observed to migrate in response to CCL19, whilst their normal counterpart B-cells do not, despite also expressing CCR7 [364]. This is not an isolated finding with migration in response to CXCL12 in CLL/SLL cells enhanced in comparison to normal B-cells [286]. Although it has also been shown that both normal and malignant CXCR4⁺ B-cells of germinal centre origin have a lower migratory response to CXCL12 than those of non-germinal centre cells origin, despite similar expression of the receptor due to differences in the intracellular pathways triggered [359]. These studies indicate that receptor expression does not always equate to migratory function with a host of factors influencing chemotaxis. This is supported by earlier data on normal B-cells, which, showed that despite high levels of CXCR4 expression a diminishing response of normal B-cells to CXCL12 was observed as they matured [370].

Finally, other functions may be gained in malignant B-cells with respect to chemokines. Interestingly, CXCL13 and CCL19 have been shown to act synergistically to induce resistance to TNF α mediated apoptosis in B-cell CLL cells but not in normal CD5⁺ B-cells [361]. This shows that chemokines do not only play a role in the trafficking of malignant cells.

7.3 CCR4 and Non-Hodgkin's Lymphoma

7.3.1 CCR4 Expression

CCR4 binds to two ligands CCL17 and CCL22 [371] and is present on Th2 cells, regulatory T (Treg) cells, skin-homing T cells and subsets of B-cells, as well as on platelets, monocytes and macrophages [340]. The ligands for CCR4 are not monogamous, and both CCL17 and CCL22 will bind the atypical receptor D6 [372].

In chapter 3, the results of CCR4 expression in the NHL samples tested revealed a higher than expected expression in certain sub-types, namely DLBCL, MCL, Burkitt's lymphoma and MALT lymphoma. At that point it was observed that the higher expression appeared to correlate with more aggressive disease subtype, with less expression noted in the more indolent follicular lymphoma and CLL/SLL. The higher expression of CCR4 in the higher-grade lymphomas may provide a reason in part, why the cytokine driven B-symptoms are

more often seen at presentation in these diseases. Studies comparing CCR4^{+/+} with CCR4^{-/-} mice following lipopolysaccharide exposure revealed a higher mortality rate in the CCR4^{+/+} mice with higher levels of cytokines such as TNF α detected [373]. Whilst CCR4 expression may help to explain some of the clinical features noted with these NHL subtypes, it does not explain the reason for the differences in receptor expression.

The implications of CCR4 expression in T-cell lymphomas has been reported, with a clear correlation between CCR4 expression and an adverse outcome [372] which has led to the development of anti-CCR4 antibody therapy by the same group. Yet, with regards to B-cell lymphomas, little can be found. Ishida et al reported a case of DLBCL, in which CCR4 expression could be detected. However, in this instance it was postulated that the CCR4 expression was due to the fact that this patient was unusual due to extensive and localised cutaneous involvement. Thus the CCR4 expression related to skin-homing lymphocytes [291] with the implicit assumption that DLBCL is not associated with expression of this receptor. This is likely to have been an erroneous assumption, and it can be argued that CCR4 expression was actually related to the DLBCL subtype, or more specifically to the normal B-cell counterpart of DLBCL lymphocytes.

A number of studies have been reported looking at the role of CCR4 in the various T cell subsets, however very little has been published relating to CCR4 expression in B-cells. One of the first studies assessed the response of normal non-germinal centre (GC) and GC B-cells, from tonsils, to CCL22. CD38 was used to characterize the B-cells as being of GC (CD38⁺) or non-GC (CD38⁻) origin. It was noted that non-GC cells, consisting of both naïve and memory B-cells, migrated in response to CCL22, whereas the GC cells did not. Subsequently, analysis of CCR4 expression supported these results with 56-70% of CD38⁻, naïve B-cells expressing CCR4 and 40-73% of memory B-cells expressing CCR4, whilst there was no expression detected in GC cells [341]. It is possible that CCR4 may aid in the migration of the naïve and antigen activated/memory B-cells along with other chemokine receptors as these cells home to specific anatomical sites or re-circulate, whilst GC cells demonstrate very little motility remaining within germinal centres.

Later, CCR4 expression at the transcriptional level was noted in a number of different subtypes of B-cell lymphoma (DLBCL, follicular lymphoma, mantle cell lymphoma, lymphocytic lymphoma and marginal lymphoma) as part of a paper on the use of CXCR4 neutralizing antibodies in the control of Raji cell induced tumours in mice [362]. However, other than a single figure in the paper, no further investigation of this expression was

undertaken, but it does confirm that CCR4 expression is not restricted to the T-cell lymphomas.

Finally, analysis of chemokine receptor expression on normal IgA⁺ and IgG⁺ cells has again revealed a population of CCR4⁺ cells. IgA⁺ B-cells are involved in mucosal and intestinal immunity, whereas IgG⁺ B cells preferentially migrate to the bone marrow and secondary lymphoid organs [295]. On reporting CCR4 expression in these two B-cell groups it was noted that both IgA⁺ and IgG⁺ B-cell populations contained subpopulations of CCR4⁺ cells. Furthermore, IgG⁺ cells had higher expression than the IgA⁺ cells, which was even more evident when the B-cells were classified as small (resting) or large (activated), with CCR4 expression noted on 5% of small IgA⁺ vs. 13.8% of small IgG⁺ B-cells, and 11.6% of large IgA⁺ vs. 25.9% of large IgG⁺ B-cells [366].

Therefore, if the results discussed in chapter 3 are related to the findings in these papers it can be argued that as with expression of the other constitutive chemokine receptors studied, CCR4 expression relates to the normal B-cell counterpart of the NHL subtype. For DLBCL the normal B-cell counterpart falls predominantly into three groups, the germinal centre B-cell (GCB) or the activated B-cell (ABC) and the primary mediastinal B-cell lymphoma (PMBCL) [366]. Unfortunately, due to the time span over which the samples were collected, information on the category of DLBCL was not available as, further classification into GCB or ABC did not become part of routine diagnostic practice until after these samples were collected. Furthermore PMBCL would not have been represented, as by definition, it only involves the mediastinum, and the samples consisted of peripheral lymph nodes. However if, as suggested by Corcione et al, CCR4 expression identifies non-GC B-cells then it is not unreasonable to postulate that the higher CCR4 expressing samples represented the ABC type of DLBCL. Yet, if this was the case, then the better outcome in the high CCR4 expressing group is unusual as ABC DLBCLs have been noted to have a poorer outcome than the GCB DLBCLs [374].

With regards to the remaining NHL subtype expressing higher levels of CCR4, MALT lymphoma and mantle cell lymphomas have post germinal-centre and naïve B-cells as their normal B-cell counterparts respectively [375]. Therefore the chemokine receptor expression is consistent with the findings of Corcione et al. Although, intriguingly, CCR4 expression was only detected in a small subset of MALT lymphomas examined in one study analysing chemokine receptor expression in this disease. Further examination of the CCR4 positive MALT lymphomas revealed that they all demonstrated adverse

cytogenetics with trisomy 3 [176], an abnormality exclusively associated with nodal MALT lymphomas [376]. Cytogenetics is not routinely performed in many centres as part of the diagnostic work up of MALT lymphomas, but it is an interesting hypothesis that the samples examined in this study may have demonstrated this cytogenetic abnormality considering that they were all lymph node samples.

However, the postulated normal B-cell counterpart in Burkitt's lymphoma has not yet been confirmed with it thought to be either of GC or post-GC origin [176]. The results in this study, may add support to the theory that the cell of origin is actually post-GC in view of the high CCR4 expression.

Finally, the lower expression of CCR4 in the follicular lymphoma samples is again consistent, with this being a lymphoma of GC B-cell origin, yet the lower expression in CLL/SLL is interesting. The expression of the GC marker, CD38, is variable in CLL/SLL and has been noted to be of adverse prognostic significance [176], it would therefore been of interest to know the CD38 status of the CLL/SLL samples. The reason for the lack of this information is the same as with the lack of information on the DLBCL samples. It is unfortunate that correlative clinical data was not available for these samples, as it could be postulated that CCR4 expression would correlate with a good outcome in keeping with CD38⁻ status.

7.3.2 CCR4 Targeted Therapy

Having shown that CCR4 is expressed in certain lymphoma subtypes, the question arises as to whether or not this is a good target for therapy. A phase I clinical study using a monoclonal anti-CCR4 antibody has certainly demonstrated some efficacy in patients with relapsed adult T-cell leukaemia/ lymphoma (ATLL) and peripheral T cell lymphomas (PTCL) [251]. The identification of CCR4 as a target in ATLL was identified by the same group, although the patient's sample were considered to be CCR4⁺ if greater than 10% of T-cells expressed the receptor, with no details given on which cells were used to calculate the proportion identified [297]. With the proportion of CCR4⁺ cells in the samples analysed in this thesis ranging from 11.84 (\pm 3.98)% in follicular lymphoma cases to 61.59(\pm 6.52)% in DLBCL cases, then the simple answer is that CCR4 is a valid target, particularly in the non-GC NHL subtypes.

Although it would appear that CCR4 would be a reasonable therapeutic target for B-cell lymphomas, it is also worth considering which other CCR4 positive cells may be depleted

as a consequence. As mentioned earlier, CCR4 is also expressed on T regulatory cells, Th2 cells, monocytes, macrophages and platelets.

In recent years, there has been a lot of interest in the role of T regulatory cells in the microenvironment of lymphomas and other malignant diseases. T regulatory cells are CD4⁺ cells that regulate the immune response by a number of mechanisms leading to self-tolerance and suppression of cellular immunosurveillance [291]. They are further identified by the expression of CD25⁺ (in a subgroup) and more specifically by expression of the transcription factor FOXP3 [377]. Additionally, Treg cells have been shown to express CCR4 and to migrate in response to both CCL17 and CCL22 [378]. The impact of increased numbers of Treg cells in solid tumours such as non-small cell lung cancer, ovarian cancer and gastrointestinal cancers, either within the tumour itself or in the peripheral blood, has been associated with poorer outcomes (379, 380). This is postulated to be related, to escape from immunosurveillance therefore providing a more hospitable environment for the malignant cells. Thus targeting of CCR4 in solid tumours may also be advantageous by depleting Treg cells and thus assisting malignant cell destruction through the recognition of tumour antigens.

However, this association has not held true for lymphoid malignancies. On the whole, higher numbers of Treg cells have been associated with improved outcomes in a range of lymphomas. The first suggestion of this association came in 2001 when higher numbers of CD4⁺ cells correlated with a longer overall survival in patients with DLBCL [379]. It was subsequently demonstrated that these represented Treg cells. Increased numbers of CD4⁺CD25⁺CTLA⁺FOXP3⁺ Treg cells were demonstrated in a variety of lymphomas by Yang et al. In this study it was noted that these cells suppressed the migration of CD4⁺CD25⁻ cells into the tumor microenvironment by suppressing the release of IFN- γ and IL-4, thus also suppressing cellular proliferation [380]. Two other interesting observations were made. Firstly, the lymphoma cells actually released CCL22 thereby attracting T regulatory cells into the microenvironment. Secondly, cell-cell interaction between CD4⁺CD25⁻ T cells and the lymphoma cells lead to the induction of CD25 on the T cells, showing that the lymphoma cells have the ability to induce Treg cells [381]. This latter observation has been confirmed in subsequent studies [381].

The majority of studies exploring Treg numbers and lymphoma have confirmed the association between higher Treg numbers and improved survival in DLBCL and follicular lymphoma [382, 383]. Although, one study has suggested the opposite, with higher

numbers of Tregs detected in both the tumour bulk and in the peripheral blood being associated with more advanced disease in a range of lymphoma subtypes [384].

The more common correlation between higher numbers of Tregs and improved survival in lymphomas appears counter-intuitive if these cells help the malignant cells to escape immune-mediated cytotoxicity, which leads to the question, why would higher numbers lead to improved outcomes in lymphomas? There are a number of potential explanations. It has been shown that they suppress T helper dependent B-cell immunoglobulin production and class switching [382] and Treg cells have also been shown to selectively induce apoptosis in activated B-lymphocytes following stimulation by CD3 or exposure to antigen [385]. Thus targeting CCR4 in lymphomas may have a detrimental affect, and finding a way to harness these suppressive and apoptotic properties of Treg cells may be a more useful therapeutic approach. However, until the studies have been performed with anti-CCR4 approaches, firm conclusions cannot be drawn.

Finally, CCR4 could be used therapeutically in a different way. The fact that Reed-Sternberg cells in Hodgkin's lymphoma express CCL17 and CCL22 has been employed to provide an elegant treatment option. Cytotoxic T-lymphocytes (CTLs) are rare in the cellular milieu surrounding Reed-Sternberg cells. CTLs were engineered to express CCR4 as well as a CD30-specific antigen receptor (CD30 is expressed by Reed-Sternberg cells). These were then adoptively transferred into SCID mice manipulated to develop tumours from a Hodgkin's lymphoma cell line. The CCR4⁺ CTLs successfully migrated towards the CCL17 and CCL22 expressing lymphoma cells with early tumour control noted and tumour regression observed by day 30 due to the cytotoxic effects of the engineered cells [386].

7.4 CCR7 and NHL

7.4.1 CCR7 Expression

As CCR7 was chosen as the chemokine receptor for testing the feasibility of targeting the chemokine system in this thesis, further exploration of this receptor in lymphoma and other malignant diseases is worthwhile. Under normal circumstances, CCR7 is expressed on dendritic cells, thymocytes, naïve and memory T-cells subsets and subsets of B-cells [387]. CCR7 and its ligands, CCL19 and CCL21, are involved in the homing of lymphocytes to, and the development of, secondary lymphoid organs thus making CCR7 an ideal receptor to study in relation to lymphomas.

In chapter 3, it was shown that, although all 6 lymphoma subtypes studied expressed CCR7 to some degree, there were significant differences in the level of expression. In particular samples from patients with mantle cell lymphoma or CLL/SLL showed significantly higher expression when compared to the remaining four subtypes with 91.03 (\pm 4.97)% of B-cells expressing this in MCL cases and 95.83 (\pm 2.1.)% of B-cells expressing the receptor in CLL/SLL cases. These findings are consistent with the published data. Higher expression of CCR7 in CLL when compared to both normal B-cell counterparts and other lymphoma subtypes has been consistently demonstrated [296, 347, 359, 364]. The data for mantle cell lymphoma are less robust with comparatively higher expression of CCR7 reported more often than not [359, 369]. However, in the one publication CCR7 expression in mantle cell lymphoma was reported as equal to that of its normal B-cell counterpart, this conclusion was based on gene expression rather than protein expression analysis [286] whereas the other papers reported on protein expression of CCR7 as with this thesis.

It is also worth pointing out that CCR7 expression is detected in other B-cell lymphoproliferative disorders such as follicular lymphoma, marginal zone lymphomas [367] [364] and Burkitt's lymphoma (cells from which the receptor was first characterised) [359]. Interestingly, aberrant or reduced expression of CCR7 has been observed in primary CNS lymphomas (PCNSL). However, on closer examination the receptor is located intracellularly rather than on the cell surface [388]. Whereas on cells from primary mediastinal B-cell lymphoma CCR7 expression is reduced in comparison with thymocytes (PMBCL arises from thymic tissues) [288]. In PCNSL and PMBCL nodal involvement is absent, by definition, which may be explained by the altered expression of CCR7. However the work by Rehm et al, also demonstrated a low level of CCR7 expression in primary DLBCL samples by immunohistochemistry. This is less easy to explain, but, as with the samples studied in this thesis, further categorisation into GB B-cell or activated B-cell type was not possible, and so these results could potentially be explained by an incidentally larger number of GC B-cell type DLBCL cases.

Functional differences between CCR7⁺ lymphoma and CCR7⁺ normal B-cells have also been described, with responses to CCL19 demonstrated in mantle cell lymphoma cells but not their normal counterparts [389]. CCR7 has also been shown to be functional in CLL, with transendothelial migration demonstrable, and higher levels of migration noted with cells from those individuals with lymph node involvement [286].

What is clear from published results and those discussed in chapter 3 is that CCR7 is a suitable target for the development of anti-lymphoma treatments. However the value of CCR7 as a target does not end with lymphoma.

Nodal metastases in solid tumours are a common occurrence; furthermore, CCR7 has been implicated in the pathogenesis of the nodal spread of numerous tumour types. It has been proposed that up regulation of CCR7 precedes nodal metastasis in a number of tumour types as evidenced by detectable CCR7 expression in cells that would normally be negative for this receptor. Such examples include oesophageal squamous cell carcinoma [390], prostate carcinoma [391], breast carcinoma [392] and melanoma [393]. In all of these instances, CCR7 expression was associated with lymph node metastasis and an adverse prognosis.

7.4.2 CCR7 Targeted Therapy

Therefore it is clear that targeting CCR7 to induce cytotoxicity is a valid approach to the treatment of not only lymphomas, but also a range of solid tumours. In particular mantle cell lymphoma and CLL/SLL would be ideal targets for such treatment. However, whilst many papers on CCR7 expression in a range of diseases conclude with the comment that inhibition of CCR7 would provide a potentially useful therapeutic approach, to date there is remarkably very little literature describing strategies to specifically target this receptor.

Neutralizing antibodies have been used in murine *in-vivo* studies. A melanoma cell line B16, was engineered to express either CCR7 (CCR7-B16) or CXCR5 (CXCR5-B16) and, along with untransfected B16 cells, were injected into the footpads of mice. In all cases tumours became detectable. However there was a faster and a higher rate of metastasis in the mice injected with the CCR7-B16 cells [394]. Following this, a neutralizing anti-CCL21 antibody was administered to those mice that had been injected with CCR7-B16 cells. This led to the regression of nodal metastasis although no mention was made of the effect on the initial tumour [395]. This study shows that CCR7 mediated migration to lymph nodes can be inhibited and may offer a therapeutic approach. However, in the case of solid tumours, anti-CCR7 therapy alone is unlikely to suffice, as the primary tumour is unlikely to be affected and a combined approach with chemotherapy will probably be required.

An anti-CCR7 monoclonal antibody has been developed, which has demonstrated the ability to induce apoptosis of CLL cells *in-vitro*. As the intensity of CCR7 expression on CLL cells is much higher than normal cells, the ability of this anti-CCR7 antibody to induce apoptosis in normal B-cells was also examined. Normal T and B-cells were relatively spared due to their lower expression of CCR7 [395]. This suggests that targeting CCR7 may not be as immunosuppressive as its normal expression profile may suggest. This is analogous to the situation seen with rituximab in which there is relative sparing of CLL cells at standard treatment doses due to relatively lower expression of CD20. The majority of CLL and mantle cell lymphoma cells express CCR7, as shown by the results in this thesis, and so it is proposed that anti-CCR7 antibody therapy could be applicable as a single agent in these diseases.

Whilst, the bias of this thesis was towards targeted cytotoxic therapy, as with CCR4, engineering cells to express CCR7 may also offer a therapeutic approach. There has been a lot of interest in the development of anti-cancer vaccines utilising dendritic cells (DC). One issue with immunotherapy has been the poor migratory properties of the DCs expressing the cancer antigen of interest. By engineering DCs to express higher levels of CCR7, migration to lymph nodes was enhanced allowing for a more robust immune response to the endogenous cancer antigen. In addition, potentially a lower number of DCs would be required [296], which is currently a problem with anti-cancer vaccinations.

Finally, although not developed specifically to target CCR7 a few agents have been observed to down-regulate CCR7. Triptolide has been used as an anti-inflammatory agent in China for many years and has been shown to reduce transplant rejection in both solid organ and bone marrow transplantation [396]. Its immunosuppressive effects have been further studied and it has been shown that one mechanism of suppression is through down-regulation of CCR7 expression on DCs [397]. Certain retinoids have also demonstrated similar effects. Two retinoids, 9-cis retinoic acid (9cRA) and retinoid fenretinide (4-HPR) also downregulate CCR7, as well as CXCR4 [397] and so may also have anti-inflammatory properties. Of interest, in the same study *all-trans* retinoic acid (ATRA), a drug used very effectively in the treatment of acute promyelocytic leukaemia [398], was also tested and did not show any down-regulation of either CCR7 or CXCR4 [399], demonstrating that not all members of this class of agents will have the same effects. It is likely that other agents have inhibitory effects on CCR7. However as with the three agents discussed above, these are not specific. Nevertheless, they may offer some therapeutic potential in lymphomas and solid tumours.

7.5 Using the Chemokine System to Target Specific Cell Populations with Cytotoxins

There has been a lot of interest and research in recent decades looking at the development of monoclonal antibodies to deliver targeted therapy. There is no doubt that this approach has been successful as evidenced by the impact that rituximab has had on the management of B-cell lymphomas. However, monoclonal antibody relies on other functioning elements of the immune system to induce cell death such as antibody dependent cell-mediated toxicity or complement dependent cytotoxicity. Additionally, at relapse, expression of the targeted antigen may be lost, meaning that repeated use of the agent may be ineffectual. Loss of CD20 expression has been noted in up to 60% of cases of diffuse large B-cell lymphoma and follicular lymphomas at relapse, and is associated with poorer outcomes [398, 400]. Therefore, theoretically at least, agents causing direct, targeted cytotoxicity could overcome some of these issues. Having established that the chemokine system, more specifically chemokine receptors, are a suitable therapeutic target for B-cell non-Hodgkin's lymphoma, the next sections of this thesis detailed ways in which the system could be targeted to directly deliver a cytotoxic agent.

7.5.1 Chemotoxins and Chemokine-toxin Conjugates

In this thesis, targeting of the chemokine system used the radioisotope ^{125}I conjugated to either CCL19 or PM2 (a mutated form of CCL3) was attempted. Unfortunately, no significant differences in cell kill were detected between the CCR7^+ and D6^+ cells compared to CCR7^- and D6^- cells exposed to the radioisotope-chemokine conjugates. There are many potential reasons for this, the main one being that the dose of ^{125}I could have been too high therefore negating any specific targeting. Repeating this work using lower concentrations of the radioisotope and using a different control cell population may be worthwhile. However, developing an alternative approach utilizing chemotoxins, may be more viable and would certainly be easier to use in the clinical setting.

As previously described, chemotoxins are defined as chemokines fused with a toxic moiety. A toxin, which will only cause cell death intracellularly would be ideal, and therefore would overcome the problems encountered with the radioisotope-chemokine conjugation. As discussed in section 1.4.5.4, this approach has been tried *in-vivo* in murine studies using CCR4 as the target in cutaneous T-cell lymphomas/leukaemias. CCL17 was fused with one of two toxins and administered to mice. Whilst initial responses were

promising, relapse occurred with reduced expression of CCR4 observed on the tumour cells [401], therefore preventing effective re-use of the agent, analogous to the situation seen with rituximab. However, as proof-of-principle, this study demonstrated that this was a valid approach. Certainly, fusing chemokines with a cytotoxic agent already in clinical use for haematopoietic malignancies such as cytosine is an interesting concept and worth exploring further. Although results from studies performed by Clare McCulloch in our laboratory with chemokine-doxorubicin conjugates were disappointing.

7.5.2 Adenoviral Vectors Gene Therapy – Oncolytic Vectors

The use of adenoviral vectors in oncology is expanding as discussed in section 1.5. However, there are a number of issues limiting their use including immunogenicity, robust and consistent gene expression and of course specificity. In chapter 5 and 6, it was demonstrated that adenoviral tropism could be successfully redirected through chemokine receptors, although a number of issues did arise meaning that final proof-of-principle studies could not be conducted.

One issue was the persistence of background infection due largely to incomplete shrouding of the virus with chemokine. As a consequence a vector had been designed incorporating an acceptor peptide (AP) into the fibre knob protein sequence of the adenovirus. The AP is able to be biotinylated by biotin ligase [298]. The theory is that the virus can then be more efficiently biotinylated and subsequently shrouded following the use of biotin ligase, thus eliminating the background infection rate whilst more efficiently redirecting the adenovirus away from its CAR receptor to the chemokine receptor. Unfortunately, time did not allow for the transfection of this vector into HEK293 cells and the subsequent creation of viral particles to test this theory. However, it is likely that background infection may not be entirely eliminated due to the residual non CAR-dependant mechanisms of viral entry such as the utilization of α -integrins [354] and additional mechanisms to block α -integrin mediated cellular entry may also be required.

Another potential problem with this approach is the promiscuity of chemokines. In this study CCR7 was the receptor predominantly under investigation, yet for a variety of reasons adenoviral experiments were performed with cell lines expressing alternative receptors such as CCR5 and the atypical chemokine receptors D6 and CCX-CKR. This led to the observation that not only could adenoviral tropism be redirected through the atypical chemokine receptors, but also led to transduction of the cell with the reporter gene LacZ.

Therefore, any adenoviral vector shrouded with CCL19 has the potential to enter a broader range of tissues and cells than initially surmised. This is because in comparison to CCR7, CCX-CKR has a broader range of expression being detectable in bone marrow, brain, heart, kidney, liver and lung tissues [319] as well as in mast cells, and both B and T cells from the lymph nodes (outlined in chapter 6). This has the obvious disadvantage that if a cytolytic adenoviral vectors is redirected by shrouding with CCL19, then all of these tissues could be affected, potentially resulting in a widely toxic therapy. The widespread expression of CCX-CKR may also explain why there were no major differences in the distribution of LacZ expression in the *in-vivo* study outlined in chapter 6 in which C57/BL6 mice were injected with the Ad5.CMV.LacZ vector with, or without, CCL19 shrouding.

However, this does not preclude this approach, as the degree of cytotoxicity may be influenced by a range of factors, not least, the intensity of surface expression of CCR7 and CCX-CKR. It has already been noted that CCR7 expression on CCR7⁺ B-cell lymphomas is often of a higher level than normal cells, and this may also be true for solid tumours, therefore there may be increased uptake in these cells, although of course an examination into the expression of CCX-CKR in lymphomas is currently lacking. It is also interesting to note that NOD/SCID mice, in which a CCR4⁺ human acute T-lymphoblastic leukaemia cell line (CEM) had been injected to induce tumours survived without any obvious (although not specifically reported) tissue toxicity following administration of a chemotoxin derived from CCL17 [349]. This is worth noting as another atypical chemokine receptor, D6, that internalizes and subsequently degrades a number of chemokines including the ligands for CCR4 namely CCL17 and CCL22 [126, 298] has wide expression including lung, heart, brain, thymus, ovary, liver and skeletal muscle [402].

Finally, as discussed in section 1.5, further levels of specificity can be introduced into adenoviral vectors using either conditionally replicative vectors or those requiring tumour specific promoters such as telomerase.

7.6 Development of a Murine Lymphoma Model

In chapter 6 the murine T-lymphoblastic lymphoma cell line EL4 was characterised to assess its suitability as a murine lymphoma model. The cell line fulfilled the first requirement in that it expressed functional CCR7, although it was subsequently shown that it also expressed CCX-CKR. Interestingly EL4 cells express neither the CAR receptor nor

α -integrins meaning that any infection detected in these cells would have to have occurred via altered tropism of the adenoviral vector.

Following this attempts at infecting the cell line with shrouded adenovirus proved challenging, although eventually, a small but not significant degree of infection was detected in the cells after increasing the multiplicity of infection (MOI) 100 fold.

Having finally successfully infected the EL4 cells, improved detection of infection was optimized by using an adenoviral vector engineered to use the EF-1 α promotor, which may improve the efficiency of transgene expression [122]. The development of the adenoviral vector containing this sequence was successful, but obtaining viral particles following transfection of HEK293 cells was not achieved due to time constraints. It would be interesting to repeat the infection experiments, not only on EL4 cells, but also other haematopoietic cell lines, using this vector to see if improvements in transgene expression can be obtained.

Prior to testing any directed therapy *in-vivo* using adenoviral vectors, it would be useful to study the induced tumors further. Using EL4 cells engineered to up regulate CCR7 or CCX-CKR, may affect the pattern of distribution and speed at which the tumor cells grow or metastasize. Conversely, using techniques such as siRNA technology to block expression of each of these receptors may also alter tumour behaviour and provide clues with regards to the likely effects of targeted therapy. Additionally, techniques such as CFSE CelltrackTM, could be employed to assess the migration of the altered cells, to add further to the characterization of this cell line.

Furthermore, experiments using neutralizing antibodies to either the receptor or its ligands, as described by Wiley et al in targeting CCR7⁺ tumours formed by the melanoma cell line B16 in mice [357], would be of interest too.

Finally, using EL4 induced tumours to provide the 'proof-of-principle' for targeted therapy with chemokine shrouded adenoviral vectors, or even chemotoxins, at least at this point, appears to be a valid approach, although further work is required. Later, an alternative model using a murine B-cell malignancy such as CLL would be desirable, as this is one of the lymphomas in which CCR7 directed therapy would appear to be most efficacious. Certainly, murine B-cell CLL models have been described [395, 403].

7.7 Summary and Future Directions

This thesis has addressed and answered a number of questions. Firstly, there are variations between lymphoma subtypes and constitutive chemokine receptor expression, and with the exception of CCR4, the expression profiles of each of the lymphoma subtypes was consistent with published data. With regards to CCR4 expression in B-cell non-Hodgkin's lymphoma, this is the first systematic analysis of this receptor, but as discussed, may well correspond with expression on the normal B-cell counterpart of the lymphoma subtypes.

The correlation between higher CCR4 expression and improved survival in diffuse large B-cell lymphoma was unexpected and not easily explained. An analysis (preferably prospective) of CCR4 expression and Treg numbers in DLBCL would be valuable, and that along with a study of CCL17 and CCL21 expression and may help to explain this phenomenon. In addition collection of clinical data including the stage of disease at presentation, response to treatment, time of relapse and survival data should be collected for further correlation with CCR4 expression. Of course, although the differences in survival were significant, the overall numbers were small, and further studies would require a larger patient population. In addition, further testing of the DLBCL samples would enable differentiation between activated-B-cell type and germinal centre cell type, allowing for correlation between CCR4 status and DLBCL subtype.

Functional studies on the lymphoma samples may also be of value. In chapters 4 and 5, the QCMTM Chemotaxis assay was used successfully albeit with less convincing results than with the Transwell[®] assay, this has the advantage of requiring fewer cells for analysis, therefore enabling more efficient use of clinical samples. Of course the absence of migration towards a ligand does not always equate with lack of signal induction and initiation of an alternative function. Calcium flux assays could be of use too. However, they can be difficult to optimize and a much larger number of cells are required, which are not always available with primary samples. Alternatively, biotin-chemokine uptake studies could be performed, requiring the same number of cells as for flow cytometry analysis. The number and range of studies that could potentially be performed on primary lymphoma cells obviously stretches beyond those detailed above.

The second aim was with regards to utilising the chemokine system to provide targeted therapy. Initial experiments with radiolabelled chemokines were disappointing and ultimately not very informative. This has been discussed earlier. However, using oncolytic

or cytolytic adenoviral vectors holds some promise although a lot more work is required. Which leads on the third aim of this study.

Can adenoviral vectors be redirected to chemokine receptors? The simple answer is yes, however, work to increase the specificity of the tropism was not completed. With time and resources, the aim would be to use the vectors created containing the acceptor peptide to attempt comprehensive adenoviral biotinylation and to subsequently assess the efficiency of chemokine shrouding by repeating the electron microscopy and infection experiments. Following this, engineering the virus to contain 'suicide' genes and potentially tissue specific promoters would need to be undertaken before progressing on to therapeutic *in-vivo* murine studies. Furthermore *in-vivo* infection experiments would need to be repeated following confirmation of more efficient chemokine shrouding.

The final aim of this study was to develop a suitable *in-vivo* mouse model for testing targeted therapy. So far, EL4 cells remain the most viable option due to the ease of obtaining them and the ability to use a standard laboratory strain of mouse for any experiments. Of course, the proposed experiments outlined previously will need to be performed first.

In summary, although a lot more work is needed, it has been established that there is an association between B-cell lymphoma subtype and constitutive chemokine receptor expression, chemokine directed targeted therapy remains a viable approach to the treatment of B-cell lymphomas, adenoviral tropism can be redirected through chemokine receptors and the identification of EL4 cells for used as an *in-vivo* mouse lymphoma model remains valid.

APPENDICES

8.1 WHO Classification of Tumours of the Lymphoid Tissues

<i>B-CELL NEOPLASMS</i>	<i>ICD-O</i>
<i>PRECURSOR LYMPHOID NEOPLASMS</i>	
B lymphoblastic leukaemia/lymphoma	
B lymphoblastic leukaemia/lymphoma, NOS	9811/3
B lymphoblastic leukaemia/lymphoma with recurrent genetic abnormalities	
B lymphoblastic leukaemia/lymphoma with t(9;22)(q34;q11.2); BCR-ABL1	9812/3
B lymphoblastic leukaemia/lymphoma with t(v;11q23); MLL rearranged	9813/3
B lymphoblastic leukaemia/lymphoma with t(12;21)(p13;q22); TEL-AML1 (ETV6-RUNX1)	9814/3
B lymphoblastic leukaemia/lymphoma with hyperdiploidy	9815/3
B lymphoblastic leukaemia/lymphoma with hypodiploidy (hypodiploid ALL)	9816/3
B lymphoblastic leukaemia/lymphoma with t(5;14)(q31;q32); IL3-IGH	9817/3
B lymphoblastic leukaemia/lymphoma with t(1;19)(q23;p13.3); E2A-PBX1 (TCF3-PBX1)	9818/3
T lymphoblastic leukaemia/lymphoma	9837/3
MATURE B-CELL NEOPLASMS	
Chronic lymphocytic leukaemia/ small lymphocytic lymphoma	9823/3
B-cell prolymphocytic leukaemia	9833/3
Splenic marginal zone lymphoma	9689/3
<i>Hairy cell leukaemia</i>	9940/3
<i>Splenic B-cell lymphoma/leukaemia, unclassifiable</i>	9591/3
<i>Splenic diffuse red pulp small B-cell lymphoma</i>	9591/3
<i>Hairy cell leukaemia-variant</i>	9591/3
Lymphoplasmacytic lymphoma	9671/3

Waldenström macroglobulinaemia	9761/3
Heavy chain diseases	9762/3
Alpha heavy chain disease	9762/3
Gamma heavy chain disease	9762/3
Mu heavy chain disease	9762/3
Plasma cell myeloma	9732/3
Solitary plasmacytoma of bone	9731/3
Extraosseous plasmacytoma	9734/3
Extranodal marginal zone B-cell lymphoma of mucosa-associated lymphoid tissue (MALT-lymphoma)	9699/3
Nodal marginal B-cell lymphoma	9699/3
<i>Paediatric nodal marginal zone lymphoma</i>	9699/3
Follicular lymphoma	9690/3
<i>Paediatric follicular lymphoma</i>	9690/3
Primary cutaneous follicle centre lymphoma	9597/3
Mantle cell lymphoma	9673/3
Diffuse large B-cell lymphoma (DLBCL), NOS	9680/3
T-cell/histiocyte rich large B-cell lymphoma	9688/3
Primary DLBCL of the CNS	9680/3
Primary cutaneous DLBCL, leg type	9680/3
EBV positive DLBCL of the elderly	9680/3
DLBCL associated with chronic inflammation	9680/3
Lymphomatoid granulomatosis	9766/1
Primary mediastinal (thymic) large B-cell lymphoma	9679/3
Intravascular large B-cell lymphoma	9712/3
ALK positive large B-cell lymphoma	9737/3
Plasmablastic lymphoma	9735/3
Large B-cell lymphoma arising in HHV8-associated multicentric Castleman disease	9738/3
Primary effusion lymphoma	9678/3
Burkitt lymphoma	9687/3
B-cell lymphoma, unclassifiable, with features intermediate between diffuse large B-cell lymphoma and Burkitt lymphoma	9680/3
B-cell lymphoma, unclassifiable, with features intermediate between diffuse large B-cell lymphoma and Hodgkin lymphoma	9596/3

MATURE T-CELL AND NK CELL NEOPLASMS	ICD-O
T-cell prolymphocytic leukaemia	9834/3
T-cell large granular lymphocytic leukaemia	9831/3
<i>Chronic lymphoproliferative disorder of NK-cells</i>	9831/3
Aggressive NK cell leukaemia	9948/3
Systemic EBV positive T-cell lymphoproliferative disease of childhood	9724/3
Hydroa vacciniforme-like syndrome	9725/3
Adult T-cell leukaemia/lymphoma	9827/3
Extranodal NK/T cell lymphoma, nasal type	9719/3
Enteropathy-associated T-cell lymphoma	9717/3
Hepatosplenic T-cell lymphoma	9716/3
Subcutaneous panniculitis-like T-cell lymphoma	9708/3
Mycosis fungoides	9700/3
Sézary syndrome	9701/3
Primary cutaneous CD30 positive T-cell lymphoproliferative disorders	
Lymphomatoid papulosis	9718/1
Primary cutaneous anaplastic large cell lymphoma	9718/3
Primary cutaneous gamma-delta T-cell lymphoma	9726/3
<i>Primary cutaneous CD8 positive aggressive epidermotropic cytotoxic T-cell lymphoma</i>	9709/3
<i>Primary cutaneous VD4 positive small/medium T-cell lymphoma</i>	9709/3
Peripheral T-cell lymphoma, unspecified	9702/3
Angioimmunoblastic T-cell lymphoma	9705/3
Anaplastic large cell lymphoma, ALK positive	9714/3
<i>Anaplastic large cell lymphoma, ALK negative</i>	9702/3
HODGKIN LYMPHOMA	
Nodular lymphocyte predominant Hodgkin lymphoma	9659/3
Classical Hodgkin lymphoma	9650/3
Nodular sclerosis classical Hodgkin lymphoma	9663/3
Lymphocyte-rich classical Hodgkin lymphoma	9651/3
Mixed cellularity classical Hodgkin lymphoma	9652/3
Lymphocyte-depleted classical Hodgkin lymphoma	9653/3

POST-TRANSPLANT LYMPHOPROLIFERATIVE DISORDERS**(PTLD)**

Early lesions

Plasmacytic hyperplasia 9971/1

Infectious mononucleosis-like PTLD 9971/1

Polymorphic PTLD 9971/3

Monomorphic PTLD (B- and T/NK-cell types)*

Classical Hodgkin lymphoma type PTLD*

** These are classified according to the lymphoma or leukaemia to which they correspond, and assigned the respective ICD-O Code*

NOS – not otherwise specified

Morphology code of the International Classification of Diseases (ICD-O), fourth edition.

Behaviour is coded /3 for malignant tumours and /1 for lesions of low or uncertain malignant potential.

The italics indicate provisional entities for the WHO working group felt that there was insufficient evidence to recognise them as distinct diseases at the time of compilation

8.2 Eastern Cooperative Oncology Group Performance Status [404]

<i>Score</i>	<i>Definition</i>
0	Asymptomatic (Fully active, able to carry on all pre-disease activities without restriction)
1	Symptomatic but completely ambulatory (Restricted in physically strenuous activity but ambulatory and able to carry out work of a light or sedentary nature. For example, light housework, office work)
2	Symptomatic, >50% in bed, but not bedbound (Capable of only limited self-care, confined to bed or chair 50% or more of waking hours)
3	Symptomatic, >50% in bed, but not bedbound (Capable of only limited self-care, confined to bed or chair 50% or more of waking hours)
4	Bedbound (Completely disabled. Cannot carry on any self-care. Totally confined to bed or chair)
5	Death

References

1. Bertrand, J.Y., et al., *Haematopoietic stem cells derive directly from aortic endothelium during development*. *Nature*, 2010. **464**(7285): p. 108-111.
2. Vassiliou, G. and A. Green, *Chapter 46. Myeloproliferative Disorders in Postgraduate Haematology*. 2005, Blackwell Publishing. p. 761-782.
3. Gordon, M., *Chapter 1. Stem Cells and Haemopoiesis.*, in *Postgraduate Haematology*. 2005, Blackwell Publishing. p. 1-12.
4. Delves, P.J., et al., *Roitt's Essential Immunology. Eleventh Edition*. 11 ed. Roitt's Essential Immunology. 2006: Blackwell Publishing.
5. Bain, B.J., *Chapter 3. Morphology of Blood Cells. Blood Cells A Practical Guide. 3rd Ed.*. 3rd ed. 2002: Blackwell Science.
6. Xing, L. and D.G. Remick, *Relative cytokine and cytokine inhibitor production by mononuclear cells and neutrophils*. *Shock*, 2003. **20**: p. 10-16.
7. Costa, J.J., P.F. Weller, and S.J. Galli, *The cells of the allergic response: mast cells, basophils, and eosinophils*. *JAMA*, 1997. **278**(22): p. 1815-22.
8. Robertson, M.J. and J. Ritz, *Biology and clinical significance of human natural killer cells*. *Blood*, 1990. **76**: p. 2421-38.
9. Farag, S.S. and M.A. Caligiuri, *Human natural killer cell development and biology*. *Blood Reviews*, 2006. **20**: p. 123-137.
10. Cooper, M.A., et al., *Human killer cells: a unique immunoregulatory role for CD56 bright subset*. *Blood*, 2001. **97**: p. 3146-3151.
11. Alpin, A.E., A.K. Howe, and R.L. Juliano, *Cell adhesion molecules, signal transduction and cell growth*. *Current Opinion in Cell Biology*, 1998. **11**: p. 737-744.
12. Clark, E.A. and J.S. Brugge, *Integrins and Transduction Pathways: The Road Taken*. *Science*, 1995. **268**: p. 233-239.
13. Oberholzer, A., C. Oberholzer, and L.L. Moldawer, *Cytokine signalling-regulation of the immune response in normal and critically ill states*. *Crit Care Med*, 2000. **28**(4): p. Supp.N3-12.
14. Parkin, J. and B. Cohen, *An Overview of the Immune System.*. *The Lancet*, 2001. **357**: p. 1777-89.
15. Strieter, R.M., J.A. Belperio, and M.P. Keane, *Cytokines in innate and host defense in the lung*. *J Clin Invest*, 2002. **109**: p. 699-705.
16. Bazzoni, F. and B. Beutler, *The Tumour necrosis factor ligand and receptor families*. *N Engl J Med*, 1996. **334**(26): p. 1717-25.
17. Issacs, A. and J. Lindenmann, *Virus Interference I. The interferon*. *Proc. Roy. Soc. London Ser. B*, 1957. **147**: p. 258-73.

18. Samuel, C.E., *Antiviral actions of Interferons*. Clinical Microbiology Reviews, 2001. **14**(4): p. 778-809.
19. Finter, N.B., *The naming of cats – and alpha interferons*. The Lancet, 1996. **348**(9024): p. 348-349.
20. Tonegawa, S., et al., *Evidence for Somatic Generation of Antibody Diversity (RNA.DNA hybridization/ κ -chain mRNA)*. Proc Natl Acad Sci, 1974. **71**(10): p. 4027-4031.
21. Coombs, R.R.A., A. Feinstein, and A.B. Wilson, *Immunoglobulin determinants on the surface of human lymphocytes*. Lancet, 1969. **294**(7631): p. 1157-1161.
22. Alt, F.W., T.K. Blackwell, and G.D. Yancopoulos, *Development of the primary antibody repertoire*. Science, 1987. **238**(4830): p. 1079-1087.
23. LeBien, T.W. and T.F. Tedder, *B lymphocytes: how they develop and function*. Blood, 2008. **112**(5): p. 1570-1580.
24. Zhang, Z., P.D. Burrows, and M.D. Cooper, *The molecular basis and biological significance of VH replacement*. Immunological Reviews, 2004. **197**(1): p. 231-242.
25. Nemazee, D.A. and K. Bürki, *Clonal deletion of B lymphocytes in a transgenic mouse bearing anti-MHC class I antibody genes*. Nature, 1989. **337**(6207): p. 562-566.
26. Corthésy, B., *Roundtrip Ticket for Secretory IgA: Role in Mucosal Homeostasis?* J Immunol, 2007. **178**: p. 27-32.
27. Janeway, C.A., et al., *Part IV. The Adaptive Immune Response. 9. The Humoral Immune Response*, in *Immunobiology*. 2001, Garland Science.
28. Reth, M., et al., *Activation of V kappa gene rearrangement in pre-B cells follows the expression of membrane-bound immunoglobulin heavy chains*. EBMO Journal, 1987. **6**(11): p. 3299-3305.
29. Le Franc, M.P., *Nomenclature of the human immunoglobulin heavy (IGH) genes*. Exp Clin Immunogenet, 2001. **18**(2): p. 100-16.
30. Early, P., et al., *An immunoglobulin heavy chain variable region gene is generated from three segments of DNA: VH, D and JH*. Cell 1980. **19**(4): p. 981-992.
31. Oettinger, M.A., et al., *RAG-1 and RAG-2, adjacent genes that synergistically activate V(D)J recombination*. Science, 1990. **248**: p. 1517-1523.
32. Tonegawa, S., *Somatic generation of antibody diversity*. Nature, 1983. **302**: p. 575-581.
33. Edwards, J.C.W. and G. Cambridge, *B-cell targeting in rheumatoid arthritis and other autoimmune diseases*. Nat Rev Immunol, 2006. **6**: p. 394-403.

34. Janeway, C.A., et al., *Part II. The Recognition of Antigen 3. Antigen Recognition by B-cell and T-cell Receptors*, in *Immunobiology*. 2001, Garland Science.
35. Kawabe, T., et al., *The immune responses in CD40-deficient mice: Impaired immunoglobulin class switching and germinal center formation*. *Immunity*, 1994. **1**(3): p. 167-178.
36. Liu, Y.J., et al., *Within germinal centers, isotype switching of the immunoglobulin occurs after the onset of somatic mutation*. *Immunity*, 1996. **4**: p. 241-259.
37. Li, Z., et al., *The generation of antibody diversity through somatic hypermutation and class switch recombination*. *Genes Dev*, 2004. **18**: p. 1-11.
38. Gross, J., et al., *TACI-Ig neutralizes molecules critical for B cell development and autoimmune disease: Impaired B cell maturation in mice lacking BLyS*. *Immunity*, 2001. **15**: p. 289-302.
39. Kehry, M., *CD40-mediated signaling in B cells: Balancing cell survival, growth and death*. *J. Immunol*, 1996. **156**(7): p. 2345-2348.
40. Coutinho, A., et al., *Mechanism of Thymus-Independent Immunocyte triggering: Mitogenic activation of B cells results in specific immune responses*. *J. Exp. Med*, 1974. **139**: p. 74-92.
41. Snapper, C., et al., *Induction of IgG3 secretions by interferon γ : A model for T cell-independent class switching in response to T cell-independent type 2 antigens*. *J. Exp. Med*, 1992. **175**: p. 1367-1371.
42. Prockop, S. and H.T. Petrie, *Cell migration and the anatomic control of thymocyte precursor differentiation*. *Seminars in Immunology*, 2000. **12**: p. 435-444.
43. Fehling, H.J. and e. al., *Crucial role of the pre-T-cell receptor alpha gene in alpha beta but not gamma delta T cells* *Nature*, 1995. **375**(6534): p. 795-798.
44. Capone, M., D. Hockett, and A. Zlotnik, *Kinetics of T cell receptor β , γ and δ rearrangements during adult thymic development: T cell receptor rearrangements are present in CD44⁺CD25⁺ pro-T thymocytes*. *Proc Natl Acad Sci*, 1998. **95**(21): p. 12522-12527.
45. Pardoll, D.M., et al., *Differential expression of two distinct T-cell receptors during thymocyte development*. *Nature*, 1987. **326**: p. 79-81.
46. Winoto, A. and D. Baltimore, *Separate lineages of T-cells expressing the alpha beta and gamma delta receptors*. *Nature*, 1989. **338**(6214): p. 430-432.
47. Xiong, N. and D.H. Raulet, *Development and selection of $\gamma\delta$ T cells*. *Immunological Reviews*, 2007. **215**: p. 15-31.
48. van Kooten, C. and J. Banchereau, *CD40-CD40 Ligand*. *Journal of Leukocyte Biology*, 2000. **67**.
49. Zúñiga-Pflücker, J.C., *T-cell development made simple*. *Nat Rev Immunol*, 2004. **4**(1): p. 67-72.

50. Young, A.J., *The physiology of lymphocyte migration through the single lymph node in vivo*. Seminars in Immunology, 1999. **11**: p. 73-83.
51. Geoffroy, J.S. and S.D. Rosen, *Demonstration that a lectin-like receptor (gp^{90MEL}) directly mediates adhesion of lymphocytes to high endothelial venules of lymph nodes*. J Cell Biol, 1989. **109**: p. 2463-2469.
52. Bajénoff, M., S. Granjeaud, and S. Guerder, *The Strategy of T Cell Antigen-presenting Cell Encounter in Antigen-draining Lymph Nodes Revealed by Imaging of Initial T Cell Activation*. J Exp Med, 2003. **198**(5): p. 715-724.
53. Dieu, M.-C., et al., *Selective Recruitment of Immature and Mature Dendritic Cells by Distinct Chemokines Expressed in Different Anatomic Sites*. J Exp Med, 1998. **188**(2): p. 373-386.
54. Banchereau, J. and R.M. Steinman, *Dendritic cells and the control of immunity*. Nature, 1998. **392**: p. 245-252.
55. Villadangos, J.A., P. Schnorrer, and N.S. Wilson, *Control of MHC class II antigen presentation in dendritic cells: a balance between creative and destructive forces*. Immunological Reviews, 2005. **207**: p. 191-205.
56. Zamoyska, R., *CD4 and CD8: Modulators of T-cell receptor recognition of antigen and of immune responses?* Current Opinion in Immunology, 1998. **10**: p. 82-87.
57. Zinkernagel, R.M., *The Nobel Lectures in Immunology. The Nobel Prize for Physiology or Medicine, 1996. Cellular immune recognition and the biological role of major transplant antigens*. Scand J Immunol, 1997. **46**: p. 421-436.
58. Weissman, A.M., *The T-cell antigen receptor; a multisubunit signaling complex*. Chem Immunol, 1994. **59**: p. 1-18.
59. June, C.H., et al., *Role of the CD28 receptor in T cell activation*. Immunology Today, 1990. **11**: p. 211-216.
60. Wang, S. and L. Chen, *T lymphocyte co-signalling pathways of the B7-CD28 family*. Cellular & Molecular Immunology, 2004. **1**(1): p. 37-42.
61. Cher, D. and T. Mosmann, *Two types of murine helper T clone. II. Delayed type hypersensitivity is mediated by Th1 clones*. J Immunol, 1987. **138**: p. 3688-94.
62. Constant, S.L. and K. Bottomly, *Induction of the TH1 and TH2 CD4+ responses: The Alternative Approach*. Annual Reviews in Immunology, 1997. **15**: p. 297-322.
63. Killar, L., et al., *Cloned, Ia-restricted T cells that do not produce interleukin 4(IL 4)/B cell stimulatory factor 1(BSF-1) fail to help antigen-specific B cells* J Immunol, 1987. **138**(6): p. 1674-1679.
64. Harrington, L.E., et al., *Interleukin 17-producing CD4+ effector T cells develop via a lineage distinct from the T helper type 1 and 2 lineages*. Nature Immunology, 2005. **6**(11): p. 1123-1132.

65. Breitfeld, D., et al., *Follicular B Helper T cells Express CXC Chemokine Receptor 5, Localize to B Cell Follicles, and Support Immunoglobulin Production*. J. Exp. Med, 2000. **192**(11): p. 1545-1551.
66. Schaerli, P., et al., *CXC Chemokine Receptor 5 Expression Defines Follicular Homing T Cells with B Cell Helper Function*. J. Exp. Med, 2000. **192**(11): p. 1553-1562.
67. Vogelzang, A., et al., *A Fundamental Role for Interleukin-21 in the Generation of T Follicular Helper Cells*. Immunity, 2008. **29**: p. 127-137.
68. Andersen, M.H., et al., *Cytotoxic T cells*. J Invest Dermatol, 2006. **126**: p. 32-41.
69. Nagata, S., *Fas-mediated apoptosis*. Adv Exp Med Biol, 1996. **406**: p. 119-124.
70. Blott, E.J. and G.M. Griffiths, *Secretory Lysosomes*. Nat Rev Mol Cell Biol, 2002. **3**: p. 122-131.
71. Peters, P.J. and e. al., *Cytotoxic T lymphocyte granules are secretory lysosomes, containing both perforin and granzymes*. J Exp. Med, 1991. **173**: p. 1099-1109.
72. Sad, S., R. Marcotte, and T.R. Mosmann, *Cytokine-induced differentiation of precursor mouse CD8+ T cells into cytotoxic CD8+ T cells secreting Th1 or Th2 cytokines*. Immunity, 1995. **2**(3): p. 271-279.
73. Cools, N., et al., *Regulatory T cells and Human Disease*. Eur J Immunol, 2007. **2007**: p. 1-11.
74. Paust, S., et al., *Engagement of B7 on effector T cells by regulatory T cells prevents autoimmune disease*. Proc Natl Acad Sci, 2004. **101**(28): p. 10398-10403.
75. Shevach, E.M., et al., *Control of T cell activation by CD4+CD25+ supressor T cells*. Immunological Reviews, 2001. **182**: p. 58-67.
76. O'Garra, A. and P. Vieira, *Regulatory T cells and mechanisms of immune system control*. Nat Medicine, 2004. **10**: p. 801-805.
77. Suntharalingam, G., et al., *Cytokine Storm in a Phase I Trial of the Anti-CD28 Monoclonal Antibody TGN1412*. N Engl J Med, 2007. **355**: p. 1018-1028.
78. Zlotnik, A. and O. Yoshie, *Chemokines: A New Classiifcation and their role in immunity*. Immunity, 2000. **12**: p. 121-127.
79. Deuel, T.F., et al., *Amino acid sequence of platelet factor 4*. Proc Natl Acad Sci, 1997. **74**(6): p. 2256-2258.
80. Feng Y, et al., *HIV-1 entry cofactor: functional cDNA cloning of a seven-transmembrane, G protein-coupled receptor*. Science, 1996. **272**(5263): p. 872-7.
81. Dragic, T., et al., *HIV-1 entry into CD4+ cells is mediated by the chemokine receptor CC-CKR-5* Nature, 1996. **381**(6584): p. 667-73.

82. Liu, R., et al., *Homozygous defect in HIV-1 coreceptor accounts for resistance of some multiply-exposed individuals to HIV-1 infection*. *Cell*, 1996. **86**: p. 367-377.
83. Dean, M., et al., *Genetic restriction of HIV-1 infection and progression to AIDS by a deletion allele of the CCR5 structural gene*. *Science*, 1996. **273**: p. 1856-1862.
84. Gulick, R.M., et al., *Maraviroc for previously treated patients with R5 HIV-1 infection*. *N Engl J Med*, 2008. **359**(14): p. 1429-1441.
85. Allen, S., S. Crown, and T. Handel, *Chemokine: Receptor structure, Interactions and antagonism*. *Annual Review of Immunology*, 2007. **25**: p. 787-820.
86. Balkwill, F., *Cancer and the Chemokine Network* *Nat Rev Cancer*, 2004. **4**: p. 540-550.
87. Ajuebor, M.N., M.G. Swain, and M. Perretti, *Chemokines as novel therapeutic targets in inflammatory diseases*. *Biochemical Pharmacology*, 2002. **63**: p. 1191-1196.
88. Förster, R., et al., *CCR7 coordinates the primary immune response by establishing functional microenvironments in secondary lymphoid organs*. *Cell*, 1999. **99**(1): p. 23-33.
89. Proudfoot, A., *Chemokine receptors: Multifaceted Therapeutic Targets*. *Nature Reviews, Immunology*, 2002. **2**: p. 106-115.
90. Gong, J.-H. and I. Clark-Lewis, *Antagonists of monocyte chemoattractant protein-1 identified by modification of functionally critical NH2-terminal residues*. *J Exp. Med*, 1994. **181**(2): p. 631-640.
91. Jarnagin, K., et al., *Identification of Surface Residues of the Monocyte Chemotactic Protein 1 That Affect Signaling through the Receptor CCR2*. *Biochemistry*, 1999. **38**(49): p. 16167-16177.
92. Strieter, R.M., et al., *CXC chemokines in angiogenesis*. *Cytokine Growth Factor Rev*, 2005. **16**(6): p. 593-609.
93. Salcedo, R. and J. Oppenheim, *Role of chemokines in angiogenesis: CXCL12/SDF-1 and CXCR4 interaction, a key regulator of endothelial cell responses*. *Microcirculation*, 2003. **10**(3-4): p. 359-370.
94. Proudfoot, A.E.I., et al., *Glycosaminoglycan binding and oligomerization are essential for the in vivo activity of certain chemokines*. *Proc Natl Acad Sci*, 2003. **100**(4): p. 1885-1890.
95. Witt, D. and A. Lander, *Differential binding of chemokines to glycosaminoglycan subpopulations*. *Current Biology*, 1994. **4**(5): p. 394-400.
96. Kuschert, G.S.V., et al., *Glycosaminoglycans interact selectively with chemokines and modulate receptor binding and cellular responses*. *Biochemistry*, 1999. **38**(39): p. 12959-12968.

97. Guan, E., et al., *Natural truncation of the chemokine MIP-1 β / CCL4 affects receptor specificity but not anti-HIV-1 activity.* J Biol Chem, 2002. **277**: p. 32348-32352.
98. Guan, E., J. Wang, and M.A. Norcross, *Amino-terminal processing of MIP-1 β /CCL4 by CD26/dipeptidyl-petidase IV.* J Cell Biochem, 2004. **92**(1): p. 53-64.
99. Palczewski, K., et al., *Crystal structure of Rhodopsin: A G protein-coupled receptor.* Science, 2000. **289**(5480): p. 739-745.
100. Skelton, N., et al., *Structure of a CXC chemokine-receptor fragment in complex with interleukin-8.* Structure, 1999. **7**: p. 157-168.
101. Blanpain, C., et al., *The Core Domain of Chemokines Binds CCR5 Extracellular Domains while Their Amino Terminus Interacts with the Transmembrane Helix Bundle.* J. Biol. Chem, 2003. **278**(14): p. 5179-5187.
102. Damaj, B., et al., *Identification of G-protein binding sites of the human interleukin-8 receptors by functional mapping of the intracellular loops.* FASEB J, 1996. **10**: p. 1426-1434.
103. Baggiolini, M., A. Walz, and S. Kunkel, *Neutrophil-activating peptide-1/Interleukin 8, a novel cytokine that activates neutrophils.* J. Clin. Invest, 1989. **84**: p. 1045-1049.
104. Mellado, M., et al., *CHEMOKINE SIGNALING AND FUNCTIONAL RESPONSES: The Role of Receptor Dimerization and TK Pathway Activation.* Annual Review of Immunology, 2001. **19**: p. 397-421.
105. Shi, G., et al., *Identification of an alternative G α_q -dependant chemokine receptor signal transduction pathway in dendritic cells and granulocytes.* J Exp. Med, 2007. **204**(11): p. 2705-2718.
106. Berman, D., T. Wilkie, and A. Gilman, *GAIIP and RGS4 are GTPase-activating proteins for the Gi subfamily of G protein α subunits.* Cell, 1996. **86**: p. 445-452.
107. Hunt, T., et al., *RSG10 is a selective activator of G α_i GTPase activity.* Nature, 1996. **383**: p. 175-177.
108. Fukui, Y., et al., *Haematopoietic cell-specific CDM family protein DOCK2 is essential for lymphocyte migration.* Nature, 2001. **412**: p. 826-831.
109. Xu, J., et al., *Divergent signals and cytoskeletal assemblies regulate self-organizing polarity in neutrophils.* Cell, 2003. **114**(2): p. 201-214.
110. Benovi, J., et al., *β -adrenergic receptor kinase: Identification of a novel protein kinase that phosphorylates the agonist-occupied form of the receptor.* Proc Natl Acad Sci, 1986. **83**(9): p. 2797-2801.
111. Goodman, O., et al., *Arrestin/Clathrin Interaction Localization of the arrestin binding locus to the clathrin terminal domain.* J Biol Chem, 1997. **272**(23): p. 15017-15022.

112. Laporte, S., et al., *The β_2 -adrenergic receptor / β arrestin complex recruits clathrin adaptor AP-2 during endocytosis*. Proc Natl Acad Sci, 1999. **96**: p. 3712-3717.
113. Warnock, D. and S. Schmid, *Dynamin GTPase, a force-generating molecular switch*. BioEssays, 1996. **18**(11): p. 885-893.
114. Neel, N., et al., *Chemokine receptor internalization and intracellular trafficking*. Cytokine & Growth Factor Review, 2005. **16**: p. 637-658.
115. Zerial, M. and H. McBride, *Rab proteins as membrane organizers*. Nat Rev Mol Cell Biol, 2001. **2**: p. 107-119.
116. Venkatesan, S., et al., *Distinct mechanisms of agonist-induced endocytosis for human chemokine receptors CCR5 and CXCR4*. Molecular Biology of the Cell, 2003. **14**: p. 3305-3324.
117. Fan, G.-H., et al., *Differential regulation of CXCR2 trafficking by Rab GTPases*. Blood, 2003. **101**(6): p. 2115-2124.
118. Otero, C., M. Groettrup, and L. DF, *Opposite fate of endocytosed CCR7 and its ligands: Recycling versus degradation*. Journal of Immunology, 2006. **177**: p. 2314-2323.
119. Bardi, G., et al., *The T cell receptor CCR7 is internalized on stimulation with ELC, but not with SLC*. Eur. J. Immunol., 2001. **31**: p. 3291-3297.
120. Signoret, N., et al., *Endocytosis and recycling of the HIV co-receptor CCR5*. J Cell Biol, 2000. **151**(6): p. 1281-1293.
121. Neote, K., et al., *Functional and biochemical analysis of the cloned Duffy Antigen: Identity with the red blood cell chemokine receptor*. Blood, 1994. **84**(1): p. 44-52.
122. Nibbs, R., et al., *Cloning and Characterization of a Novel Promiscuous Human β -Chemokine Receptor D6*. J Biol Chem, 1997. **272**: p. 32078-83.
123. Hadley, T. and S. Peiper, *From Malaria to Chemokine Receptor: The Emerging Physiologic Role of the Duffy Blood Group Antigen*. Blood, 1997. **89**(9): p. 3077-3091.
124. Jamieson, T., et al., *The chemokine receptor D6 limits the inflammatory response in vivo*. Nat Immunol, 2005. **6**: p. 403-411.
125. Feng, L.-Y., et al., *Involvement of a Novel Chemokine Decoy Receptor CCX-CKR in Breast Cancer Growth, Metastasis and Patient Survival*. Clinical Cancer Research, 2009. **15**(9): p. 2962-2970.
126. Weber, M., et al., *The chemokine receptor D6 constitutively traffics to and from the cell surface to internalize and degrade chemokines*. Mol. Cell. Biol, 2004. **15**: p. 2492-2508.
127. Comerford, I., et al., *The chemokine receptor CCX-CKR mediates effective scavenging of CCL19 in vitro*. Eur. J. Immunol., 2006. **36**(7): p. 1904-1916.

128. Springer, T.A., *Traffic signals for lymphocyte recirculation and leukocyte emigration: the multi-step paradigm*. Cell, 1994. **76**: p. 301-314.
129. Cinamon, G., et al., *Sphingosine 1-phosphate receptor 1 promotes B cell localization in the splenic marginal zone*. Nat Immunol, 2004. **5**: p. 713-720.
130. Misslitz, A., et al., *Thymic T cell development and progenitor localization depend on CCR7*. J Exp. Med, 2004. **200**(4): p. 481-491.
131. Kwan, J. and N. Killeen, *CCR7 directs migration of thymocytes into the thymic medulla*. J Immunol, 2004. **172**: p. 3999-4007.
132. Plotkin, J., et al., *Critical role for CXCR4 signalling in progenitor localization and T cell differentiation in the postnatal thymus*. J Immunol, 2003. **171**: p. 4521-4527.
133. Hernández-López, C., et al., *Stromal cell-derived factor 1/CXCR4 signaling is crucial for early T-cell development*. Blood, 2002. **99**(2): p. 546-554.
134. Benz, C., K. Heinzel, and C. Bleul, *Homing of immature thymocytes to the subcapsular microenvironment within the thymus is not an absolute requirement for T cell development*. Eur. J. Immunol., 2004. **34**: p. 3652-3663.
135. Annuziato, F., et al., *Macrophage-derived chemokine and EB11-ligand chemokine attract human thymocytes in different stage of development and are produced by distinct subsets of medullary epithelial cells: Possible implications for negative selection*. J Immunol, 2000. **165**: p. 238-246.
136. Campbell, D.J., C.H. Kim, and E.C. Butcher, *Chemokines in the systemic organization of immunity*. Immunological Reviews, 2003. **195**: p. 58-71.
137. Ueno, T., et al., *Role for CCR7 ligands in the emigration of newly generated T lymphocytes from the neonatal thymus*. Immunity, 2002. **16**: p. 205-218.
138. Stein, J.V. and C. Nombela-Arrieta, *Chemokine control of lymphocyte trafficking: a general overview*. Immunology 2005. **116**: p. 1-12.
139. Egawa, T., et al., *The earliest stages of B cell development require a chemokine stromal cell-derived factor/Pre-B cell growth-stimulating factor*. Immunity, 2001. **15**: p. 323-334.
140. Ma, Q., D. Jones, and T.A. Springer, *The chemokine receptor CXCR4 is required for the retention of B lineage and granulocytic precursors within the bone marrow microenvironment*. Immunity, 1999. **10**: p. 463-471.
141. Glodek, A., et al., *Sustained activation of cell adhesion is a differentially regulated process in B lymphopoiesis*. J Exp. Med, 2003. **197**(4): p. 461-473.
142. Wurbel, M.-A., et al., *Mice lacking the CCR9 CC-chemokine receptor show a mild impairment of early T- and B-cell development and a reduction in T-cell receptor $\gamma\delta^+$ gut intraepithelial lymphocytes*. Blood, 2001. **98**(9): p. 2626-2632.
143. Bowman, E., et al., *Developmental switches in chemokine response profiles during B cell differentiation and maturation*. J Exp. Med, 2000. **191**(8): p. 1303-1317.

144. Nakano, H., et al., *Genetic defect in T lymphocyte-specific homing into peripheral lymph nodes*. Eur. J. Immunol., 1997. **27**(1): p. 215-221.
145. Mori, S., et al., *Mice lacking expression of chemokines CCL21-Ser and CCL19 (plt Mice) demonstrate delayed but enhanced T cell immune responses*. J. Exp. Med., 2001. **193**(2): p. 207-217.
146. Okada, T., et al., *Chemokine requirements for B cell entry to lymph nodes and Peyer's patches*. J. Exp. Med., 2002. **196**(1): p. 65-75.
147. Nie, Y., et al., *The Role of CXCR4 in Maintaining Peripheral B Cell Compartments and Humoral Immunity*. J Exp. Med, 2004. **200**(9): p. 1145-1156.
148. Miller, M., et al., *Autonomous T cell trafficking examined in vivo with intravital two-photon microscopy*. Proc Natl Acad Sci, 2003. **100**(5): p. 2604-2609.
149. Wei, S., et al., *A stochastic view of lymphocyte trafficking within the lymph node*. Immunological Reviews, 2003. **195**: p. 136-159.
150. Matloubian, M., et al., *Lymphocyte egress from thymus and peripheral lymphoid organs is dependant on SIP receptor 1*. Nature, 2004. **427**(6972): p. 355-360.
151. Kunkel, E.J., et al., *Lymphocyte CC chemokine receptor 9 and epithelial thymus-expressed chemokine (TECK) expression distinguish the small intestinal immune compartment: epithelial expression of tissue-specific chemokines as an organizing principle in regional immunity*. J Exp Med, 2000. **192**: p. 761-768.
152. Svenson, M., et al., *CCL25 mediates the localization of recently activated CD8 $\alpha\beta$ ⁺ lymphocytes to the small-intestinal mucosa*. J Clin Invest, 2002. **110**(8): p. 1113-1121.
153. Sigmundsdottir, H., et al., *DCs metabolize sunlight-induced vitamin D3 to 'program' T cell attraction to the epidermal chemokine CCL27*. Nat Immunol, 2007. **8**(3): p. 285-293.
154. Iwata, M., et al., *Retinoic Acid Imprints Gut-Homing Specificity on T Cells*. Immunity, 2004. **21**(4): p. 527-538.
155. Wang, C., et al., *Retinoic acid determines the precise tissue tropism of inflammatory Th17 cells in the intestine*. J Immunol, 2010. **184**: p. 5519-5526.
156. Dutton, R.W., L.M. Bradley, and S.L. Swain, *T cell memory*. Annual Review of Immunology, 1998. **16**: p. 201-223.
157. Sallusto, F., et al., *Two subsets of memory T lymphocytes with distinct homing potentials and effector functions*. Nature, 1999. **401**: p. 708-12.
158. Román, E., et al., *CD4 Effector T cell subsets in Response to Influenza: Heterogeneity, migration and function*. J. Exp. Med, 2002. **196**(7): p. 957-968.
159. Weninger, W., et al., *Naive T cell recruitment to nonlymphoid tissues: A role for endothelium expressed CC chemokine ligand 21 in autoimmune disease and lymphoid neogenesis*. J. Immunol, 2002. **170**: p. 4638-4648.

160. Unsoeld, H. and H. Pircher, *Complex memory T-cell phenotypes revealed by coexpression of CD67 and CCR7*. Journal of Virology, 2005. **79**(7): p. 4510-4513.
161. Bonecchi, R., et al., *Differential expression of chemokine receptors and chemotactic responsiveness of type 1 T helper cells (Th1s) and Th2s*. J. Exp. Med, 1998. **187**(1): p. 129-134.
162. Ward, S., K. Bacon, and J. Westwick, *Chemokines and lymphocytes: More than an attraction*. Immunity, 1998. **9**: p. 1-11.
163. Campbell, D.J., C.H. Kim, and E.C. Butcher, *Separable effector T cell populations specialized for B cell help or tissue inflammation*. Nat Immunol, 2001. **2**(9): p. 876-81.
164. Sato, W., T. Aranami, and T. Yamamura, *Cutting Edge: Human Th17 cells are identified as bearing CCR2⁺CCR5⁻ phenotype*. J. Immunol, 2007. **178**: p. 7525-7529.
165. Lim, H., et al., *Human Th17 cells share major trafficking receptors with both polarized effector cells and FOXP3⁺ regulatory T cells*. J. Immunol, 2008. **180**: p. 122-129.
166. Lehmann, J., et al., *Expression of the integrin $\alpha_E\beta_7$* . Proc Natl Acad Sci, 2002. **99**(20): p. 13031-13036.
167. Huehn, J., et al., *Developmental stage, phenotype and migration distinguish naive- and effector/memory- like CD4⁺ regulatory T cells*. J. Exp. Med, 2004. **199**(3): p. 303-313.
168. Allen, C., et al., *Germinal center dark and light zone organization is mediated by CXCR4 and CXCR5*. Nat Immunol, 2004. **5**(9): p. 943-952.
169. Cyster, J., et al., *Follicular stromal cells and lymphocyte homing to follicles*. Immunological Reviews, 2000. **176**: p. 181-193.
170. Hodgkin, T., *On some appearances of the absorbent glands and spleen*. Med Chir Soc Trans, 1832. **17**: p. 68-114.
171. Wilks, S., *Cases of enlargement of the lymphatic glands and spleen (or Hodgkin's disease) with remarks*. Guy's Hops Rep, 1865. **11**: p. 56-67.
172. Sternberg, C., *Über eine eigenartige unter dem Bilde der Pseudoleukämie verlaufende Tuberculose des lymphatischen Apparates*. Ztschr Heilk, 1898. **19**: p. 21-90.
173. Reed, D., *On the pathological changes in Hodgkin's disease, with special reference to its relation to tuberculosis*. Johns Hopkins Hosp Rep, 1902. **10**: p. 133-96.
174. Goodman, L., et al., *Nitrogen mustard therapy. Use of methyl-bis(beta-chloroethyl)amine hydrochloride and tris(beta-chloroethyl)amine hydrochloride for Hodgkin's disease, lymphosarcoma, leukemia, and certain allied and miscellaneous disorders*. J Am Med Assoc, 1946. **105**: p. 475-476.

175. Rappaport, H., *Tumors of the Hematopoietic System. Atlas of Tumor Pathology, Section III, Fascicle 8*. Armed Forces Institute of Pathology, Washington DC, 1966: p. 97-98.
176. Swerdlow, S.H., et al., *WHO Classification of Tumours of Haematopoietic and Lymphoid Tissues*. 4th ed, ed. IARC. 2008, Lyon: IARC. 440.
177. Rosenberg, S., *Report of the committee on the staging of Hodgkin's disease*. Cancer Res, 1966. **26**: p. 1310.
178. Lister, T.A., et al., *Report of a committee convened to discuss the evaluation and staging of patients with Hodgkin's disease: Cotswolds meeting* J Clin Oncol, 1989. **7**(11): p. 1630-6.
179. ISD, *Trends in Cancer Survival in Scotland, 1980-2004*. ISD, National Services Scotland, 2007.
180. CRUK. *Cancer Incidence for common cancers - UK Statistics*. 2009; Available from: <http://info.cancerresearchuk.org/cancerstats/index.htm>.
181. Karipidis, K., et al., *Occupational exposure to ionizing and non-ionizing radiation and risk of non-Hodgkin lymphoma*. Int Arch Occup Environ Health, 2007. **80**: p. 663-67-.
182. Zhang, Y., et al., *Hair-coloring product use and risk of non-Hodgkin's lymphoma: A population-based case-control study in Connecticut*. Am J Epidemiol, 2004. **159**(2): p. 148-154.
183. Schöllkopf C, Ekström Smedby K, Hjalgrim H, Rostgaard K, Adami H-O, Melbye M. *Cigarette smoking and risk of non-Hodgkin's lymphoma - A population-based case-control study*. Cancer Epidemiol Biomarkers Prev. 2005; **14**(7):1791-6.
184. Cocco, P., et al., *Occupational exposure to solvents and risk of lymphoma subtypes: results from the EpiLymph case-control study*. Occup Environ Med, 2010. **67**: p. 341-347.
185. Richardson, D., C. Terschüren, and W. Hoffmann, *Occupational risk factors for non-Hodgkin's lymphoma: A population-based case-control study in Northern Germany*. Am J Ind Med, 2008. **51**: p. 258-268.
186. Li, S. and A. Lee, *Silicone implant and primary breast ALK1-negative anaplastic large cell lymphoma, fact or fiction?* Int J Clin Exp Pathol, 2010. **3**(1): p. 117-127.
187. Morton, L., et al., *Alcohol consumption and risk of non-Hodgkin lymphoma: a pooled analysis*. Lancet Oncology, 2005. **6**(7): p. 469-476.
188. Krickler, A., et al., *Personal sun exposure and risk of non-Hodgkin lymphoma: A pooled analysis from the Interlymph Consortium*. Int J Cancer, 2008. **122**: p. 144-154.
189. Burkitt, D., *A sarcoma involving the jaws in African children*. B J Surg, 1958. **46**(197): p. 218-23.

190. Epstein, M., B. Achong, and Y. Barr, *Virus particles in cultured lymphoblasts from Burkitt's lymphoma*. *Lancet*, 1964. **1**: p. 702-703.
191. Ziegler, J., et al., *Outbreak of Burkitt's-like lymphoma in homosexual men*. *Lancet*, 1982. **2**: p. 631-633.
192. MacMahon, E., et al., *Epstein-Barr virus in AIDS-related primary central nervous system lymphoma*. *Lancet*, 1991. **338**(8773): p. 969-973.
193. Blattner, W., et al., *The human type-C retrovirus, HTLV, in blacks from the Caribbean region, and relationship to adult T-cell leukemia/lymphoma*. *Int J Cancer*, 1982. **30**: p. 257-64.
194. Pozzato, G., et al., *Low-grade malignant lymphoma, hepatitis C virus infection, and mixed cryoglobulinemia*. *Blood*, 1994. **9**: p. 3047-3053.
195. Carbone, A. and G. Gaidano, *HHV-8 positive body cavity-based lymphoma: a novel lymphoma entity*. *Br J Haematol.*, 1997. **97**: p. 515-522.
196. Parsonnett, J., et al., *Helicobacter pylori Infection and Gastric Lymphoma*. *N Engl J Med*, 1994. **330**: p. 1267-1271.
197. Wündisch, T., et al., *Long-Term Follow-Up of Gastric MALT Lymphoma After Helicobacter Pylori Eradication*. *J Clin Oncol*, 2005. **23**(31): p. 8018-8024.
198. Ferreri, A., et al., *Evidence for an Association Between Chlamydia psittaci and Ocular Adnexal Lymphomas*. *J Natl Cancer Inst*, 2004. **96**(8): p. 586-94.
199. Garbe, C., et al., *Borrelia burgdorferi—associated cutaneous B cell lymphoma: Clinical and immunohistologic characterization of four cases*. *J Am Acad Derm*, 1991. **24**(4): p. 584-590.
200. Ekström Smedby, K., E. Baecklund, and J. Askling, *Malignant lymphomas in autoimmunity and inflammation: A review of risks, risk factors, and lymphoma characteristics*. *Cancer Epidemiol Biomarkers Prev*, 2006. **15**(11): p. 2069-2077.
201. Gottschalk, S., C. Rooney, and H. Heslop, *Post-transplant lymphoproliferative disorders*. *Annu. Rev. Med.*, 2005. **56**: p. 29-44.
202. Raghavan, S., et al., *A non-B-DNA structure at the Bcl-2 major breakpoint region is cleaved by the RAG complex*. *Nature*, 2004. **428**(6978): p. 88-93.
203. Reed, J., *Bcl-2 and the regulation of programmed cell death*. *J Cell Biol*, 1994. **124**(1&2): p. 1-6.
204. Swerdlow, S.H. and M.E. Williams, *From centrocytic to mantle cell lymphoma: A clinicopathologic and molecular review of 3 decades*. *Hum Pathol*, 2002. **33**(1): p. 7-20.
205. Tsai, A.G., et al., *Human chromosomal translocations at CpG sites and a theoretical basis for their lineage and stage specificity* *Cell*, 2008. **135**: p. 1130-1142.

206. Muramatsu, M., et al., *Class switch recombination and hypermutation require activation-induced cytidine deaminase (AID), a potential RNA editing enzyme*. *Cell*, 2000. **102**: p. 553-63.
207. Lenz, G. and L. Staudt, *Mechanisms of Disease. Aggressive Lymphomas*. *N Engl J Med*, 2010. **362**(15): p. 1417-1429.
208. Pasqualucci, L., et al., *Hypermutation of multiple proto-oncogenes in B-cell diffuse large B-cell lymphoma*. *Nature*, 2001. **412**: p. 341-346.
209. Robbiani, D., et al., *AID is required for the chromosomal breaks in c-myc that lead to c-myc/IgH translocations*. *Cell*, 2008. **135**: p. 1028-1038.
210. Hancock, B., et al., *Chlorambucil versus observation after anti-Helicobacter therapy in gastric MALT lymphomas: results of the international randomised LY03 trial*. *B J Haem*, 2009. **144**(3): p. 367-375.
211. Thieblemont, C., et al., *Treatment of splenic marginal zone B-cell lymphoma: an analysis of 81 patients*. *Clin Lymphoma*, 2002. **3**(1): p. 41-47.
212. Dave, S., et al., *Prediction of survival in Follicular lymphoma based on molecular features of tumour-infiltrating immune cells*. *N Engl J Med*, 2004. **351**(21): p. 2159-2169.
213. de Jong, D., *Molecular pathogenesis of follicular lymphoma: A cross talk of genetic and immunologic factors*. *J Clin Oncol*, 2005. **23**: p. 6358-6363.
214. Lenz, G., et al., *Stromal gene signatures in Large-B-cell lymphomas*. *N Engl J Med*, 2008. **359**(22): p. 2313-2323.
215. Avivi, I. and A. Goldstone, *Chapter 45. Aetiology and management of non-Hodgkin's lymphoma*, in *Postgraduate Haematology*. 2005, Blackwell Publishing Ltd. p. 735-760.
216. Wotherspoon, A., et al., *Chapter 2. Pathology and Cytogenetics*, in *Lymphoma Pathology, Diagnosis and Treatment*. 2007, Cambridge University Press. p. 12-18.
217. Jerusalem, G., et al., *Whole-body positron emission tomography using 18F-fluorodeoxyglucose for posttreatment evaluation in Hodgkin's disease and non-Hodgkin's lymphoma has a higher diagnostic and prognostic value than classical computed tomography scan imaging*. *Blood*, 1999. **94**(2): p. 429-433.
218. Coiffier, B., et al., *CHOP Chemotherapy plus Rituximab Compared with CHOP Alone in Elderly Patients with Diffuse Large-B-Cell Lymphoma*. *N Engl J Med*, 2002. **346**(4): p. 235-242.
219. Haque, T., et al., *Treatment of Epstein-Barr-virus-positive post-transplantation lymphoproliferative disease with partly HLA-matched allogeneic cytotoxic T cells*. *Lancet*, 2002. **360**(9331): p. 436-442.
220. Fisher, F., et al., *Multicenter Phase II Study of Bortezomib in Patients With Relapsed or Refractory Mantle Cell Lymphoma*. *J Clin Oncol*, 2006. **24**(30): p. 4867-4874.

221. Olsen, E., et al., *Phase IIB Multicenter Trial of Vorinostat in Patients With Persistent, Progressive, or Treatment Refractory Cutaneous T-Cell Lymphoma*. *J Clin Oncol*, 2007. **25**(21): p. 3109-3115.
222. Richardson, S., et al., *Activity of thalidomide and lenalidomide in mantle cell lymphoma*. *Acta Haematol*, 2010. **123**(1): p. 21-29.
223. Bastard, C., et al., *LAZ3 rearrangements in non-Hodgkin's lymphoma: Correlation with histology, immunophenotype, karyotype, and clinical outcome in 217 patients*. *Blood*, 1994. **83**(9): p. 2423-2427.
224. Weiss, L., et al., *Molecular analysis of the t(14;18) chromosomal translocation in malignant lymphomas*. *N Engl J Med*, 1987. **317**(19): p. 1185-1189.
225. Le Gouill, S., et al., *The clinical presentation and prognosis of diffuse large B-cell lymphoma with t(14;18) and 8q24/c-MYC rearrangement*. *Haematologica*, 2007. **92**(10): p. 1335-1342.
226. Hans, C., et al., *Confirmation of the molecular classification of diffuse large B-cell lymphoma by immunohistochemistry using a tissue microarray*. *Blood*, 2004. **103**(1): p. 275-282.
227. Sehn, L., et al., *The revised international prognostic index (R-IPI) is a better predictor of outcome than the standard IPI for patients with diffuse large B-cell lymphoma treated with R-CHOP*. *Blood*, 2007. **109**(5): p. 1857-1861.
228. Armitage, J., *How I treat patients with diffuse large B-cell lymphoma*. *Blood*, 2007. **110**(1): p. 29-36.
229. Pfreundschuh, M., et al., *CHOP-like chemotherapy plus rituximab versus CHOP-like chemotherapy alone in young patients with good-prognosis diffuse large-B-cell lymphoma: a randomised controlled trial by the MabThera International Trial (MInT) Group*. *Lancet Oncol.*, 2006. **379**(5): p. 379-391.
230. DeAngelis, L., et al., *Combination Chemotherapy and Radiotherapy for Primary Central Nervous System Lymphoma: Radiation Therapy Oncology Group Study 93-10*. *J Clin Oncol*, 2002. **20**(24): p. 4643-4648.
231. Gisselbrecht, C., et al., *Salvage Regimens With Autologous Transplantation for Relapsed Large B-Cell Lymphoma in the Rituximab Era*. *J Clin Oncol*, 2010. **28**(27): p. 1-19.
232. Fisher, F., et al., *New Treatment Options Have Changed the Survival of Patients With Follicular Lymphoma*. *J Clin Oncol*, 2005. **23**: p. 8847-8452.
233. Anon, *A Clinical Evaluation of the International Lymphoma Study Group Classification of Non-Hodgkin's Lymphoma. The Non-Hodgkin's Lymphoma Classification Project*. *Blood*, 1997. **89**: p. 3909-3918.
234. Solal-Céligny, P., et al., *Follicular Lymphoma International Prognostic Index*. *Blood*, 2004. **104**(5): p. 1258-1265.

235. Federico, M., et al., *Follicular Lymphoma International Prognostic Index 2: A New Prognostic Index for Follicular Lymphoma Developed by the International Follicular Lymphoma Prognostic Factor Project*. J Clin Oncol, 2009. **27**(27): p. 4555-4562.
236. Ardeschna, K., et al., *Long-term effect of a watch and wait policy versus immediate systemic treatment for asymptomatic advanced-stage non-Hodgkin lymphoma: a randomised controlled trial*. Lancet, 2003. **362**(9383): p. 516-522.
237. Marcus, R., et al., *CVP chemotherapy plus rituximab compared with CVP as first-line treatment for advanced follicular lymphoma*. Blood, 2005. **105**(4): p. 1417-1423.
238. Hiddemann, W., et al., *Frontline therapy with rituximab added to the combination of cyclophosphamide, doxorubicin, vincristine, and prednisone (CHOP) significantly improves the outcome for patients with advanced-stage follicular lymphoma compared with therapy with CHOP alone: results of a prospective randomized study of the German Low-Grade Lymphoma Study Group*. Blood, 2005. **106**(12): p. 3725-3732.
239. Salles, G., et al., *Rituximab maintenance for 2 years in patients with untreated high tumour burden follicular lymphoma after response to immunochemotherapy*. J Clin Oncol, 2010. **28**(7s): p. Abstract No: 8004.
240. Schouten, H., et al., *High-Dose Therapy Improves Progression-Free Survival and Survival in Relapsed Follicular Non-Hodgkin's Lymphoma: Results From the Randomized European CUP Trial*. J Clin Oncol, 2003. **21**(21): p. 3918-3927.
241. Gribben, J., *How I treat indolent lymphoma*. Blood, 2007. **109**: p. 4617-4626.
242. van Oers, M., et al., *Rituximab maintenance improves clinical outcome of relapsed/resistant follicular non-Hodgkin lymphoma in patients both with and without rituximab during induction: results of a prospective randomized phase 3 intergroup trial*. Blood, 2006. **108**(10): p. 3295-3301.
243. de Boer, C., et al., *Cyclin D1 messenger RNA overexpression as a marker for mantle cell lymphoma*. Oncogene, 1995. **10**(9): p. 1833-40.
244. Salar, A., et al., *Gastrointestinal involvement in mantle cell lymphoma: a prospective clinic, endoscopic, and pathologic study*. Am J Surg Pathol, 2006. **30**(10): p. 1274-80.
245. Hoster, E., et al., *A new prognostic index (MIPI) for patients with advanced-stage mantle cell lymphoma*. Blood, 2008. **111**(2): p. 558-565.
246. Leitch, H., et al., *Limited-stage mantle-cell lymphoma*. Ann Oncol., 2003. **14**: p. 1555-1561.
247. Geisler, C., et al., *Long-term progression-free survival of mantle cell lymphoma after intensive front-line immunochemotherapy with in-vivo-purged stem cell rescue: a nonrandomised phase 2 multicenter study by the Nordic Lymphoma Group*. Blood, 2008. **112**(2687-2693).

248. Ghielmini, M. and E. Zucca, *How I treat mantle cell lymphoma*. *Blood*, 2009. **114**: p. 1469-1476.
249. Matutes, E. and A. Polliack, *Morphological and immunophenotypic features of chronic lymphocytic leukaemia*. *Rev Clin Exp Hematol.*, 2000. **4**(1): p. 22-47.
250. Wiestner, A., et al., *ZAP-70 expression identifies a chronic lymphocytic leukaemia subtype with unmutated immunoglobulin genes, inferior clinical outcome, and distinct gene expression profile*. *Blood*, 2003. **101**: p. 4944-4951.
251. Damle, R., et al., *IgV gene mutation status and CD38 expression as novel prognostic indicators in chronic lymphocytic leukaemia*. *Blood*, 1999. **94**: p. 1840-1847.
252. Döhner, H., et al., *Genomic aberrations and survival in chronic lymphocytic leukaemia*. *N Engl J Med*, 2000. **343**(26): p. 1910-1916.
253. Binet, J., A. Auquier, and G. Dighiero, *A new prognostic classification of chronic lymphocytic leukaemia derived from a multivariate survival analysis*. *Cancer* 1981. **48**(1): p. 198-206.
254. Rai, K., et al., *Clinical staging of chronic lymphocytic leukaemia*. *Blood*, 1975. **46**(2): p. 219-234.
255. Hallek, M., et al., *Guidelines for the diagnosis and treatment of chronic lymphocytic leukemia: a report from the International Workshop on Chronic Lymphocytic Leukemia updating the National Cancer Institute–Working Group 1996 guidelines*. *Blood*, 2008. **111**(12): p. 5446-5456.
256. Hallek, M., et al., *First-Line Treatment with Fludarabine (F), Cyclophosphamide (C), and Rituximab (R) (FCR) Improves Overall Survival (OS) in Previously Untreated Patients (pts) with Advanced Chronic Lymphocytic Leukemia (CLL): Results of a Randomized Phase III Trial On Behalf of An International Group of Investigators and the German CLL Study Group*. *Blood*, 2009. **114**(22): p. abstract 535.
257. Gribben, J., *How I treat CLL up front*. *Blood*, 2010. **115**(187-197).
258. Wayne, A. and W. Wilson, *Chapter 13. Burkitt's and Lymphoblastic Lymphomas, in Lymphoma Pathology, Diagnosis and Treatment*. 2007, Cambridge University Press. p. 182-199.
259. Reiter, A., et al., *Improved Treatment Results in Childhood B-Cell Neoplasms With Tailored Intensification of Therapy: A Report of the Berlin-Frankfurt-Münster Group Trial NHL-BFM 90*. *Blood*, 1999. **94**(10): p. 3294-3306.
260. Mead, G., et al., *An international evaluation of CODOX-M and CODOX-M alternating with IVAC in adult Burkitt's lymphoma: results of United Kingdom Lymphoma Group LY06 study*. *Ann Oncol.*, 2002. **13**: p. 1264-1274.
261. Dunleavy, K., et al., *A prospective study of dose-adjusted (DA) EPOCH with rituximab in adults with newly diagnosed Burkitt lymphoma: a regimen with high efficacy and low toxicity*. *Ann Oncol.*, 2009. **19**(S4): p. Abstract 009.

262. Doglioni, C., et al., *High incidence of primary gastric lymphoma in northeastern Italy*. *Lancet*, 1992. **339**: p. 834-835.
263. Zucca, E. and F. Bertoni, *Chapter 9. MALT lymphoma and other marginal zone lymphomas*, in *Lymphoma Pathology, Diagnosis and Treatment*. 2007, Cambridge University Press. p. 126-140.
264. Thieblemont, C., *Clinical presentation and management of marginal zone lymphomas*. *Hematology*, 2005. **2005**: p. 307-313.
265. Franco, V., et al., *Splenectomy influences bone marrow infiltration in patients with splenic marginal zone cell lymphoma with or without villous lymphocytes*. *Cancer*, 2001. **91**(2): p. 294-301.
266. Mestdagt, M., et al., *Transactivation of MCP-1/CCL2 by β -catenin/TCF-4 in human breast cancer cells*. *Int J Cancer*, 2006. **118**: p. 35-42.
267. Richmond, A., *NF- κ B, chemokine gene transcription and tumour growth*. *Nat Rev Immunol*, 2002. **2**: p. 664-674.
268. Mantovani, A., et al., *Chemokines in the recruitment and shaping of the leucocyte infiltrate of tumours*. *Semin Cancer Biol*, 2004. **14**(3): p. 155-160.
269. Mantovani, A., et al., *The chemokine system in cancer biology and therapy*. *Cytokine & Growth Factor Review*, 2010. **21**(2010): p. 27-39.
270. Aalinkeel, R., et al., *Gene expression of angiogenic factors correlates with metastatic potential of prostate cancer cells* *Cancer Res*, 2004. **64**: p. 5311-21.
271. Metas, J., et al., *The role of CXCR2/CXCL2 ligand biological axis in renal cell carcinoma*. *J Immunol*, 2005. **175**: p. 5351-5357.
272. Kryczek, I., et al., *CXCL12 and vascular endothelial growth factor synergistically induce neoangiogenesis in human ovarian cancers*. *Cancer Res*, 2005. **65**: p. 465-472.
273. Vetrano, S., et al., *The lymphatic system controls intestinal inflammation and inflammation-associated colon cancer through the chemokine decoy receptor D6*. *Gut*, 2010. **59**(2): p. 197-206.
274. Nibbs, R.J.B., et al., *The atypical chemokine receptor D6 suppresses the development of chemically induced skin tumors*. *J Clin Invest*, 2007. **117**: p. 1884-1892.
275. Pals, S., D. de Gorter, and M. Spaargaren, *Lymphoma dissemination: the other face of lymphocyte homing*. *Blood*, 2007. **110**(9): p. 3102-3111.
276. Hjelmström, P., *Lymphoid neogenesis: de novo formation of lymphoid tissue through expression of homing chemokines*. *J Leuk Biol*, 2001. **69**: p. 331-339.
277. Fan, L., et al., *Cutting Edge: Ectopic expression of chemokine TCA4/SLC is sufficient to trigger lymphoid neogenesis*. *J Immunol*, 2000. **164**: p. 3955-3959.
278. Luther, S.A., et al., *BLC expression in pancreatic islets causes B cell recruitment and lymphotoxin-dependant lymphoid neogenesis*. *Immunity*, 2000. **12**: p. 471-481.

279. Lam, K.Y., et al., *Malignant lymphoma of the thyroid. A 30-year clinicopathologic experience and an evaluation of the presence of Epstein-Barr virus*. *Am J Clin Pathol*, 1999. **112**(2): p. 263-270.
280. Aust, G., et al., *The role of CXCR5 and its ligand CXCL13 in the compartmentalization of lymphocytes in thyroids affected by autoimmune thyroid diseases*. *Eur. J. Endocrine*, 2004. **150**: p. 225-234.
281. Holm, L.E., H. Blomgren, and T. Lowhagen, *Cancer risks in patients with chronic lymphocytic thyroiditis*. *N Engl J Med*, 1985. **312**(10): p. 601-604.
282. Burger, J.A., et al., *The microenvironment in mature B-cell malignancies: a target for new treatment strategies*. *Blood*, 2009. **114**(16): p. 3367-3375.
283. Kurtova, A.V., et al., *Mantle cell lymphoma cells express high levels of CXCR4, CXCR5 and VLA-4 (CD49d): importance for interactions with the stromal microenvironment and specific targeting*. *Blood*, 2009. **113**: p. 4604-4613.
284. Grogg, K.L., et al., *Expression of CXCL13, a chemokine highly upregulated in germinal center T-helper cells, distinguishes angioimmunoblastic T-cell lymphoma from peripheral T-cell lymphoma, unspecified*. *Modern Pathology*, 2006. **19**: p. 1101-1107.
285. Dunleavy, K. and W.H. Wilson, *Angioimmunoblastic T-cell lymphoma: Immune modulation as a therapeutic strategy*. *Leuk Lymphoma*, 2007. **48**(3): p. 449-451.
286. Corcione, A., et al., *CCL19 and CXCL12 trigger in vivo chemotaxis of human mantle cell lymphoma B cells*. *Clin Cancer Res*, 2004. **10**: p. 964-971.
287. Sokolowska-Wojdylo, M., et al., *Circulating clonal CLA+ and CD4+ cells in Sézary Syndrome express the skin-homing chemokine receptors CCR4 and CC10 as well as lymph node-homing chemokine receptor CCR7*. *British Journal of Dermatology*, 2005. **152**(2): p. 258-264.
288. Jahnke, K., et al., *Expression of the chemokine receptors CXCR4, CXCR5, and CCR7 in primary central nervous system lymphoma*. *Blood*, 2005. **106**(1): p. 384-385.
289. Kallinich, T., et al., *Chemokine receptor expression on neoplastic and reactive T cells in the skin at different stages of mycosis fungoides*. *J Invest Dermatol*, 2003. **121**: p. 1045-1052.
290. Crazzolaro, R., et al., *High expression of the chemokine receptor CXCR4 predicts for extramedullary organ infiltration in childhood acute lymphoblastic leukaemia*. *B J Haem*, 2001. **115**: p. 545-553.
291. Ishida, T., et al., *Clinical Significance of CCR4 Expression in Adult T-Cell Leukemia/Lymphoma, Its Close Association with Skin Involvement and Unfavorable Outcome*. *Clin Cancer Res*, 2003. **9**: p. 3625-3634.
292. Yamamoto, H., et al., *Significance of CXCR3 expression in gastric low-grade B-cell lymphoma of mucosa-associated lymphoid tissue type for predicting responsiveness to Helicobacter pylori eradication*. *Cancer Sci*, 2008. **99**(9): p. 1769-1773.

293. Devine, S., et al., *Rapid Mobilization of CD34+ Cells Following Administration of the CXCR4 Antagonist AMD3100 to Patients With Multiple Myeloma and Non-Hodgkin's Lymphoma*. *Journal of Clinical Oncology*, 2004. **22**(6): p. 1095-1102.
294. Fruehauf, S., et al., *Mobilization of peripheral blood stem cells for autologous transplant in non-Hodgkin's lymphoma and multiple myeloma patients by plerixafor and G-CSF and detection of tumour cell mobilization by PCR in multiple myeloma patients*. *Bone Marrow Transplantation*, 2009. **45**: p. 269-275.
295. Bertolini, F., et al., *CXCR4 neutralization, a novel therapeutic approach for Non-Hodgkin's lymphoma*. *Cancer Res*, 2002. **62**: p. 3106-3112.
296. Alfonso-Pérez, M., et al., *Anti-CCR7 monoclonal antibodies as a novel tool for the treatment of chronic lymphocytic leukemia*. *J Leuk Biol*, 2006. **79**: p. 1157-1165.
297. Yamamoto, K., et al., *Phase I study of KW-0761, a defucosylated humanized anti-CCR4 antibody, in relapsed patients with adult T-cell leukemia-lymphoma and peripheral T-cell lymphoma*. *J Clin Oncol*, 2010. **28**(9): p. 1591-1598.
298. Baatar, D., et al., *CCR4-expressing T-cell tumours can be specifically controlled via delivery of toxins to chemokine receptors*. *J Immunol*, 2007. **179**: p. 1996-2004.
299. Hütter, G., et al., *Long-term control of HIV by CCR5 Delta32/Delta32 Stem-cell transplantation*. *N Engl J Med*, 2009. **360**(7): p. 692-698.
300. Kanerva, A. and A. Hemminki, *Modified adenovirus for cancer gene therapy*. *Int J Cancer*, 2004. **110**: p. 475-480.
301. Zubietta, C., et al., *The structure of the Human Adenovirus 2 Penton*. *Mol. Cell*, 2005. **17**: p. 121-135.
302. Blair, G.E. and M.E. Blair-Zajdel, *Evasion of the immune system by adenoviruses*. *Current Topics in Microbiology and Immunology*, 2004. **273**: p. 3-28.
303. Endter, C. and T. Dobner, *Cell transformation by Human Adenoviruses*. *Current Topics in Microbiology and Immunology*, 2004. **273**: p. 163-214.
304. Volpers, C. and S. Kochanek, *Adenoviral vectors for gene transfer and therapy*. *J Gene Med*, 2004. **2004**(6): p. S164-171.
305. Bergelson, J.M., et al., *Isolation of a common receptor for Coxsackie B viruses and adenoviruses 2 and 5*. *Science*, 1997. **275**: p. 415-419.
306. Roelvink, P.W., et al., *Identification of a conserved receptor-binding site on the fiber proteins of CAR-recognizing adenoviridae*. *Science*, 1999. **286**(5444): p. 1568-1571.
307. Philipson, L. and R.F. Pettersson, *The Coxsackie-Adenovirus Receptor - A new receptor in the immunoglobulin family involved in cell adhesion*. *Current Topics in Microbiology and Immunology*, 2004. **273**: p. 87-111.

308. Huang, S., et al., *Adenovirus interactions with distinct integrins mediates separate events in cell entry and gene delivery to hematopoietic cells*. J Virol, 1996. **70**(7): p. 4502-4508.
309. Asher, D.R., et al., *Coxsackievirus and adenovirus receptor is essential for cardiomyocyte development*. Genesis, 2005. **42**(2): p. 77-85.
310. Patzke, C., et al., *The Coxsackievirus–Adenovirus Receptor Reveals Complex Homophilic and Heterophilic Interactions on Neural Cells*. J Neuroscience, 2010. **30**(8): p. 2897-2910.
311. Meier, O. and U. Greber, *Adenovirus endocytosis*. Journal of Gene Medicine, 2003. **6**: p. S152-163.
312. Roelvink, P.W., et al., *The coxsackievirus-adenovirus receptor protein can function as a cellular attachment protein for adenovirus serotypes from subgroups A, C, D, E, and F*. J Virol, 1998. **72**(10): p. 7909-7915.
313. Wickham, T.J., et al., *Integrins $\alpha_v\beta_3$ and $\alpha_v\beta_5$ promote adenovirus internalization but not virus attachment*. Cell, 1993. **73**(2): p. 309-319.
314. Li, E., et al., *Adenovirus endocytosis requires actin cytoskeleton reorganization mediated by Rho family GTPases*. J Virol, 1998. **72**(11): p. 8806-8812.
315. Greber, U.F., et al., *Stepwise dismantling of adenovirus 2 during entry into cells*. Cell, 1993. **75**(3): p. 477-486.
316. Horwood, N.J., et al., *High-efficiency gene transfer into nontransformed cells: utility for studying gene regulation and analysis of potential therapeutic targets*. Arthritis Research, 2002. **4**(suppl 3): p. 215-225.
317. Alemany, R. and D.T. Curiel, *CAR-binding ablation does not change biodistribution and toxicity of adenoviral vectors*. Gene Therapy, 2001. **8**: p. 1347-1353.
318. Yun, C.O., et al., *Coxsackie and adenovirus receptor binding ablation reduces adenovirus liver tropism and toxicity*. Hum Gene Ther, 2005. **16**(2): p. 248-61.
319. Lyle, C. and F. McCormick, *Integrin $\alpha v\beta 5$ is a primary receptor for adenovirus in CAR-negative cells*. Virology Journal, 2010. **7**(148): p. 1-13.
320. Shayakhmetov, D.M., et al., *Adenovirus binding to blood factors results in liver cell infection and hepatotoxicity*. J Virol, 2005. **79**(12): p. 7478-7490.
321. Parker, A., et al., *Multiple vitamin K-dependant coagulation zymogens promote adenovirus-mediated gene delivery to hepatocytes*. Blood, 2006. **108**(8): p. 2554-2561.
322. Graham, F.L., et al., *Characteristics of a Human Cell Line transformed by DNA from Human Adenovirus Type 5*. J Gen Virol, 1977. **36**: p. 59-72.

323. Raper, S.E., et al., *A pilot study of in vivo liver-directed gene transfer adenoviral vector in partial ornithine transcarbamylase deficiency*. Hum Gene Ther, 2002. **13**(1): p. 163-175.
324. Windeatt, S., et al., *Adenovirus-mediated Herpes Simplex Virus Type-1 thymidine kinase gene therapy suppresses oestrogen-induced pituitary prolactinomas*. JCEM, 2000. **85**(3): p. 1296-1305.
325. Bilsland, A.E., et al., *Selective ablation of human cancer cells by telomerase-specific adenoviral suicide gene therapy vectors expressing bacterial nitroreductase*. Oncogene, 2003. **22**: p. 370-380.
326. Bischoff, J.R., et al., *An adenovirus mutant that replicates selectively in p53-deficient tumor cells*. Science, 1996. **274**(5286): p. 373-377.
327. Small, E.J., et al., *A phase I trial of intravenous CG7870, a replication-selective, prostate specific antigen-targeted oncolytic adenovirus for the treatment of hormone-refractory metastatic prostate cancer*. Mol Ther, 2006. **14**(1): p. 107-117.
328. Bilsland, A.E., et al., *Modulation of telomerase promoter tumor selectivity in the context of oncolytic adenoviruses*. Cancer Res, 2007. **67**(3): p. 1299-1307.
329. Shay, J.W. and W.N. Keith, *Targeting telomerase for cancer therapeutics*. B J Cancer, 2008. **98**(4): p. 677-683.
330. Wickham, T.J., et al., *Adenovirus targeted to heparan-containing receptors increases its gene delivery efficiency to multiple cell types*. Nature Biotechnology, 1996. **14**: p. 1570-1573.
331. Belousova, N., et al., *Modulation of adenovirus vector tropism via incorporation of polypeptide ligand into the fiber protein*. J Virol, 2002. **76**(17): p. 8621-8631.
332. Douglas, J.T., et al., *Targeted gene delivery by tropism-modified adenoviral vectors*. Nature Biotechnology, 1996. **14**: p. 1574-1578.
333. Smith, J.S., et al., *Redirected infection of directly biotinylated recombinant adenovirus vectors through cell surface receptors and antigens*. Proc Natl Acad Sci, 1999. **96**: p. 8855-8860.
334. Jin, J., et al., *Effective gene-viral therapy of leukaemia by a new fiber chimeric oncolytic adenovirus expressing TRAIL: in vitro and in vivo evaluation*. Mol Cancer Ther, 2009. **8**(5): p. 1387-1397.
335. Drouin, M., M.-P. Cayer, and D. Jung, *Adenovirus 5 and chimeric adenovirus 5/F35 employ distinct B-lymphocyte intracellular trafficking routes that are independent of their cognate surface receptor*. Virology 2010. **401**: p. 305-313.
336. Nakayama, T., et al., *Human B Cells Immortalized with Epstein-Barr Virus Upregulate CCR6 and CCR10 and Downregulate CXCR4 and CXCR5* J Virol, 2002. **76**(6): p. 3072-3077.

337. Youn, B.S., et al., *Blocking of c-FLIP(L)—independent cycloheximide-induced apoptosis or Fas-mediated apoptosis by the CC chemokine receptor 9/TECK interaction*. *Blood*, 2001. **98**: p. 925-933.
338. Power, C.A., et al., *Molecular cloning and functional expression of a novel CC chemokine receptor cDNA from a Human Basophilic cell line*. *J Biol Chem*, 1995. **270**(33): p. 19495-19500.
339. Campbell, J. and E. Butcher, *Rapid acquisition of tissue-specific homing phenotypes by CD4⁺ T cells activated in cutaneous or mucosal lymphoid tissues*. *J Exp. Med*, 2002. **195**(1): p. 135-141.
340. Imai, T., et al., *Selective recruitment of CCR4-bearing Th2 cells toward antigen-presenting cells by the CC chemokines thymus and activation-regulated chemokine and macrophage-derived chemokine*. *Int Immunol*, 1999. **11**(1): p. 81-88.
341. Ishida, T., et al., *CC Chemokine Receptor 4-Positive Diffuse Large B-Cell Lymphoma Involving the Skin: A Case Report*. *Int J Haem*, 2005. **82**(2): p. 148-151.
342. Rodig, S.J., et al., *CCR6 is a functional chemokine receptor that serves to identify select B-cell Non-Hodgkin's lymphomas*. *Human Pathology*, 2002. **33**(12): p. 1227-1234.
343. Banfield, G., et al., *CC Chemokine Receptor 4 (CCR4) in human allergen induced late nasal responses*. *Allergy*, 2010. **65**: p. 1126-1233.
344. Lundgren, A., et al., *Helicobacter pylori-Specific CD4 T Cells Home to and Accumulate in the Human Helicobacter pylori-Infected Gastric Mucosa*. *Infection and Immunity*, 2005. **73**(9): p. 5612-5619.
345. Geissmann, F., et al., *Homing Receptor $\alpha 4\beta 7$ Integrin Expression Predicts Digestive Tract Involvement in Mantle Cell Lymphoma*. *Am J Pathol*, 1998. **153**(6): p. 1701-1705.
346. Campbell, J.J., et al., *CCR7 Expression and Memory T Cell Diversity in Humans*. *J Immunol*, 2001. **166**: p. 877-884.
347. Förster, R., A.C. Davalos-Miszlitz, and A. Rot, *CCR7 and its ligands: balancing immunity and tolerance*. *Nat Immunol Reviews*, 2008. **8**: p. 362-371.
348. Shields, J.D., et al., *Autologous Chemotaxis as a Mechanism of Tumor Cell Homing to Lymphatics via Interstitial Flow and Autocrine CCR7 Signaling*. *Cancer Cell*, 2007. **11**: p. 526-538.
349. Townsen, J.R. and R.J.B. Nibbs, *Characterization of mouse CCX-CKR, a receptor for the lymphocyte-attracting chemokines TECK/mCCL25, SLC/mCCL21 and MIP-3 /mCCL19: comparison to human CCX-CKR*. *Eur J Immunol*, 2002. **32**(5): p. 1230-1241.
350. Press, O.W., et al., *Phase II trial of ¹³¹I-B1 (anti-CD20) antibody therapy with autologous stem cell transplantation for relapsed B cell lymphomas*. *Lancet*, 1995. **346**(8971): p. 336-340.

351. Narra, V.R., et al., *Radiotoxicity of some iodine-123, iodine-125 and iodine-131-labeled compounds in mouse testes: Implications for radiopharmaceutical design.* J Nuclear Med, 1992. **33**(12): p. 2196-2201.
352. Xia, D., et al., *Crystal structure of the receptor-binding domain of adenovirus type 5 fiber protein at 1.7Å resolution.* Structure, 1994. **2**(12): p. 1259-1270.
353. Kim, M., et al., *The therapeutic efficacy of adenoviral vectors for cancer gene therapy is limited by a low level of primary adenovirus receptors on tumour cells* Eur J Cancer, 2002. **38**(14): p. 1917-1926.
354. Howarth, M., et al., *Targeting quantum dots to surface proteins in living cells with biotin ligase.* Proc Natl Acad Sci, 2005. **102**(21): p. 7587.
355. Gorer, P.A., *Antibody response of mice to tumour inoculation.* Br J Cancer, 1950. **4**(4): p. 372-379.
356. Salem, M.L., *Systemic treatment with n-6 polyunsaturated fatty acids attenuates EL4 thymoma growth and metastasis through enhancing specific and non-specific anti-tumor cytolytic activities and production of TH1 cytokines* Int Immunopharmacology, 2005. **5**(6): p. 947-960.
357. Teschendorf, C., et al., *Comparison of the EF-1 alpha and the CMV promoter for engineering stable tumor cell lines using recombinant adeno-associated virus.* Anticancer Res, 2002. **22**(6A): p. 3325-3330.
358. Leon, R.P., et al., *Adenoviral-mediated gene transfer in lymphocytes.* Proc Natl Acad Sci, 1998. **95**: p. 13159-13164.
359. López-Giral, S., et al., *Chemokine receptors that mediate B cell homing to secondary lymphoid tissues are highly expressed in B cell chronic lymphocytic leukaemia and non-Hodgkin lymphomas with widespread nodular dissemination.* J Leuk Biol, 2004. **76**: p. 462-471.
360. Förster, R., et al., *A putative Chemokine Receptor, BLR1, Directs B Cell Migration to Defined Lymphoid Organs and Specific Anatomic Compartments of the Spleen.* Cell, 1996. **87**: p. 1037-47.
361. Honczarenko, M., et al., *SDF-1 responsiveness does not correlate with CXCR4 expression levels of developing human bone marrow B cells.* Blood, 1999. **94**(9): p. 2990-2998.
362. Corcione, A., et al., *Chemotaxis of human tonsil B lymphocytes to CC chemokine receptor (CCR) 1, CCR2 and CCR4 ligands is restricted to non-germinal center cells.* Int Immunol, 2002. **14**(8): p. 883-892.
363. Caron, G., et al., *CXCR4 expression functionally discriminates centroblasts versus centrocytes within human germinal center B cells.* J Immunol, 2009. **182**: p. 7595-7602.
364. Wong, S.W.J. and D.A. Fulcher, *Chemokine receptor expression in B-cell lymphoproliferative disorders.* Leuk Lymphoma, 2004. **45**(12): p. 2491-2496.

365. Cook, D.N., et al., *CCR6 mediates dendritic cell localization, lymphocyte homeostasis, and immune responses in mucosal tissue*. *Immunity*, 2000. **12**: p. 495-503.
366. Johansson, C., et al., *Differential expression of chemokine receptors on human IgA+ and IgG+ B cells*. *Clinical and Experimental Immunology*, 2005. **141**: p. 279-287.
367. Ek, S., et al., *Mantle cell lymphomas express a distinct genetic signature affecting lymphocyte trafficking and growth regulation as compared with subpopulations of normal human B cells*. *Cancer Res*, 2002. **62**: p. 4398-4405.
368. Kunkel, E.J., et al., *CCR10 expression is a common feature of circulating and mucosal epithelial tissue IgA Ab-secreting cells*. *J Clin Invest*, 2003. **111**(7): p. 1001-1010.
369. Ghobrial, I.M., et al., *Expression of the Chemokine Receptors CXCR4 and CCR7 and Disease Progression in B-Cell Chronic Lymphocytic Leukaemia/ Small Lymphocytic Lymphoma*. *Mayo Clin Proc*, 2004. **79**: p. 318-325.
370. Piovan, E., et al., *Differential Regulation of Hypoxia-Induced CXCR4 Triggering during B-cell development and Lymphomagenesis*. *Cancer Res*, 2007. **67**(18): p. 8605-8614.
371. Chunsong, H., et al., *CXC Chemokine Lignad 13 and CC Chemokine Ligand 19 Cooperatively Render Resistance to Apoptosis in B Cell Lineage Acute and Chronic Lymphocytic CD23⁺CD5⁺ B Cells*. *J Immunol*, 2006. **177**: p. 6713-6722.
372. Chvatchko, Y., et al., *A key role for CC Chemokine receptor 4 in lipopolysaccharide-induced endotoxic shock*. *J Exp. Med*, 2000. **191**(10): p. 1755-1763.
373. Bonecchi, R., et al., *Differerential recognition and scavenging of native and truncated macrophage-derived chemokine (macrophage-derived chemokine/ CC ligand 22) by the D6 decoy receptor*. *J Immunol*, 2004. **172**: p. 4972-4976.
374. Alizadeh, A., et al., *Distinct types of diffuse large B-cell lymphoma identified by gene expression profiling*. *Nature*, 2000. **403**: p. 503-511.
375. Rosenwald, A., et al., *The use of molecular profiling to predict survival after chemotherapy for diffuse large B-cell lymphoma*. *N Engl J Med*, 2002. **346**(25): p. 1937-1947.
376. Deutsch, A.J.A., et al., *Distinct signatures of B-cell homeostatic and activation-dependent chemokine receptors in the development and progression of extragastric MALT lymphomas*. *J Pathol.*, 2008. **215**: p. 431-444.
377. Sakaguchi, S., *Regulatory T cells: key controllers of immunologic self-tolerance*. *Cell*, 2000. **101**(5): p. 455-458.
378. Hori, S., T. Nomura, and S. Sakaguchi, *Control of regulatory T cell development by the transcription factor FOXP3*. *Science*, 2003. **299**(5609): p. 1057-1061.

379. Iellem, I., et al., *Unique chemotactic response profile and specific expression of chemokine receptors CCR4 and CCR8 by CD4⁺CD25⁺ Regulatory T cells*. J. Exp. Med, 2002. **194**(6): p. 847-853.
380. Ansell, S.M., et al., *CD4⁺ T-cell immune response to diffuse large B-cell Non-Hodgkin's lymphoma predicts patient outcome*. J Clin Oncol, 2001. **19**(3): p. 720-726.
381. Yang, Z.-Z., et al., *Intratumoral CD4⁺CD25⁺ regulatory T-cell-mediated suppression of infiltrating CD4⁺ T cells in B-cell non-Hodgkin's lymphoma*. Blood, 2006. **107**(9): p. 3639-3646.
382. Mittal, S., et al., *Local and systemic induction of CD4⁺CD25⁺ regulatory T-cell population by non-Hodgkin's lymphoma*. Blood, 2008. **111**(11): p. 5359-5370.
383. Tzankov, A., et al., *Correlation of high numbers of intratumoural FOXP3⁺ regulatory T cells with improved survival in germinal centre-like diffuse large B-cell lymphoma, follicular lymphoma and classical Hodgkin's lymphoma*. Haematologica, 2008. **93**(2): p. 193-200.
384. Lee, N.-R., et al., *Prognostic impact of tumor infiltrating FOXP3 positive regulatory T cells in diffuse large B-cell lymphoma at diagnosis*. Leuk Lymphoma, 2008. **49**(2): p. 247-256.
385. Lim, H.W., P. Hillsamer, and C.H. Kim, *Regulatory T cells can migrate to follicles upon T cell activation and suppress GC-Th cells and GC-Th cell-driven B cell responses*. J Clin Invest, 2004. **114**(11): p. 1640-1649.
386. Zhao, D.-M., et al., *Activated CD4⁺CD25⁺ T cells selectively kill B lymphocytes*. Blood, 2006. **107**: p. 3639-3646.
387. Di Stasi, A., et al., *T lymphocytes coexpressing CCR4 and a chimeric antigen receptor targeting CD30 have improved homing and antitumour activity in a Hodgkin tumor model*. Blood, 2009. **113**(25): p. 6392-6402.
388. Birkenbach, M., et al., *Epstein-Barr Virus-Induced Genes: First Lymphocyte-Specific G Protein-Coupled Peptide Receptors*. J Virol, 1993. **67**(4): p. 2209-2220.
389. Rehm, A., et al., *Identification of a chemokine receptor profile characteristic for mediastinal large B-cell lymphoma*. Int J Cancer, 2009. **125**(10): p. 2367-2374.
390. Till, K.J., et al., *The chemokine receptor CCR7 and α 4 integrin are important for migration of chronic lymphocytic leukaemia cells into lymph nodes*. Blood, 2002. **99**(8): p. 2977-2984.
391. Ding, Y., et al., *Association of CC Chemokine Receptor 7 with Lymph Node Metastasis of Esophageal Squamous Cell Carcinoma*. Clin Cancer Res, 2003. **9**: p. 3406-3412.
392. Heresi, G.A., et al., *Expression of the chemokine receptor CCR7 in prostate cancer presenting with generalized lymphadenopathy: report of a case, review of the literature, and analysis of chemokine receptor expression*. Urol Oncol., 2005. **23**(4): p. 261-7.

393. Müller, A., et al., *Involvement of chemokine receptors in breast cancer metastasis*. Nature, 2001. **410**(6824): p. 50-56.
394. Shields, J.D., et al., *Chemokine-mediated migration of melanoma cells towards lymphatics--a mechanism contributing to metastasis*. Oncogene, 2007. **10**(26): p. 2997-3005.
395. Wiley, H.E., et al., *Expression of CC Chemokine Receptor-7 and Regional Lymph Node Metastasis of B16 Murine Melanoma*. J Natl Cancer Inst, 2001. **93**(21): p. 1638-1643.
396. Okada, N., et al., *Augmentation of the migratory ability of DC-based vaccine into regional lymph nodes by efficient CCR7 gene transduction*. Gene Therapy, 2005. **12**(2): p. 129-139.
397. Liu, Q., et al., *Triptolide impairs dendritic cell migration by inhibiting CCR7 and COX-2 expression through PI3-K/Aky and NF- κ B pathways*. Mol Immunol, 2007. **44**: p. 2686-2696.
398. Villablanca, E.J., et al., *Selected natural and synthetic retinoids impair CCR7- and CXCR4-dependent cell migration in vitro and in vivo*. J Leuk Biol, 2008. **84**: p. 871-879.
399. Hu, J., et al., *Long-term efficacy and safety of all-trans retinoic acid/arsenic trioxide-based therapy in newly diagnosed acute promyelocytic leukaemia*. Proc Natl Acad Sci, 2009. **106**(9): p. 3342-3347.
400. Kennedy, G.A., et al., *Incidence and nature of CD20-negative relapses following rituximab therapy in aggressive B-cell non-Hodgkin's lymphoma: a retrospective review*. Br J Haematol., 2002. **119**(2): p. 412-416.
401. Haider, J., et al., *Loss of CD20 expression in relapsed lymphomas after rituximab therapy*. Haematologica, 2003. **70**(5): p. 330-2.
402. Whitehead, G.S., et al., *The chemokine receptor D6 has opposing effects on allergic inflammation and airway reactivity*. Am J Respir Crit Care Med, 2007. **175**: p. 243-247.
403. Nakagawa, R., J.W. Soh, and A.M. Michie, *Subversion of Protein Kinase CA Signaling in Hematopoietic Progenitor Cells Results in the Generation of a B-Cell Chronic Lymphocytic Leukemia-Like Population In vivo*. Cancer Res, 2006. **66**(1): p. 527-534.
404. ter Brugge, P.T., et al., *A mouse model for chronic lymphocytic leukaemia based on expression of the SV40 large T antigen*. Blood, 2009: epub.